NASA CR-130186

OCT 5 - 1970

DESIGN STUDY REPORT
VOLUME 1
TRANSPORT UNIT

CONTRACT NO: NAS5-11643

GODDARD SPACE FLIGHT CENTER

PREPARED BY:

RCA/DEFENSE COMMUNICATIONS SYSTEM DIVISION
DEFENSE ELECTRONIC PRODUCTS
CAMDEN, NEW JERSEY

FOR:

GODDARD SPACE FLIGHT CENTER
GREENBELT, MARYLAND

2/73

379

DESIGN STUDY REPORT
VOLUME 1
TRANSPORT UNIT

CONTRACT NO: NAS5-11643

GODDARD SPACE FLIGHT CENTER

CONTRACTING OFFICER: H. ARISTA
TECHNICAL MONITOR: J. HAYES 731

PREPARED BY:

RCA/DEFENSE COMMUNICATIONS SYSTEMS DIVISION
DEFENSE ELECTRONIC PRODUCTS
CAMDEN, NEW JERSEY
PROGRAM MANAGER: F. DONALD KELL
TECHNICAL DIRECTORS: STANLEY CLURMAN
FRANZ PUTZRATH

FOR:

GODDARD SPACE FLIGHT CENTER
GREENBELT, MARYLAND

TABLE OF CONTENTS

TABLE OF CONTENTS (Continued)

TABLE OF CONTENTS (Continued)

TABLE OF CONTENTS (Continued)

TABLE OF CONTENTS (Continued)

LIST OF ILLUSTRATIONS

LIST OF ILLUSTRATIONS (Continued)

LIST OF TABLES

1.0 INTRODUCTION

The wideband recorder development covered by Contract NAS5-11643 has goals which are typical for a satellite equipment program; long life, high reliability, minimum power consumption and minimum weight. This report documents the efforts toward these goals on the Transport Unit portion of the recording system. The analyses and tests conducted on the other portion of the recording system, the Electronics Unit, will be covered in Volume 11 of the Design Study Report.

The division of the recording system into two discrete packages is a requirement of NASA Specification S-731-P-79, which calls for a minimum of electronics in the hermetically-sealed enclosure which houses the tape transport. Hence, the major elements of the Transport Unit are a transverse scan headwheel panel; a negator-spring reeling system; a urethane coated, mylar-belt coupled, hysteresis motor driven capstan assembly and 2,000 feet of special 2" wide video recording tape. Miscellaneous guides, auxiliary heads, $I\omega$ balancing elements, end-of-tape sensors, pressure and temperature sensors and electronics are also contained in the Transport Unit.

The recording system is required to record and reproduce wideband data from either of the two primary ERTS sensors. The input from one, the RBV Camera, is an analog signal with a bandwith from dc to 3.5 MHz. This signal is accommodated through fm recording techniques which provide a recorder signal-to-noise ratio in excess of 42 dB, pp/rms over the specified bandwidth. The second sensor is a Multi-Spectral Scanner (MSS) which provides, as initial output, twenty-six narrow-band channels. These channels are multiplexed prior to transmission or recording into a single 15 Megabit/sec. digital data stream. Within the recorder, the 15 Megabit/sec., NRZ_L signal is processed through the same fm electronics as the RBV signal, but the basic fm standards are modified to provide an internal, 10.5 MHz baseband response with S/N ratio of about 25 dB. Following fm demodulation, however, the MSS signal is digitally re-shaped and re-clocked so that good bit stability and signal-to-noise exist at the recorder output.

Two additional, longitudinally-recorded channels are also included in the recording system. One of these channels (Auxiliary Channel) is available for recording of housekeeping or audio data and has a bandwidth and S/N of dc-5 kHz and 30 dB, pp/rms, respectively. The second longitudinal track (Search Track) is a pre-recorded digital channel which outputs a discrete word for every 6" of tape movement. The output bit rate is 2.5 dbps or 10 dbps for the playback or wind modes, respectively.

The electronics within the Transport Unit consist primarily of record amplifiers for the wide band auxiliary channels, and playback amplifiers for all three channels.

In addition, portions of the control elements for motor switching and shoe engagement are also located in the Transport Unit. To minimize the possibilities of tape path contamination, the electronics and most of the transport wiring are located on the side of the motorboard opposite to the tape path.

The specification for the recorder life requires "one year in orbit after considerable ground testing" with a design goal of "4,000 full length record and playback cycles". In the studies and tests conducted during the design phase of the program, drift during three years was considered for the electronics and 4,000 record/playback cycles (5,000 operating hours) was the minimum goal for all limited life mechanical components except for the head-to-tape interface. In this latter area, a goal of 1,000 hours was established by RCA's proposal and this goal represented a two-to-one improvement over the best previous results. Two tests of the most recent head/tape configuration have now exceeded this goal without failure and the wear rates experienced do not preclude an extension of life to beyond 4,000 record/playback cycles.

Realization of this life, however, will depend on the ability to

1) minimize the build-up of contaminants on the video heads, and

2) prevent the occurrence of premature component failures. Design efforts in these areas for the Transport Unit are described in this report, together with the other related analyses and tests.

1.1 General Design Discussion

This study presents mechanical and thermal analyses of the transport mechanism and its pressurized enclosure, and electrical and thermal analyses of those circuits within the enclosure.

The complete transport mechanism is mounted on a ribbed magnesium deck. Figure 1-1 shows the ERTS Feasibility Unit transport with all functional components mounted in place. The deck is fastened at 8 points to the lower half of the pressurized enclosure. The deck is electrically isolated from the enclosure by rubber spacers. The compliance of the isolators also provides strain relief between the deck and the enclosure. Figure 1-2 shows the partially assembled ERTS Engineering Model transport mounted in the lower half of the pressurized enclosure; the upper half of the enclosure is shown so as reveal its inner stiffening structure. Figure 1-3 shows the full pressurized enclosure, minus the hermetic seal connectors.

The discussions which follow provide a brief functional description, where called for, and then analyze the basic functional modes. In the mechanical analyses, worst case loads or stresses are computed, and, where required, life estimates are

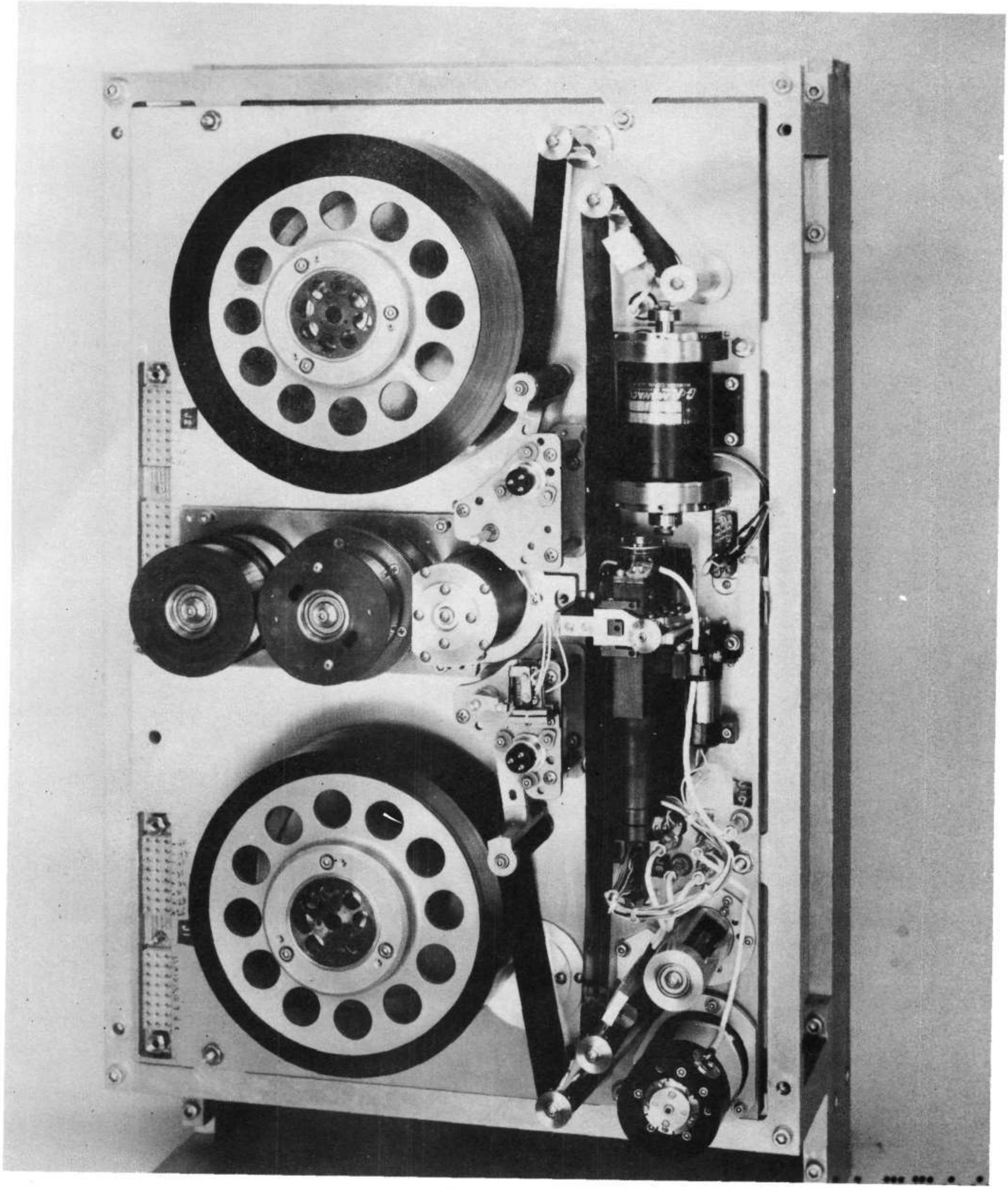

Figure 1-1. Front View of Erts Feasibility Unit Transport with Transmission Cover Removed

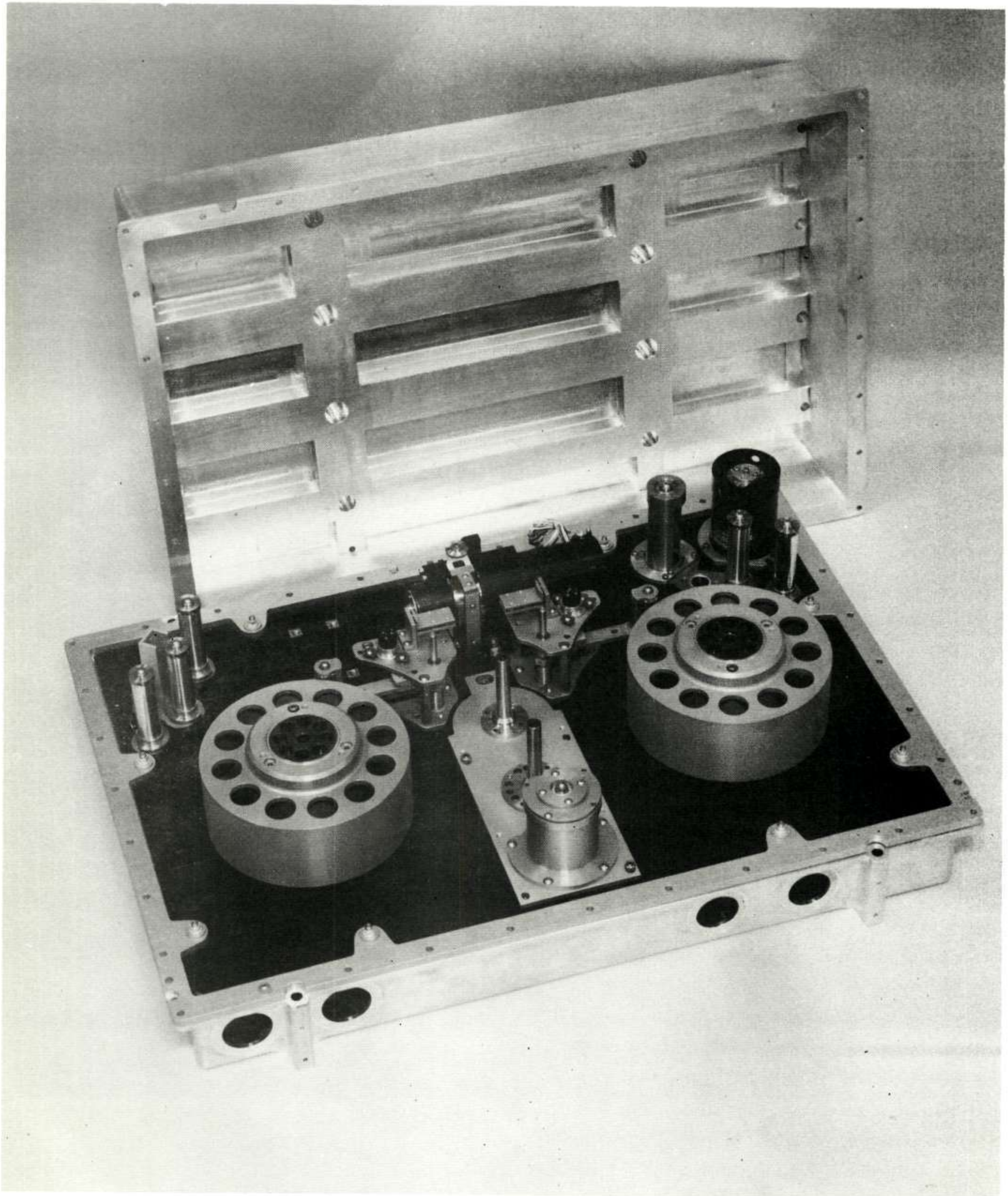

Figure 1-2. Engineering Model Transport Unit

Figure 1-3, Pressurized Enclosure

made. In the case of circuitry, worst case analyses, stress analyses, and failure mode and effects analyses are presented. A thermal analysis of the internal assemblage has been made and temperature rise predicted.

1.2 External Drawings

The outline dimensions and mounting information for the ERTS Transport Unit are shown in Figure 1-4 (RCA 8671011). Four mounting pads are provided to minimize case distortion while maximizing heat transfer. In order to minimize case distortion, the four spacecraft mounting pads or areas, corresponding to the Transport Unit mounting pads, should be flat and parallel to each other within .005 total.

1.3 Key Assemblies

The key sub-assemblies include the Reel Assembly, the Capstan Assembly, the Negator/Differential Assembly, and the Headwheel Assembly. The basic construction of these assemblies is shown in Figures 1-5 through 1-8, respectively.

1.4 Tape Transport Assembly

The various elements of the Tape Transport Unit are shown in the top assembly drawing (RCA 8358497) of Figure 1-9. A family tree for the unit is diagrammed in Figure 1-10 while preliminary parts lists for the unit are contained in Appendix 1A.

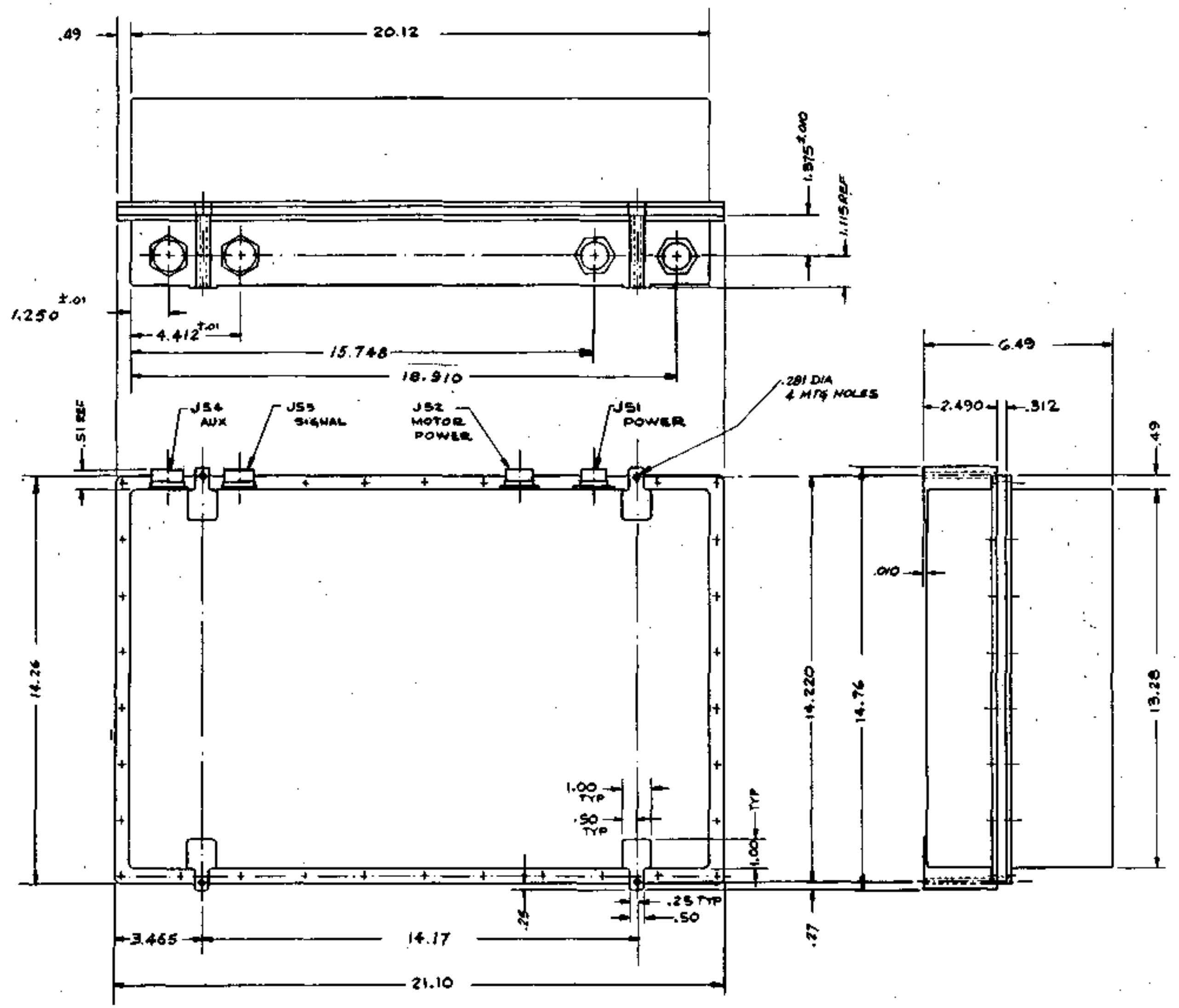

Figure 1-4 OUTLINE DWG TRANSPORT UNIT ERTS

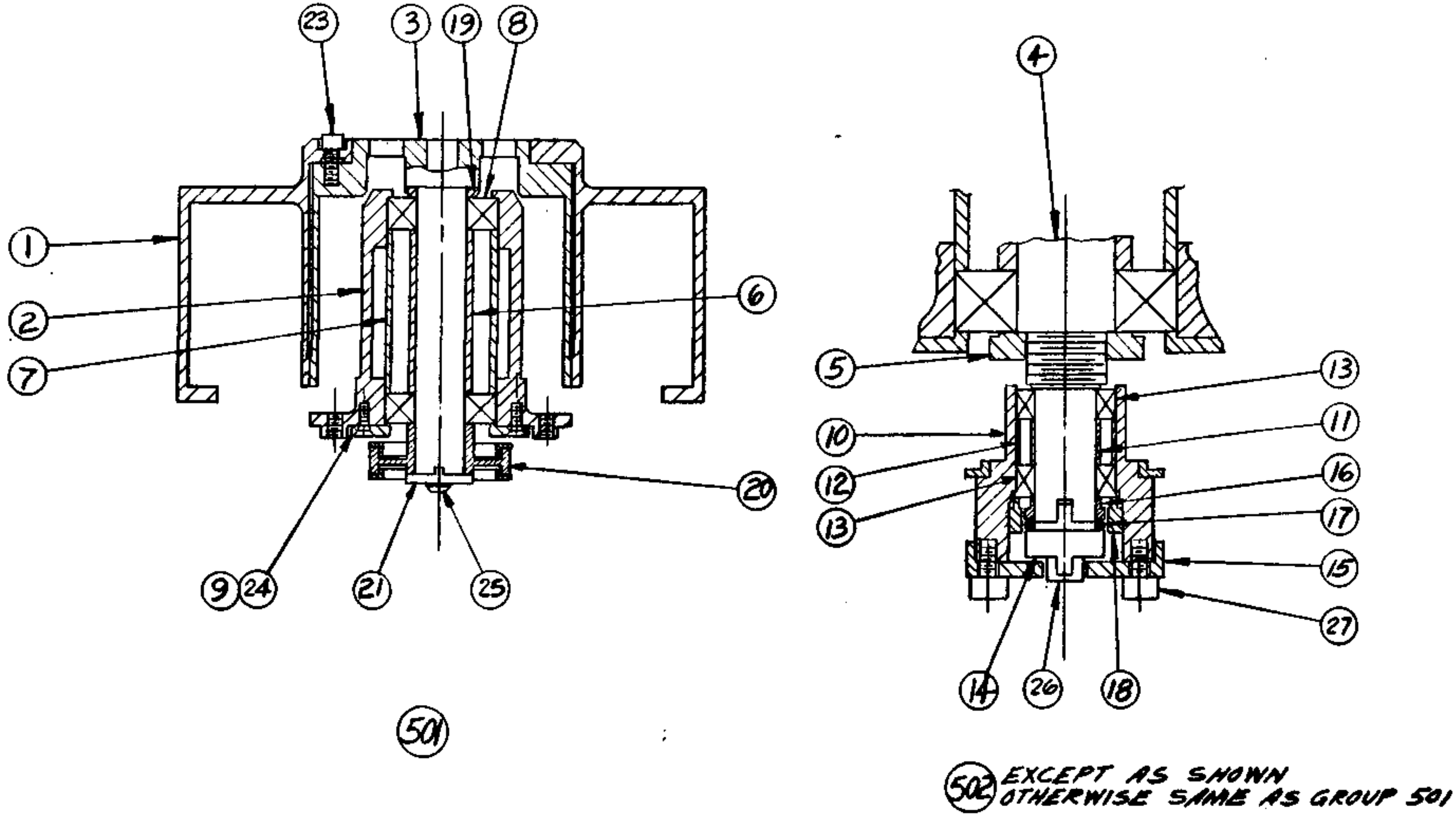

Figure 1-5 REEL, ASSEMBLY

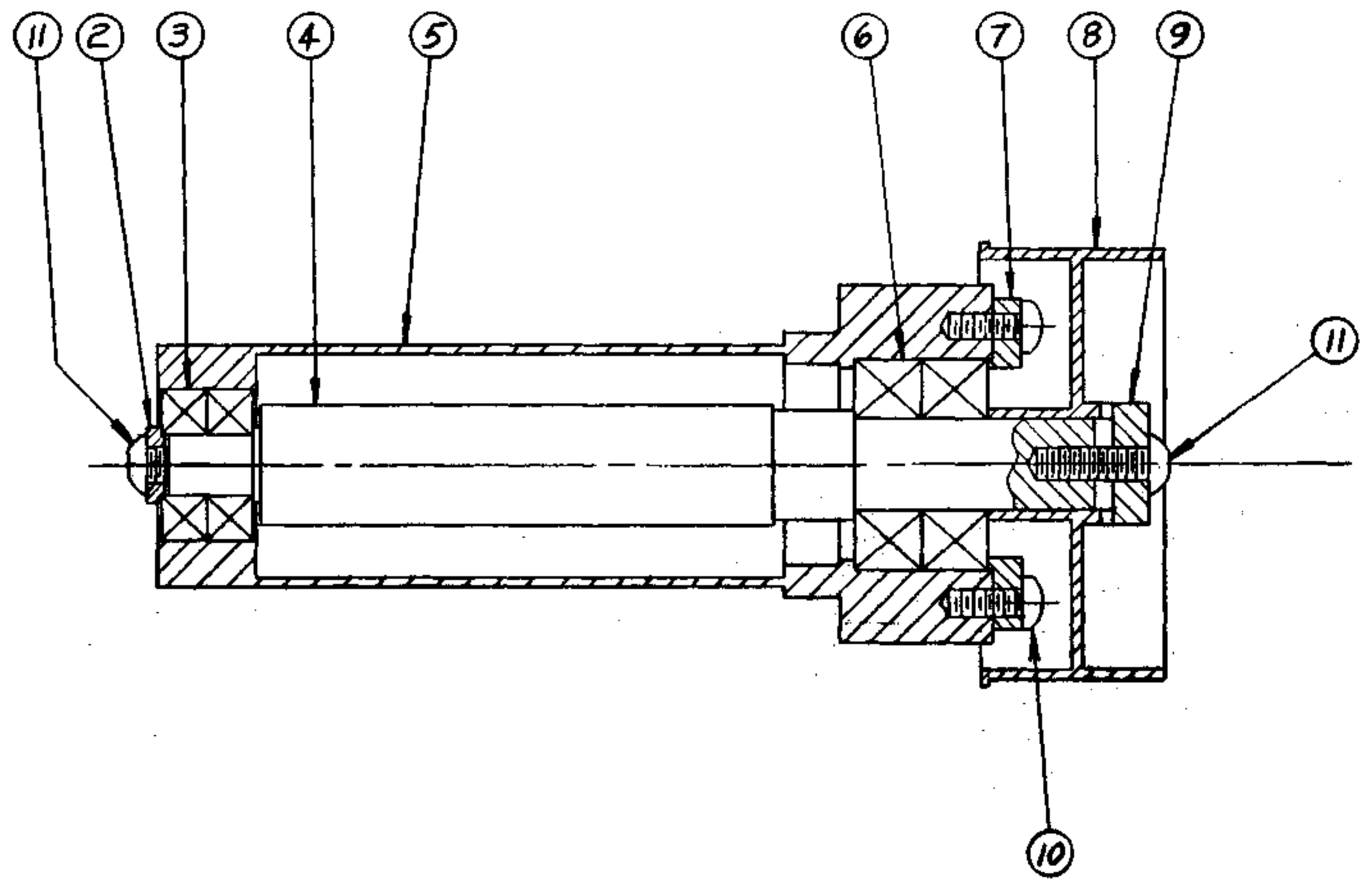

Figure 1-6 CAPSTAN ASSEMBLY

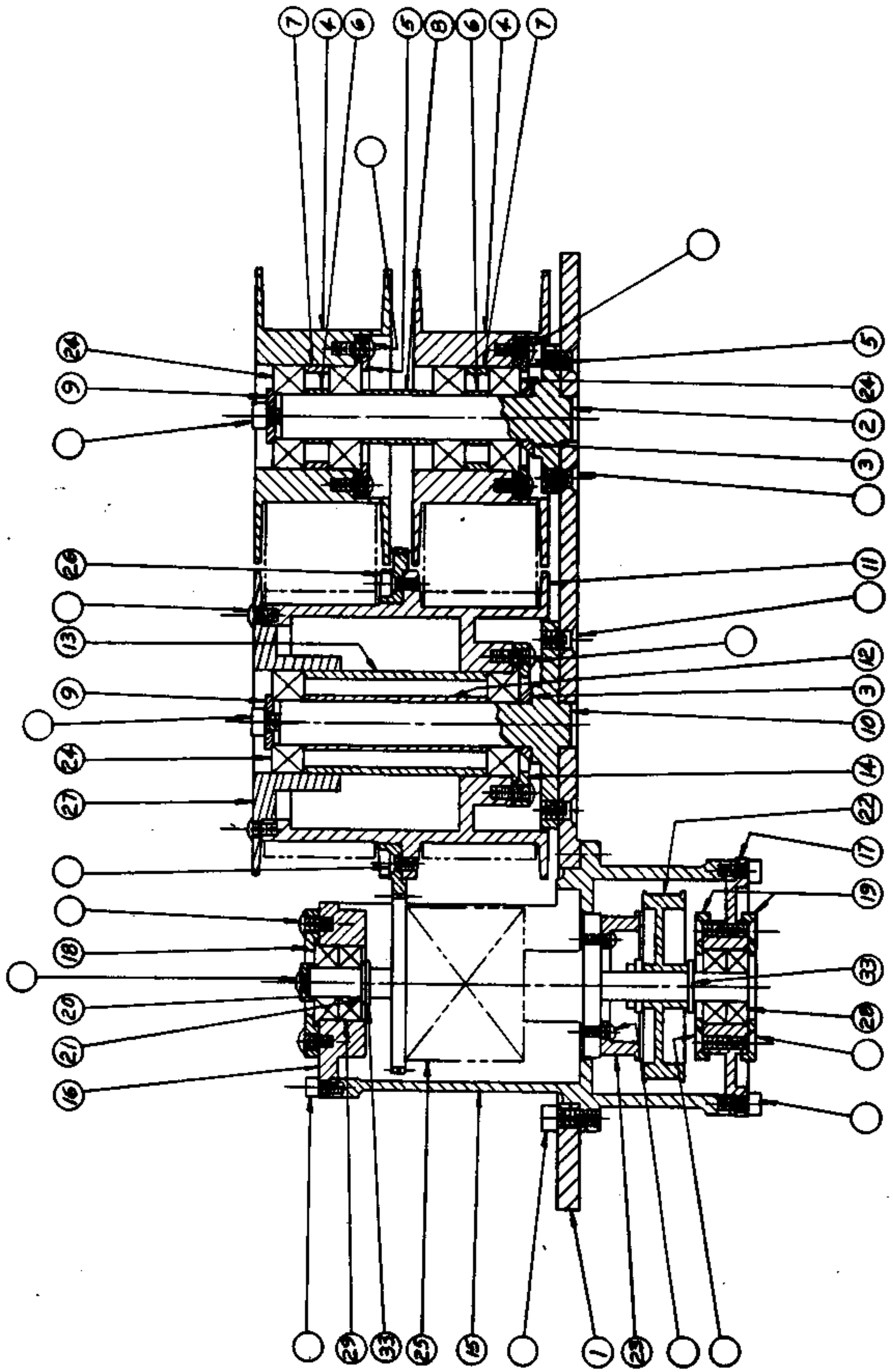

Figure 1-7 NEGATOR/DIFFERENTIAL ASSEMBLY

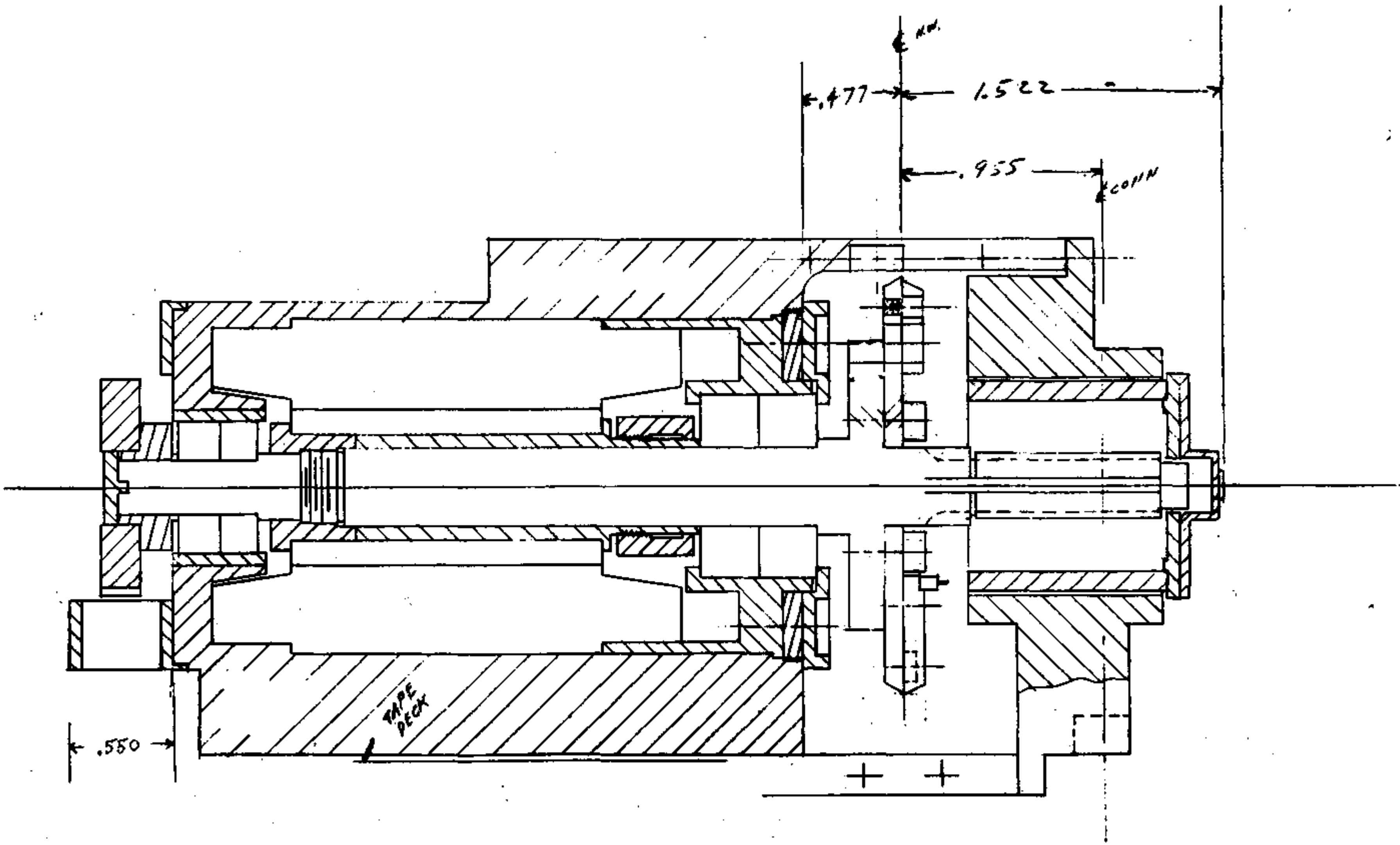

Figure 1-8   ERTS HEADWHEEL ASSEMBLY CONSTRUCTION

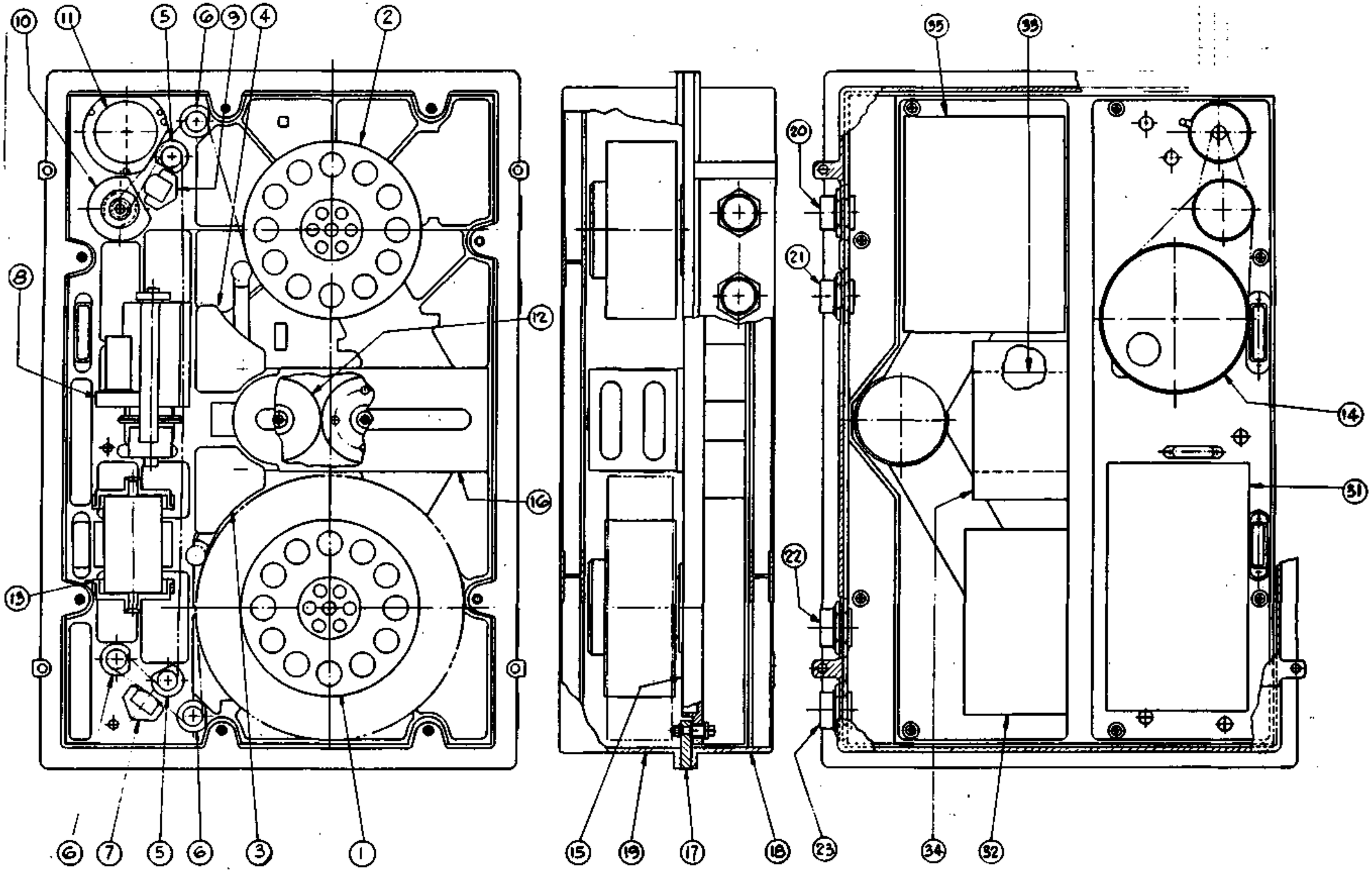

Figure 1-9 TAPE TRANSPORT UNIT ERTS

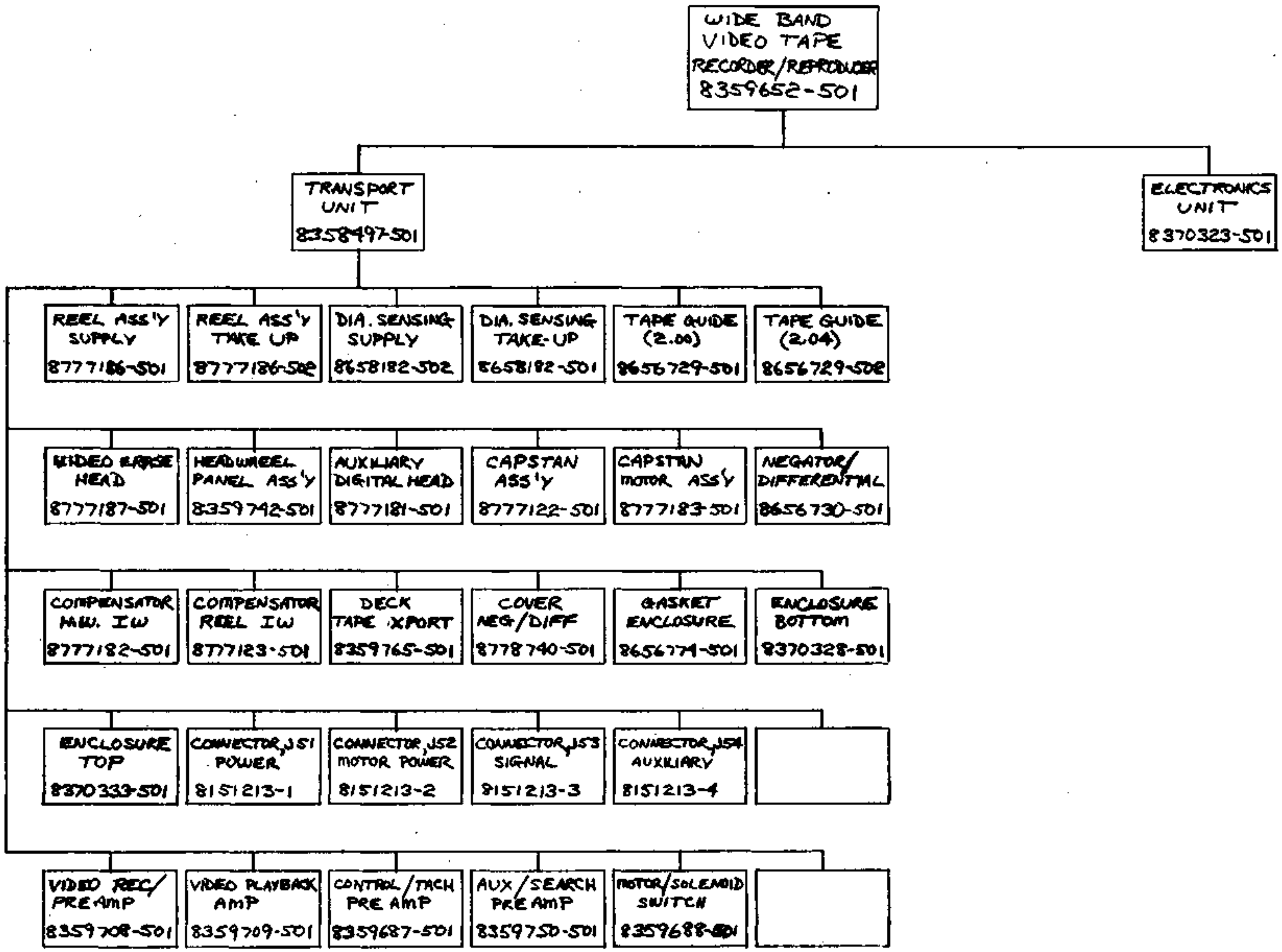

Figure 1-10 ERTS RECORDER FAMILY TREE TRANSPORT UNIT

2.0 MECHANICAL DESIGN STUDIES

2.1 Tape Tensioning System

Tape Tension is maintained by torquing the two tape reels in opposite directions by means of the Negator-differential mechanism. A schematic drawing of this subsystem is shown in Figure 2-1. Two Negator springs torque an input shaft of the differential. The gear and belt ratios are such that each reel "sees" 1/2 this torque, or the torque of a single Negator coil, assuming no frictional losses. The differential rotation between the two reels is exactly twice the rotation of the Negator power drum. An analysis diagram of the tape tensioning system is shown in Figure 2-2.

Under steady-state conditions, the tape tension approaching the control track head and headwheel will be the tension leaving the supply reel plus the drag effects of elements between the supply reel and the control track head. These elements are, in sequence, the reel follower roller, two idler rollers, the erase head and a third idler roller.

The torque on the supply reel would be, nominally, that of a single Negator spring, if there were no frictional losses in the transmission. Actually, the supply reel torque is increased by these friction effects.

Measurements were made on the Feasibility Model of tape tension, reel diameters, and turns of the Negator output drum, and these values are shown in Figure 2-3, as a function of recording time. At the time of this test, the transport was set up for 28 minutes of recording time. The values shown in Figure 2-3 will be slightly modified for the full 30 minutes of recording time. In its application, the takeup sprocket on the differential is driving the takeup reel (refer to Figure 2-2), and the supply sprocket is braking the supply reel. In order to analyze the action within the differential, however, the supply belt can be considered as driving its differential shaft. The reasoning for this is based on the condition that the high tension side of the takeup belt is torquing shaft no. 1 of the differential in the same direction as its rotation. By the same logic, the takeup sprocket on shaft no. 2 can be considered as transmitting a load into the takeup belt. Thus, the analysis can be made for a gear transmission in which the supply sprocket is on the input shaft and the takeup sprocket is on the output shaft. For the moment, assume no motion of the Negator spur gears, as will be the case at the center of tape. For this type of gear transmission, the following relationships apply:

(1) $M2/2M_1 = E_1 = 1-\nu_1$

and for static equilibrium,

(2) $M_3 = M_2 - M_1 = 2(1-\nu_1)\,M_1 - M_1 = (1-2\,\nu_1)\,M_1$

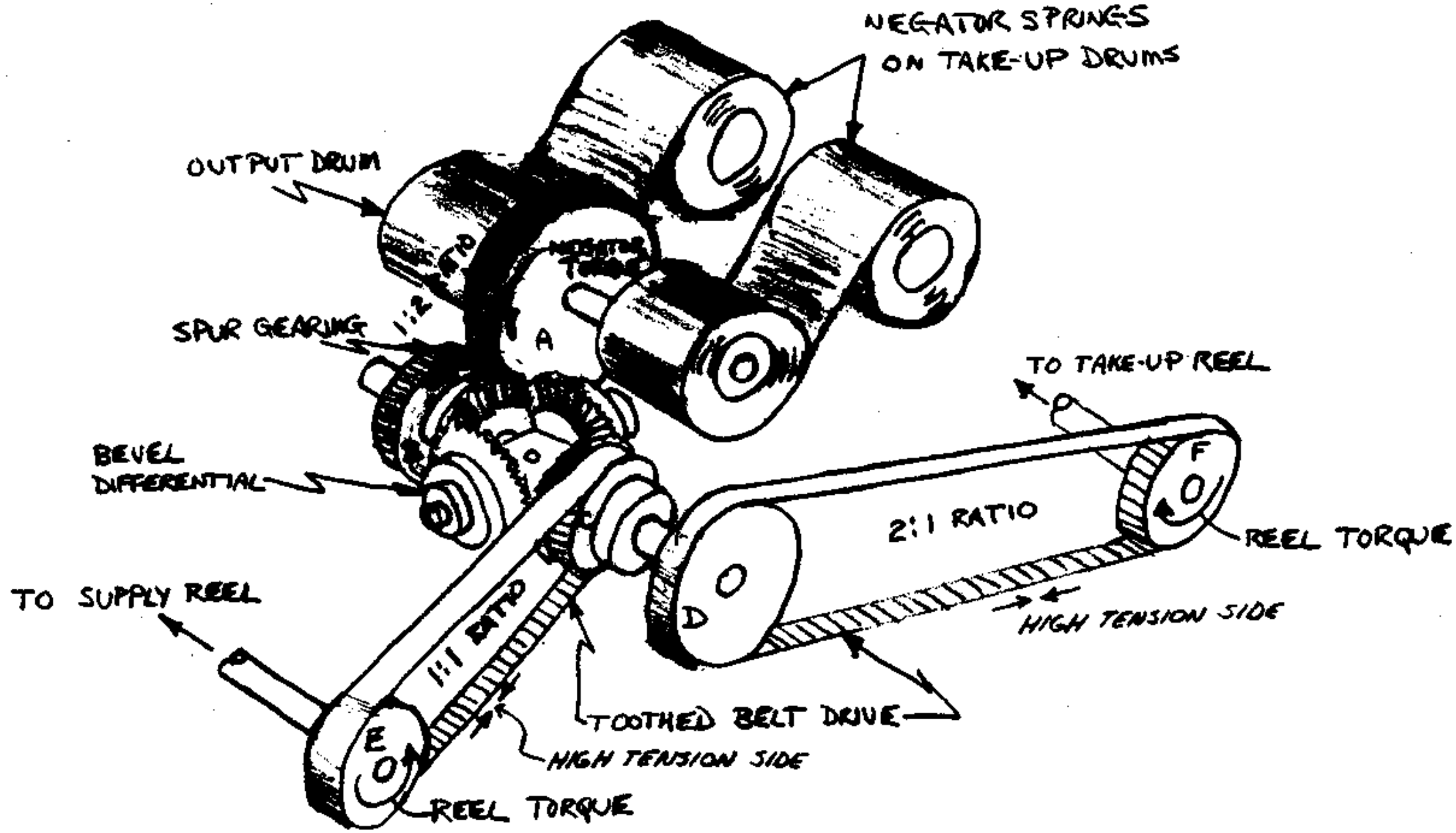

Figure 2-1 SCHEMATIC OF REEL TORQUING SYSTEM

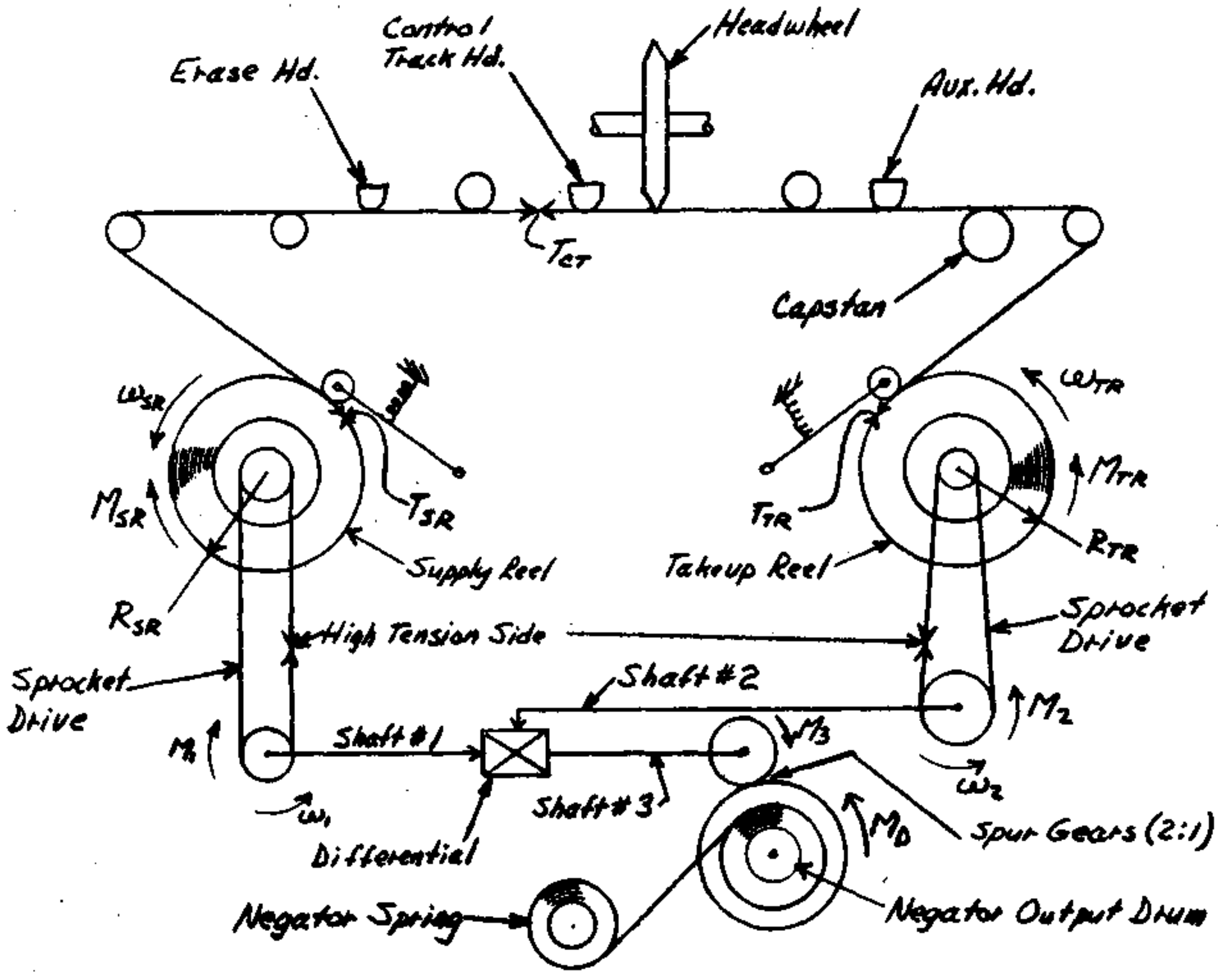

T_{CT} = Tension Approaching Control Track Hd.

T_{SR} = Tension Leaving Supply Reel

T_{TR} = Tension Entering Takeup Reel

M_{SR} = Torque on Supply Reel

M_{TR} = Torque on Takeup Reel

M_1 = Torque on Shaft #1

M_2 = Torque on Shaft #2

M_3 = Torque on Shaft #3

M_D = Torque at Negator Output Drum

Figure 2-2 ANALYSIS DIAGRAM OF TAPE TENSIONING SYSTEM

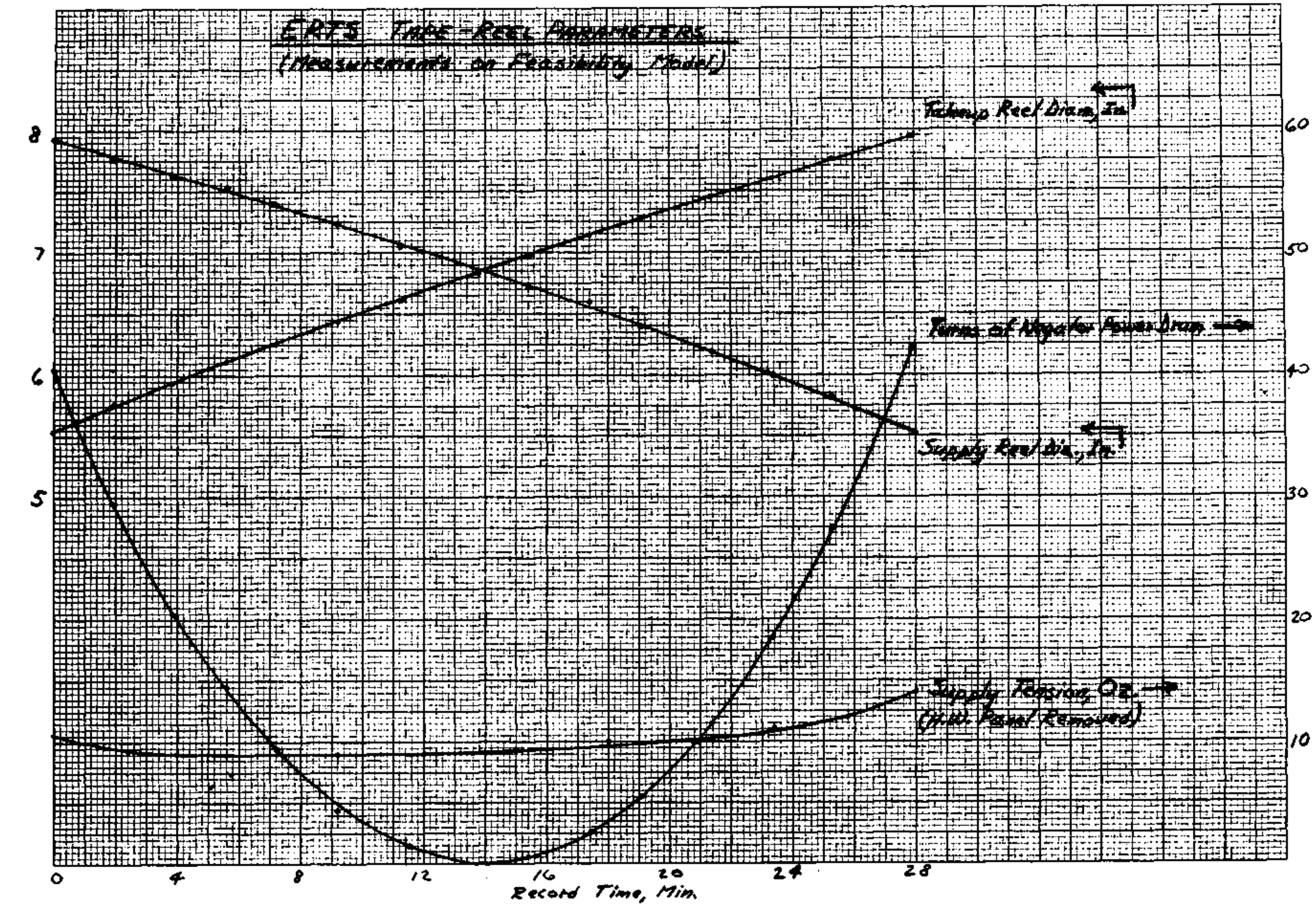

Figure 2-3 ERTS TAPE-REEL PARAMETERS

where:

M_1 = the torque on the differential supply sprocket

M_2 = the torque on the differential takeup sprocket

M_3 = the torque on the differential spur gear

E_1 = the efficiency of one mesh of the bevel gears

ν_1 = the loss in one mesh of the bevel gears

When the two reel speeds are unequal, the Negator output drum and its spur gear rotate slowly. When the supply reel speed is less than that of the takeup reel (SOT - COT), the springs are unwinding, and the drum gear is driving its mate on shaft no. 3. When the supply reel speed is greater than that of the takeup reel (COT - EOT), the drum gear is being driven by the shaft no. 3. Since these spur gears have a ratio of 2:1, the following equations may be written:

$$(3)\quad M_3 = E_2\left(\frac{MD}{2}\right) \approx (1 - \nu_2)\left(\frac{MD}{2}\right), \text{ between SOT and COT}$$

$$(4)\quad M_3 = \frac{1}{E_2}\left(\frac{MD}{2}\right)(1 + \nu_2)\left(\frac{MD}{2}\right), \text{ between COT and EOT}$$

where:

MD = torque of the Negator output drum

E_2 = efficiency of the spur gear mesh

ν_2 = loss in the spur gear mesh

Combining equations (2) and (3), and also (2) and (4) leads to:

$$(5)\quad \frac{M_1}{(1/2\ MD)} = (1 + 2\,\nu_1 - \nu_2) \text{ between SOT and COT}$$

$$(6)\quad \frac{M_1}{(1/2\ MD)} = (1 + 2\,\nu_1 + \nu_2) \text{ between COT and EOT}$$

Finally, the torque at the supply reel sprocket is increased by any small losses in the sprocket drive and the consequent equations are:

$$(7) \quad \frac{MSR}{(1/2\ MD)} = \frac{1}{E_3} (1+2\nu_1-\nu_2) = (1+2\nu_1-\nu_2+\nu_3) \text{ between SOT and COT}$$

$$(8) \quad \frac{MSR}{(1/2\ MD)} = \frac{1}{E_3} (1+2\nu_1+\nu_2) = (1+2\nu_1+\nu_2+\nu_3) \text{ between COT and EOT}$$

where:

E_3 = the efficiency of the sprocket drive

ν_3 = the loss in the sprocket drive

Some sample calculations will be made for correlation with the experimental data for 28 minutes of tape length at two points during the record mode. The points to be chosen will be at positions having equal Negator turns in order to reduce the ambiguities due to lack of a specific calibration curve for the Negators in the Feasibility Model.

Using 20 turns of the Negator power drum, Figure 2-3 shows this to occur at the 4 minute point and the 23.6 minute point. At these two points, the supply reel diameters and tape tensions are, respectively, 7.62 inches and 9 ounces (at 4 minutes), and 5.97 inches and 11 ounces (at 23.6 minutes).

On Figure 2-4 are plotted available Negator data. A composite envelope of the torque of 10 Havar Negators is shown. Since, at the time of this writing, there was not similar data for stainless steel Negator, the curve for a single specimen is shown. A reasonable estimate for the torque at 20 turns is 1.75 in.-lb. per coil, or 3.5 in.-lb. (56 in. oz.) total torque at the output drum.

The effect of the bearings in the Negator spools should be evaluated. There is a single pair of R-6 bearings in the output drum and two pairs of R-6 bearings in the Negator storage spools. These bearing pairs are preloaded to 5 lbs., and the nominal friction torque per pair is estimated from vendor data to be 0.084 in.-oz. The drag value of the bearings in the output drum is directly additive. The drag of the bearings in the storage spools is modified by a variable mechanical advantage, depending on the change in the ratio of diameters of the output drum coil to the storage spool coil. For 20 turns, this diameter ratio was calculated to be 1.06 (this ratio varies between approximately 0.85 at COT to approximately 1.85 at SOT/EOT). This bearing drag, effective at the output drum is:

$$0.084 + 2\ (1.06)\ (0.084) = 0.279 \text{ in.-oz.}$$

C

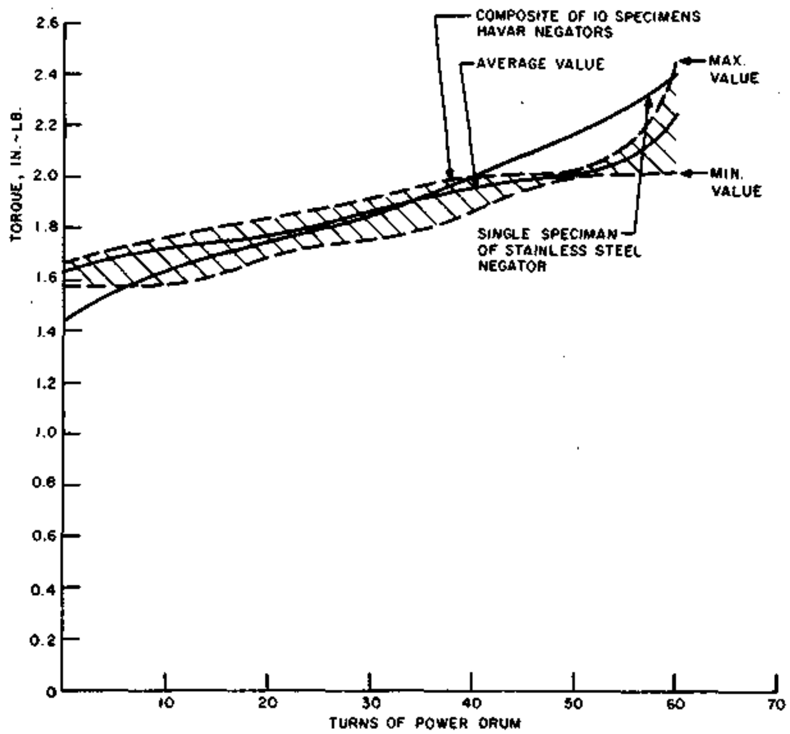

Figure 2-4 ERTS NEGATOR CHARACTERISTICS

For 20 turns of the output drum:

MD = 56 - 0.279 = 55.72 in.-oz. between SOT and COT

MD = 56 + 0.279 = 56.28 in.-oz. between COT and EOT

Regarding the efficiency of gears, this is usually considered to be around 98% for precision gears. A more specific approach will be taken however. A theoretical equation for the efficiency of a single gear mesh is:

$$(9)\quad E = 1 - \pi\mu \left(\frac{1}{N_1} + \frac{1}{N_2}\right) \;*$$

Where,

μ = the coefficient of friction

N_1 = number of teeth in the driver gear

N_2 = number of teeth in the driven gear

*Mechanical Design Analysis, M.F. Spotts, Prentice Hall, Inc. (1964)

or, alternatively, the loss in a single mesh is:

$$(10)\ \nu = \pi \mu \left(\frac{1}{N_1} + \frac{1}{N_2} \right)$$

For a single mesh of bevel gears in the differential:

$$\nu_1 = \pi\mu \ (1/54 + 1/32) = 0.1553\ \mu$$

For the Negator spur gearing:

$$\nu_2 = \pi\mu \ (1/106 + 1/212) = 0.0445\ \mu$$

Since all the gears are made of 416 stainless steel and may be presumed to have about the same value of $\underline{\mu}$, it is seen that the spur gears have less than 1/3 the loss of a single mesh of the differential gears. If we assume a gear coefficient of friction of $\mu = 0.3$:

$$\nu_1 = 0.1553\ (0.3) = 0.0466$$

$$\nu_2 = 0.0445\ (0.3) = 0.01335$$

In the case of the toothed belt and sprocket drive, there is no specific data at the present. It is believed their efficiency is high since they do not have the basic sliding contact which occurs in gearing, and, at all times, the majority of contacting tooth pairs have no relative motion. A nominal loss (ν_3) of 1% will be assumed.

The torque delivered to the supply reel is calculated from Equations (7) and (8).

$$\text{MSR} = [\ 1 + 2(0.0466) - 0.0134 + 0.010\ ]\ \frac{55.72 \text{ in.-oz.}}{2}$$

$$= 30.36 \text{ in.-oz. at 4 minutes}$$

$$\text{MSR} = [\ 1 + 2(0.0466) + 0.0134 + 0.010\ ]\ \frac{56.28 \text{ in.-oz.}}{2}$$

$$= 31.42 \text{ in.-oz. at 23.6 minutes}$$

An allowance should be made for the drag of the reel bearings. These are R-8 bearings preloaded to 10 pounds, and their nominal torque is estimated at 0.1 in.-oz. (for worst case fit and temperature, this becomes 1.12 in.-oz.).

The tape tension leaving the supply reel is:

$$TSR = \frac{(30.36 + 0.01) \text{ in.-oz.}}{3.81 \text{ inches}} \text{ at 4 minutes}$$

$$= 7.96 \text{ oz.}$$

$$TSR = \frac{(31.42 + 0.01) \text{ in.-oz.}}{2.985 \text{ inches}} \text{ at 23.6 minutes}$$

$$= 10.53 \text{ oz.}$$

The bearing drag of the three idler rollers is very low and their effect on tape tension, based on estimated bearing torque, is 0.16 oz. The follower roller has bearings with negligible torque. The effective drag of the urethane roller has not been studied, but, based on experience with it, it is also believed to be low and nominal drag of 0.2 oz. is assigned to it.

The drag of the erase head is calculated by the rope-and-pulley equation of classical mechanics. For a tape wrap angle of 12° and a coefficient of friction of 0.333:

$$\text{Head Tension Ratio} = e^{0.0696} = 1.072$$

The calculated tension approaching the control track head is:

$$T_{CT} = [\,7.96 + (0.16 + 0.2)\,] \text{ oz.} \times 1.072 \text{ at 4 minutes}$$

$$= 8.894 \text{ oz.}$$

$$T_{CT} = [\,10.52 + (0.16 + 0.2)\,] \text{ oz.} \times 1.072 \text{ at 23.6 minutes}$$

$$= 11.68 \text{ oz.}$$

2.2 Mechanical Transmission Components

2.2.1 Differential. - The requirements of the differential are shown schematically in Figure 2-1. This system results in the two reels torqued in opposite directions, giving tape tension at all times.

The actual capabilities of the differential were derived as follows:

The dimensions of the tape load were obtained through an RCA computer program that calculates tape loads by the "Area Method". From various combinations of reel diameters, delta turns between reels and negator torque capabilities, the most optimum were:

Tape O.D.	=	8.000
Tape Thickness	=	0.0018 (tape + trapped air)
Tape Speed	=	12.000
Time, Minutes	=	33
Tape Length, Feet	=	1980
Tape I.D.	=	5.320
Average Dia.	=	6.793
Delta Turns	=	113.10

Assuming an 8 ounce tension at midtape (equal tape on both reels), the required torque at each reel shaft is:

$$T_R = 8.02 \times \frac{6.793 \text{ in.}}{2} = 27.172 \text{ in.-oz. or } 1.696 \text{ in.-lb.}$$

By definition, if end gear B is held stationary, end gear C will rotate twice as fast as spider shaft gear D. Therefore, a 2:1 ratio is inserted between gear D and the take-up reel gear F to maintain proper reel to reel rotation ratio. The torque required at end gear B equals the torque at either reel, T_R.

The Negator package is kept to a minimum by inserting a 1:2 ratio to reduce the number of Negator turns and using two springs to obtain the necessary torque, T_R. Applying a 1.10 factor to the required torque, due to the length of spring, the torque input to the end gear is (1.693) (1.10) = 1.865 in.-lb., or 30 in.-oz. The torque at the end gear is equivalent to 60 in.-oz. at the spider shaft where differentials are rated.

The differential design by Dynamic Gear is nearly the same as used in an Apollo digital recorder and is capable of handling up to 200 in.-oz. for speeds of 20 to 200 rpm. This torque handling capability results in a safety factor of approximately 3:1.

2.2.2 Toothed Belt Drive. - The Power Transmission Capability P of the drive belt is:

$$P = \frac{NRTW}{1.2 \times 10^5}$$

where

P = horsepower

N = drive pulley speed, rpm

R = pulley pitch diameter

T = belt strength per inch of width, pounds

W = belt width, inches

The minimum drive pulley speed, N, occurs at maximum reel diameter at 12 ips and is:

$$N = \frac{12 \text{ in./sec.}}{(\pi)\ (8.00 \text{ in.})} \times 60 \text{ sec./min.} = 28.7 \text{ rpm}$$

$R = 0.910$ for 35 tooth pulley

$J = 400$ pounds for B-1096-4 belt

$W = 1/4$ in.

Therefore,

$$P = \frac{(28.7)\ (0.910)\ (400)\ (1/4)}{1.2 \times 10^5} = 2.185 \times 10^{-2} \text{ horsepower}$$

The actual horsepower transmitted by the belt is:

$$hp = \frac{\left(T_1 - T_2\right)V}{33,000}$$

Where,

T_1 = belt tension on tight side $= 2.3 \times \frac{1.00}{0.455} = 5.05$ lb.

T_2 = belt tension on slack side $= 0$

V = belt velocity $= \frac{(\pi)\ (0.910)}{12}\ 28.7 = 6.84$ ft./min.

Therefore,

$$\text{RUNNING HP} = \frac{(5.05)\ (6.84)}{33 \times 10^{3}} = 1.05 \times 10^{-3}$$

During startup, an increase in tension is applied to the belt:

$$M = \frac{I\omega}{t} = \frac{0.2772}{0.25} = 1.1 \text{ in.-lb.}$$

where,

$I\omega$ = Reel $I\omega$, in.-lb.-sec.

t = startup time, sec.

The tension increase is:

$$\frac{1.000}{0.455} \times 0.9 = 2.44 \text{ lb.}$$

Therefore, the horsepower transmitted during startup is:

$$\text{hp} = \frac{(5.05 + 2.44)\ (6.84)}{33 \times 10^{3}} = \frac{(7.49)\ (6.84)}{33 \times 10^{3}} = 1.55 \times 10^{-3}$$

Hence the maximum transmitted horsepower is less than one-tenth of capability of the toothed belt.

2.2.3 <u>Negator Assembly</u>

2.2.3.1 <u>General Discussion.</u> - The torquing of the two tape reels is effected by two Negator coils on separate, coaxial storage spools which wrap about a common power drum as shown in the schematic of Figure 2-1. The design configuration of each single coil is shown in Figure 2-5.

A Negator coil consists of a long strip of spring material which has been cold-worked so as to leave a natural curvature along the leaf length. With no restraining forces on any section of leaf length, it will have a natural radius. Immediately after the cold working stage, the natural radius is nominally constant along the entire length. Negators are usually given a stress relief treatment after cold working, and this is done with the leaf tightly coiled. The leaf material in the coil is constrained to a slightly larger radius than the natural radius, with a resultant flexure stress, and this stress increases with the radius of the coil. During the stress relief heat treatment,

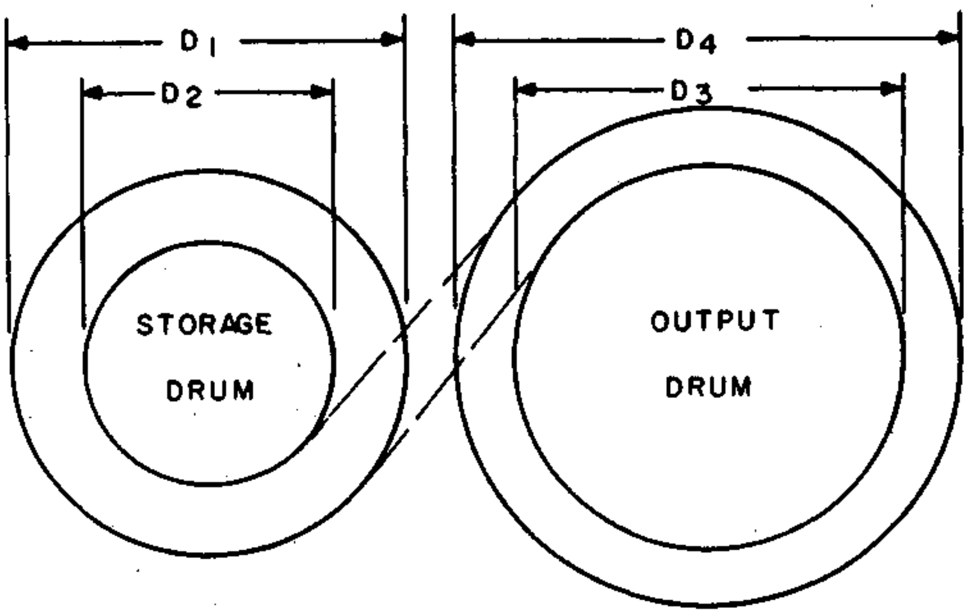

D_2 = 1.44" $D_1 \approx$ 2.485"
D_3 = 2.00" $D_4 \approx$ 2.845" NBR Output Turns = 65
t = 0.006" Spring Length = 510"
b = 1.000"

Torque = 1.73 in. # ± 10% with 4 turns on output Drum
Torque = 2.4 in-# maximum with 61 turns on output Drum

REF ONLY
(Chart "X"-"M" value is 1.9 in-# for 13,000 min. Life for S. S)
Outer R_n = 0.661
Inner R_N = 0.591

1 Mat'l - Type 301 High Yield Stainless Steel
2 Mat'l - Hamilton Precision Metals "HAVAR"

Figure 2-5 ERTS NEGATOR SPRINGS

the degree of stress relaxation which occurs is a function of the original residual stress. As a consequence of all this, the final leaf natural curvature, R_n, varies slightly along the leaf length, increasing with the coil diameter. The expected variation of R_n along the length of our spring is estimated to be 12% (based on empirical data for 1095 spring steel).

In its application, the leaf is coiled about a storage spool with a radius slightly larger than R_n. The outer length is then payed out and reverse-wrapped around a power drum or output drum. The reverse-wrapped leaf material has a much higher flexural stress than that on the storage spool, and, therefore, more elastic energy per inch of leaf length. This, then, is the basis of the torquing mechanism; energy is required to unwind leaf from the storage spool, and reverse flex it around the power drum.

In the ERTS recorder, two alternate Negator coil designs have been explored; one made of high yield 301 stainless steel, and the other made of Havar alloy. In general, the stainless steel coils have surpassed the original life estimate of 22,000 cycles, averaging over 42,000 cycles. The Havar coils, which were expected to reach very high values ($\approx$ 180,000 cycles), have not achieved this goal but still demonstrated an average life comparable to that of the stainless steel.

A group of theoretical equations for Negator stress and torque are assembled in Figure 2-6. Equations (1) through (5) are exact derivations. Equations (6) through (9) are simplified expressions, equivalent to those used in the Negator design manual, which uses the approximation $R_B = R_n$ (i.e., the natural radius of the leaf matches the stack radius on the storage spool at all places, and, therefore, the flexure stress is zero on throughout the stack on the storage spool).

The simplified equations will yield values of amplitude of stress fluctuation which are higher than the actual values. When the analysis of fatigue life is based upon conventional material parameters, plus an endurance diagram (such as the Goodman diagram), the simplified equation will be more pessimistic than the exact equations. On the other hand, when the material data is actual Negator test history plotted against the "stress factor", the approximation inherent in the simplified equations is compensated, more or less. Such a body of data is available for the stainless steel Negators and is shown in Figure 2-7. In the case of Havar, such data is not available and the more basic approach must be used.

2.2.3.2 Fatigue Analysis of Stainless Steel Negators. - Assuming nominal material properties equal to those inherent for the plot of Figure 2-7 (which entails a high degree of quality control), the parameters which are slightly variable are the natural leaf radius, R_n, and the leaf thickness, $\underline{t}$. The leaf width may be considered controlled to a negligible percentage of the nominal value. R_n, and $\underline{t}$ are not specified directly, but they are implicit in the torque which is specified with a 10% tolerance. Referring to equation (7), the torque is seen to be proportional to:

$$t^3\left(\frac{1}{R_n} + \frac{1}{R_A}\right)^2 = t\left[t\left(\frac{1}{R_n} + \frac{1}{R_A}\right)\right]^2 = t\,S_f^{\,2}$$

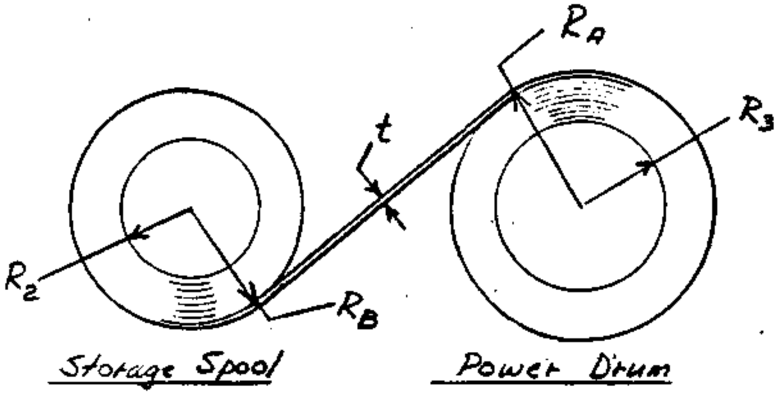

Definitions

M = Torque, In.-Lb.
t = Leaf Thickness, In.
b = Leaf Width, In.
R_A = Stack Radius on Pwr. Drum
R_B = Stack Radius on Storage Spool
E = Elastic Modulus, P.S.I.
ν = Poisson's Ratio (≈ 0.3)
S_A = Max. Flexure Stress at R_A
S_B = Max. Flexure Stress at R_B
S_p = Peak Alternating Stress
S_M = Mean Value of Stress
S_f = "Stress Factor"

(1) $$S_A = \frac{tE}{2\,(1-\nu^2)}\left(\frac{1}{R_n} + \frac{1}{R_A}\right)$$

(2) $$S_B = \frac{tE}{2\,(1-\nu^2)}\left(\frac{1}{R_n} - \frac{1}{R_B}\right)$$

(3) $$M = \frac{E}{24\,(1-\nu^2)}\,bt^3\left[\frac{2}{R_n} + \frac{1}{R_A} - \frac{1}{R_B}\right]\left(1 + \frac{R_A}{R_B}\right)$$

(4) $$S_p = \frac{1}{2}\,(S_A - S_B) = \frac{6M}{bt^2}\left(\frac{1}{1 + 2\,R_A/R_n - R_A/R_B}\right) = \frac{Et}{4\,(1-\nu^2)}\left(\frac{1}{R_A} + \frac{1}{R_B}\right)$$

(5) $$S_M = \frac{1}{2}\,(S_A + S_B) = \frac{6M}{bt^2}\left(\frac{1}{1 + R_A/R_B}\right)$$

Equations (1) -(5) are exact. If the simplifying approximation ($R_B = R_n$) is used, and also the Hunter Spring Co. "Stress Factor", $S_f = t\,(1/R_n + 1/R_A)$, the equations become

(6) $$S_A = \frac{tE}{2\,(1-\nu^2)}\left(\frac{1}{R_n} + \frac{1}{R_A}\right) = \frac{E}{2\,(1-\nu^2)}\,S_f$$

(7) $$M = \frac{Ebt^3R_A}{24\,(1-\nu^2)}\left(\frac{1}{R_n} + \frac{1}{R_A}\right)^2 = \frac{EbtR_A}{24\,(1-\nu^2)}\,S_f^2$$

(8) $$M = \frac{1}{12}\,bt\,R_A S_f S_A$$

(9) $$S_p = \frac{6M}{btR_A}\quad\frac{1}{S_f}$$

(10) $$S_B = 0$$

(11) $$S_M = S_p$$

Figure 2-6 NEGATOR EQUATIONS

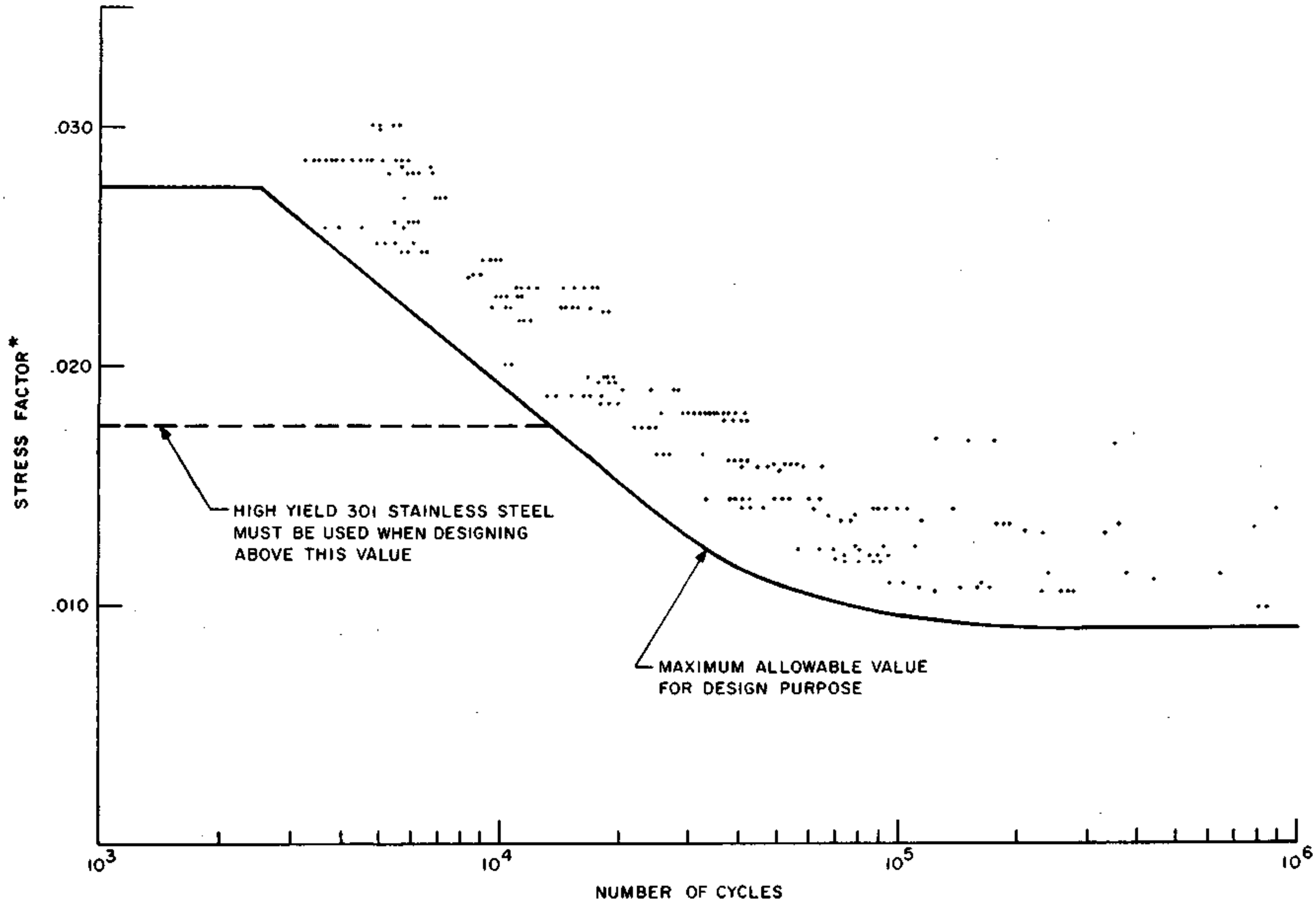
.030
.020
.010
STRESS FACTOR*
HIGH YIELD 301 STAINLESS STEEL
MUST BE USED WHEN DESIGNING
ABOVE THIS VALUE
MAXIMUM ALLOWABLE VALUE
FOR DESIGN PURPOSE
10^3
10^4
10^5
10^6
NUMBER OF CYCLES

Figure 2-7

We might reasonably approximate the 10% torque variation as being due to 10% change in Sf^2 only, and estimate worst case life. The maximum stress will occur at the start of wind of the power drum when the reverse flexural stress is maximum. Since the power drum will have approximately four inactive coils on it, the minimum radius of repeated reverse bending is:

$$R_A = \frac{2.00}{2} + 4(0.006) = 1.024''$$

also,

$$R_B = \sqrt{\left(\frac{2.485}{2}\right)^2 - \frac{\pi\,(2.024)\,(0.006)}{\pi/4}} = 1.222''$$

Equation (3) is used to estimate the nominal value of R_n for the nominal torque of 1.73 in.-oz.

$$1.73 = \frac{28 \times 10^6}{24(1-0.09)} \ (1) \ (6 \times 10^{-3})^3 \left[\frac{2}{R_n} + \frac{1}{1.024} - \frac{1}{1.222}\right]\left(1 + \frac{1.024}{1.222}\right)$$

Solving for R_n:

R_n = 0.617", nominal value

and,

$$S_f = 0.006\left(\frac{1}{0.617} + \frac{1}{1.024}\right) = 0.01557, \text{ nominal value}$$

Referring to Figure 2-7, the nominal design life is seen to be 19,000 cycles. If the torque is high by 10%, then:

$$\text{Maximum } S_f = 0.01557 \ \sqrt{1.10} = 0.0163$$

and the worst case design life is 16,300 cycles.

Some further consideration should be given to the curve of Figure 2-7, upon which the foregoing fatigue estimates were based. Examining the locations of the large number of data points, it is obvious that the curve is quite conservative. An estimate based on the data points near our stress level (S_f between 0.015 and 0.017) indicates that the curve appears to be of the order of minus three times the standard deviation below the mean life of any group tested. This consideration should only be applied to the nominal life of 19,000 cycles. The worst case life due to a smaller R_n is one of the factors tending to cause specimens in any test group to fall below the mean value.

Correlation with our own test experience with 4 stainless steel Negators shows the mean life of 42,700 cycles to be 225% greater than the nominal design life. Fatigue tests at Hunter Spring of a group of Negators with a nominal life of 2,500 cycles yielded values ranging between 6,000 and 9,000 cycles, and a comparable margin over the design life.

2.2.3.3 Fatigue Analysis of Havar Negators. - The Havar springs were made to the same torque and dimensional specifications as those for the 301 high yield stainless steel. The difference in material properties are mainly: the Havar modulus of elasticity is 30×10^6 psi compared to a nominal 28×10^6 psi for stainless steel, and the predicted fatigue life for Havar is higher. This last consideration was not borne out in an initial test of Havar springs; and this will be discussed further on.

To obtain the nominal value of R_n at start of windup (after 4 "dead" turns in the power drum), we again use equation (3).

$$1.73 = \frac{30 \times 10^6}{24\ (1-0.09)}\ (1)\ (6 \times 10^{-3})\left[\frac{2}{R_n} + \frac{1}{1.024} - \frac{1}{1.222}\right]\left(1 + \frac{1.024}{1.222}\right)$$

and R_n = 0.664", nominal value.

Since there is no body of empirical test data for Havar Negators, the fatigue life will be estimated from the peak alternating stress, S_p, and the average fluctuating stress, S_M.

From equation (4):

$$S_p = \frac{6\ (1.73)}{(1)\ (6 \times 10^{-3})^2}\left(\frac{1}{1 + \frac{2 \times 1.024}{0.664} - \frac{1.024}{1.222}}\right)$$

and,

$$S_p = 88{,}820 \text{ psi, nominal value.}$$

From equation (5):

$$S_M = \frac{6\ (1.73)}{(1)\ (6 \times 10^{-3})^2}\left(\frac{1}{1 + \frac{1.024}{1.222}}\right)$$

$$S_M = 156{,}850 \text{ psi, nominal value.}$$

When these values are plotted on a Goodman diagram (Figure 2-8), an equivalent reversed flexure stress is found to be 156,000 psi. The fatigue of Havar in reversed flexure is shown in Figure 2-9. The indicated life for this reversed stress value is seen to be 180,000 cycles (nominal design).

The +10% increase in torque can be caused by either or both an increase in t or a decrease in R_n. In equation (4), the extreme right hand optional form shows Sp to be proportional to t and independent of M and R_n. Equation (5) shows S_M to be proportional to M and to vary inversely with t^2.

It is understood that the tolerance on 0.006" Havar is ±0.1 mil, or ±1.67%. For the case of +10% increase in torque, accompanied by +0.1 mil in thickness, Sp would increase +1.67% and S_M would increase ±6.7%. If the 10% torque increase were due to a smaller R_n only, and t were at the nominal value, Sp would not increase, and S_M would, again, increase 6.7%. Thus, the first case is slightly worse and the new stresses are:

Sp = 90,300 psi, worst case

S_M = 167,350 psi, worst case

These values are also plotted in Figure 2-8, and the equivalent reversed flexure stress (worst case) is 172,000 psi. Referring to Figure 2-8 again shows the worst case fatigue life to be 120,000 cycles.

The test of 4 Havar Negators produced a mean life 42,000 cycles. One specimen failed at 34,000 cycles, and the other 3 had multiple, severe edge cracks after 45,000 cycles when the test was stopped.

Because these results were considerably lower than expected, some attention has been given to possible causes. The Havar sheet is cold rolled to a high degree of cold working and its hardness is believed to be approximately Rockwell C-58. This is the state at which the sheet is slit into 1" wide strips. Since cutting at this hardness may leave edges with damaged surfaces or unfavorable residual stress, five Havar samples were given a physical examination. The samples examined were 1" long pieces, cut from new, untested Negator coils. Three of these five 1" samples showed surface imperfections in the form of pitting of the edge corners. Considering that each coil is 500 inches long, the probability seems high that each coil had a substantial number of these surface imperfections.

It is planned to further evaluate Havar Negators after suitable rework. Four of the remaining untested coils will be given a light grind on each coil face (i.e., edges of the 1" strips) in order to remove damaged material and surfaces. The sharp corners will be broken. These springs will then be put through another life test. There has been some discussion about the merits of peening the edge surfaces, however, it is questionable whether this approach can be evaluated at this stage.

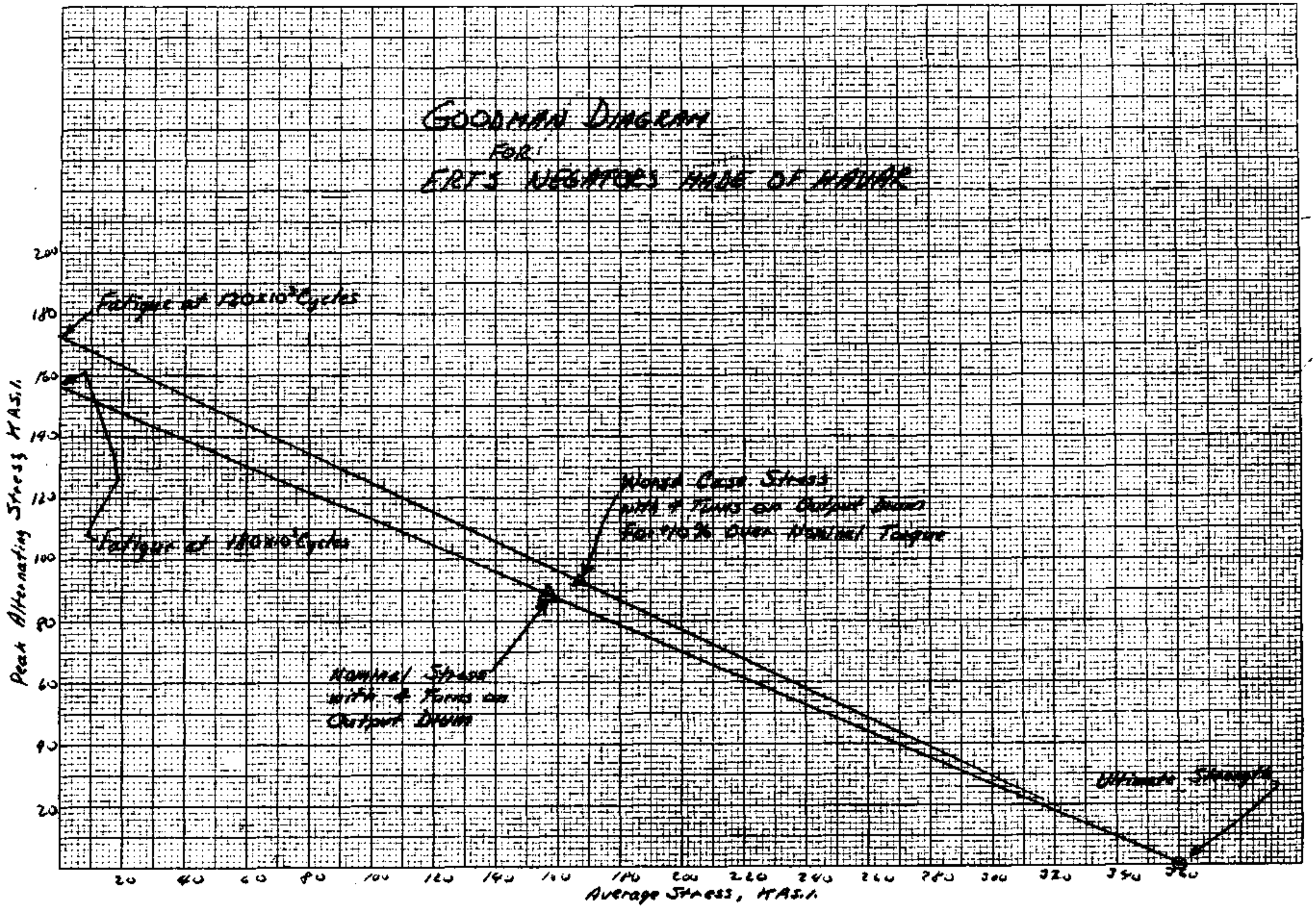

Figure 2-8 GOODMAN DIAGRAM FOR ERTS NEGATORS MADE OF HAVAR

D

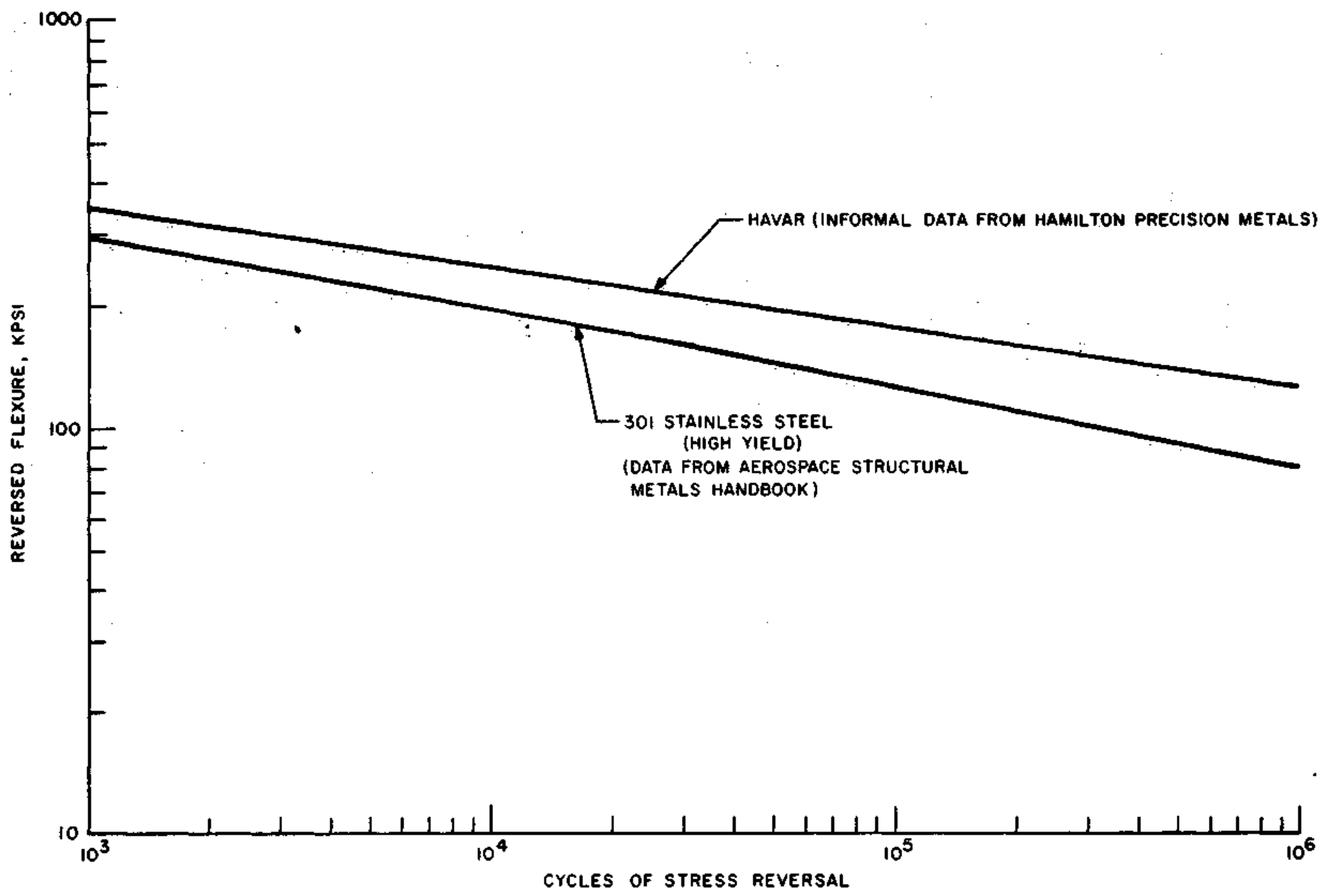

Figure 2-9 FATIGUE CURVES FOR NEGATOR MATERIALS

2.2.4 Mylar Belt Drives. - Two Mylar belts are used, one coupling the capstan shaft to the capstan motor, and the second coupling the $I\omega$ compensation fly-wheel to the capstan shaft. The geometry of the two belts is shown in Figure 2-10.

The belts have been designed to transmit more than the maximum motor torque without slippage, and to have a large margin over fatigue failure throughout the life of the mission. The nominal mission requirement is established on the basis of 4,000 Record-Playback cycles. One Record-Playback cycle involves passing 2,000 feet of tape four times around a 1/2 diameter capstan.

$$\text{No. of Capstan Revolutions} = 2{,}000 \text{ ft.} \times \frac{12 \text{ in.}}{\text{ft.}} \times \frac{1}{0.5\,\pi \text{ in.}} \times (4)\ (4{,}000)$$

$$= 2.45 \times 10^{8}$$

$$\text{Required No. of Capstan Belt Cycles} = 2.45 \times 10^{8} \times \frac{1.790\,\pi \text{ in.}}{8.19 \text{ in.}} = 1.68 \times 10^{8}$$

$$\text{Required No. of } I\omega \text{ Belt Cycles} = 2.45 \times 10^{8} \times \frac{1.790\,\pi \text{ in.}}{17.30 \text{ in.}} = 0.80 \times 10^{8}$$

The initial tension in the belts is adjusted by measuring the slippage torque rather than by measuring the tension directly. Theoretical belt slippage calculations are based on the equations:

$$\frac{T_1}{T_2} = e^{\mu\theta}$$

and,

$$T_o = \frac{M}{D}\ \frac{e^{\mu\theta} + 1}{e^{\mu\theta} - 1}$$

where:

T_1/T_2 = Belt tension ratio at slippage

M = Pulley torque at slippage

T_o = Initial belt tension to develop a torque, M

D = Pully diameter

μ = Coefficient of friction

θ = Angle of belt wrap

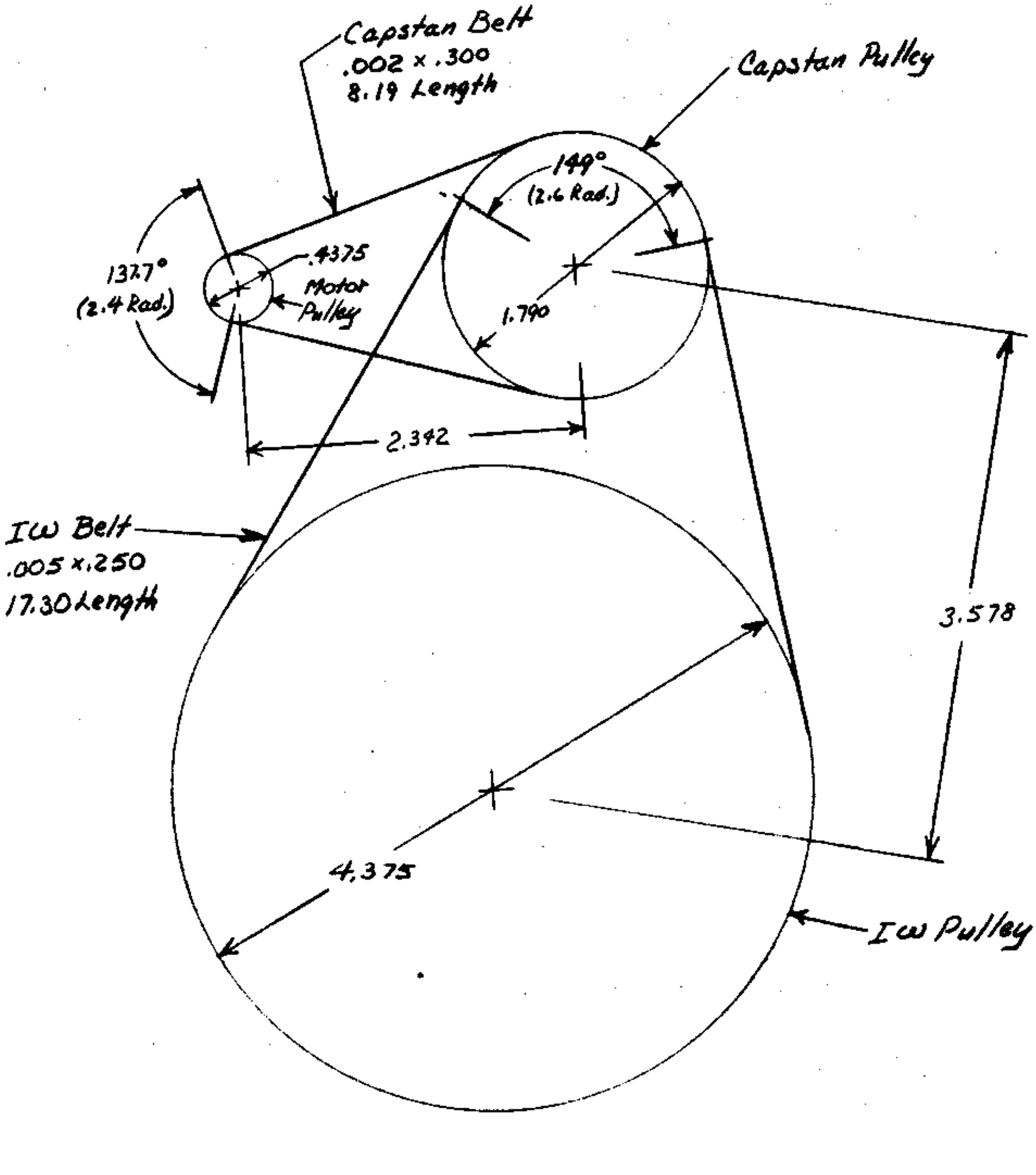

Figure 2-10 MYLAR BELT GEOMETRY

These equations are, of course, exact if one transfers the responsibility for any inaccuracies to the establishment of a suitable value for μ. For a condition of gross belt slippage, a value of $\mu \approx 0.2$ has been measured on numerous occasions. For steady state operation with minimum open loop deviations in pulley speed, it is highly desirable to stay within the linear "creep" region. This has been defined, in a study of Mylar belts by the Kinelogic Corporation*, as the point where the slope of the creep-differential stress curve increases 100% over that of the linear portion. For stainless steel pulleys, this definition, applied to the test data, yields an empirical value of $\mu = 0.075$.

The belt design is based upon a nominal slippage torque of 5 inch-ounces reflected at the motor shaft. The stall torque of the capstan motor is 4.25 in.-oz. on the "start" winding, and 2.25 in.-oz. on the "run" winding (which is the present mode of acceleration). During acceleration, however, all of this torque is not transmitted through the belt since some must be used to accelerate the inertia of the motor itself. At steady-state, the belt torque is considerably less, the worst case calculated value being 0.71 in.-oz.

2.2.4.1 <u>Analysis of Capstan Belt.</u> - The tension ratio at slippage is:

$$e^{\mu\theta} = e^{(.2)(2.4)} = 1.615$$

The nominal initial tension is:

$$T_o = \frac{5 \text{ in.-oz.}}{0.4375 \text{ in.}} \times \frac{1.615 + 1}{1.615 - 1} = 48.7 \text{ oz.}$$

The exponential value for linear "creep" is:

$$e\ (0.075)\ (2.4) = 1.197$$

and, the maximum torque in the linear "creep" region is:

$$M = T_o D \frac{e^{\mu\theta} - 1}{e^{\mu\theta} + 1} = (48.7 \text{ oz.})\ (0.4375 \text{ in.}) \frac{1.197 - 1}{1.197 + 1} = 1.92 \text{ in.-oz.} \quad \text{(at the motor)}$$

For an average running torque of, say 0.5 in.-oz., the differential belt tension is:

$$\Delta T = \pm \frac{0.5 \text{ in.-oz.}}{0.4375 \text{ in.}} = 1.14 \text{ oz.}$$

*"Tape Recorder Belt Study", prepared for Jet Propulsion Laboratory, Accession No. N66-23678.

$$\text{Maximum direct stress} = \frac{(48.7 + 1.14)\ \text{oz.}}{(0.002 \times 0.300)\ \text{in.}^2} \times \frac{1\ \text{lb.}}{16\ \text{oz.}} = 5{,}190\ \text{psi}$$

$$\text{Minimum direct stress} = \frac{(48.7 - 1.14)\ \text{oz.}}{(0.002 \times 0.300)\ \text{in.}^2} \times \frac{1\ \text{lb.}}{16\ \text{oz.}} = 4{,}950\ \text{psi}$$

$$\text{Maximum flexure stress} = E\,\frac{t}{D} = 0.75 \times 10^6 \times \frac{0.002}{0.4375} = 3{,}440\ \text{psi}$$

$$\text{Maximum tensile stress} = 5{,}190 + 3{,}440 = 8{,}630$$

$$\text{Peak Alternating stress} = \frac{8{,}630 - 4{,}950}{2} = 1{,}840\ \text{psi}$$

$$\text{Mean Fluctuating stress} = \frac{8{,}630 + 4{,}950}{2} = 6{,}790\ \text{psi}$$

A Goodman diagram for predicting belt life has been constructed in Figure 2-11. An "Indefinite Life" line has been drawn between the yield strength value of 18,000 psi on the horizontal axis and a data point from the original Licht-White study of Mylar belts. This data point locates the nominal stresses for which their logarithmic plot of stress versus life becomes virtually asymptotic. The "Indefinite Life" plot has been confirmed by numerous tests which have gone through many millions of cycles without failure in the programs for Nimbus, OGO and HDRSS recorders.

The stress values for the capstan belt are plotted as a point on Figure 2-11, and it is 81% of an equivalent "Indefinite Life" value.

2.2.4.2 Analysis of the $I\omega$ Belt. - The tension ratio at slippage is:

$$e^{\mu\theta} = e^{(.2)(2.6)} = 1.682$$

The nominal initial tension is:

$$T_o = \frac{5\ \text{in.-oz.}}{0.4375\ \text{in.}} \times \frac{1.682 + 1}{1.682 - 1} = 45\ \text{oz.}$$

The exponential value for linear "creep" is:

$$e^{(0.075)(2.6)} = 1.218$$

and, the maximum torque in the linear "creep" region is:

$$M = (45\ \text{oz.})\ (0.4375\ \text{in.})\ \frac{1.218 - 1}{1.218 + 1} = 1.94\ \text{in.-oz.}\ \text{(at the motor)}$$

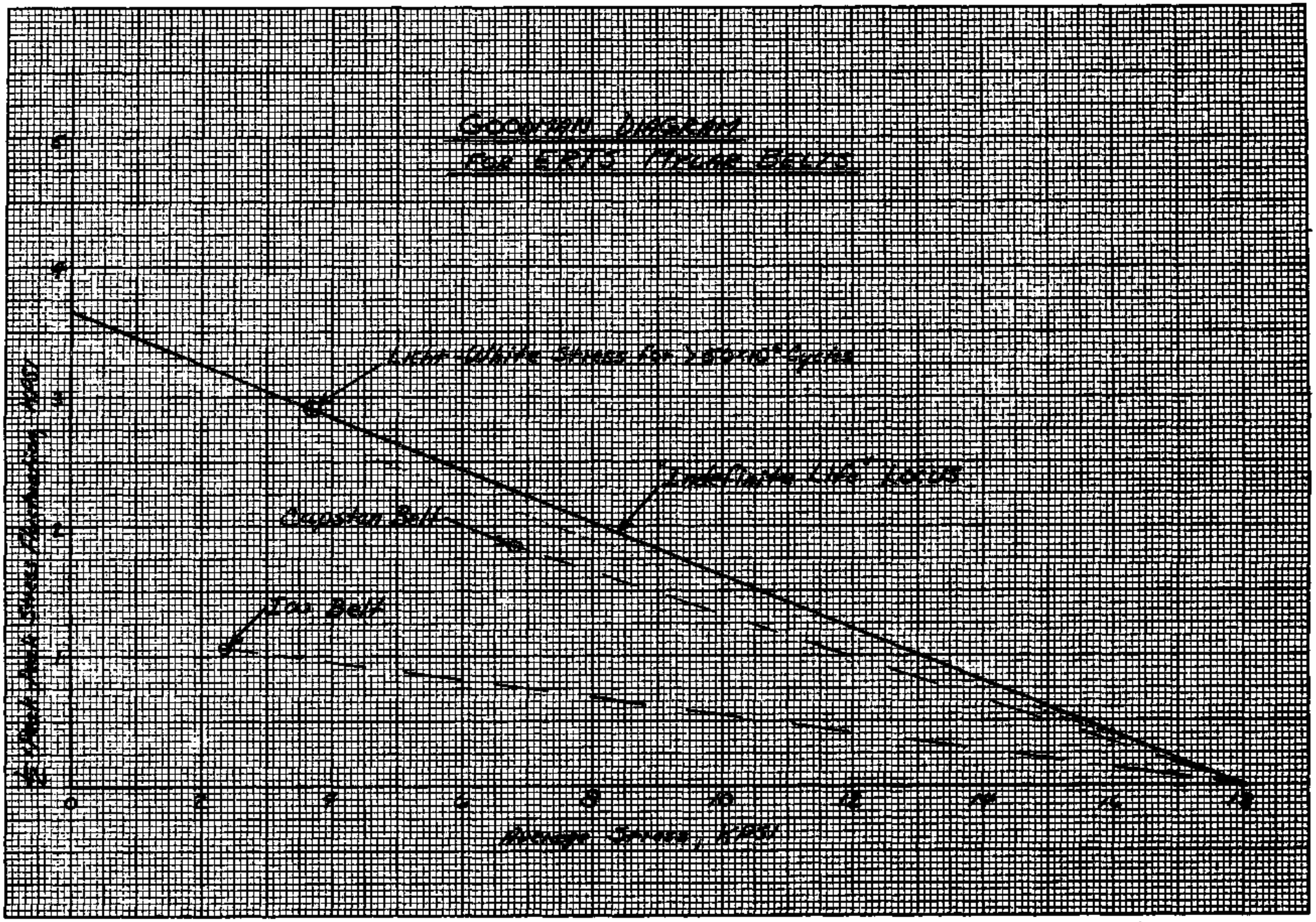

Figure 2-11 GOODMAN DIAGRAM FOR ERTS MYLAR BELTS

The belt stresses due to acceleration torque occur for a relatively small fraction of the total belt flexure cycles. For the fatigue estimate, only the steady running stress should be considered. In the case of the $I\omega$ belt, the steady-state torque is that due to the bearing friction of the $I\omega$ compensation flywheel. This has been "worst-cased" for 0°C as 0.314 in.-oz. at the flywheel. Reflected at the motor shaft, this is 0.0314 in.-oz.

$$\Delta T = \pm \frac{0.0314 \text{ in.-oz.}}{0.4375 \text{ in.}} = \pm 0.0718 \text{ oz.}$$

The stress due to ΔT is:

$$\frac{0.0718 \text{ oz.}}{(0.005 \times 0.250) \text{ in.}^2} \times \frac{1 \text{ lb.}}{16 \text{ oz.}} = \pm 3.6 \text{ psi, which may be neglected.}$$

$$\text{Direct tensile stress} = \frac{45. \text{ oz.}}{(0.005 \times 0.25) \text{ in.}^2} \times \frac{1 \text{ lb.}}{16 \text{ oz.}} = 2{,}250 \text{ psi}$$

$$\text{Maximum flexure stress} = 0.75 \times 10^6 \times \frac{0.005 \text{ in.}}{1.790 \text{ in.}} = 2{,}100 \text{ psi}$$

$$\text{Peak alternating stress} = \frac{2{,}100}{2} = 1{,}050 \text{ psi}$$

$$\text{Mean fluctuation stress} = \frac{2{,}250 + 2{,}100}{2} = 2{,}175 \text{ psi}$$

These stress values have also been plotted as a point on Figure 2-11, and the point is 33% of an equivalent "Indefinite Life" value.

At the time of the writing, a life test of two capstan belts and three $I\omega$ belts has completed 5,586 hours without failure at a capstan speed of 60 rps (7.85 x "record" speed). Since 1,135 hours of test time represents 16,000 full tape passes, the currently logged time is very close to 5 times the nominal mission requirement. In terms of belt flexural stress cycles, the capstan belts have completed 8.23×10^8 cycles and the $I\omega$ belts have completed 3.9×10^8 cycles, both without failure. At irregular intervals throughout the test, the slippage torque was measured. In all cases, this has increased, the increase varying from +10% to +230%. This increase is attributable to some combination of increased residual tension and increased coefficient of friction. Determination of the exact combination seems somewhat moot since the extended life has been demonstrated while the original torque capacity has been maintained or surpassed.

2.2.5 Capstan-Tape Interface. - Experiments were carried out to study the frictional grip between the urethane covered capstan and the surface of the tape base which contacts the capstan. In general, this appeared to be a highly variable factor, even when restricted to two single specimens of urethane covered capstan and magnetic tape. The tape tension ratio at incipient slippage increased with higher ambient humidity, and also increased with the state of cleanliness (becoming highest immediately after being cleaned with chlorothane). The results were also dependent upon the testing technique.

Two types of tests were run, each using the same new ERTS capstan, with a urethane hardness of 90 durometer reading, and a sample of 2" wide 3M400 tape ("velvet" backing). Each test was made with a tape wrap angle of 180°, and a constant load of 10 gm on one end of the tape. The two techniques were as follows:

Method 1 - With 10 gms on one end of the tape, the other end was loaded with progressively increasing weights. The tape was held to the capstan by hand during each change of weight, and thereafter released, followed by observation of whether or not slippage occurred. This was repeated for several sections of tape.

Method 2 - With 10 gms on one end of the tape, the weight on the other end was progressively increased. After each new weight was added, the tape was slipped over the capstan to a new section of tape, and then released and observed for the presence of continued slippage. This technique was intended to more closely approximate the tension distribution around the capstan which exists during the natural "creepage" progression around the capstan.

The highest tension ratio values ranged between 80 and 100, for Method #1, at high ambient humidity (humidity was not measured). The lowest tension ratios were obtained by Method #2 at a lower ambient humidity: these ranged between 18 and 22 for a clean (but not washed with chlorothane) ERTS capstan, and between 15 and 17 for a "dirty" older capstan which had been used intermittently and left exposed to ambient contamination for several years. These last ratios are the values used in the design study for a more conservative position.

Figure 2-12 is a semi-logarithmic plot of the theoretical function $T_1/T_2 = e^{\mu\theta}$. The dotted line represents the function for $\theta = 180°$, the value used in bench tests of tape slippage. The minimum bench test ratios of 15-17 are indicated on the dotted line. The solid line represents the function for $\theta = 190°$, the ERTS capstan wrap angle. The bench test values have been extrapolated by vertical projection onto the solid line. This extrapolation predicts a minimum tension ratio of 17.6 at incipient slippage. In Section 2.4, the tape tensions have been calculated for transport acceleration near end-of-tape operating at 0°C. The calculated tension ratio is 4.42, and this is also indicated on the solid line. The factor of safety, then, is 4.

2.3 Review of Motor Characteristics

2.3.1 Headwheel Motor. - The headwheel motor is a two-pole, two-phase, 312.5 Hz hysteresis synchronous motor. The detailed specifications, mechanical description and electrical schematic are shown in Figure 2-13 (RCA drawing 8778736).

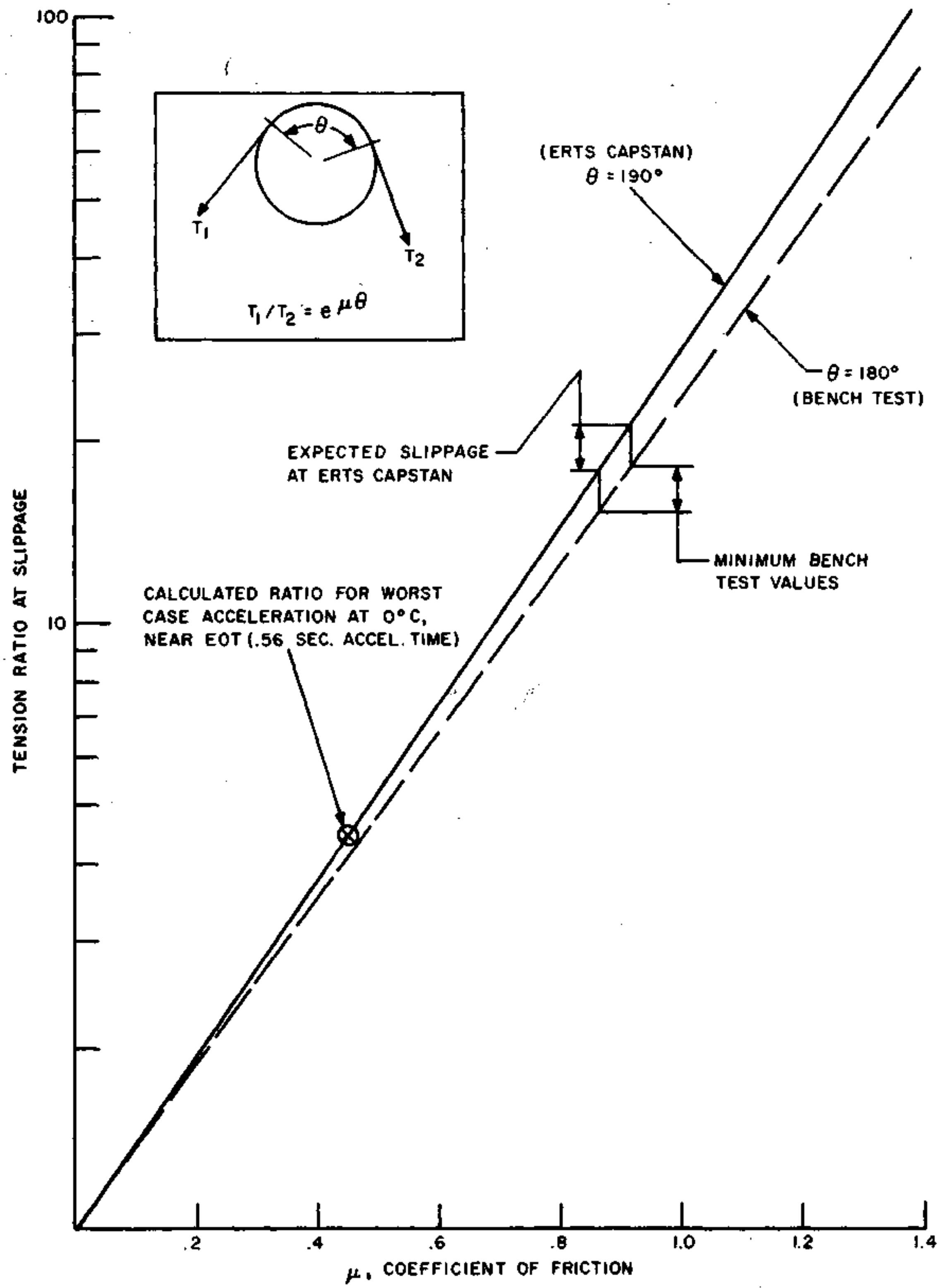

Figure 2-12 ERTS CAPSTAN-TAPE INTERFACE

During startup, the motor is accelerated while being driven through low-impedance, high power taps in the windings. At synchronous speed, the drive voltage is switched to high impedance, low power taps. The original performance data was obtained from a breadboard motor which was electrically identical to that in the head-wheel panel, but was assembled in a conventional motor configuration. As such, this motor had relatively low windage and bearing losses, and this data indicates the basic capability of the motor design, with minimal mechanical losses.

Figure 2-14 shows the characteristics of the breadboard motor operating at synchronous speed on the "run" winding, after acceleration on the "start" winding. The dc current, rotor phase angle, output power and efficiency are plotted against the applied torque load. Figure 2-15 shows the subsynchronous characteristics of the motor during acceleration on the "start" winding.

In the headwheel panel, the identical rotor is mounted on a shaft which rotates in two matched R-6 bearings at the headwheel end of shaft and two matched R-4 bearings at the opposite end. Both bearing pairs are preloaded to a nominal 2 pounds. The useful torque of the motor in this assembly will be reduced from that of the breadboard motor by the small incremental friction of the bearings and the increased windage, predominantly due to the 2" diameter headwheel.

Before assembly into the headwheel panel, each motor stator is tested in a fixture with a standard rotor shaft and bearings. No headwheel is mounted at this time, and the windage losses are still low. The setup of the fixture is such that the two R-4 bearings are preloaded, but the two R-6 bearings are not, and the bearing drag is comparable to that of the breadboard motor.

Tests of 5 stators in this fixture showed very close correlation with the bread-board torque-current curve. The synchronous pull-out torques were grouped closely about those of the breadboard. The measured stall torques were grouped reasonably closely together, and all were slightly higher than that of the breadboard. This last effect was probably due to the superior motor circuit used at this later date. The test fixture data is shown below:

Stator Serial No.	Pull-Out Torque, In-Oz	Stall Torque, In-Oz
S/N 101 (used in Feas. Model Panel)	1.25	7
S/N 102	1.25	6.9
S/N 103	1.1	6.75
S/N 104	1.225	6.5
S/N 105	1.3	6.75

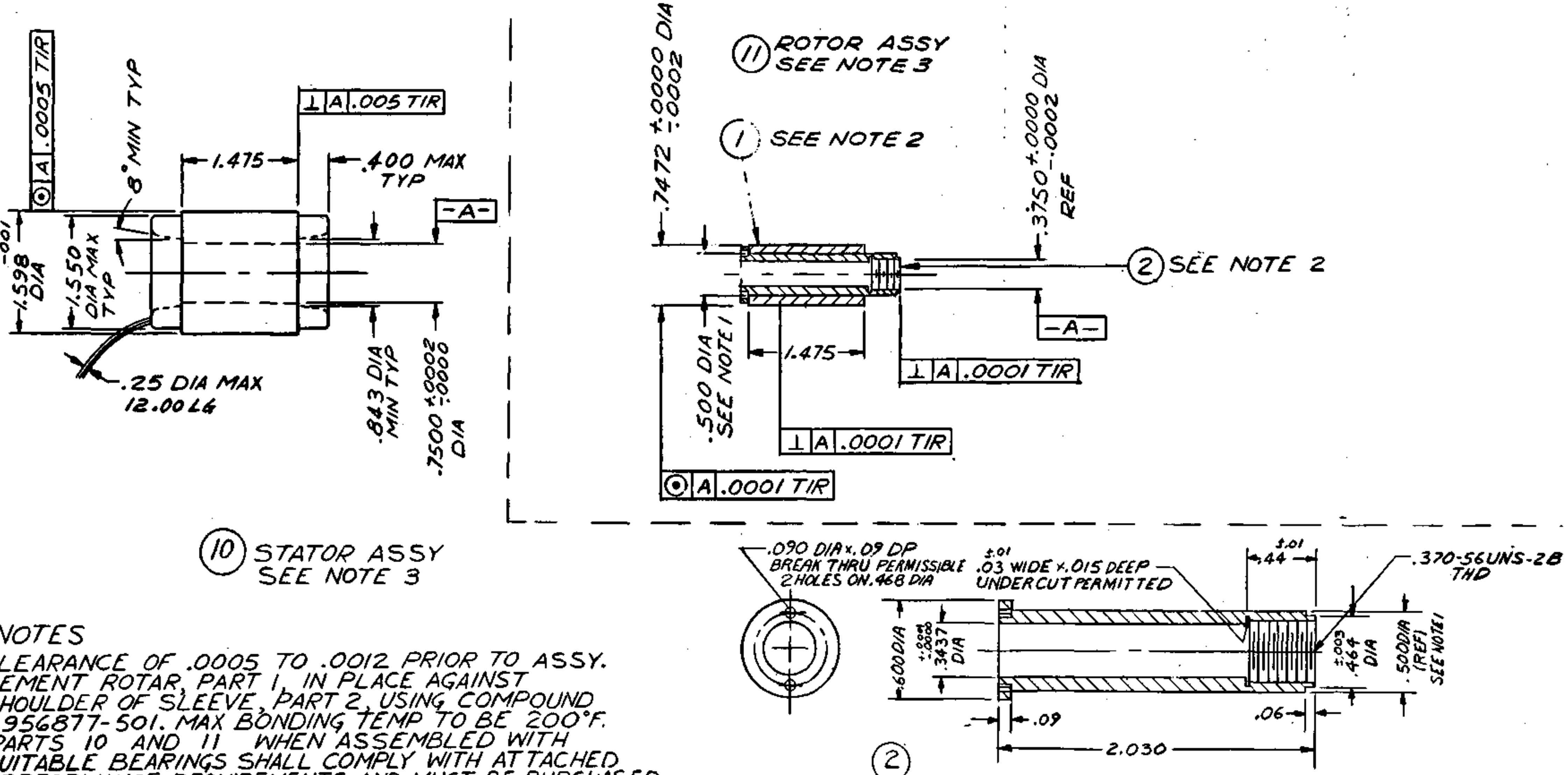

NOTES

1. CLEARANCE OF .0005 TO .0012 PRIOR TO ASSY.
2. CEMENT ROTAR, PART 1, IN PLACE AGAINST SHOULDER OF SLEEVE, PART 2, USING COMPOUND 8956877-501. MAX BONDING TEMP TO BE 200°F.
3. PARTS 10 AND 11 WHEN ASSEMBLED WITH SUITABLE BEARINGS SHALL COMPLY WITH ATTACHED PERFORMANCE REQUIREMENTS AND MUST BE PURCHASED IN SETS TO BE ASSEMBLED TOGETHER.

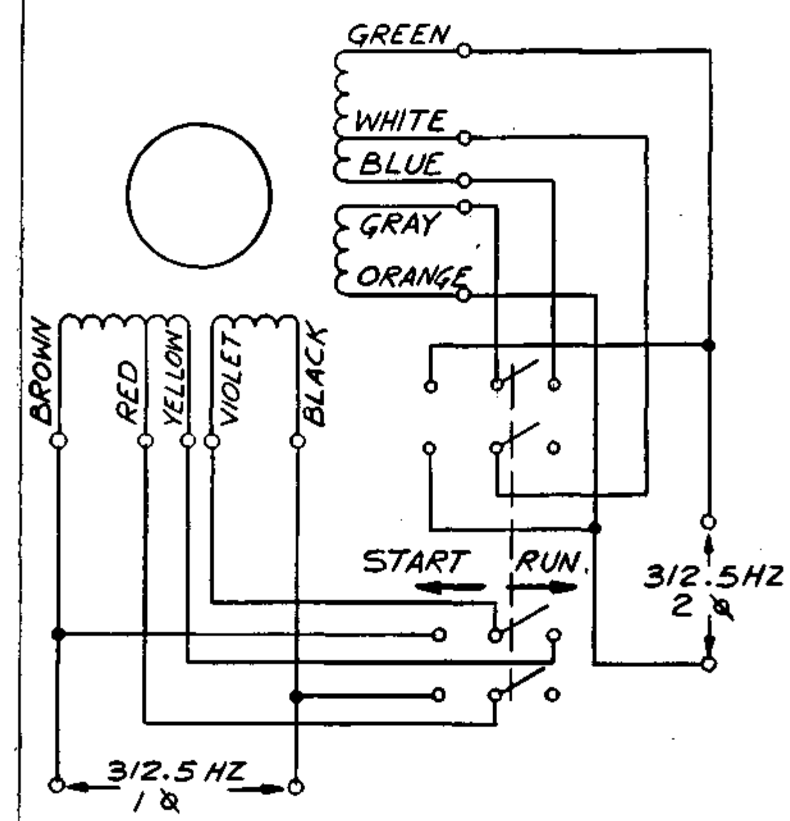

Figure 2-13 MOTOR HEAD WHEEL

FOLDOUT FRAME -1

FOLDOUT FRAME -2

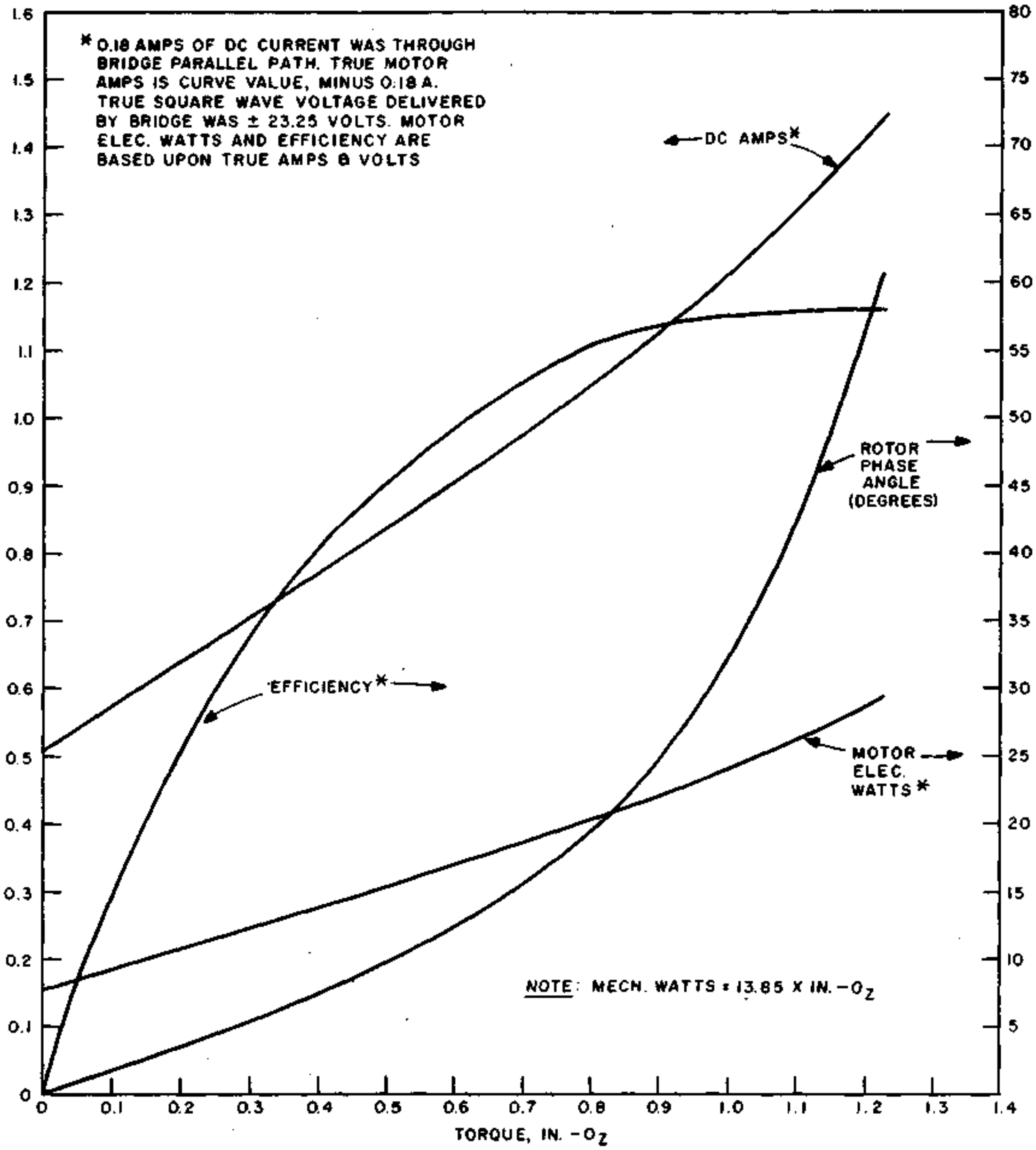

Figure 2-14 BENCH TEST DATA ERTS HEADWHEEL MOTOR (SER. NO. 69-2-1)

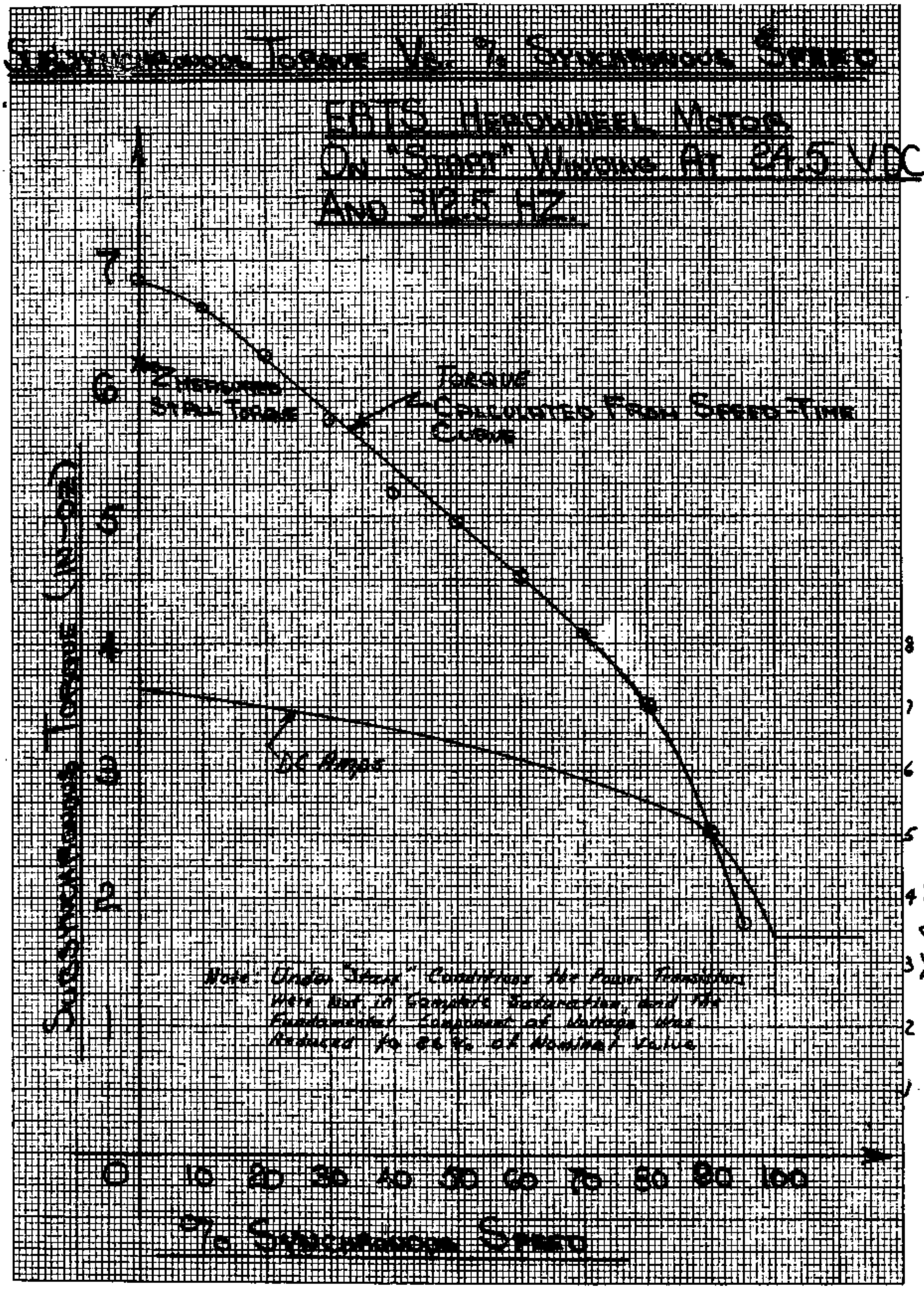

Figure 2-15 SUBSYNCHRONOUS TORQUE VS. % SYNCHRONOUS SPEED

The Feasibility Unit headwheel panel was assembled, using stator S/N 101. The quantitative data taken at this point was not as extensive, as in the case of the breadboard motor. The dc current and torque were tested at no-load and pull-out, and, also at several intermediate points, at ambient temperature. This was repeated at no-load and pull-out for two extreme temperatures of +50°C and 0°C. This data is shown in Figure 2-16, plotted against dc current in the X-axis. For reference, the breadboard motor data is replotted here with its current values reduced by a constant 0.18 amps which was peculiar to the early drive circuit. The test fixture values for stator S/N 101 are shown to fall close to the breadboard motor curve. Any further changes in motor current may be assumed to indicate a torque increment.

When assembled into the headwheel panel, the increased no-load ambient current reflects the higher windage and bearing losses. Extrapolation from the breadboard curve indicates this torque increment to be 0.26 in.-oz. There is a comparable reduction in pull-out torque value amounting to 0.31 in.-oz. The performance of the assembled motor at +50°C appeared to be unchanged. Operation at 0°C introduces a further torque load. In this case, the motor was given a cold soak with no rotation or electrical inputs to the winding. Immediately after acceleration on the "start" winding, the no-load and pull-out values were obtained. The no-load current indicates a further bearing load of 0.35 in.-oz., and the pull-out torque was reduced to 0.7 in.-oz., a further reduction of 0.2 in.-oz. The acceleration characteristics of the headwheel panel at ambient temperature are shown in Figure 2-17. The acceleration time here is seen to be 2.7 seconds on the "start" winding. Estimates of acceleration time during the temperature tests indicated that acceleration at 0°C took 0.3 to 0.4 seconds longer than at 50°C.

2.3.2 Capstan Motor. - The capstan motor is a four-pole, two-phase hysteresis synchronous motor. It is a two-speed motor with independent windings for each speed. When driven by 62.5 Hz through its low speed winding, the synchronous speed is 32.5 rps. When driven by 250 Hz through its high speed winding, the synchronous speed is 125 rps. It also has a dc braking winding for rapid deceleration using dc current. The brake winding is wound in a two-pole configuration so as to eliminate transformer coupling with the ac-drive windings, and avoid high induced voltage when the motor is powered. The detailed specifications, mechanical description and electrical schematics are shown in Figure 2-18 (RCA drawing 8778735).

The torque-amps characteristics of the capstan motor at the two synchronous speeds are shown in Figure 2-19. "Start" and "run" taps have been provided in both the 62.5 Hz windings and the 250 Hz windings. At both synchronous speeds, there is obviously an increase in pull-out torque and operating efficiency if the motor is first pulled into synchronism on the "start" winding and then switched to the "run" winding. At 62.5 Hz, however, the torque is higher for either starting mode.

The accelerating capability of the motor in each of the four modes was measured in two ways. The stall torque was measured with a torque watch. Also, a mean acceleration time of a known total shaft inertia. The subsynchronous torque, for a given

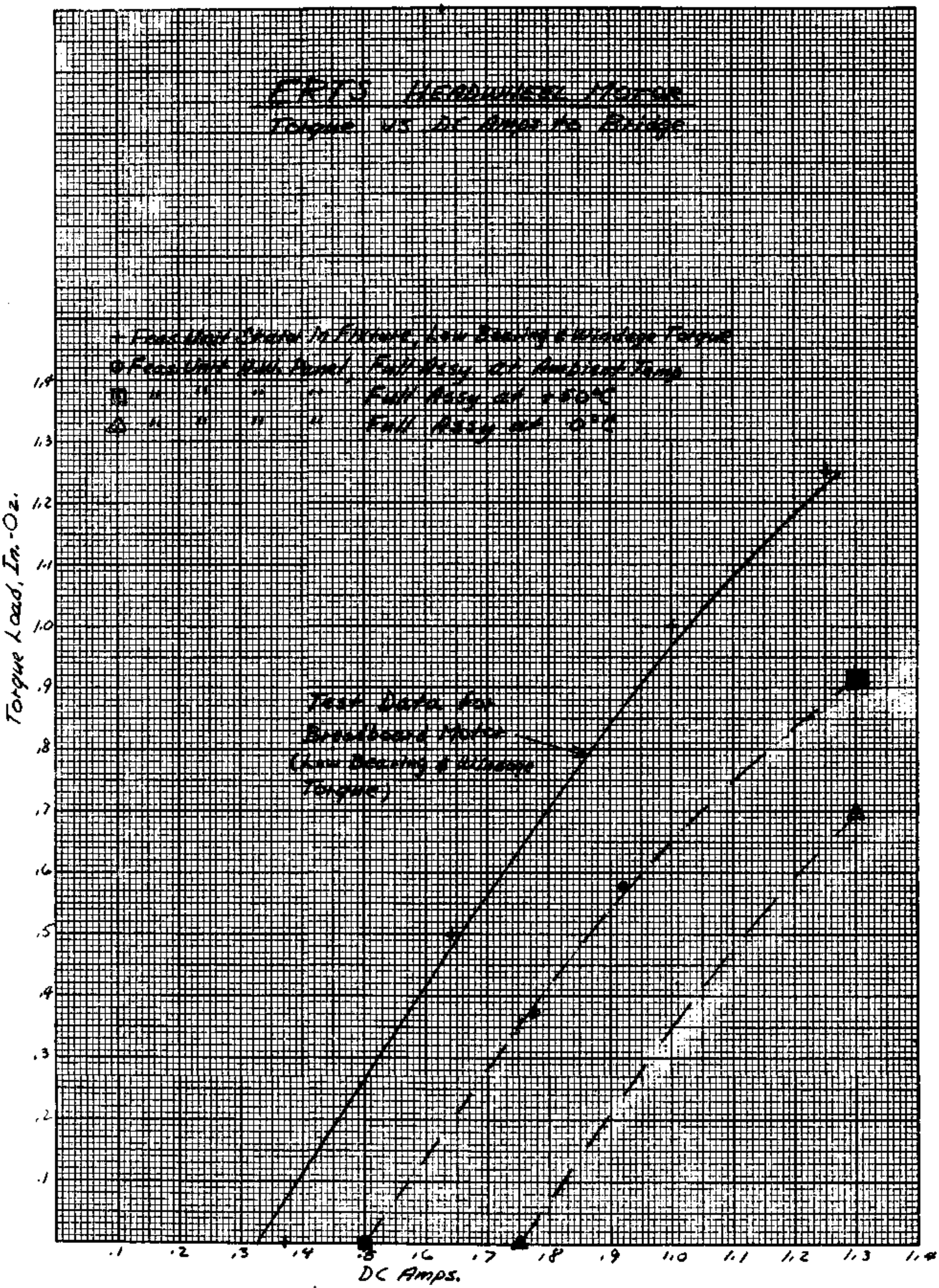

Figure 2-16 ERTS HEADWHEEL MOTOR

electrical excitation, is a function of the instantaneous speed (or, of slip speed). The mean acceleration torque is only dependent on this function as shown in the following simple derivation.

Acceleration,

$$\frac{d\omega}{dt} = \frac{M}{I}$$

$$dt = \frac{I}{M}\, d\omega$$

$$t_a = I \int_{o}^{\omega s} \left[\frac{d\omega}{M}\right] = \frac{I\omega s}{Mav.}$$

and,

$$M_a = \frac{\omega s}{\int_{o}^{\omega s} \left[\frac{d\omega}{M}\right]} = \frac{I\omega s}{t_a}$$

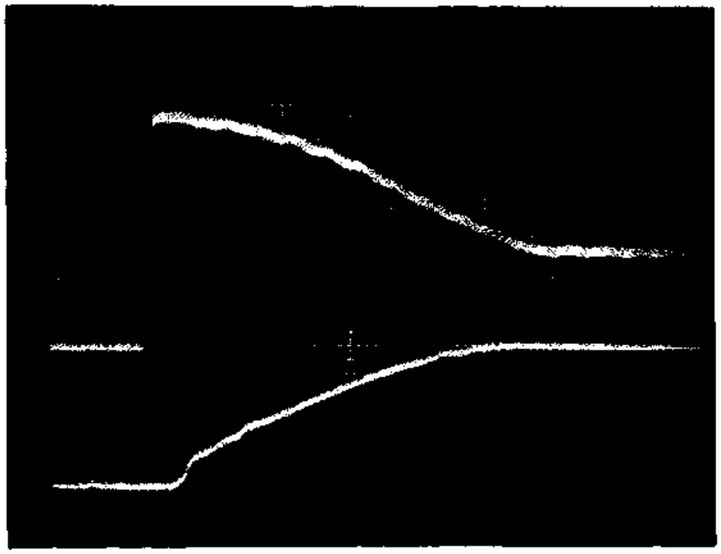

Upper Trace: DC Current, 2 Amp./cm.
Lower Trace: Relative Speed, Stall-to-Sync.
Horizontal Scale: 0.5 sec./cm

Figure 2-17 ACCELERATION CHARACTERISTICS OF ERTS HEADWHEEL PANEL

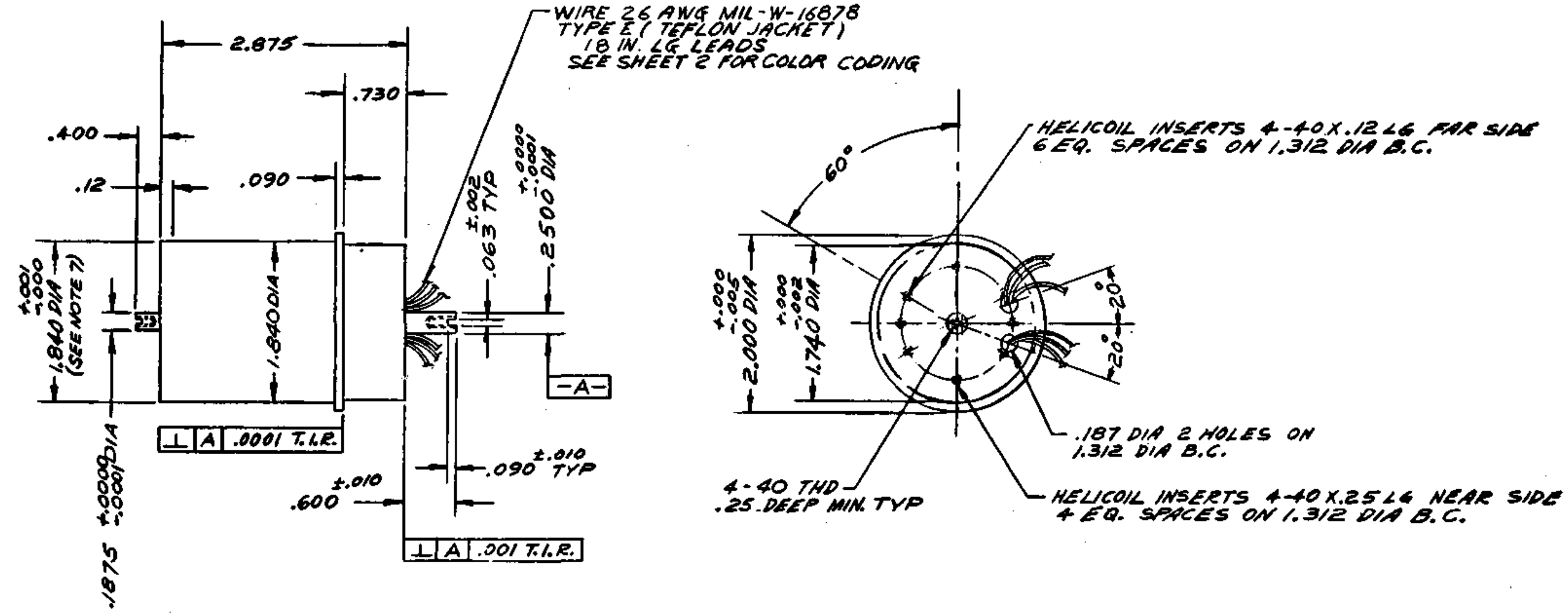

NOTE.
WITH THE MOTOR ENERGIZED AT FULL VOLTAGE ON "RUN" WINDINGS AT EITHER SPEED, THE AC VOLTAGE ACROSS "BRAKE" WINDING SHALL NOT EXCEED 2.5 VRMS

NOTES.
1. HOUSING MAT'L TO BE ALUM ALLOY 7075-T6.
2. SHAFT MAT'L TO BE STN STEEL TYPE 303
3. MAX SHAFT RUNOUT .0001 T.I.R.
4. BEARINGS AT .2500 DIA TO BE MATCHED PRELOADED PAIR BARDEN SR4A55ER2DF2CG-6
5. BEARING AT .1875 DIA TO BE BARDEN SR3 SSW5ER2CG-6, OUTER RACE TO BE FIXED, INNER RACE TO BE PRELOADED 6 TO 10 OZ.
6. MAT'L FOR BUSHING BETWEEN OUTER RACE & HOUSING BORE BOTH ENDS TO BE STN STEEL TYPE 416, .060 MIN WALL THICKNESS
7. DIMENSION 1.840 TOLERANCES $\pm$.000 TO BE HELD FOR .12

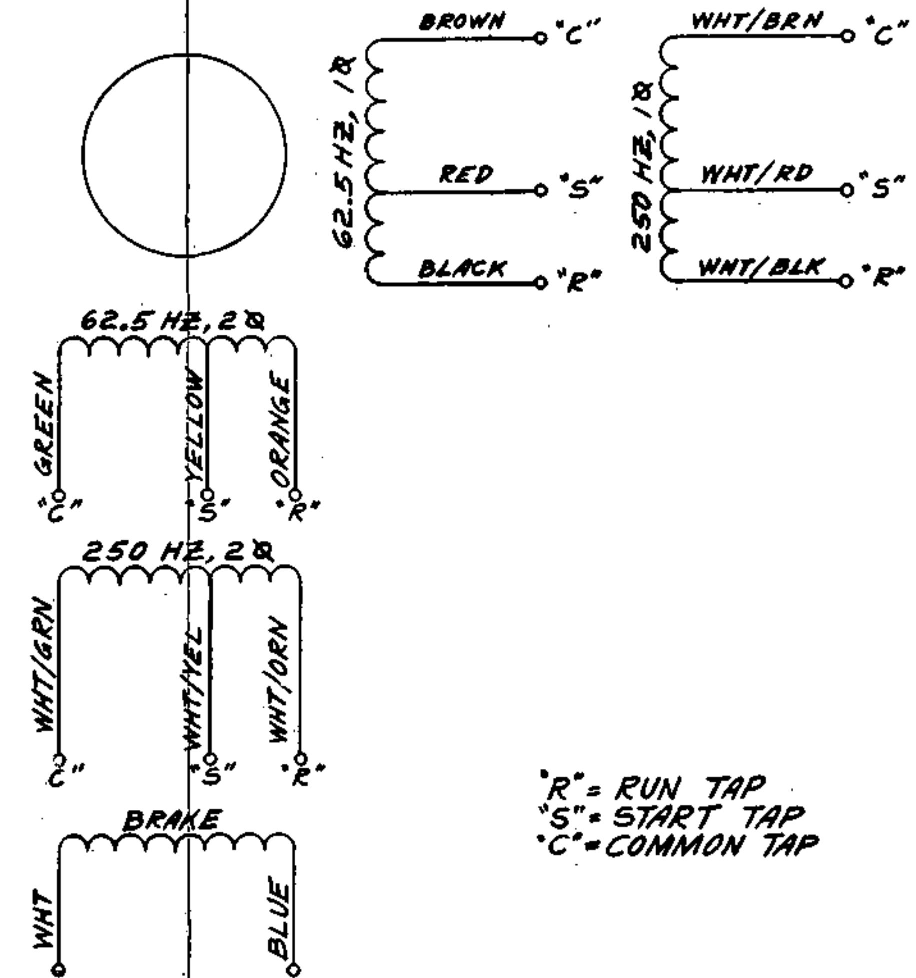

"R" = RUN TAP
"S" = START TAP
"C" = COMMON TAP

Figure 2-18 MOTOR CAPSTAN

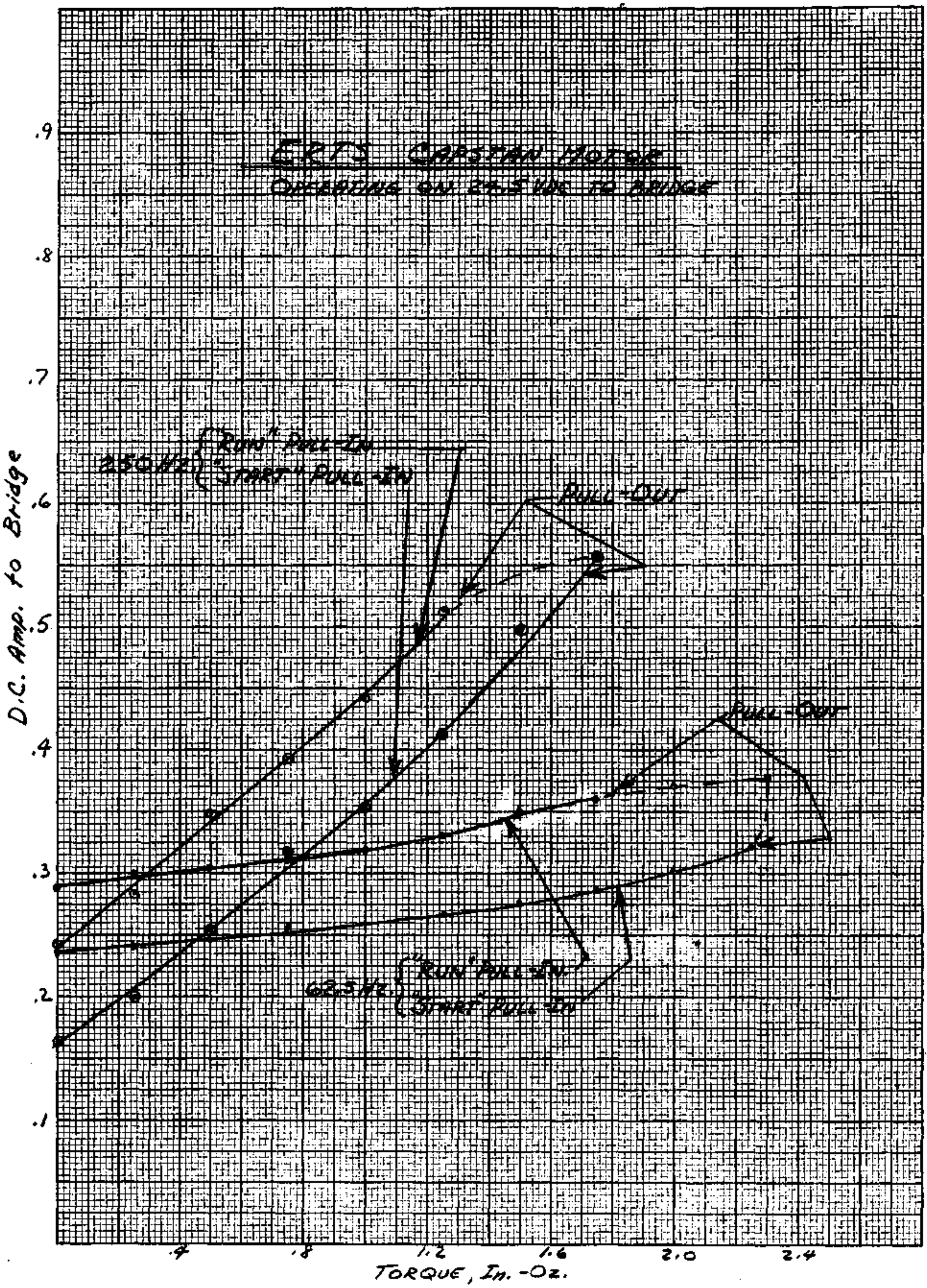

Figure 2-19 ERTS CAPSTAN MOTOR

where:

ω = motor angular velocity

ω_s = motor synchronous angular velocity

I = moment of inertia

t_a = time to reach sync speed

M = $M(\omega)$, instantaneous torque, as a function of speed

M_a = mean acceleration torque

The subsynchronous parameters measured for the capstan motor are given below.

		Stall Power Watts	Stall Torque In.-Oz.	Mean Accel. Torque In.-Oz.
62.5 Hz Oper.	"run" Winding	14.2	2.25	1.96
	"start" Winding	43.0	4.0	3.06
250 Hz Oper.	"run" Winding	19.7	1.7	1.40
	"start" Winding	68.0	4.25	4.47

It was decided not to use the "start" taps in the low speed, record/playback modes. The advantages of this approach are:

a) It eliminates actuation of a relay at every record command.

b) It eliminates the explicit sequencing of sync speed detection and relay actuation.

c) Elimination of the "start"-"run" transient plus (b), above, means that a steady-state tape speed is reached more quickly.

The torque margins are still quite adequate for "run" only operation in record mode. The motor pull-out torque is 1.7 inch-ounce. Elsewhere in this report, the worst case torque has been calculated for end-of-tape operation at 0°C. Reflected at the motor shaft, this value is 0.996 in.-oz. The acceleration time under this worst case condition, using the mean acceleration torque of 1.96 in.-oz. will be 0.715 second.

The dc brake operation is equivalent to accelerating a hysteresis motor in reverse. The stator field is stationary and the rotor slip speed equals the absolute speed. Figure 2-20 shows the torque of the brake as a function of voltage although it will only be operated at the nominal 24.5 Vdc line voltage. Since the brake winding is a two-pole configuration, in order to avoid transformer coupling with the ac windings, it should be expected to have 1/2 the nominal torque of a four-pole configuration. This is evident when the maximum brake torque is compared with the maximum "start" torques at stall.

2.3.3 $I\omega$ Motor. - The $I\omega$ motor is a four-pole, two-phase hysteresis synchronous motor operating at a synchronous speed of 78.125 rps and powered by 156.25 Hz. The detailed specifications, mechanical description and electrical schematic are shown in Figure 2-21 (RCA drawing 877734).

The torque-current characteristics at synchronous speed are shown in Figure 2-22 for "start" pull-in and "run" pull-in. The only function of this motor, however, is to accelerate an inertia to synchronous speed so as to compensate the angular momentum of the headwheel. At synchronous speed, there is no external torque capacity requirement. The compensation inertia consists of two flywheels, one at each end of the motor shaft, and each weighing approximately 1/3 pound. Because of the requirement to survive the vibration environment, unusually heavy duty bearings are used in this motor. At each end of the motor, there is a matched pair of R4A bearings preloaded to 7 pounds. The estimated torque of these four bearings for the worst case fits and 0°C is 0.38 in.-oz., and this constitutes the only real torque load, other than the high accelerating torque required during startup. The "start" winding data obtained for this motor are:

dc Current at Stall	3.6 amp
dc Current at Synch Speed (on "start" winding)	3.2 amp
Stall Torque	5.5 in.-oz. (approx.)

2.4 Torque Margins

This section deals with the mechanical losses in the tape transport mechanism due to bearing drag, transmission losses and friction in the tape path. The losses in these elements under worst case conditions are then used to establish the torque margins of the three motors in the transport. For convenience, the key transport elements are shown schematically in Figure 2-23. Throughout the computations, minor factors such as belt losses and tape guide inertias have been ignored. Section 2.4.1 establishes the bearing mechanical torque loads at thermal extremes, while section 2.4.2

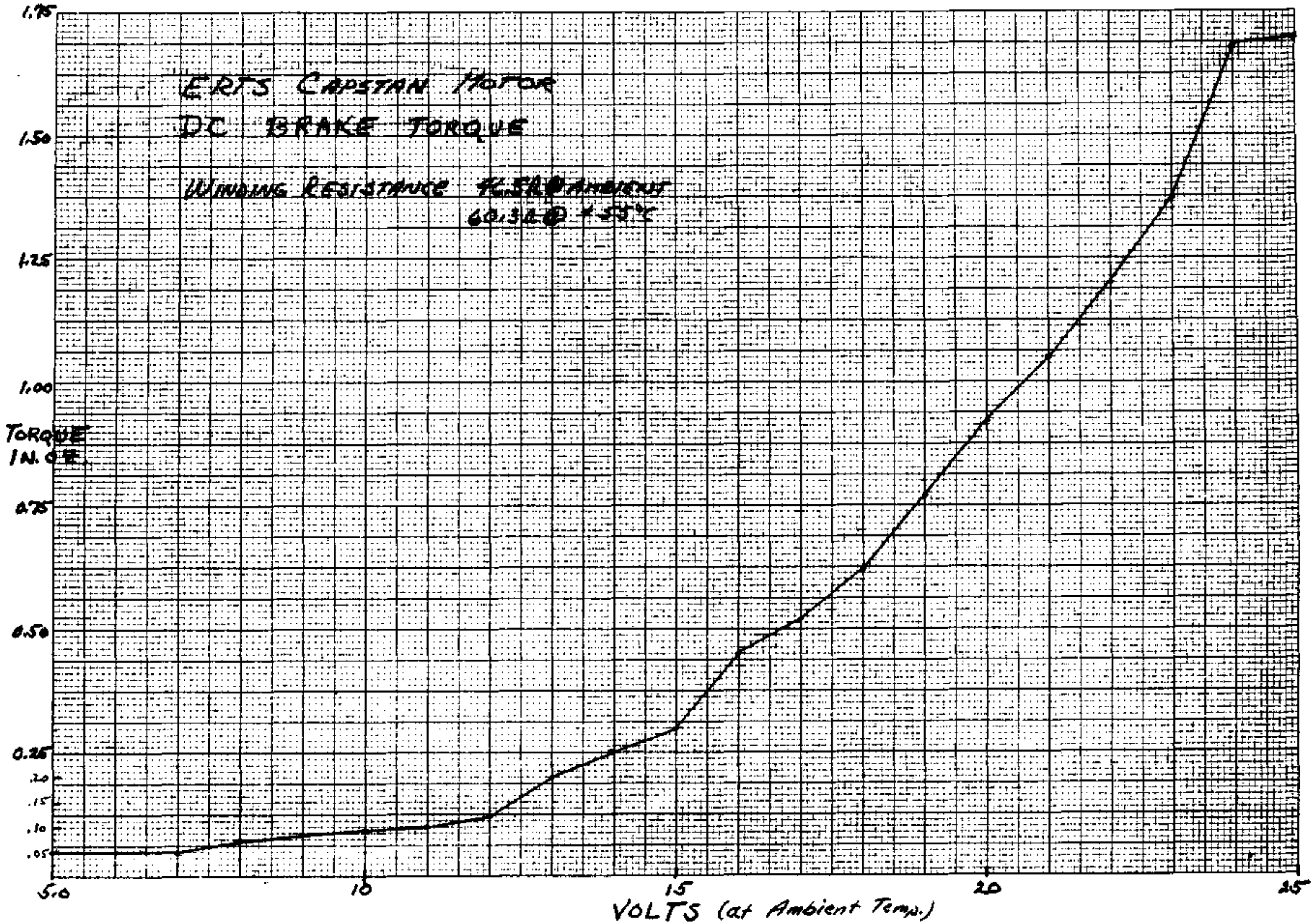

Figure 2-20 ERTS CAPSTAN MOTOR DC BRAKE TORQUE

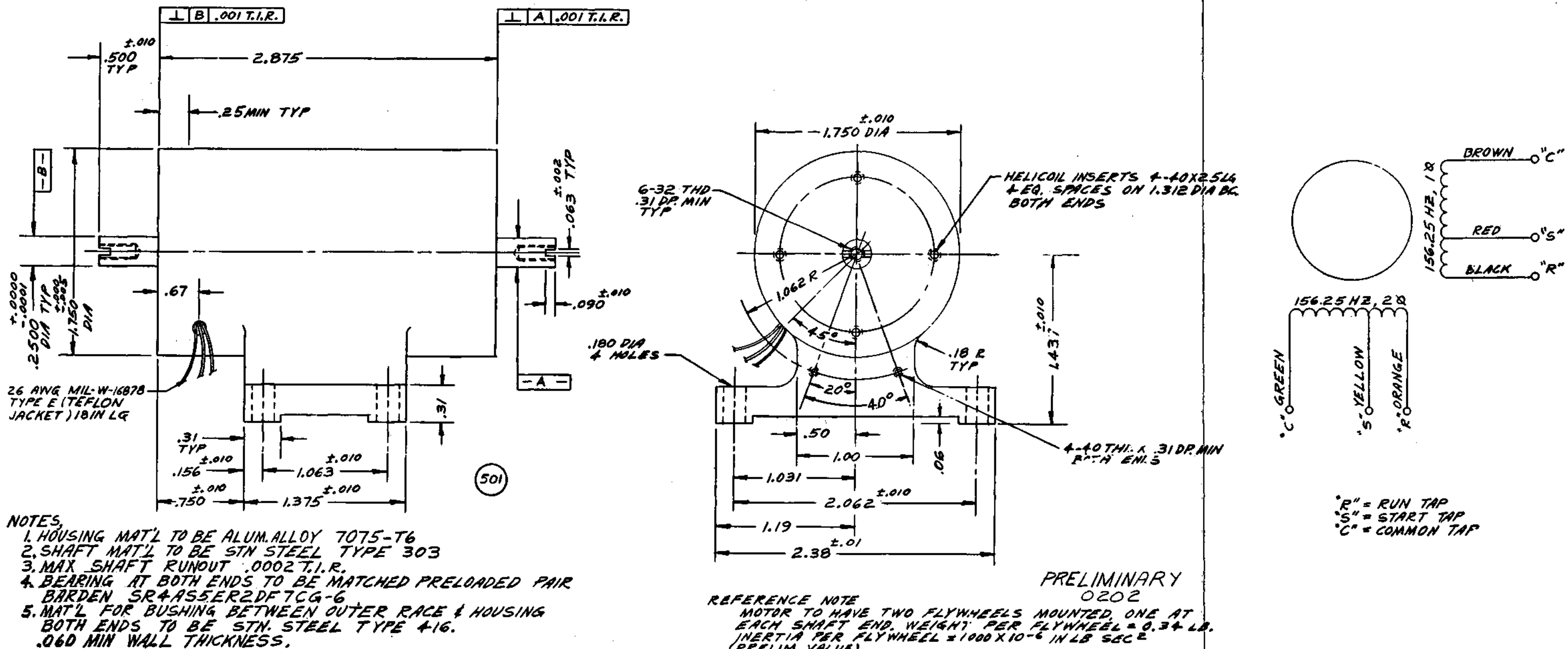

Figure 2-21 MOTOR MOMENTUM-COMPENSATION

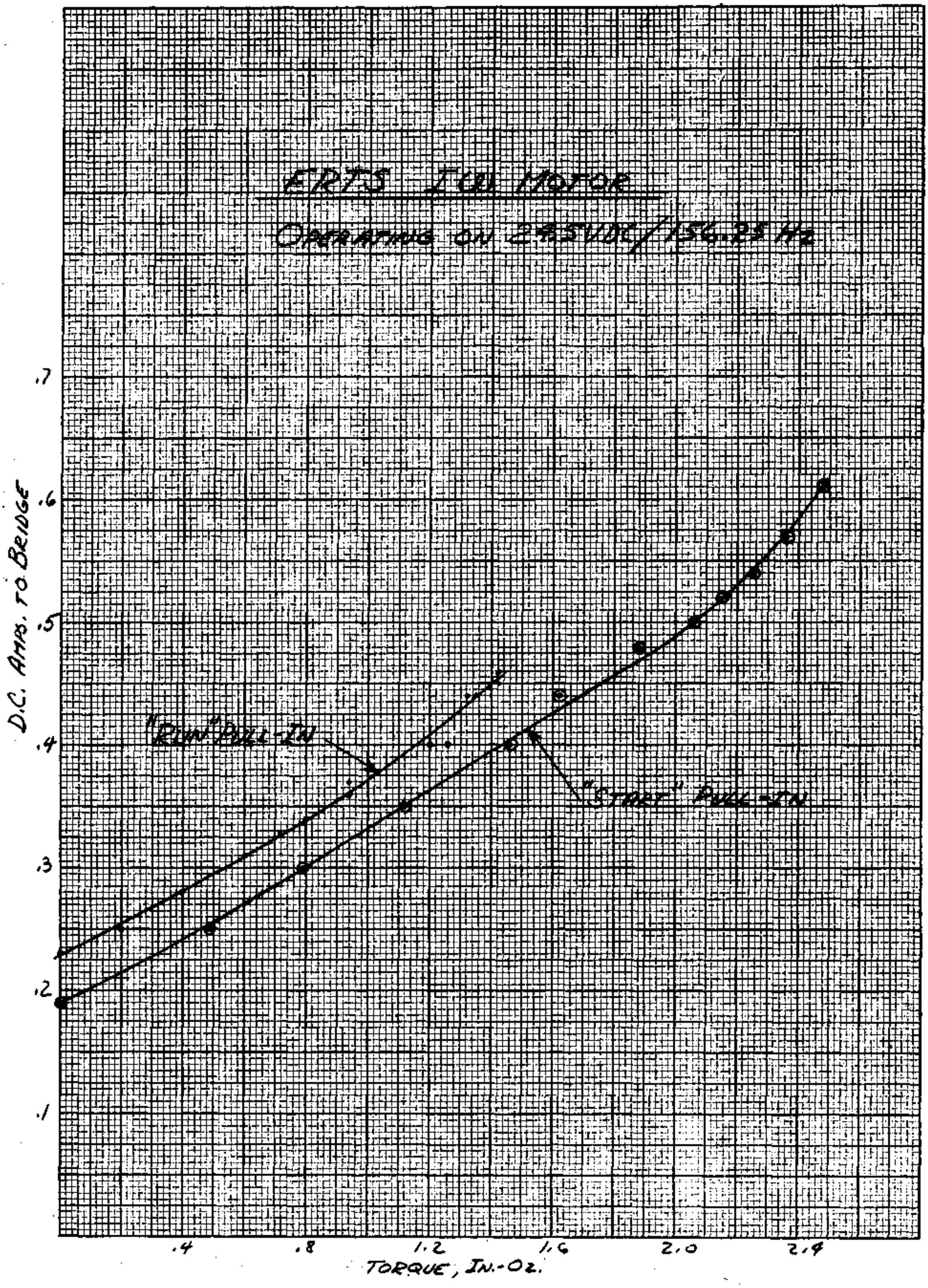

Figure 2-22 ERTS Iω MOTOR

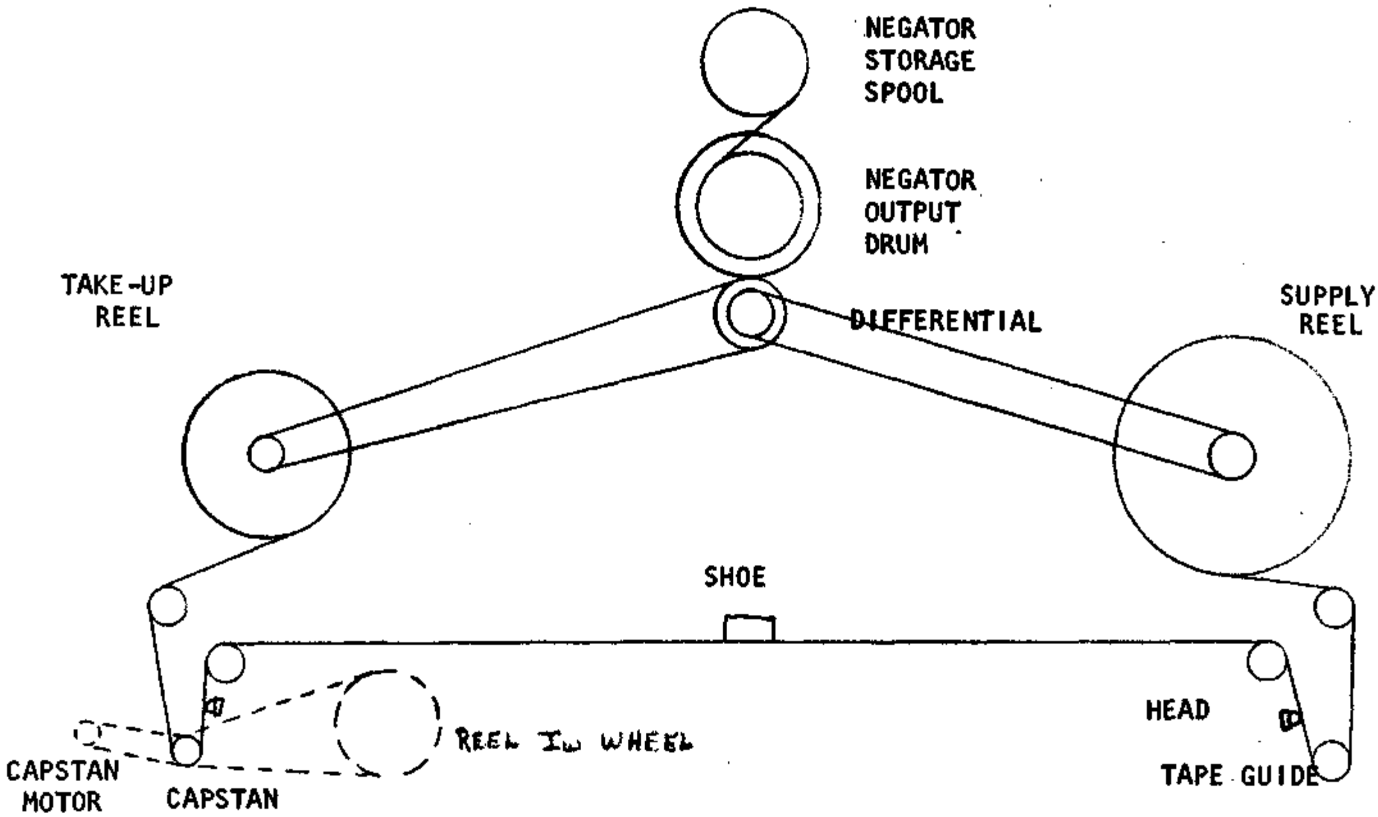

Figure 2-23 TRANSPORT SCHEMATIC

establishes the drag due to lubricants. Parameters used in the computation of individual mechanical torque loads are tabulated in Table 2-1 while Table 2-2 contains the parameters for the lubricant drag computations and summarizes the total drag torque for each transport sub-assembly. The relationship of drag torque to available torque (i.e., torque margin) is discussed in Section 2.4.3 for each of the three transport motors.

2.4.1 <u>Bearing Mechanical Torque Loads.</u> - The majority of the rotating subassemblies in the Transport Unit employ a bearing housing construction like that shown in Figure 2-24. This arrangement provides a primary structural element of aluminum for minimum equipment weight, with inserts or jackets of stainless steel (416) at the bearing seats to minimize thermal stressing of the bearing. Since the coefficient of thermal expansion is larger for aluminum than steel, the housing attempts to shrink around the jacket when the temperature is lowered. This mechanism stresses the steel jacket and the bearing outer race and causes a radial shrinkage of the outer race which results in additional loading on the balls. After establishing the various part stiffnesses and clearances, the radial shrinkage of the inner diameter of the outer race of the bearing was computed. This radial shrinkage was converted to an axial deflection. The axial deflection, preload deflection, and preload tolerance were added to give an effective axial thrust which was then converted to a mechanical torque. Values for the mechanical torques of the various bearings are listed in Table 2-1.

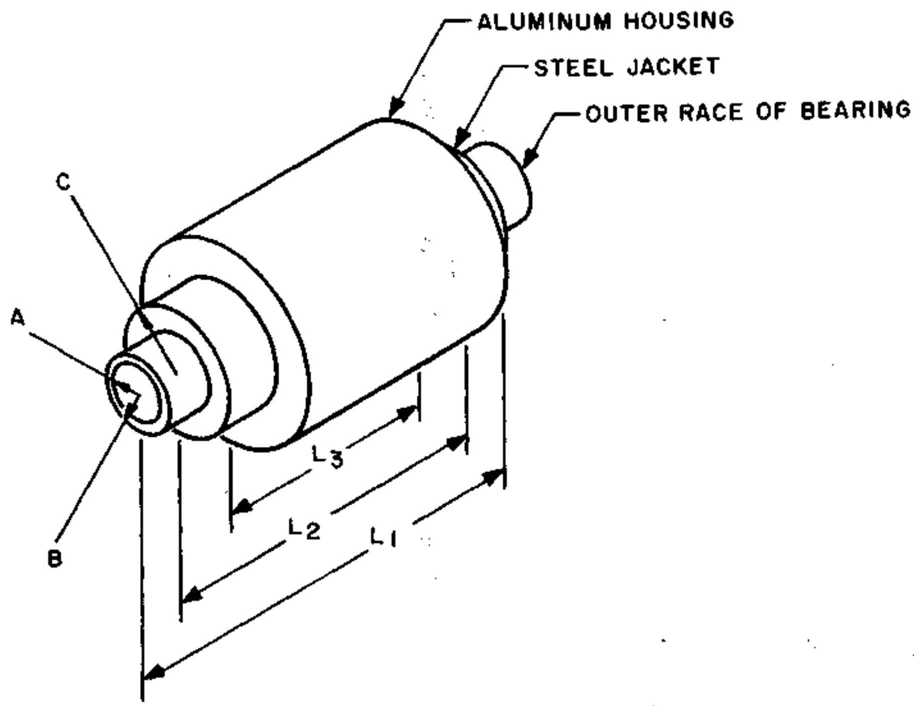

Figure 2-24 TYPICAL BEARING/HOUSING CONSTRUCTION

For uniform external radial pressure

$$\Delta A = -P \frac{1}{E} \left(\frac{2 A B^2}{B^2 - A^2} \right)$$

$$\Delta B = -P \frac{B}{E} \left(\frac{A^2 + B^2}{B^2 - A^2} - \nu \right)$$

For uniform internal radial pressure

$$\Delta B = P \frac{B}{E} \left[\frac{C^2 + B^2}{C^2 - B^2} + \nu \right]$$

$$\Delta C = P \frac{C}{E} \left[\frac{2 B^2}{C^2 - B^2} \right]$$

F

2.4.1.1 Basis of Mechanical Torque Computations

2.4.1.1.1 Physical Constants

Poisson's Ratio (ν)

AL = .33 S.S. = .27

Young's Modulus (E)

AL = 10.6×10^6 psi, S.S. = 29×10^6 psi

Coefficient of Thermal Expansion (Q)

AL = 12.9×10^{-6} in./in.-°F S.S. = 5.6×10^{-6} in./in.-°F

Temperature Change (Δ T)

25°C - (-5°C) = 30°C = 54°F

2.4.1.1.2 Equations Used to Find Radial Shrinkage

$$K_1 = P/\Delta B_B = \left[E_{ss}/B\right] \left[(A^2 + B^2) / (B^2 - A^2) - \nu_{ss}\right]^{-1}$$

$$K_2 = P/\Delta B_R = \left[E_{ss}/B\right] \left[(C^2 + B^2) / (C^2 - B^2) + \nu_{ss}\right]^{-1}$$

$$\Delta B_B = D_7 / (1 + K_1 L_1 / K_2 L_2)$$

$$P_1 = (K_1)(\Delta B_B)$$

$$\Delta A_B = P_1 (2 AB^2) / \left[E_{ss} (B^2 - A^2)\right]$$

$$\Delta C_R = P_1 (2 CB^2) / \left[E_{ss} (C^2 - B^2)\right]$$

$$\Delta C = C (Q_{AL} - Q_{ss}) \Delta T + \Delta C_R$$

$$K_7 = P/\Delta C_{BR} = E_{ss} / \left[C \left(\frac{C^2 + A^2}{C^2 - A^2} - \nu_{ss} \right) \right]$$

$$K_3 = P/\Delta C_{AR} = E_{AL} / \left[C \left(\frac{D^2 + C^2}{D^2 - C^2} + \nu_{AL} \right) \right]$$

$$\Delta C_{BR} = \Delta C/(1 + K_7 L_7 / K_3 L_3)$$

$$P_2 = K_7 (\Delta C_{BR})$$

$$\Delta A_{BR} = P_2 (2 AC^2) / E_{ss} (C^2 - A^2)$$

$$\text{Radial Shrinkage} = \Delta A_B + \Delta A_{BR}$$

where

P is interface pressure, psi

K_1 is the relative radial stiffness of bearing, lbs/in^3

K_2 is the relative radial stiffness of steel ring, lbs/in^3

L_1, L_2 are lengths shown in Figure 2-24

A, B, C are the radii shown in Figure 2-24

ν, E, Q, ΔT are the constant defined in para 2.4.1.1.1

ΔB_B and ΔA_B are the radial change of the bearing OD and ID respectively

ΔB_R is the radial change of the steel ring I.D.

ΔA_{BR} is the radial and subscripts with (7) denote the parameters effectively derived by combination of the bearing (1) and steel sleeve (2)

In the case of an initial clearance ($-D_7$) between the bearing and ring, the following procedure was used.

$$P_3 = (-D_7)\, E_{ss} \left(\frac{C^2 - B^2}{2\, BC^2} \right)$$

$S_{CR} = P_3/K_2$

$$S_C = S_{CR} \left(1 + \frac{K_2\, L_2}{K_3\, L_3}\right)$$

$\Delta T_1 = S_C/C\ (Q_{AL} - Q_{ss})$ This is the temperature change needed to close the clearance.

$\Delta T_2 = \Delta T - \Delta T_1$

$\delta = C\ (Q_{AL} - Q_{ss})\ T_2$

$\delta_{CBR} = \delta/(1 + K_7 L_7/K_3 L_3)$

$P_4 = \delta_{CBR}\, K_7$

S_{ABR} = Radial Shrinkage = $P_4\ (2\ AC^2)/(E_{ss}\ \ (C^2 - A^2)\ )$

Axial deflection = (radial deflection) Cot φ where φ = contact angle of bearing.

2.4.1.1.3 R8 Running Torque. - Data on the Average Running Torque of a SR8K5 type bearing was not included in the Barden catalog. A SR6K5 bearing was the closest bearing to a SR8K5 whose data was listed. Therefore, the SR6K5 data was converted to the SR8K5 type.

SR8K5: 10, 5/32" dia. balls

$$\bar{R}_8 = \frac{L_0 + L_1}{4} = \frac{.972 + .736}{4} = .427''$$

SR6K5: 7, 5/32" dia. balls

$$\bar{R}_6 = \frac{L_0 + L_1}{4} = \frac{.692 + .463}{4} = .289''$$

For SR8K5 Case:

Normal force on balls = $F_n = T/\text{Sin}\,\varphi$

$F_n = 88/\sin 33.9° = 157.6$ lb. F_n/ball = 15.76 lb./ball

$F_n = 118/\sin 34.7° = 207$ lb. F_n/ball = 20.7 lb./ball

For SR6K5 Case:

T (lb.)	φ (°)	F_n (lb.)	F_n/Ball (lb./ball)	Running Torque for Bearing (mg-mm)
2	12.18	9.47	1.35	12.5 K
6	12.82	27.0	3.86	38.0 K
10	13.27	43.5	6.22	66.0 K
20	14.10	82.1	11.73	145.0 K
30	14.73	117.7	16.83	210.0 K

from Figure 2-25, 15.76 lb./ball $\Longrightarrow$ 197 K mg-mm

for SR8K5 Running Torque $= 197 \left(\frac{10}{7}\right) \left(\frac{.427}{.289}\right)$

$=$ 403 K mg-mm @ top bearing

20.7 lb./ball $\Longrightarrow$ 298 K mg-mm $\therefore$ 608 K mg-mm @ bottom bearing

2.4.2 Bearing Lubricant Torque. - The viscosity of G-6 lubricant was computed based on an experiment with a headwheel motor. This value was then used to compute the drag of all the other bearings. The high speed mode was used in evaluating the velocity of each bearing.

In this experiment, there was negligible change in frictional torque between 50°C and ambient; it is therefore assumed that the lubricant drag was small. When the temperature was 0°C, there was a significant increase in friction. Part of this was possibly due to the aluminum contracting on the bearing as well as the increase in viscosity of the grease. As a worst case assumption, the total increase in drag (0.35 in.-oz. at 0°C) will be assumed to be due to the viscous effects alone.

$$M = 16\,(1.42 \times 10^{-5})\, f_o\, (n\nu)^{2/3}\, dm^3$$

(Rolling Bearing Analysis, Harris, Pg. 447)

$$.35 = 16\,(1.42 \times 10^{-5})\,(2)\,(18{,}750)^{2/3}\, \nu^{2/3}\; 2\,(.438^3 + .632^3)$$

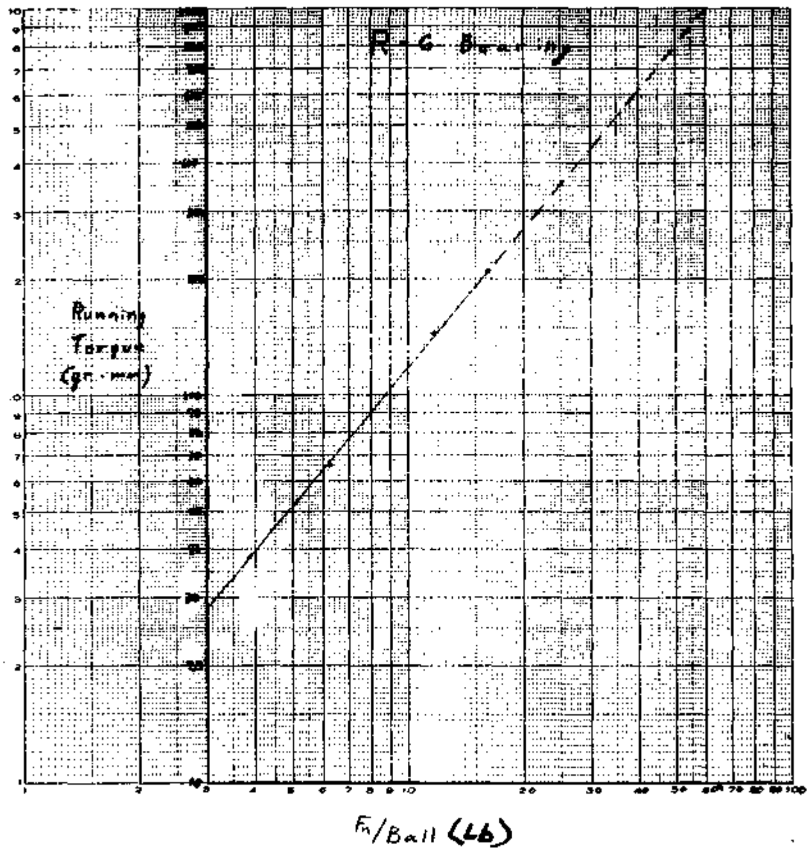

Figure 2-25 TORQUE CURVE FOR R-6 BEARING

$\nu^{2/3} = 1.623$

$\nu = 2.07$ cs

$\therefore \; T_{lub.} = 7.38 \times 10^{-4} \, n^{2/3} \, dm^3$

where:

M = Torque, in.-oz.

f_o = Bearing geometry factor

n = rpm

ν = Kinematic Viscosity, centistokes

dm = Bearing pitch dia., inches

2.4.3 Summary of Torque Margins

2.4.3.1 Headwheel Motor. - From Table 2-2, the worst case drag torque on the headwheel motor is 0.431 oz.-in. As discussed in paragraph 2.3.1, pull-out torque of the headwheel motor is approximately 1.25 oz.-in. Hence, even under worst case conditions sufficient margin will be present to accommodate the load introduced by the tape during shoe engagement. This latter load has been measured under various circumstances and is less than 0.1 oz.-in.

2.4.3.2 I ω Motor. - As shown in Table 2-2, the total drag torque on the I ω motor is 0.377 oz.-in. As indicated in Figure 2-22 of paragraph 2.3.3, the pull-out torque of this motor is in excess of 1 in.-oz., and no other torque loads other than acceleration are applied to the motor. Hence, adequate torque margin exists.

2.4.3.3 Capstan Motor. - The loads imposed on the capstan motor are considerably more complicated than those imposed on the other two motors in the transport. The following sections describe the two parameters which are critical to the capstan drive. These include transport acceleration time and tension ratio across the capstan, and are considered for "worst case" tape position during both normal and high speed operations. As a result of these calculations, it can be seen that sufficient margin is available for transport acceleration even under worst case conditions.

2.4.3.3.1 Tension Ratios and Transport Acceleration Time

2.4.3.3.1.1 Normal Speed at EOT

Torque per Negator = 2.4 lb.-in. = 38.4 oz.-in.

Drum Torque = 2 (Negator torque) + bearing torque

$$Md = 2(38.4) + (.540 + .331)$$

$$Md = 77.67 \text{ oz.-in.}$$

Takeup Reel Torque (Mtur) = $1/2\ Md\ (1 + \nu_1 + \nu_2 - \nu_3)$ + bearing torque

where:

ν_1 = the loss in one bevel gear mesh

ν_2 = the loss in the spur gear mesh

ν_3 = the loss in the sprocket drive

$$\text{Mtur} = \frac{77.67}{2}\ (1 + .0466 + .0134 + .0100) + .03$$

$$\text{Mtur} = 40.75 \text{ oz.-in.}$$

$$\text{Takeup Reel Force (Ftur)} = \frac{\text{Mtur - (inertial torque)}}{\text{Radius}}$$

$$\text{Ftur} = \frac{40.75 - 16\ (.0924) \left(\frac{.25}{4.00}\right) \left(\frac{.2187}{.895}\right)\ \alpha\text{cm}}{4.00}$$

$$\text{Ftur} = 10.19 - 5.65 \times 10^{-3}\ \alpha\,\text{cm}$$

where:

αcm = the acceleration of the capstan motor

Force on the Takeup Side of the Capstan (Ftus) = Ftur - (tape guide force)

$$\text{Ftus} = 10.19 - 5.65 \times 10^{-3}\ \alpha\text{cm} - \left(\frac{.069}{.3125}\right)$$

$$\text{Ftus} = 9.97 - 5.65 \times 10^{-3}\ \alpha\text{cm}$$

Supply Reel Torque (Msr) = 1/2 Md $(1 + 2\nu_1 + \nu_2 + \nu_3)$ + bearing torque

$$\text{Msr} = \frac{77.66}{2}\ (1 + 2\ (.0466) + .0134 + .0100) + .03$$

$$\text{Msr} = 43.40 \text{ oz.-in.}$$

$$\text{Supply Reel Force (Fsr)} = \frac{\text{Msr + (inertial torque)}}{\text{radius}}$$

$$\text{Fsr} = \frac{43.40 + 16(.0079) \left(\frac{25}{2.66}\right) \left(\frac{.2187}{.895}\right)\ \alpha\text{cm}}{2.66}$$

$$\text{Fsr} = 16.32 + 1.093 \times 10^{-3}\ \alpha\text{cm}$$

Force on the supply side of the capstan (Fss) = Fsr + 2 (tension loss across a single head) (tape tension) + (shoe force) + 4 (tape guide force).

$$Fss = 16.32 + 1.093 \times 10^{-3}\,\alpha cm + 2\,(.07)\,Fss + 1.75 + 4\left(\frac{.069}{.3125}\right)$$

$$.86\ Fss = 18.95 + 1.093 \times 10^{-3}\,\alpha cm$$

$$Fss = 22.06 + 1.280 \times 10^{-3}\,\alpha cm$$

Capstan torque = (bearing torque) + (Fss - Ftus) (capstan radius) +

$$(I\omega \text{ wheel torque}) \left(\frac{\text{capstan radius}}{I\omega \text{ wheel radius}}\right)$$

$$Mcap = .227 + (22.06 + 1.280 \times 10^{-3}\,\alpha cm - 9.97 + 5.65 \times 10^{-3}\,\alpha cm)$$

$$(.25) + \left[.314 + 16(1.525 \times 10^{-2})\ \frac{1}{10}\ \alpha cm\right] \frac{.895}{2.187}$$

$$Mcap = 3.38 + 11.71 \times 10^{-3}\,\alpha cm$$

Capstan Motor Torque (Mcm) = (bearing torque)

$$+ \ Mcap \frac{\text{capstan pulley radius}}{\text{capstan motor pulley radius}}$$

+ (capstan motor inertial torque)

$$Mcm = .169 + (3.38 + 11.71 \times 10^{-3}\,\alpha cm) \left(\frac{.2187}{.895}\right) + 8 \times 10^{-4}\,\alpha cm$$

$$Mcm = .996 + 3.66 \times 10^{-3}\,\alpha cm$$

$$Mcm = 2.00 = .996 + 3.66 \times 10^{-3}\,\alpha cm$$

$$\alpha cm = \frac{1.004}{3.66 \times 10^{-3}} = 274 \text{ rad./sec}^2.$$

$$\omega cm = 2\,\pi\, f = 2\,\pi\ (31.25) = 196 \text{ rad./sec.}$$

$$\text{Acceleration time} = \frac{\omega}{\alpha} = \frac{196}{274} = .715 \text{ sec.}$$

Tension Ratio across the Capstan

$$Fss/Ftus = \left[22.06 + 1.280(.274)\right] / \left[9.97 - 5.65(.274)\right] = 2.66$$

TABLE 2-1. PARAMETERS FOR MECHANICAL TORQUE CALCULATIONS

Part	Bearing #	D_7* (M")	A (")	B (")	C (")	D (")	L_1 (")	L_2 (")	L_7 (")	L_3 (")	Radial Shrinkage (μ")	φ (°)	Cot φ	δ axial	Preload (lbs)	δ Preload (μ")	Preload Tolerance (μ")	δ Total (μ")	Effective Axial Thrust (lbs)	Mechanical Torque (mg-mm)	Mechanical Torque (oz-in)
Reel Ass. top	SR8FFW5DB10CG-6	60	.5625	.5625	.71	.8125	.3125	.53	.46	.8	105.5	33.9	1.487	157	10	83	75	315	88	403K	.561
bottom	SR8FFW5DB10CG-6	60	.5625	.5625	.71	.94	.3125	.50	.42	.8	149.3	34.7	1.443	215	10	87	75	373	118	608K	.845
Tape Guide	SFR1810SSW5DB2CG-6	- 5	.223	-	.25	.3125	.1562	-	.1562	1.0	6.6	21.3	2.56	17	2	94	75	186	6.1	22K	.0278
Capstan top	SR4SW5DB2ER2CG-6	-40	.2735	.3125	.37	.55	.392	.407	.4	.407	10	16.5	3.36	54	2	158	25	237	3.8	14K	.0195
bottom	SR6SW5DF2ER2CG-6	-40	.392	.4375	.495	.742	.5624	.65	.61	.65	43.3	12.0	4.37	189	2	238	50	478	6.3	41K	.057
IW Reel	SFR6SSW5DB5CG-6	-40	.392	.4375	.5075	2.00	.2812	.4515	.73	.7	72.2	13.7	4.10	298	5	415	50	771	14.5	102K	.142
Neg. Take Up	SFR6SSW3DB5CG-6	-40	.392	.4375	.5075	.9	.2812	.505	.79	1.01	65.3	13.5	4.17	272	5	415	50	737	13.3	96K	.133
Neg. Supply top	SFR6SSW5DB5CG-6	-40	.392	.4375	.5075	.825	.2812	.75	.52	.75	55.0	13.6	4.13	227	5	415	100	741	13.6	95K	.132
bottom	SFR6SSW5DB5CG-6	-40	.392	.4375	.5075	1.01	.2812	.45	.37	1.	99.9	14.0	4.01	400	5	415	100	915	20.3	140K	.195
Diff. top	SFR4FW5DB2CG-6	-40	.2735	.3125	.3825	.812	.196	.2	.4	.4	34.5	16.9	3.30	114	2	158	25	297	5.6	28K	.037
bottom	SFR4FW5DF2CG-6	-40	.2735	.3125	.3825	.84	.392	.375	.38	.375	27.3	16.8	3.32	91	2	158	25	274	4.8	22K	.031
IW Motor																					
front outboard	SR4AS5ER2DF7CG-6	-40	.323	.375	.435	.875	.2812	.315	.30	.28	36.3	14.3	3.92	142	7	528	25	695	11.3	62K	.096
2 inboard	SR4AS5ER2DF7CG-6	-40	.323	.375	.435	.50	.2812	.315	.30	.35	3.9	14.0	4.01	16	7	528	25	569	8.1	43K	.060
rear outboard	SR4AS5ER2DF7CG-6	-40	.323	.375	.435	.875	.2812	.315	.30	.15	15.9	14.1	398	63	7	528	25	616	9.3	51K	.071
Capstan Motor																					
front	SR3SSW5ER2CG-6	-40	.215	.25	.31	.92	.190	.5	.35	.15	0	0	0	0	.625	114	-	114	.625	2.2K	.003
rear inboard	SR4AS5ER2DF2CG-6	-40	.323	.375	.435	.50	.2812	.315	.30	.35	3.9	12.1	4.67	18	2	247	25	290	2.7	13K	.018
rear outboard	SR4AS5ER2DF2CG-6	-40	.323	.375	.435	.875	.2812	.315	.30	.15	15.8	13.3	4.23	67	2	247	25	339	3.05	15K	.021
HW Motor																					
rear outboard	SR4STA5DB2ER2CV2CG-6	-80	.2735	.3125	.367	.875	.196	.22	.21	.22	4.55	16.4	3.39	15	2	158	25	198	2.85	13K	.0181
rear inboard	SR4STA5DB2ER2CV2CG-6	-80	.2735	.3125	.367	.875	.196	.22	.21	.14	-	-	-	-	2	158	25	183	2.8	11.5K	.0160
front inboard & outboard	SR6STA5DB2ER2CV2CG-6	-80	.392	.4375	.79925	.875	.2812	.5	.4	1.5	-	-	-	-	2	238	50	298	2.82	17K	.0236

*The reduction interference due to Surface Condition for accurately ground surface is 80 μ" minimum so that these numbers are 80 μ" less than the interference. (Rolling Bearing Analysis, Harris, pp. 84)

TABLE 2-2. LUBRICATION & TOTAL SUB-ASSEMBLY TORQUES

Part		dm (11)	dm^3	n (rpm)	$n^{2/3}$	Lub. Torque (oz-in)	Mech. Torque (oz-in)	Total Bearing Torque	Total Subassembly Torque (oz-in)
Reel Ass'y	top	.854	.622	172	30.9	.0142	.561	.575	1.434
	bottom	.854	.622	172	30.9	.0142	.845	.859	
Tape Guide		.410	.0689	1468	129.2	.00657	.0278	.0344	.069
Capstan	top	.438	.0840	1836	150.1	.00931	.0195	.029	
	bottom	.632	.252	1836	150.1	.0279	.057	.0849	.227
Iω Reel		.632	.252	750	82.5	.01536	.142	.157	.314
Neg. Take Up		.632	.252	43	12.3	.00228	.133	.135	.540
Neg. Supply	top	.632	.252	43	12.3	.00228	.132	.134	
	bottom	.632	.252	43	12.3	.00228	.195	.197	.331
Diff.	top	.438	.0840	86	19.5	.00121	.037	.038	
	bottom	.438	.0840	86	19.5	.00121	.031	.032	.140
Iω Motor									
front outboard		.491	.1183	4680	281	.0245	.086	.111	
2 inboard		.491	.1183	4680	281	.0245	.060	.085	
rear outboard		.491	.1183	4680	281	.0245	.071	.096	.377
Capstan Motor									
front		.344	.0352	7500	383	.00995	.003	.013	
rear inboard		.491	.1183	7500	383	.0334	.018	.051	
rear outboard		.491	.1183	7500	383	.0334	.021	.054	.169
HW Motor									
rear outboard		.438	.0840	18750	706	.0437	.0181	.0618	
rear inboard		.438	.0840	18750	706	.0437	.0160	.0597	
front inboard & outboard		.632	.252	18750	706	.1313	.0236	.1549	.431

2.4.3.3.1.2 High Speed. - In this mode, the "Takeup Reel" is on the supply side of the capstan, and the "Supply Reel" is on the takeup side of the capstan.

Supply Side

$$Mtur = 1/2\ Md\ (1 + \nu_1 + \nu_2 + \nu_3) + Mbearing$$

$$= \frac{77.67}{2}\ (1 + .0466 + .0134 + .0100) + .03$$

$$= 41.59\ \text{oz.-in.}$$

$$Ftur = \frac{Mtur + (\text{inertial torque})}{\text{radius}}$$

$$= \frac{41.59 + 16\ (.0079) \left(\frac{.25}{2.66}\right) \left(\frac{.2187}{.895}\right)\ \alpha cm}{2.66}$$

$$= 15.63 + 1.093\ X\ 10^{-3}\ \alpha cm$$

$$Fss = Ftr + (\text{tape guide force})$$

$$Fss = 15.63 + 1.093\ X\ 10^{-3}\ \alpha cm + \left(\frac{.069}{.3125}\right)$$

$$Fss = 15.85 + 1.093\ X\ 10^{-3}\ \alpha cm$$

Takeup Side

$$Msr = 1/2\ Md\ (1 + 2\ \nu_1 + \nu_2 - \nu_3) - Mbearing$$

$$Msr = \frac{77.67}{2}\ (1 + 2\ (.0466) + .0134 - .0100) - .03$$

$$Msr = 42.56\ \text{oz.-in.}$$

$$Fsr = \frac{Msr - (\text{inertial torque})}{\text{radius}}$$

$$Fsr = \frac{42.56 - 16\ (.0924) \left(\frac{.25}{4.00}\right) \left(\frac{.2187}{.895}\right)\ \alpha cm}{4.00}$$

$$Fsr = 10.64 - 5.65 \times 10^{-3} \ \alpha cm$$

$$Ftus = Fsr - 2 \text{ (head loss ratio)(Ftus)} - \text{(shoe loss)} - 4 \text{ (tape guide loss)}$$

$$Ftus = 16.64 - 5.65 \times 10^{-3} \ \alpha cm - 2\,(.07)\,Ftus - 1.75 - 4 \left(\frac{.069}{.3125}\right)$$

$$1.14\ Ftus = 8.01 - 5.65 \times 10^{-3} \ \alpha cm$$

$$Ftus = 7.03 - 4.96 \times 10^{-3} \ \alpha cm$$

$$Mcap = Mbearing + (Fss - Ftus) \text{ (capstan radius)} + (I\omega \text{ wheel torque})$$

$$Mcap = .227 + (15.85 - 7.03 + 4.96 \times 10^{-3} \ \alpha cm + 1.093 \times 10^{-3} \ \alpha cm)\,(.25)$$
$$+ \left[.314 + 16\,(1.525 \times 10^{-2})\left(\frac{1}{10}\right) \ \alpha cm\right]\left(\frac{.895}{2.187}\right)$$

$$Mcap = 2.56 + 11.49 \times 10^{-3} \ \alpha cm$$

$$Mcm = Mbearing + \text{(capstan motor inertial torque)}$$
$$+ \ Mcap \left(\frac{\text{capstan pulley radius}}{\text{capstan motor pulley radius}}\right)$$

$$Mcm = .169 + 8 \times 10^{-4} \ \alpha cm + (2.56 + 11.49 \times 10^{-3} \ \alpha cm) \left(\frac{.2187}{.895}\right)$$

$$Mcm = .795 + 3.61 \times 10^{-3} \ \alpha cm$$

$$Mcm = 4.00 = .795 + 3.61 \times 10^{-3} \ \alpha cm$$

$$\alpha cm = \frac{3.205}{3.61 \times 10^{-3}} = 888 \text{ rad./sec.}^2$$

$$Fss/Ftus = \left[15.85 + (1.093)\,(.888)\right] / \left[7.03 - 4.96\,(.888)\right] = 6.40$$

$$\text{Acceleration time} = \frac{\omega}{\alpha} = \frac{4(196)}{888} = .883 \text{ sec.}^2$$

Experimental results show that static slip will occur with a tension ratio of about 17.

2.5 Status of Life Tests and Present Conclusions

2.5.1 Negator Life Tests. - Fatigue tests of the Negator springs were conducted, using a test fixture which cycled 4 negators simultaneously through 61 turns of each power drum. The cycling rate was 530 full wind-unwind cycles per 24 hour day. Tests were run on 4 springs made of high yield 301 stainless steel, and, subsequently, on 4 springs made of Havar alloy.

The test results for the stainless steel Negators were as follows:

Specimen No.	No. of Test Cycles	Equiv. No. R/PB Cycles	Comments
1	46,488	11,622	Complete fracture
2	52,719	13,180	Partial failure, test terminated
3	21,770	5,442	Complete fracture
4	46,488	11,622	Partial fracture
	49,884	12,471	Complete fracture

The test results for the Havar Negators were as follows:

Specimen No.	No. of Test Cycles	Equiv. No. R/PB Cycles	Comments
H1	30,725	7,681	3/16" crack observed on left edge.
	34,765	8,691	First crack 1/2" long, 14 cracks on right edge. Test terminated.
H2	41,275	10,319	Numerous small cracks along one edge.
	45,772	11,443	Increase in number and size of cracks on one edge. Test terminated.
H3	41,275	10,319	Numerous small cracks along one edge.

Specimen No.	No. of Test Cycles	Equiv. No. R/PB Cycles	Comments
H3 (cont)	45,772	11,443	Increase in number and size of cracks on one edge. Test terminated.

Both Negator types met the requirements for the present mission by a substantial margin. Because of interest in other applications, where a significant improvement in life may be required, some brief discussion of results may be in order.

The following general observations are made. The stainless steel Negators surpassed the design life estimate by an expected margin, however, the deviation of specimen no. 3 from the group mean is somewhat interesting. The Havar Negators, while suitable for this program, were far from the design life estimate. Here, also, one specimen was well below the group mean value. All fatigue cracks started at the edges, and, in the case of Havar, it is striking that virtually all the many fine cracks formed along only one of two possible edges of each leaf.

The theory is advanced that the slitting operation, which produces 1" wide strips from the rolled sheet, may be responsible for these effects, by means of two different mechanisms. Firstly, the slitting of hard cold rolled sheet may leave a number of fine surface irregularities along the cut edges: this was confirmed in physical examination of new Havar specimens. These irregularities will act as stress raisers. Ultra high-strength alloys tend to have high notch sensitivity; in the case of Havar, this is believed to be a prominent characteristic.

The second postulated mechanism leading to an earlier failure involves residual stresses left by the slitting. It is assumed that shearing operation will leave some residual stresses which are predominantly tension near one surface and predominately compression near the opposite surface. It is also believed that, for either given surface of the original uncut sheet stock, the newly cut surfaces on opposite sides of the cutting tool will have opposite polarity of residual edge stress. If the slitting of 1" strips is considered analogous to slicing a loaf of bread, then, each strip will have a residual tension at one edge corner and residual compression at the opposite edge corner (both corners on the same surface).

It is accepted fairly widely that failures start in areas of tensile stress. During Negator functioning only one surface is cycled through large tension amplitudes. Therefore, only one corner out of four will reach the highest absolute tension stress by adding its residual tension to the tension caused by flexure of the leaf.

It is suggested that the foregoing discussion explains the marked preference for one edge of the formation of fatigue cracks in Havar Negators.

Consideration is being given to post-slitting edge treatment, such as rounding the corners and possibly inducing residual compression at the corners. Any evaluation of this would be oriented towards future extended life applications.

2.5.2 Mylar Belt Life Test. - An accelerated life test has been conducted on 2 capstan belts and 3 $I\omega$ belts, simultaneously. The capstan belts were driven by the periphery of a long drum representing the capstan pulley which ran at 3,600 rpm. This is 7.85 x the capstan speed in the Record mode. Each capstan belt passed around a separate idler, representing the motor pulley and having an adjustable position to permit independent tensioning of each capstan belt. The $I\omega$ belts were also driven by the drum, and, in similar fashion, each belt passed around a separate idler, representing the $I\omega$ pulley, which permitted independent belt tensioning.

The tension of each belt was adjusted so that slippage occurred at a minimum torque corresponding to 5 in.-oz. at the motor shaft. At the speed of the test setup, the equivalent of 4,000 R-W-P-W recorder cycles would be completed in 1,135 hours of test time. At the time of this report, 5 times this requirement has been completed without belt failure, loss of torque capacity or re-tensioning of the belts. As a matter of interest, the capstan belts have completed 8.23×10^8 flexural cycles, and the $I\omega$ belts have completed 3.9×10^8 flexural cycles.

2.5.3 Transmission Life Test. - An accelerated life test was run on a transmission system under simulated load. Because of the complexity of duplicating the continuously changing ratio of the two reel speeds, the test was run with identical speed at the two test "reels" (as in the case at center-of-tape). A schematic of this test set-up is shown in Figure 2-26. The two test "reels" are coupled together by a PIC belt, and, so, are constrained to operate at the same speed. The "Negator shaft", therefore, has no motion, and it provides the convenience of torquing by a weight hanging from a cord wrapped around a drum.

The first test was run with a "reel" speed of 900 rpm. This is 27.3 x the reel speed at center-of-tape in the Record/Playback Mode. There are 4,540 reel revolutions in one Record-Rewind-Playback-Rewind cycle, and, at 900 rpm, these are completed in 5.044 minutes. The test time to complete 4,000 R/W/P/W cycles is 336 hours.

The first test completed 412 test hours, at which time there was a failure of the belt to the "takeup reel". This represents 123% of the operational cycles required for the mission. It is, nevertheless, less than had been expected based on component derating. It is believed the test components were subjected to some dynamic load, superimposed upon the steady "Negator load". This is based on observing small

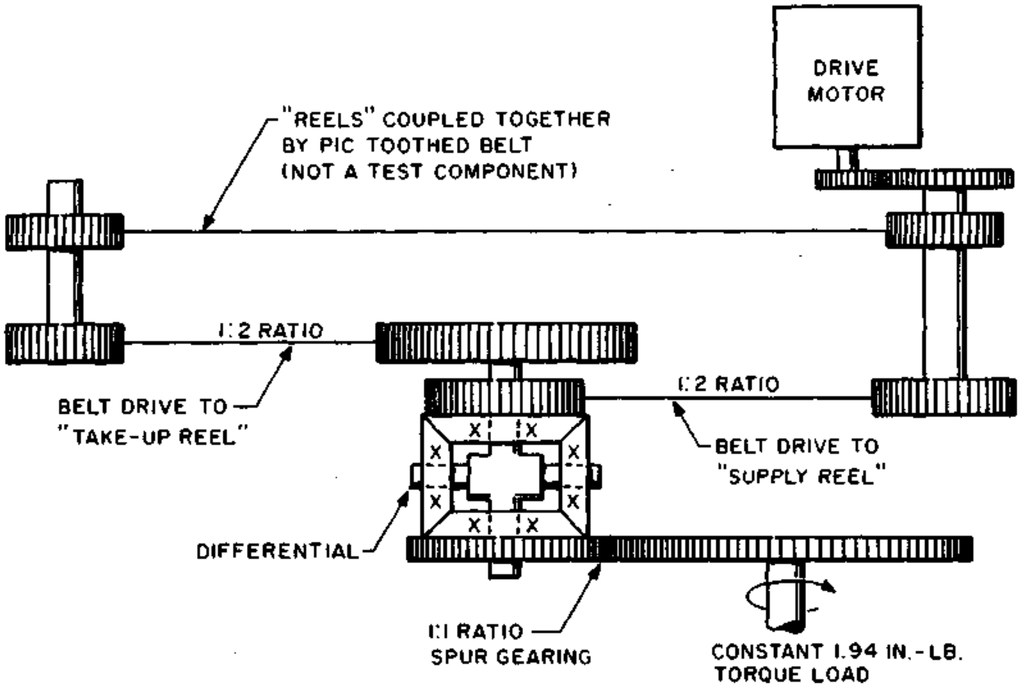

Figure 2-26 LIFE TEST SETUP FOR REEL TRANSMISSION

oscillations in the handing weight which provided the torque loading. It is possible that this dynamic load was due to the nature of the test setup. The source of this unknown load is currently under study. It is planned to resume life testing when this question has been resolved.

2.5.4 Life Test of Start-Run Relays. - A life test has been underway to evaluate the Leach, Type J, relay in its function as a start-run relay for the headwheel motor. Because of the unique character of the current and voltage being switched, no attempt was made to simulate this in a passive electrical circuit. An actual motor with a flywheel has been sequenced through a start-run-stop cycle once every minute. The motor used is an AT-70 motor operating at 250 rps, driven by 500 Hz, 20 volts peak-to-peak. This motor was used because it permitted the earliest programming of the test, and because it has a current profile and rms value very similar to that of the ERTS headwheel motor, except for the higher electrical frequency. The motor is powered by ERTS motor drive circuitry, which includes 2 Leach relays as part of its normal complement.

The test sequence was as follows:

Time, Seconds	Action
0	Relays switch to "Start", bridge circuit not energized.
1	Bridge circuit energized, motor accelerated.
3-4	Motor reaches synch speed.
7	Relay switched to "Run".
20	Bridge circuit de-energized, motor coasts to stop.
<60	Motor at rest.

The relays were tested initially and at regular intervals during the test by measuring critical parameters in accordance with MIL-R-5757D. These parameters were:

a) Contact resistance with 10 amp/6 volts contact current.

b) Pickup and dropout coil current.

c) Contact bounce with 28 Vdc across the coils.

d) Operate and release times with 28 Vdc across the coils.

The pickup and dropout currents were measured rather than pickup and dropout voltage, because it was felt these would provide a sensitive indication of relay degradation which would be less affected by temperature variations. These measurements have been made at intervals of approximately 4,000 actuate cycles. At the time of this report, 2,100 hours of testing have been completed with no evidence of any relay degradation. This represents 126,000 start-run cycles.

2.5.5 Head/Tape Life Tests. - The initial direction for the ERTS head/tape effort was based largely on experience derived from RCA's DSU Program, which requires similar, transverse-scan recording equipment operating at a head-to-tape speed of 2500 inches/second. This experience had provided an extensive background in the area of magnetic tape where considerable funds have been expended to obtain a tape binder system which would not produce excessive debris products even through a broad operating temperature range (35° F - 160° F). The tape which was proven to be most successful on the DSU Program was a product developed specifically for the application by the 3M Company. In the configuration required for the DSU Program (2" wide, 0.0075" Mylar base; coated both sides with magnetic oxide coating 0.0002" thick), this tape is assigned 3M Part No. MT-24070 and has been verified in many tests (about 12) for the specified 150 hours of head/tape contact. In the one test conducted to failure with this tape, the equipment performed for about 650 hours with failure resulting due to erosion of the gap material in the video heads.

At the beginning of the ERTS Program, efforts were undertaken with 3M to obtain a single coated version of this product, and, since many problems had been encountered with the 0.00075" Mylar base used in MT-24070, a standard 0.00092" base was selected for the ERTS tape. Finally, based on discussions with 3M technical personnel, a new back coating* was also specified for the ERTS tape. Ten reels of this tape were initially ordered to RCA Specification ERTS-564-2 (Appendix 2A), and the product was eventually assigned 3M Product No. MTA-20237.

When the tape was received, it is subjected to a 100% visual inspection and all ten reels were rated as being flight quality (vs a 20% yield for MT-24070). High temperature (150° F) tests were next run in a DSU recorder with a sample of the tape to verify that the binder system was adequate. Relative abrasivity and output measurements were also made in a standard broadcast recorder. The output of the ERTS tape measured about 2.5 dB lower than the DSU tape, and the abrasivity during 100 hours averaged about one micro-inch/hour. This wear rate is nearly equivalent to DSU levels and considerably less than the wear rate experienced with most standard video tapes.

In use, the MTA-20237 tape continued to exhibit properties superior to the MT-24070, particularly in transport handling and tape stack. Hence, tests thus far on the ERTS Program have used this tape exclusively, and, so far (over 6000 passes), no limitation in life has been found which could be attributed to the tape.

With this background in the tape area, the next major area of discussion centers on efforts undertaken on the heads and the scanning geometry. It is significant to the discussion at this point to mention that the efforts undertaken in these areas were augmented by a program for an improved DSU recorder based on the ERTS design. Hence, additional MTA-20237 tape was procured (100% yield, 10 rolls) for DSU, and an additional breadboard (1580 ips head-to-tape speed) was made available for head/tape tests. In the discussions which follow, results under both programs will be reported.

Efforts in the head and scanning geometry so far have verified improvements in three areas and have yielded unsuccessful results in one area. The initial improvement which was verified derived from a change in the head gap material from beryllium copper to alumina oxide. The latter material more closely approximates the hardness of the head material, and hence is less prone to the erosion which causes failure at

---

*Advantages of this back coating are described in 3M product sheets M-ILI37 (79.5) JO and M-VL-152(391)MP.

650 hours in the DSU test mentioned above. With the new material, no significant erosion of the gap material has been evident, even after the 1700 hour test which is discussed below.

Initial tests employing the new gap material, the new tape and the standard DSU scanning geometry were run at about the same time in the DSU and the ERTS breadboards. The heads in the ERTS unit were constructed of ferrite while those in the DSU unit were of standard alfecon. Both units exhibited pick-up on the rim of the scanning wheel at about 150 hours, and the ERTS unit failed completely (loss of at least one head output) at about 200 hours. The exact cause of the ERTS failure appeared to be due to erosion or cracking of the ferrite in the area of the gap. This failure mode is typical of earlier ferrite panels and the failure, when coupled with the extended life attained subsequently with alfecon, resulted in a de-emphasis of the efforts on ferrite. The panel in the DSU unit did not fail during 350 hours of testing, but a significant increase in drop-out rate resulted from the rim pick-up.

The next set of tests centered on minimizing the build-up of contaminants (glazing) on the rim of the headwheel. Three specific parameters were evaluated; the shoe span width (See Figure 2-27), the wheel diameter and the profile of the land on the wheel rim. Two of these parameters, the shoe span width and the wheel land profile, were modified, respectively, to reduce the overall head-to-tape pressure and to minimize the localize tape pressure on the edges of the wheel land. This configuration was tested initially in the DSU unit (terminated at 1700 hours for other tests) and subsequently in the ERTS breadboard unit (still in operation with 1600 hours as of 5/14/70). Both tests showed a significant reduction in the tendency toward glaze built-up, but in both units moderate glazing was observed at about 1000 hours. In neither test, however, did the glazing cause any significant change in drop-out count or in the level of the high frequency video response. The wear of the standard alfecon heads during the 1700 hour test amounted to only 0.0004" (vs 0.002" of wear to end of head life). Wear in the ERTS unit will not be measured until the test is terminated.

The final test which was conducted as a possibility for the reduction of wheel glazing centered on a short evaluation of a headwheel panel with an undersized wheel. In the standard configuration, the wheel size is arranged so that the wheel land will just brush the tape (size-to-size, ±0.0001"), while the heads deflect the tape into the shoe span by nearly 0.003 inches at beginning of life. This arrangement derives from broadcast experience which has shown that the close proximity of wheel-to-tape tends to damp the shock waves created in the tape by the scanning of the heads. This damping action tends to minimize geometric time base errors, especially during the interchange of tapes or headwheel panels. The test conducted for the ERTS program with the undersized wheel (no contact between wheel and tape) showed no measurable change in geometric time base errors. This arrangement is thus a possibility for further evaluation, but additional refinements of the current geometry will be evaluated before any extended testing with an undersized wheel is attempted.

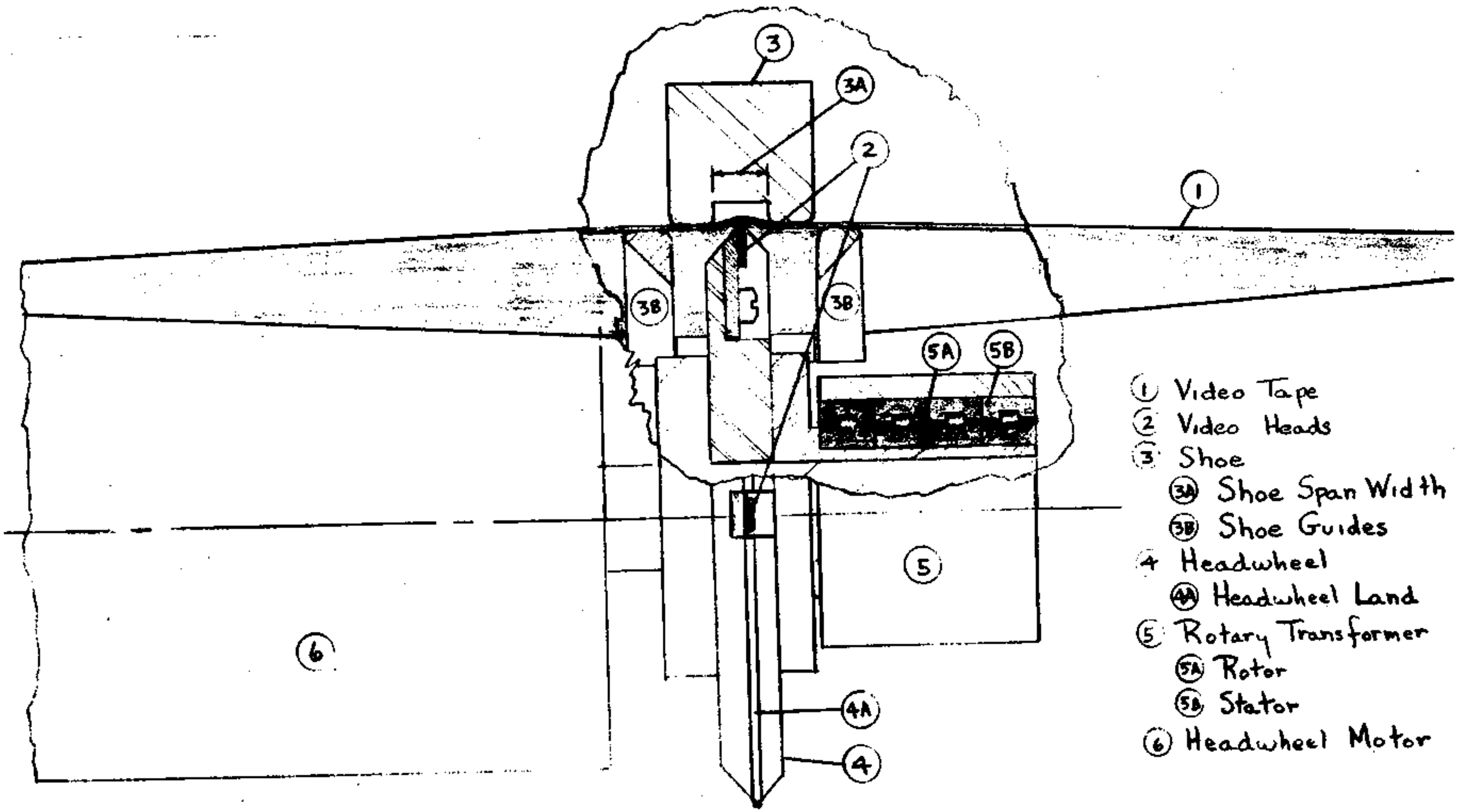

Figure 2-27 HEADWHEEL SCANNING ARRANGEMENT

Efforts are now underway to produce a headwheel in which the land profile is generated by scanning abrasive lapping tape in an otherwise normal recorder arrangement. This should produce a wheel land profile which performs with extremely uniform land to tape contact.

Additional efforts are also underway to evaluate the use of a modified alfecon material which has recently been developed by the RCA Laboratories. This material, which has been named Alfecon II, has been subjected to extensive testing by the RCA broadcast recording activity and has demonstrated a wear rate of about 1/3 that of the standard alfecon material. Initial tests with the new material on the ERTS program will center on electrical tests in the Feasibility Model, and, if satisfactory, a new life test will be undertaken in the Breadboard Unit with the new material and the new wheel land profile. The shoe span width (0.090 inches) and tape (MTA-20237) which have been proven in previous tests will be maintained during the next life test. Additional procurement and testing of tape, however, will also be undertaken to ensure that repeatable results can be attained.

2.6 Structural Considerations

2.6.1 Tape Transport

2.6.1.1 Tape Transport Deck Stress. - With its many cut-outs, holes, ribs and loading irregularities, the tape deck is impractical to analize exactly. Because of this, some assumptions were made to get a reasonable estimate of what maximum stress might occur in the plate. These assumptions are listed at the beginning of each topic.

2.6.1.1.1 Tape Deck as a Plate

A. Assume Simply Supported Plate

(ridge around perimeter, and being supported in 8 places, makes this assumption seem valid)

B. Assume an Equivalent Uniform Mass Distribution and Stiffness

(Rather even distribution of components, components having their own mounting plates, and most reinforcement ribs in the area of greater loading make this assumption also seem valid)

C. Simply Supported Plate less T-Beam.

The calculations will show that the plate is safe even without considering the support of the T-beam.

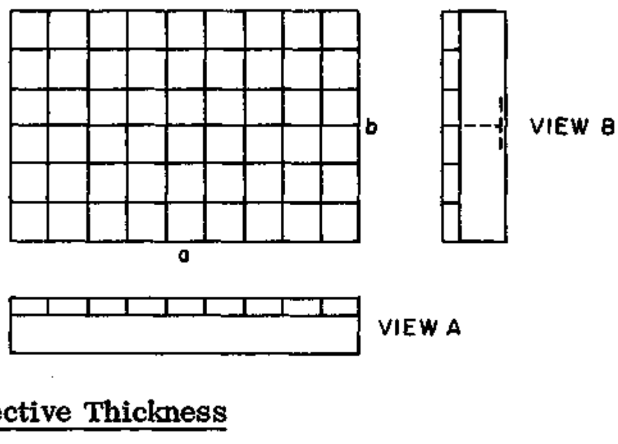

D. Effective Thickness

An effective thickness for an equivalent uniform plate was found, based on the moment of inertia of the deck.

1) View A

There appeared to be about 8, .12 inch wide by .50 inch high ridges across the plate in this sectional view.

Neutral Axis

$8\ (.12)\ (.5) = .48 \text{ in.}^2$

$(.125)\ (19.6) = 2.45 \text{ in.}^2$

$(.48)\ (.375) + (.0625)\ (2.45) = .3331 \text{ in.}^3$

$$\bar{x} = \frac{.3331}{2.93} = .1136 \text{ in.}$$

Moment of Inertia

$$I = \frac{1}{12}\ (19.6)\ (.125)^3 + 2.45\ (.1136 - .0625)^2$$

$$+ \frac{1}{12}\ (.96)\ (.5)^3 + .48\ (.375 - .1136)^2 = 5.24 \times 10^{-2} \text{ in.}^4$$

$$t_{eff} = \sqrt[3]{12I/b} = \sqrt[3]{12\ (5.24 \times 10^{-2})/19.6} = .318 \text{ in.}$$

2) View B

There appeared to be about 5, .12 inch wide by .5 inch high ridges across the plate in this sectional view.

Neutral Axis

$5\ (.12)\ (.5) = .3 \text{ in.}^2$

$(.125)\ (12.76) = 1.595 \text{ in.}^2$

$(.3)\ (.375) + (.0625)\ (1.595) = .2122 \text{ in.}^3$

$$\bar{x} = \frac{.2122}{1.895} = .1120 \text{ in.}$$

Moment of Inertia

$$I = \frac{1}{12}\ (12.76)\ (.125)^3 + 1.595\ (.1120 - .0625)^2$$

$$+ \frac{1}{12}\ (.60)\ (.5)^3 + .3\ (.375 - .1120)^2 = 3.29 \times 10^{-2} \text{ in.}^4$$

$$t_{eff} = \sqrt[3]{\frac{12\,I}{b}}$$

$$t_{eff} = \sqrt[3]{12\ (3.29 \times 10^2)/\ 12.76} = .314 \text{ in.}$$

2.6.1.1.2 Stress Concentrations. - (Machine Design, Black and Adams, pg 537)

$$r/d = \frac{.025}{.125} = .2 \qquad D/d = \frac{1.0}{.125} = 8$$

$$K_{SC} \approx 1.60$$

These curves are probably based on static loading of steel samples, but because no information was obtainable on magnesium, this value was assumed.

2.6.1.1.3 <u>Vibration of the Plate</u> (as a single-degree-of-freedom system)

2.6.1.1.3.1 <u>ω_n of the Plate (Marks, pg. 5-102)</u>

$$f = \frac{\pi}{2}\left(\frac{m^2}{a^2} + \frac{n^2}{b^2}\right)\sqrt{\frac{gD}{dh}}$$

where:

$$D = \frac{Et^3}{12\ (1-\gamma^2)}$$

$$h = t$$

$$d = \rho = \frac{P}{tab}, \text{ equiv. density}$$

P = Total weight, lb.

Lowest f:

$m = 1$,

$n = 1$

$$f = \frac{\pi}{2}\left(\frac{1}{a^2} + \frac{1}{b^2}\right)\sqrt{\frac{gE\ t^3\ ab}{12\ (1 - \nu^2)\ P}}$$

$$f = \frac{\pi}{2}\left(\frac{1}{12.76^2} + \frac{1}{19.6^2}\right)\sqrt{\frac{386\ (6.5 \times 10^6)\ (.314)^3\ (12.76)\ (19.6)}{12\ (1 - (.281)^2)\ (30.6)}}$$

$$f = 104.3 \text{ Hz}$$

$$\omega_n = (104.3)\ 2 \quad = 655 \text{ rad/sec.}$$

2.6.1.1.3.2 Vibration of the Plate on Rubber Supports

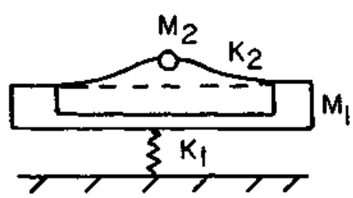

$$K_2 = \frac{W_2}{y} = \frac{Et^3}{\alpha b^2} \quad \text{(Roark, Plate Eq. No. 37, pg. 225)}$$

where

α = .1673 for a/b = 1.537 (by interpolation)

$$K_2 = \frac{(6.5 \times 10^6)\ (.314)^3}{(.1673)\ (12.76)^2} = 7{,}420 \text{ lb./in.}$$

M_2 was evaluated such that it gave the proper ωn for the plate with a concentrated mass at the center of the plate.

$$M_2 = \frac{K_2}{\omega^2} = \frac{7420}{(655)^2} = 1.731 \times 10^{-2}\ \frac{\text{lb.-sec.}^2}{\text{in.}}$$

$$M_1 = \frac{W_{total}}{g} - M_2 = \frac{30.6}{386} - 1.731 \times 10^{-2} = 6.20 \times 10^{-2} \quad \frac{\text{lb.-sec.}^2}{\text{in.}}$$

$$K_1 = 8E \left(\frac{A_1}{L_1} + \frac{A_2}{L_2} \right) \quad (E_{rubber} \approx 10^3 \text{ psi})$$

Rubber Gasket Type 1

Compression area $A_1 = \pi (.25^2 - .164^2) = .1117 \text{ in.}^2$

Thickness $L_1 = .06$ in.

Rubber Gasket Type 2

$$\text{Compression area } A_2 = (.82)(.4) + \frac{150^\circ}{360^\circ} \quad \pi(.4)^2 - \pi(.164)^2$$

$$= .453 \text{ in.}^2$$

Thickness $L_2 = .04$ in.

$$K_1 = 8(10^3)\left(\frac{.1117}{.06} + \frac{.453}{.04} \right) = 10.55 \times 10^4 \quad \text{lb./in.}$$

The resonant frequency of a two degree of freedom system is derived from:

$$\omega^4 - \left(\frac{K_1 + K_2}{M_1} + \frac{K_2}{M_2} \right) \omega^2 + \frac{K_1 K_2}{M_1 M_2} = 0$$

Vibration Theory & Applications, Thomson, pg. 162.

$$\omega^4 - \left[\frac{(10.55 + .742)}{6.20} + \frac{.742}{1.731} \right] \times 10^6 \ \omega^2 + \frac{(10.55)(.742)}{(6.20)\ (1.731)} \times 10^{12} = 0$$

$\omega_{1,2}$ = 627, 1363 rad./sec.

$f_{1,2}$ = 99.7, 217 Hz

2.6.1.1.3.3 Q of the Plate System (ξ's assumed)

ξ_1 = .25 (rubber hysteresis)

$$C1 = 2\xi_1 \sqrt{K_1 M_1} = 2(.25)\sqrt{(10.55)(6.20)\ X10^2} = 40.5\ \frac{\text{lb.-sec.}}{\text{in.}}$$

$$\omega_{n1} = \sqrt{K_1/M_1} = \sqrt{\frac{10.55}{6.20}\ X10^6} = 1305 \text{ rad./sec.}$$

ξ_2 = .08 (plate hysteresis)

$$C_2 = 2\xi_2 \sqrt{K_2 M_2} = 2(.08)\sqrt{(.742)(1.731)\ X10^2} = 1.811\ \frac{\text{lb.-sec.}}{\text{in.}}$$

ω_{n_2} = 655 rad./sec.

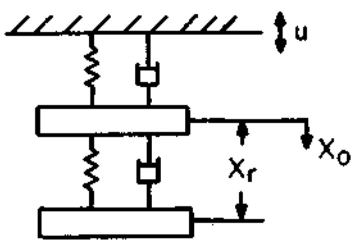

(Harris & Crede, pgs. 6-3 to 6-7)

M_2 equivalent is the effect of M_2 on M_1

$$M_2\text{ eq.} = \frac{(1-\beta_a^{\,2}) + (2\,\xi_2\,\beta_a)^2}{(1-\beta_a^{\,2})^2 + (2\,\xi_2\,\beta_a)^2}\ M_2 - \frac{2\,\xi_2\,\beta_a^{\,3}}{(1-\beta_a^{\,2})^2 + (2\,\xi_2\,\beta_a)^2}\ M_2\, j$$

1) Q for ω = 627 rad./sec.

$$\beta_a = \frac{\omega}{\omega n2} = \frac{627}{655} = .9573$$

$$\beta_a^{\,2} = .9163$$

$$M_2\text{ eq.} = \frac{(.0837) + [.16(.957)]^2}{(.0837)^2 + [.16(.957)]^2}(1.731\ X10^{-2}) - \frac{(.16)(.957)^2(1.731\ X10^{-2})j}{(.0837)^2 + [.16(.957)]^2}$$

$$M_2\text{ eq.} = 6.10\ X10^{-2} - 7.99\ X10^{-2}\ j$$

$$\frac{xo}{u} = \frac{(M_1 + M_2\text{ eq.})\ \omega^2}{-(M_1 + M_2\text{ eq.})\ \omega^2 + C_1\ \omega_j + K_1}$$

$$\frac{xo}{u} = \frac{(6.20 + 6.10 - 7.99j)\ X10^{-2}(627)^2}{-(6.20 + 6.10 - 7.99j)\ X10^{-2}(627)^2 + (40.5)(627)j + 10.55\ X10^4}$$

$$\frac{xo}{u} = .1504 - .699j$$

$$\frac{xr}{u} = \frac{M_2\ \omega^2}{-M_2\ \omega^2 + C_2\ \omega_j + K_2}$$

$$\frac{xr}{xo} = \frac{(1.731\ X10^{-2})(627)^2}{-(1.731\ X10^{-2})(627)^2 + (1.811)(627)j + 7420}$$

$$\frac{xr}{xo} = 2.50 - 4.66j$$

$$\frac{xr}{u} = \left(\frac{xr}{xo}\right)\left(\frac{xo}{u}\right) = (2.50 - 4.66j)(.1504 - .699j)$$

$$\frac{xr}{u} = -2.88 - 2.45j$$

$$Q = \left|\frac{xr}{u}\right| = \sqrt{2.88^2 + 2.45^2} = 3.78$$

2) Q for ω = 1363 rad./sec.

$$\beta_a = \frac{\omega}{\omega n2} = \frac{1363}{655} = 2.08$$

$$\beta_a^{\ 2} = 4.33$$

C2

$$M_2 \text{ eq.} = \frac{(3.33) + [.16(2.08)]^2}{(3.33)^2 + [.16(2.08)]^2} (1.731 \text{ X}10^{-2}) - \frac{.16(2.08)^3 (1.731 \text{ X}10^{-2}) j}{(3.33)^2 + [.16(.208)]^2}$$

$$M_2 \text{ eq.} = .532 \text{ X}10^{-2} - .216 \text{ X}10^{-2} j$$

$$\frac{xo}{u} = \frac{(M_1 + M_2 \text{ eq.})\, \omega^2}{-(M_1 + M_2 \text{ eq.})\, \omega^2 + C_1 \omega_j + K_1}$$

$$\frac{xo}{u} = \frac{(6.20 + .532 - .216j) \text{ X}10^{-2} (1363)^2}{-(6.20 + .532 - .216j) \text{ X}10^{-2} (1363)^2 + (40.5)(1363)j + 10.55 \text{ X}10^4}$$

$$\frac{xo}{u} = -.686 - 1.888j$$

$$\frac{xr}{xo} = \frac{M_2 \omega^2}{-M_2 \omega^2 + C_2 \omega_j + K_2}$$

$$\frac{xr}{xo} = \frac{(1.731 \text{ X}10^{-2})(1363)^2}{-(1.731 \text{ X}10^{-2})(1363)^2 + (1.811)(1363)j + 7420}$$

$$\frac{xr}{xo} = -1.288 - .128j$$

$$\frac{xr}{u} = \left(\frac{xr}{xo}\right)\left(\frac{xo}{u}\right) = (-1.288 - .128j)(-.686 - 1.888j)$$

$$\frac{xr}{u} = .641 + 2.52j$$

$$\left|\frac{xr}{u}\right| = \sqrt{.641^2 + 2.52^2} = 2.59$$

3) <u>Plate Stress</u>

For a uniformly loaded plate, the maximum stress can be expressed in terms of the displacement. (<u>Roark</u>, Plate Eq. No. 36, Pg. 225)

$$a/b = \frac{19.6}{12.76} = 1.537$$

$\therefore\ \alpha = .0863 \quad B = .497$ by interpolation

$$\sigma = \frac{B\,b^2 W}{t^2} \qquad W = \frac{Et^3 y}{\alpha b^4}$$

$$\sigma = \frac{.497\,b^2}{t^2}\left(\frac{C}{t}\right)\left(\frac{Et^3 y}{.0863\,b^4}\right) = 5.76\,\frac{EC}{b^2}\,y$$

This is the stress of the plate for the short direction (b). Since the "T" beam has the most extreme fiber, the stress in the long dimension is needed. Timoshensko gives the value of the stress in each direction which allows the stress in the long direction (a) to be found. (<u>Theory of Plates and Shells</u>, Timoshenko, pg. 120).

$$\frac{\sigma a}{\sigma b} = \frac{M_a}{M_b} = \frac{.0496}{.0830} = .597 \text{ for } a/b = 1.537$$

$$\therefore\ \sigma a = .597\,(5.76\,\frac{ECy}{b^2})$$

$$\sigma a = (.597)\,(5.76)\left(\frac{6.5 \times 10^6\,(1.25 + .112)}{(12.76)^2}\right) y$$

$$\sigma a = 1.864 \times 10^5\, y$$

for $\omega = 627$ rad./sec.

$$u = \frac{G}{\omega^2} = \frac{10\,(386)}{(627)^2} = 9.82 \text{ mils}$$

$$y = xr = \left|\frac{xr}{u}\right| u = (3.78)\,(9.82) = 37.1 \text{ mils}$$

$$\sigma b = (1.864 \times 10^5)\,(37.1 \times 10^{-3}) = 6.93 \text{ K psi}$$

$$(K_{sc})\,(\sigma b) = 11.1 \text{ K psi}$$

Fatigue Stress of AZ 31B-0 at 100,000 cycles is 20 K psi.

The factor of safety is 1.80.

This analysis is believed to be a pessimistic estimate since there are two areas of simplification which tend to elevate the calculated stresses.

The "T" beam was neglected for any additional strengthening effect although consideration of its extreme fiber stress was not neglected. The "T" beam will make the plate capable of supporting more weight, and will also increase its natural frequency which will make the amplitude of the input displacement (u) at its natural frequency smaller.

It is hoped there will be some additional damping due to the various mechanical components on the deck. A more accurate assessment will be made after an instrumented vibration survey has been completed.

2.6.1.2 Bearing Loads. - In this section, the loads on the various transport bearings are analyzed and compared with the vendor stated capability. The loads considered are the steady forces due to tension of the tape and belts, plus peak inertia forces which occur during prototype qualification testing. For this latter component, a resonant amplification of 5 is assumed to be present during the 10g peak sinusoidal sweep.

2.6.1.2.1 Guide

Radial

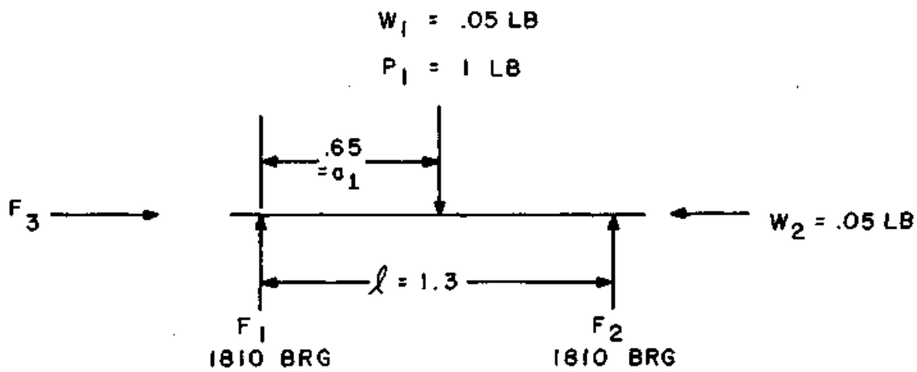

From equations of static equilibrium:

For 10g and Q of 1, $Z_1 = 10$

For 10g and Q of 5, $Z_2 = 50$

$$F_1 = \frac{(P_1 + Z_1W_1)\ (\ell - a)}{\ell} = .75\#$$

$$F_2 = \frac{(P_1 + Z_1W_1)\ a_1}{\ell} = .75\#$$

Thrust

$$F_3 = Z_2W_2 = 2.5\#$$

Capability

Bearing 1810 capable of:

Radial - 27#

Thrust - 56#

2.6.1.2.2 Reel

Radial

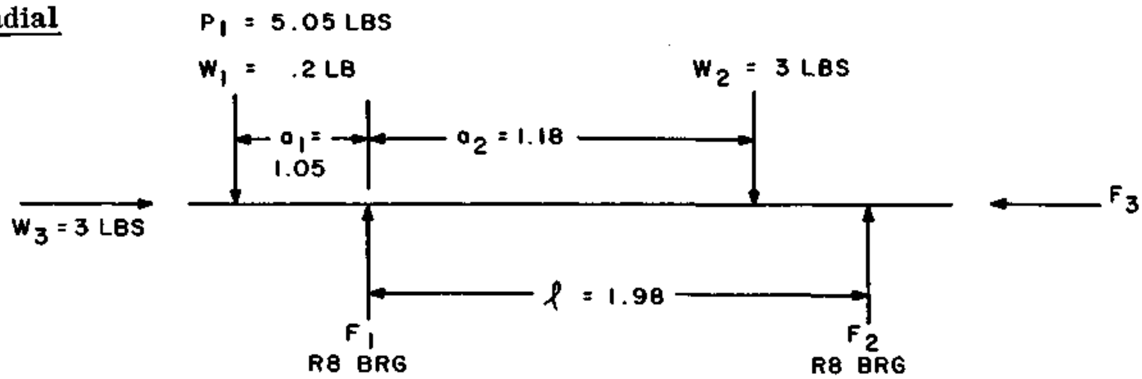

$$F_1 = \frac{1}{\ell}[(P_1 + Z_1W_1)\ (\ell + a_1) + (Z_1W_2)\ (\ell - a_2)] = 22.9\#$$

$$F_2 = \frac{1}{\ell}[Z_1W_2a_2 - (Z_1W_1 + P_1)\ (a_1)] = 14.15\#$$

Thrust

$$F_3\ Z_2 = (3)\ (50) = 150\#$$

Capability

Bearing R8 capable of

Radial - 508#

Thrust - 900#

2.6.1.2.3 Headwheel

Radial

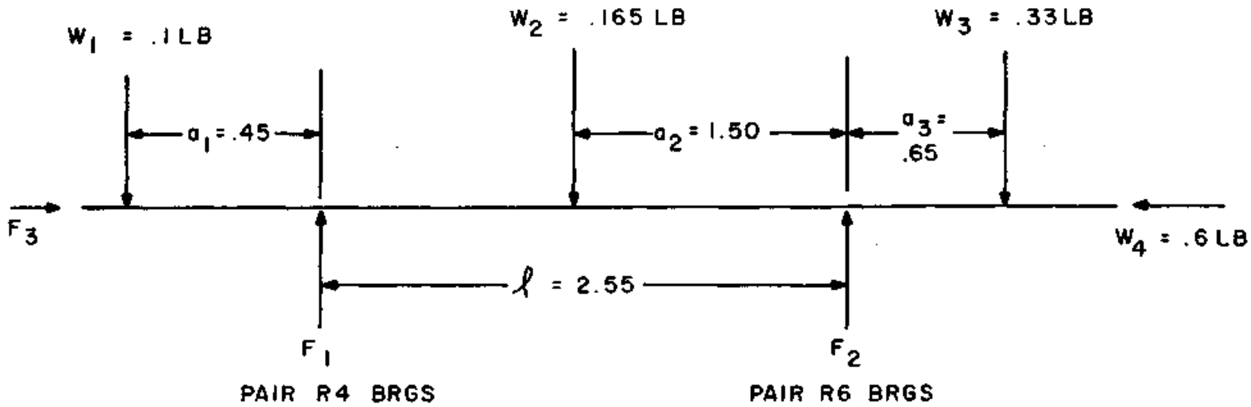

$$F_1 = \frac{W_1 (\ell + a_1) + W_2 a_2 - W_3 a_3}{\ell} = .131\#$$

$$F_1 Z_2 = (.131)(50) = 6.51\#$$

$$F_2 = \frac{W_2 (\ell - a_2) + W_3 (\ell + a_3) - W_1 a_1}{\ell} = .216\#$$

$$F_2 Z_2 = (.216)(50) = 10.80\#$$

Thrust

$$F_3 Z_1 = (.6)(10) = 6.0\#$$

Capability

Pair R6 bearings capable of

Radial - 334#

Thrust - 287#

Pair R4 bearings capable of

Radial - 140#

Thrust - 132#

2.6.1.2.4 Capstan

Radial

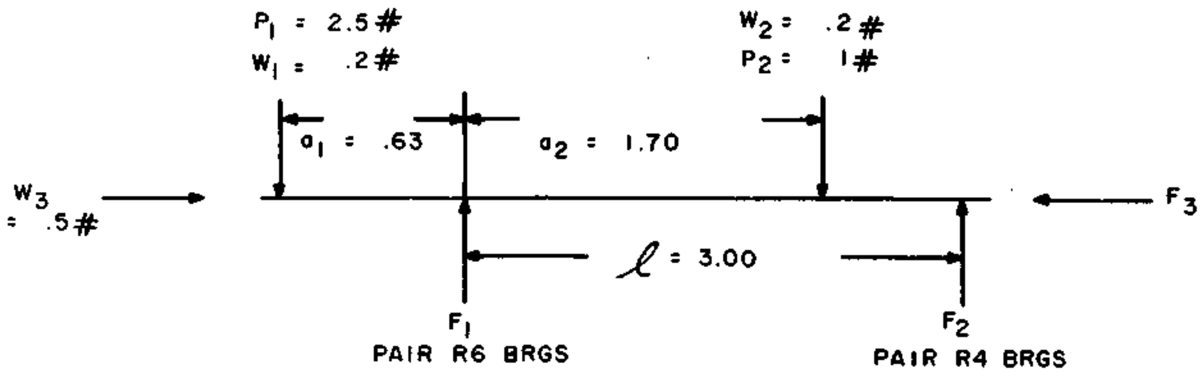

$$F_1 = \frac{1}{\ell} \left[(P_1 + Z_1 W_2) (\quad + \ell\, a_1) + (Z_1 W_2 + P_2) (\ell - a_2) \right] = 6.8\#$$

$$F_2 = \frac{1}{\ell} \left[(Z_1 W_2 + P_2) (a_2) - (P_1 + Z_1 W_1) (a_1) \right] = .75\#$$

Thrust

$F_3 Z_2 = (.5) (50) = 150\#$

Capability

Bearing pair R6 capable of

Radial - 334# each

Thrust - 273# each

Bearing pair R4 capable of

Radial - 140# each

Thrust - 125# each

2.6.1.2.5 Capstan Motor

Radial

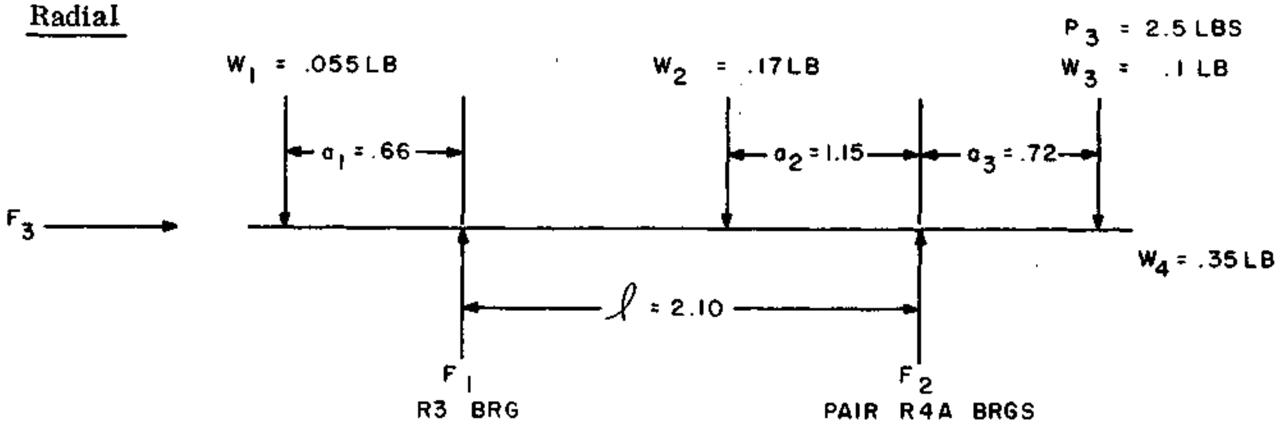

$$F_1 = \frac{Z_1W_1\,(\ell + a_1) + Z_1W_2a_2 - (P_3 + Z_1W_3)\,(a_3)}{\ell} = .46\#$$

$$F_2 = \frac{Z_1W_2\,(\ell - a_2) + (P_3 + Z_1W_3)\,(\ell + a_3) - Z_1W_1a_1}{\ell} = 5.31\#$$

Thrust

$$F_3Z_2 = (.35)\,(50) = 17.5\#$$

Capability

Bearing R3 capable of

Radial - 60#

Thrust - 105#

Pair of R4A capable of

Radial - 228#

Thrust - 210#

2.6.1.2.6 Differential

Radial

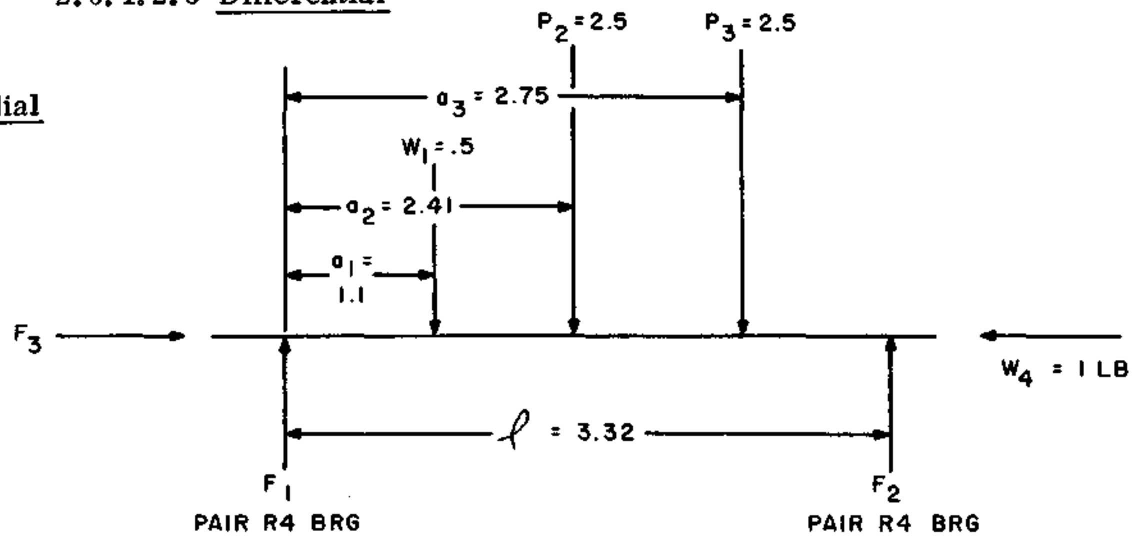

$$F_1 = \frac{Z_1W_1\ (\ell - a_1) + P_2\ (\ell - a_2) + P_3\ (\ell - a_3)}{\ell} = 4.47\#$$

$$F_2 = \frac{(Z_1W_1a_1) + (P_2a_2) + (P_3a_3)}{\ell} = 5.55\#$$

Thrust

$F_3 = 1\#$

$F_3Z_2 = (1)\ (50) = 50\#$

Capability

Bearing pair capable of

Radial - 140#

Thrust - 125#

2.6.1.2.7 Headwheel Iw

Radial

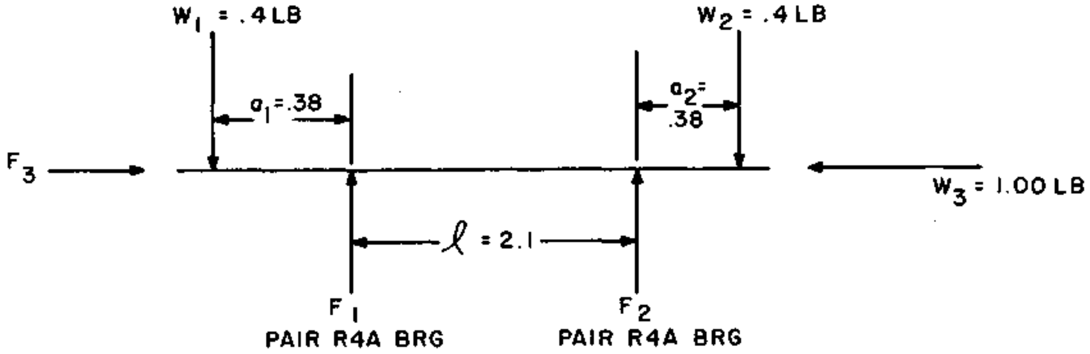

$F_1 = .4$

$F_1Z_2 = (.4)\ (50) = 20.0\#$

$F_2 = .4$

$F_2Z_2 = (.4)\ (50) = 20.0\#$

Thrust

$F_3 = 1.00\#$

$F_3Z_1 = (1)\ (10) = 10\#$

Capability

Bearing R4A capable of

Radial - 114# each

Thrust - 192# each

2.6.1.2.8 Reel Iw

Radial

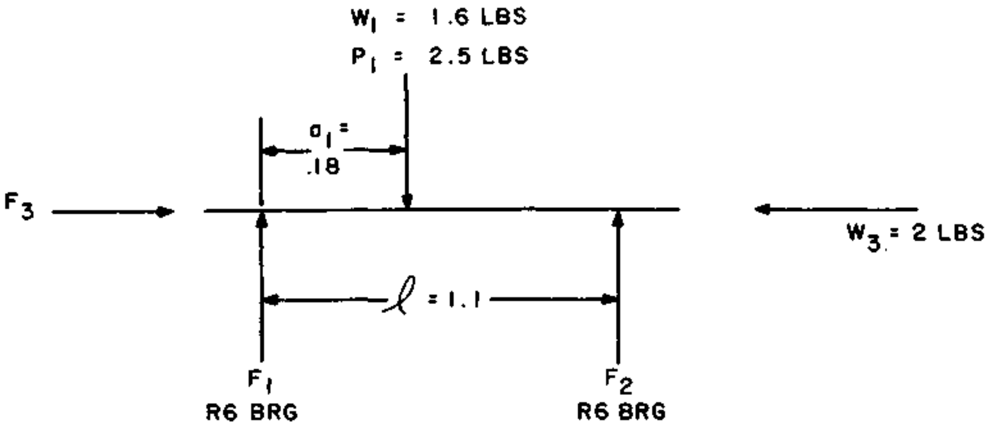

$$F_1 = \frac{(P_1 + Z_1 W_1)\ (\ell - a_1)}{\ell} = 15.5\#$$

$$F_2 = \frac{(P_1 + Z_1 W_1)\ (a_1)}{\ell} = 3.03\#$$

Thrust

$$F_3 Z_2 = (2)\ (50)\ -\ 100\#$$

Capability

Bearing R6 capable of

Radial - 167#

Thrust - 273#

2.6.1.2.9 Negator Drum

Radial

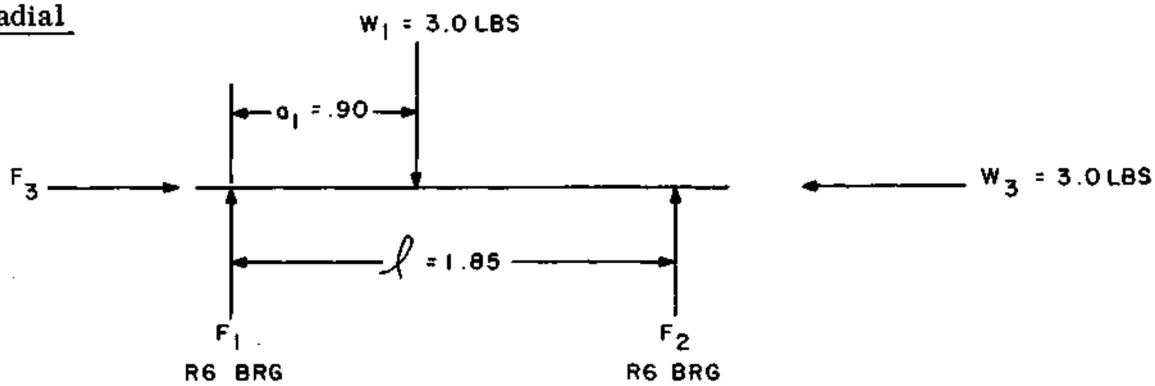

$$F_1 = \frac{W_1 (\ell - a_1)}{\ell} = 1.54\#$$

$$F_2 = \frac{W_1 a_1}{\ell} = 1.46\#$$

$$F_2 Z_1 = (1.46)\ (10) - 14.6\#$$

Thrust

$$F_3 = 3.0$$

$$F_3 Z_2 = (3)\ (50) = 150\#$$

Capability

Bearing R6 capable of

Radial - 167#

Thrust - 273#

2.6.2 Pressurized Enclosure

2.6.2.1 Stress Analysis

2.6.2.1.1 Structural Configuration

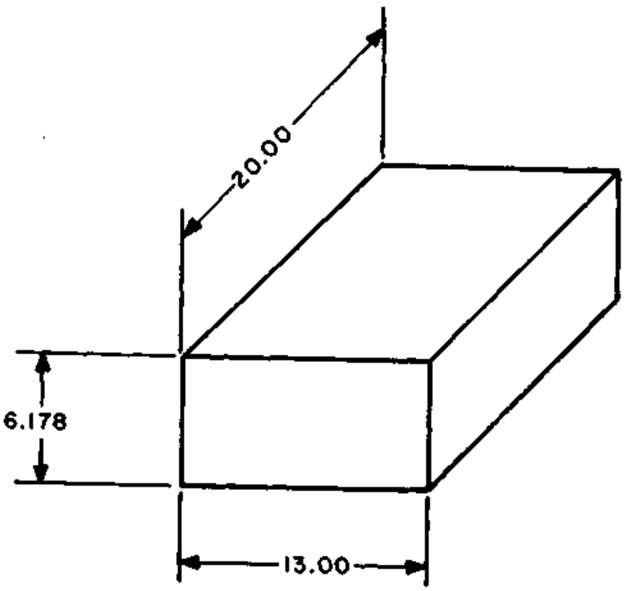

The enclosure is considered as a pressure vessel whose nominal dimensions are shown above. The highest pressure loads occur on the upper and lower walls, and consideration of their strength, stiffness, and weight has more or less controlled the structural configuration. To minimize the weight of these walls, the general approach has been to provide each wall with two thin load carrying surfaces, separated by a series of spacers, or webs. The two thin surfaces will develop the flexural stresses of a plate under a pressure load, analagous to the action of the flanges in an I-beam.

Two types of construction were considered: In the first type, the full enclosure outer shell would be machined from a solid block, with the webs integral with the upper and lower skins. An inner sheet would then be bolted at many points (46, each, top and bottom walls) to serve as the second stressed surface. In the second type of construction, shown in Figure 2-28, the total enclosure is machined from a solid block, with integral webs and flanges on the upper and lower skins.

In a comparative evaluation of the two types, it was found that the respective weights were close, with, perhaps, a small advantage in the bolted construction. The final judgement, however, was based upon the bolting concept itself. The validity of the stress analysis depends on the assumption that the clamped surfaces at the bolted junctions do not shift from their unloaded locations when load is applied. While the proposed fastened joint was designed to insure against this very situation, it was felt that it would be desirable to eliminate this consideration altogether.

B

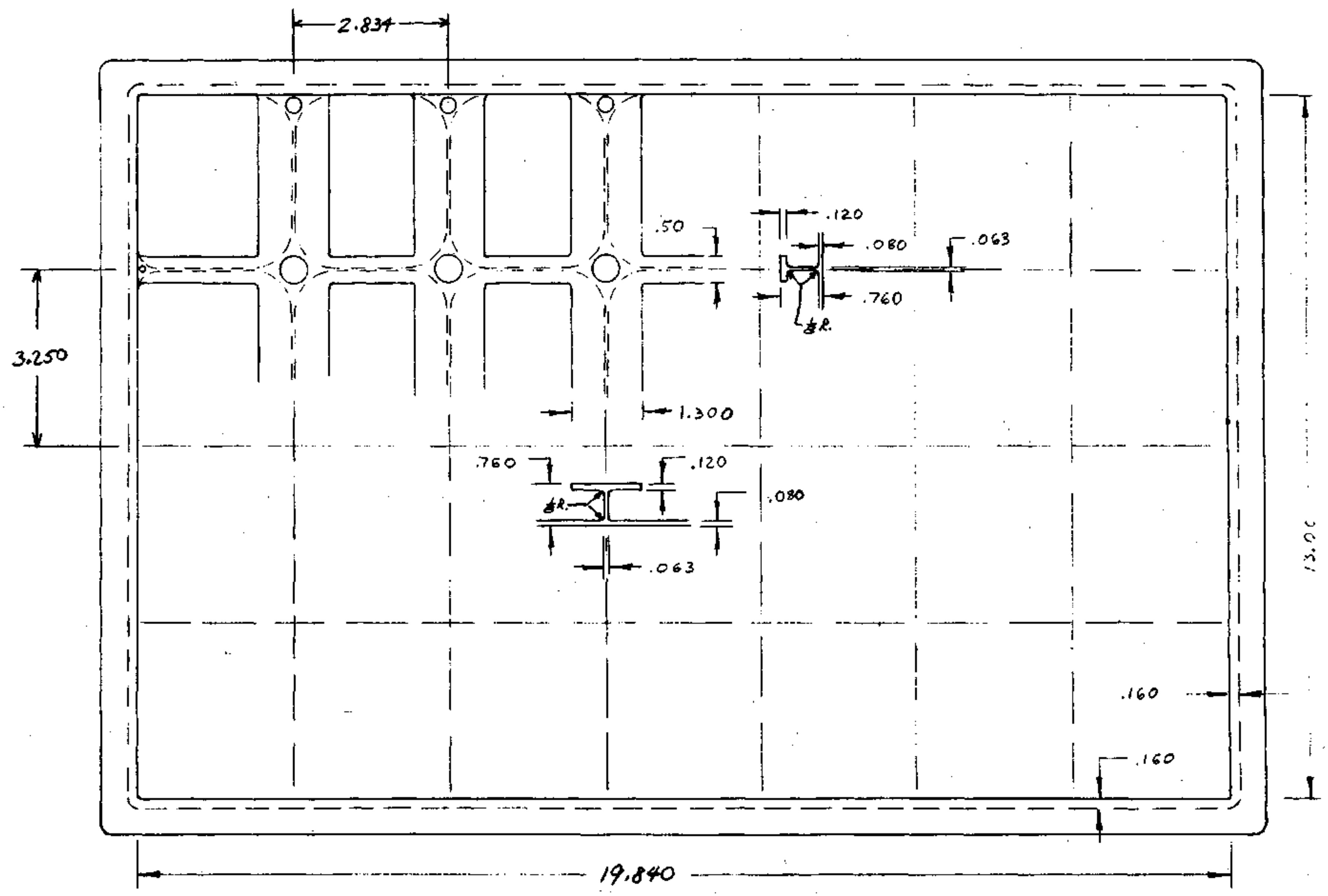

Figure 2-28. Integral Design Constructional Sketch ERTS Enclosure Second Revision

Further, tradeoffs were made in comparing the use of aluminum versus magnesium. In the design of the upper and lower walls, aluminum would have a competitive weight, but only if the outer skin thickness were of the order .045" to .050", compared to .080" for magnesium. Since the skin is formed by machining away most of a 3.7" thick plate, magnesium is preferred for a practical machining operation. In the case of the side walls and end walls, which are solid thin plates, for equal margins of safety in stress, the weight of aluminum is 1.05 greater than magnesium, and the stiffness of aluminum is 0.53 less than that of magnesium. The final material chosen for the enclosure is a ZK60A magnesium alloy hand forging. The magnesium will be in the T5 condition before machining, and will be treated to the T6 condition after all rough machining. The strength properties of this alloy are somewhat directional, relative to the direction of metal flow during forming, and the lowest value is the compressive yield stress in the transverse direction. Based upon references 1 and 2, as well as private communication with the Dow Chemical Company, this value is taken as 20,000 psi for the T6 condition.

2.6.2.1.2 Outline of Stress Analusis Procedure

(1) The upper and lower walls are considered to be joined to the side walls and analyzed as a two-dimensional problem for maximum side wall stress and maximum transverse "large plate stress" in the upper and lower walls.

(2) The longitudinal center-line deflection of the upper and lower walls are calculated as anisotropic plates with simply supported edges, for various longitudinal cross sections. The minimum longitudinal cross section is chosen by stress values based upon curvature of the deflection curve.

(3) The "small plate stress" is calculated for the upper and lower skin, considered as small plates bounded adjacent stiffener ribs.

(4) The end walls are analyzed by considering them joined to the much stiffer upper and lower walls. This is analyzed as a two-dimensional problem with the condition of the upper and lower walls having the values of deflection and slope at outboard ribs, as developed in (3) above.

(5) Summary of maximum stress values.

2.6.2.1.3 Upper, Lower and Side Walls, as a Two-Dimensional Problem

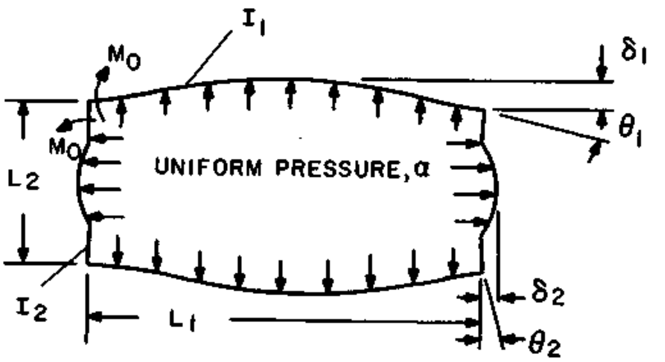

For the above rectangular flexure the boundary conditions are: the end moments and slopes are identical for both vertical and horizontal beams.

For a beam with uniform loading, α, and simply supported ends:

$$Y_m = \frac{5}{384}\frac{\alpha L^4}{E1}$$

$$Y^1{}_m = \frac{1}{24}\frac{\alpha L^3}{E1} \qquad \text{(Ref. 5, pg. 106)}$$

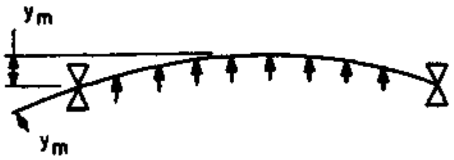

For a beam with end moments, M_o

$$Y^{11} = \frac{M_o}{E1}$$

$$Y^1 = \frac{M_o}{E1} X + C_1$$

$$Y = 1/2 \frac{M_o}{E1} X^2 + C_1 X + C_2$$

$$Y(o) = 0 \rightarrow C_2 = 0$$

$$Y(L) = 0 \qquad C_1 = -1/2 \frac{M_o L}{E1}$$

and

$$Y_m = Y(L/2) = -\frac{1}{8}\frac{M_o}{E1} L$$

$$Y^1{}_m = Y^1(0) = -\frac{1}{2}\frac{M_o}{E1} L$$

Combining the two loadings:

(1) Net tip slope, $\theta_1 = \frac{1}{24}\frac{\alpha L^3}{E_1} - \frac{1}{2}\frac{M_o L}{E_1}$

(2) Net center deflection, $\delta_1 = \frac{5}{384}\frac{\alpha L^4}{E_1} - \frac{1}{8}\frac{M_o L}{E_1}$

(3) Moment at ends of beam $= -M_o$

(4) Moment at center of beam $= \frac{1}{8}\alpha L^2 - M_o$

Imposing the condition of identical tip slopes for horizontal and vertical beams:

$$\theta_1 = -\theta_2$$

$$\frac{1}{24}\frac{\alpha L_1^3}{EI_1} - \frac{1}{2}\frac{M_o L_1}{EI_1} = \frac{1}{2}\frac{M_o L_2}{EI_2} - \frac{1}{24}\frac{\alpha L_2^3}{EI_2}$$

$$\frac{1}{2} M_o\left(\frac{L_1}{I_1} + \frac{L_2}{I_2}\right) = \frac{1}{24}\alpha\left(\frac{L_1^3}{I_1} + \frac{L_2^3}{I_2}\right)$$

and

(5) $$M_o = \frac{1}{12}\alpha L_1^2 \frac{(I_2/I_1) + (L_2/L_1)^3}{(I_2/I_1) + (L_2/L_1)}$$

For plates, the ratio (I_2/I_1) is replaced by (D_2/D_1) where D_1 and D_2 are the flexural regidities of the respective two plates. The effective flexural rigidity of the upper and lower plates is calculated below, after establishing the effective flexural width of the outer skin and the stiffener flanges.

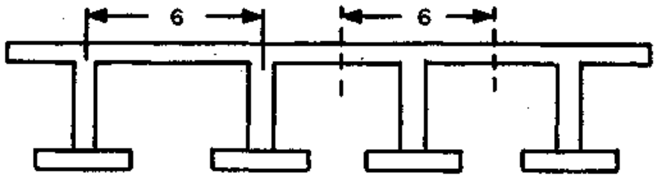

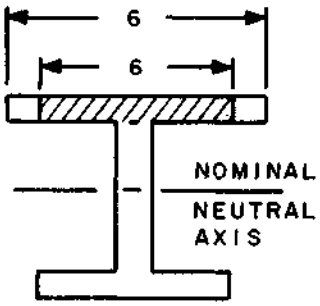

For sheet-and-stiffener construction the sheet acts as a flange, referred to the nominal neutral axis, but with an effective width less than nominal.

(b^1/b) is a function of the ratio L/b where L is the beam length; it is also dependent on the type of beam loading and end supports. The closest available analysis if for a simply supported beam with a uniform load. The values of (b^1/b) plotted in Figure 2-29, were taken from Ref. 5, pg. 136.

<u>Transverse Stiffness of Upper Wall</u>

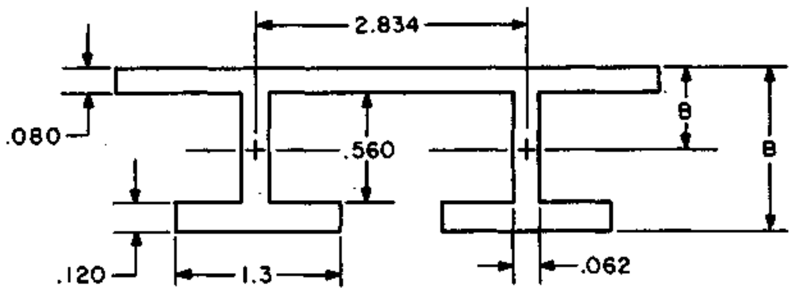

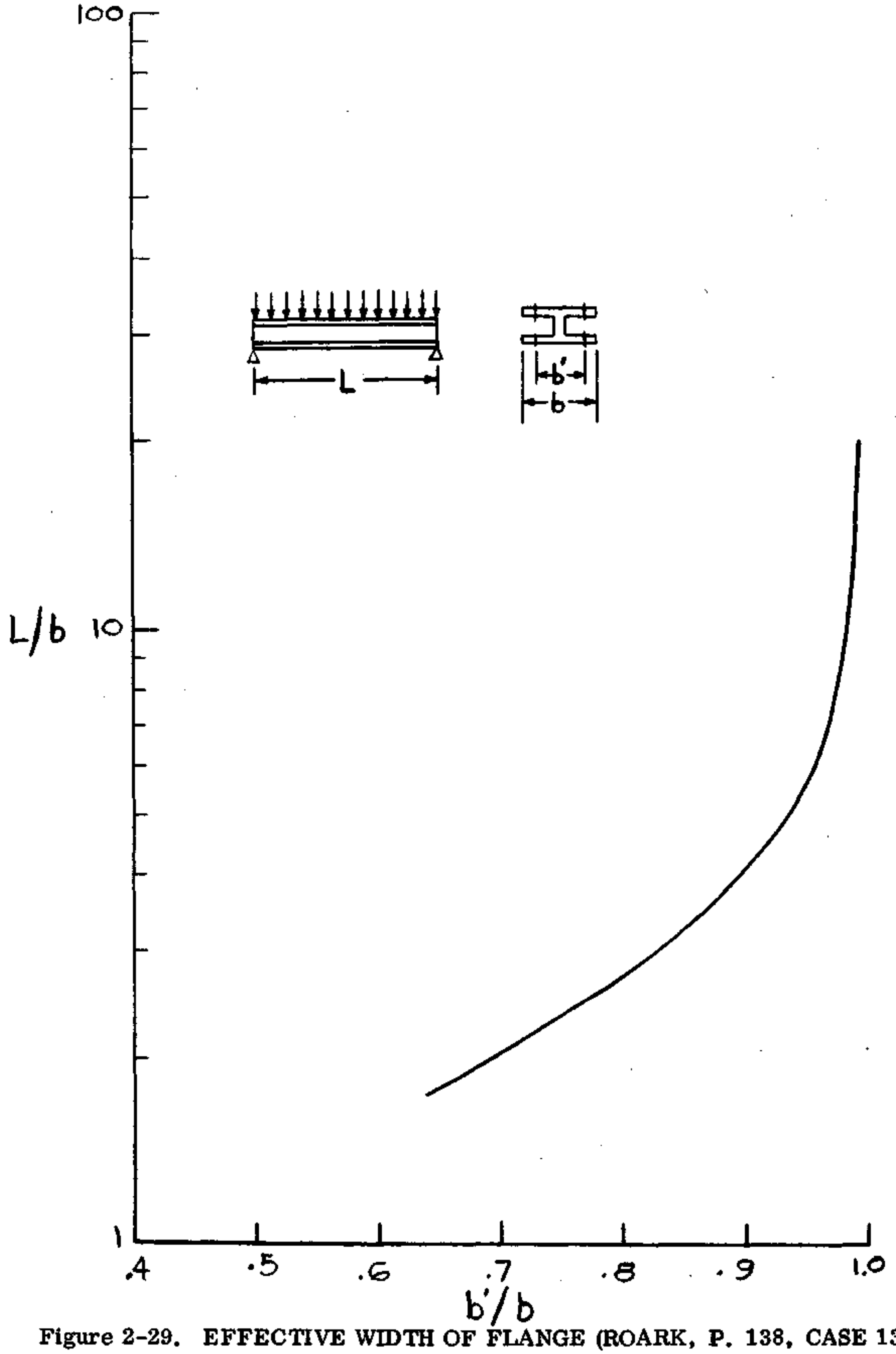

Figure 2-29. EFFECTIVE WIDTH OF FLANGE (ROARK, P. 138, CASE 13) FOR BEAMS WITH VERY WIDE FLANGES

	Area	Distance of C.G. from Top	Area Moment about Top
.080 Skin	2.834 x .080 = .226	.040	.00904
Web	.560 x .062 = .0347	.360	.01249
Flange	1.3 x .120 = .156	.700	.1090
	A = .4167		M = .1305

$$B = \frac{.1305}{.4167} = .3132''$$

<u>Skin</u>

Distance of its center from centroid = .3132 - .040 = .2732

I about centroid = $.226(.2732)^2 = .01687 \text{ in}^4$

Effective width of skin for $\frac{L}{b} = \frac{13}{2.834} = 4.58$ is $\frac{b^1}{b} = .923$

Effective I of skin = $.923 \times .01687 = .01557 \text{ in}^4$

<u>Web</u>

$$\left.\begin{array}{ll} \text{I about its own center} & = \frac{.062}{12}(.56)^3 = .0000906 \\ \text{I about centroid} & = .0347(.045)^2 = .00007 \end{array}\right\} .0001606 \text{ total for web}$$

<u>Flange</u>

I about centroid = $.156(.387)^2 = .0233 \text{ in}^4$

Effective width of flange for $\frac{L}{b} = \frac{13}{1.3} = 10$ is $\frac{b^1}{b} = .985$

Effective I = $.985 \times .0233 = .02295 \text{ in}^4$

$\Sigma I = .01557 + .0016 + .02295 = .03868 \text{ in}^4$

I per inch = $\frac{.03868}{2.834} = .01365 \text{ in}^3$

$D_1 = E \times 1/\text{inch} = 6.5 \times 10^6 \times .01365 = 88,725$ lb. in.

Extreme Fibre distance of Flange = .760 - .3132 = .4468"

Extreme Fibre distance of Skin = B = .3132"

Transverse Stiffness of Side Walls

$$D = \frac{Et^3}{12\,(1 - \nu^2)}$$

for .160" thick wall

$$D_1 = \frac{6.5 \times 10^6 \times (.160)^3}{12\,(1 - .35^2)} = 2426 \text{ lb. in.}$$

Transverse Stresses, Center of Enclosure

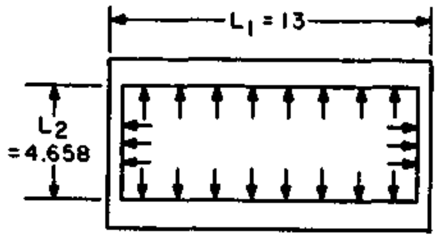

Take effective height of side wall as total distance between stiffener flanges.

$$\frac{I_2}{I_1} = \frac{D_2}{D_1} = \frac{2426}{88,725} = .0273$$

$$\frac{L_2}{L_1} = \frac{4.658}{13} = .3583$$

Using equation (5) and taking α = 17 psi pressure,

$$M_o = \frac{17(13)^2}{12} \times \frac{.0273 + (.3583)^3}{.0273 + .3583} = 45.48 \text{ in. lb./in.}$$

from equation (4).

Moment at center of side wall = $\frac{17}{8}\,(4.658)^2 - M_o = 46.11 - 45.48$

$= 0.63$ in. lb./in.

Moment at center of top wall = $\frac{17}{8}\,(13)^2 - M_o = 359.12 - 45.48$

$= 313.64$ in. lb./in.

$$\text{Maximum side wall stress} = \frac{6\ M_o}{t^2} = \frac{6(45.48)}{(.160)^2} = 10,660 \text{ psi}$$

Maximum transverse "large Plate stresses" in upper and lower walls are:

$$\text{Max Flange Stress} = \frac{313.64 \times .4468}{.01365} = 10,232 \text{ psi}$$

$$\text{Max Skin Stress} = \frac{313.64 \times .3122}{.01365} = 7,149 \text{ psi (large plate stress, only)}$$

Deflection of upper wall as a two-dimensional problem, from equation (2):

$$\delta_1 = \frac{5}{384} \times \frac{(17)(13)^4}{88,725} - \frac{1}{8} \times \frac{(45.48)(13)}{88,725}$$

$$\delta_1 = .0712 - .00083 = .0704''$$

Note, that M_o has a negligible effect on the deflection of the upper wall. It is only 1.16% less than that for a simply supported upper wall (i.e., $M_o = 0$). This will servo to justify the deflection analysis, further on, of the upper wall, considered as a simply supported plate.

The above stress calculations are reasonable, slightly pessimistic estimates of the transverse "large plate stress" in the upper, lower and side walls. To estimate the longitudinal stresses in the upper and lower walls and the effects in the end walls, the analysis can no longer be considered a two-dimensional problem. An estimate of the longitudinal deflection curve of the upper and lower walls is now required.

2.6.2.1.4 Deflection of the Upper Wall as an Anisotropic Plate

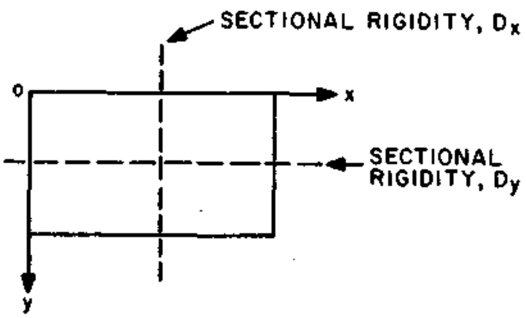

For a plate which does not have the same elastic constants in all directions, the differential equation of deflection is:

$$\text{(6)}\quad D_X \frac{\partial^4 w}{\partial X^4} + 2H \frac{\partial^4 w}{\partial X^2\, \partial Y^2} + D_Y \frac{\partial^4 w}{\partial Y^4} = \qquad \text{(Ref. 4, Pg. 365)}$$

where:

w = deflection of the plate at any point

D_x = flexural rigidity in bending in the x direction

D_Y = flexural rigidity in bending in the Y direction

$H = D_1 + 2D_{xy}$

D_1 = cross-coupling rigidity, due to the Poisson's Ratio effect ($D_1 = \nu D$ for an isotropic plate)

D_{xy} = rigidity in a twisting mode

α = the normal pressure

For a rectangular plate, simply supported at all edges, and uniformly loaded with pressure α_o, the solution is the double trigonometric series.

$$(7) \quad w = \sum_{m=1,3,5}^{\infty} \sum_{n=1,3,5}^{\infty} a_{mn} \sin \frac{m\pi X}{a} \sin \frac{n\pi y}{b}$$

where:

$$(8) \quad a_{mn} = \frac{16\,\alpha_o}{\pi^6} \frac{1}{mn\left(\frac{m^4}{a^4} D_X + 2\frac{m^2 n^2}{a^2 b^2} H + \frac{n^4}{b^4} D_Y\right)}$$

For a plate which obtains most of its stiffness from a series of ribs, the cross-coupling rigidity, D_1, can be taken as zero. Now, H can be rewritten as:

$$(9) \quad H = 2D^1_{xy} + \frac{C_1}{b_1} + \frac{C_2}{b_2}$$

where:

D^1_{xy} = twisting rigidity of the plate without the ribs $\left(= \frac{Gh^3}{12}\right)$

C_1 = torsional stiffness of a single rib in the x direction

b_1 = spacing of ribs in the x direction

C_2 = torsional stiffness of a single rib in the Y direction

b_2 = spacing of ribs in the Y direction

G = modulus of rigidity ($=2.4 \times 10^6$ for magnesium)

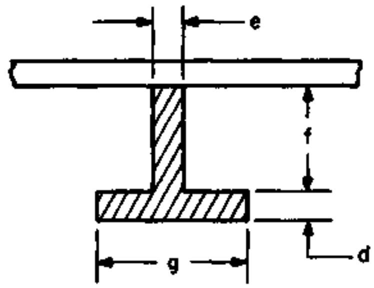

For the T-section stiffener, at left, the torsional stiffness is:

$C = KG$

where:

(10) $K = \frac{1}{3} (fe^3 + gd^3)$

This last expression is a simplification of Roark's expression (ref. 5, pg. 198), from which secondary effect terms have been dropped.

Using equations (7) and (8) deflection curves of the 20" center line were obtained by computer for 3 longitudinal ribs, 3.25" apart. Solutions were obtained for 3 different longitudinal flange widths: 1/2", 1" and 1-3/8". A solution was also obtained for the case of no longitudinal ribs to serve as reference, and also to show the need for some longitudinal stiffness. The final calculated rigidity parameters used in the four computer solutions were as follows:

Flange Width of Longitudinal Stiffener, in.	D_Y lb.-in.	D_X lb.-in.	H lb.-in.
0	88,725	277.3	856
.500	88,725	38,524	1073
1.000	88,725	66,939	1232
1.375	88,725	83,896	1372

The center line deflection curves for the four cases are plotted in Figure 2-30.

The values of the curvature of the deflection curves were also obtained by computer in order to calculate the longitudinal bending stresses in the upper wall. Sample computer runoff sheets for the deflection and curvature with 1/2" flanges are shown on the following pages.

The 1/2" wide flange is the one selected for the actual design. Its maximum center-line curvature is .00198, located 3.8" from either end.

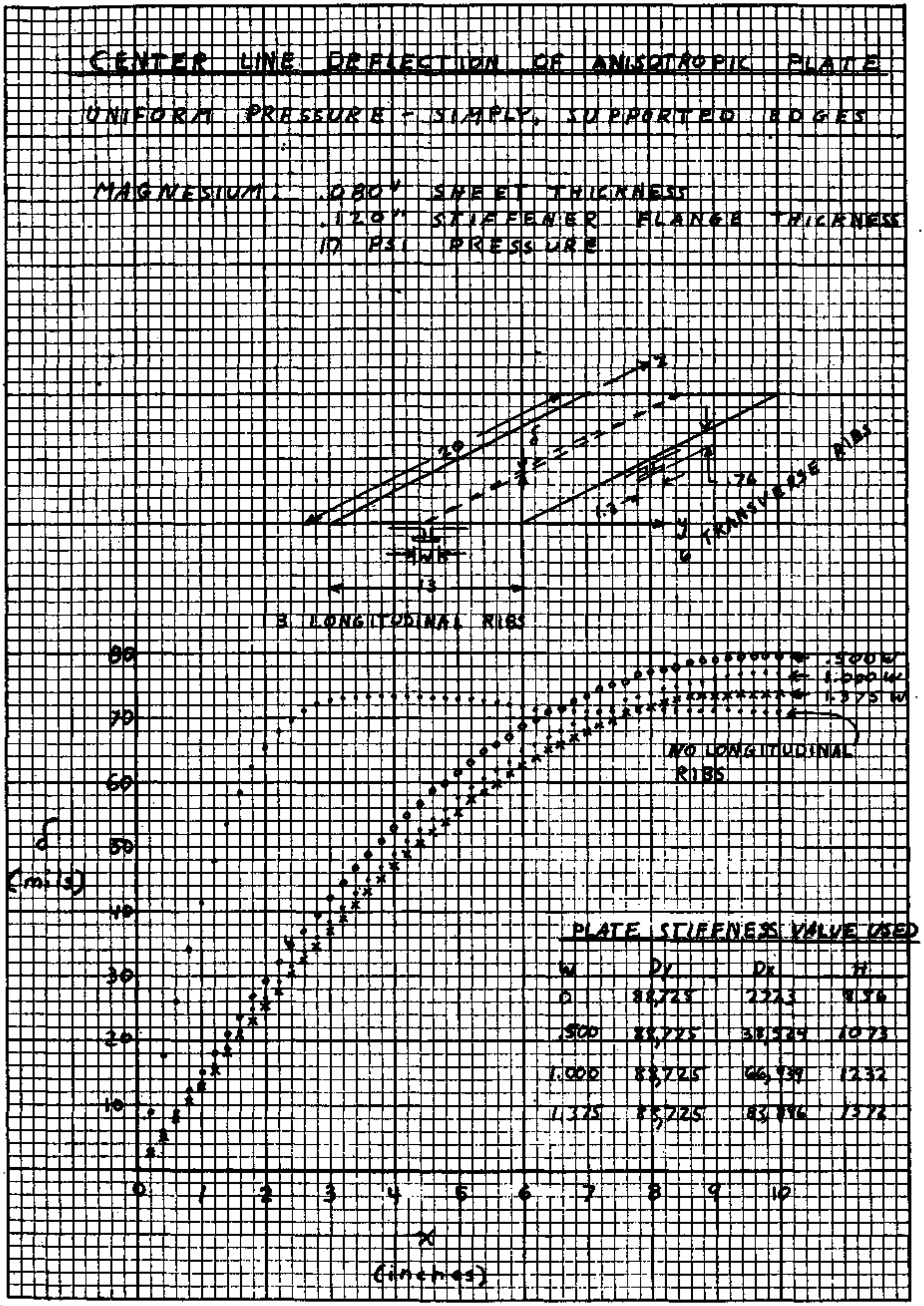

Figure 2-30. CENTER LINE DEFLECTION OF ANISOTROPIC PLATE

The longitudinal flexure stresses are obtained by combining the two basic beam equations:

$$Y'' = \frac{M}{El}$$

$$S = \frac{M_C}{I}$$

leading to:

(11) $S = E_{Y''} \times C$

For three 1/2" longitudinal flanges, the calculated neutral axis was 0.1374 from the top surface:

Outer skin "large plate stress" $= (6.5 \times 10^6)\ (.00198)\ (.1374)$

$= 1766$ psi

Flange Stress $= (6.5 \times 10^6)\ (.00198)\ (.760 - .1374)$

$= 8000$ psi

2.6.2.1.5 "Small Plate Stress". - The outer skin stresses previously calculated were essentially pure tension stresses, due to the skin acting as a flange of a web-and-flange section, 0.76" deep. The outer skin, however, is also a series of .080" thick panels between the stiffener ribs, and it will experience flexure stresses as a consequence of this.

These "small plate stresses" must be superimposed on the "large plate stresses".

The distance between the ribs along the 20" dimension is 2.86" and the distance between ribs in the 13" dimension is 2.86". Analyzing the small plates, as clamped on all edges:

$$b/a = \frac{3.25}{2.86} = 1.135$$

From Ref. 4, pg. 202 for b/a = 1.1,

$(M_X)\text{max.} = .0581\, \alpha\, a^2$ (longitudinal direction)

$(M_Y)\text{max.} = .0538\, \alpha\, a^2$ (transverse direction)

Longitudinal "Small Plate Stress"

$$(M_x)\text{max.} = .0581(17)\ (2.86)^2 = 8.07 \text{ in. lb. /in.}$$

$$S = \frac{6(8.07)}{(.080)^2} = 7580 \text{ psi}$$

Transverse "Small Plate Stress"

$$(M_Y)\text{max.} = .0538(17)\ (2.86)^2 = 7.47 \text{ in. lb. /in.}$$

$$S = \frac{6(7.47)}{(.080)^2} = 7019 \text{ psi}$$

2.6.2.1.6 Bending Moments in End Walls. - The end walls will be analyzed as a two-dimensional problem, similarly to that done for the side wall. In this analysis, however, the upper wall will be assumed to have a deflection curve between its outermost ribs identical to that previously calculated for a simply supported anisotropic plate.

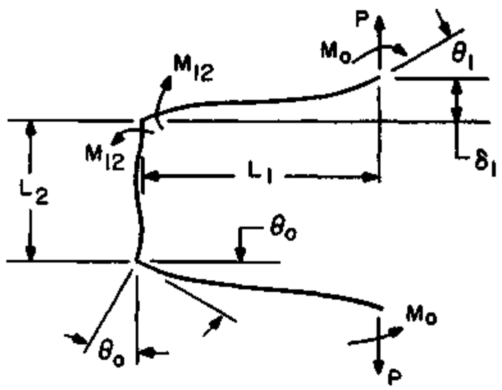

The end wall is considered as a vertical beam joined to two horizontal beams, of length, L_1, equal to the distance from the ends to the outermost ribs. δ_1 and θ_1, the tip deflection and slope, are equal to those of the upper wall center line at the outermost ribs.

Horizontal Beams

$$EI_1\ Y_1'' = P(L_1 - x) - M_o$$

$$EI_1\ Y_1' = (PL_1 - M_o)\ x - 1/2\ Px^2 + EI_1\ \theta_o$$

$$(12)\quad EI_1 Y_1 = (PL_1 - M_o)\ \frac{x^2}{2} - \frac{1}{6}\ Px^3 + EI_1\ \theta_o x$$

$$(13)\quad \text{Max. } Y_1 = \frac{1}{EI_1}\left(\frac{1}{3}\ PL_1{}^3 - M_o\ \frac{L_1{}^2}{2}\right) + \theta_o L_1$$

Vertical Beam

$$Y_2'' = \frac{1}{EI_2} M_{12}$$

$$Y^1{}_2 = \frac{1}{EI_2} M_{12}\, x + \theta_o$$

$$Y_2 = \frac{1}{2}\frac{M_{12}}{EI_2} x^2 + \theta_o x$$

$$Y_2(L_2) = \frac{1}{2}\frac{M_{12}}{EI_2} L_2{}^2 - \theta_o L_2 = 0$$

$$(14) \quad \theta_o = -\frac{1}{2}\frac{M_{12} L_2}{EI_2}$$

Using the boundary condition $Y_1{}^1 (L) = \theta_1$ and equation (14)

$$\frac{1}{EI_1}\left[P(L_1{}^2 - \frac{1}{2} L_1{}^2) - M_o L_1\right] - \frac{1}{2}\frac{M_{12}L_2}{EI_2} = \theta_1$$

and, defining $R = \left(\frac{EI_2}{EI_1}\right)$

$$(15) \quad PL_1{}^2 = 2\, M_o L_1 + 2EI_1\, \theta_1 + \frac{L_2}{R} M_{12}$$ using the boundary condition

$Y_1(L_1) = \delta_1$

$$(16) \quad PL_1{}^2 = \frac{3}{2} M_o L_1 + 3EI_1 \left(\delta_1 - \frac{1}{2}\frac{M_{12}L_2}{EI_2}\right)$$

from the summation of moments on the horizontal beam.

$$(17) \quad PL_1 = M_{12} + M_2$$

Solving (15), (16) and (17) simultaneously, and introducing the term

$$Q = \frac{EI_1 L_2}{EI_2 L_1}$$

$$(18) \quad M_{12} = \frac{EI_1}{L_1^2} \times \frac{6\,\delta_1 - 2\,\theta_1 L_1}{1 + 2\,Q}$$

$$(19) \quad M_o = 6EI_1 \frac{\delta_1}{L_1^2} \left[\frac{1 + Q}{1 + 2Q} - \frac{1}{3} L_1 \frac{\theta_1}{\delta_1} \left(\frac{2 + 3Q}{1 + 2Q} \right) \right]$$

Stresses in the End Walls. - The total moment acting on the end wall is obtained by the super-position of the effects of M_{12} and the pressure load α.

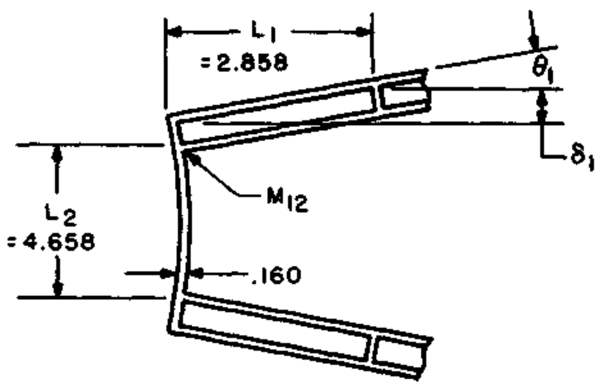

The parameter Q is evaluated with the respective values of plate flexural rigidity instead of the beam (EI)

$$Q = \frac{D_1 L_2}{D_2 L_1}$$

$$Q = \frac{88725 \times 4.658}{2426 \times 2.858} = 59.6$$

From the computer solution of the upper wall deflection curve for $x = 2.858 \approx 2.8''$

$$\delta_1 = .03964$$

and by incremental calculation:

$$\theta_1 = \frac{\Delta w}{\Delta x} \approx \frac{.00246}{.2} = .0123$$

From Equation (18),

$$M_{12} = \frac{88725}{(2.858)^2} \times \frac{6(.03964) - 2(.0123)(2.858)}{1 + 2\ (59.6)} = 15.12 \text{ in. lb./in.}$$

The end plate flexure stress due to M_{12} is:

$$S_{12} = \frac{6M_{12}}{t^2} = \frac{6 \times 15.12}{(.160)^2} = 3544 \text{ psi}$$

The maximum stress in the end wall, considered as a plate clamped on all edges, with a uniform pressure load, occurs at the edges of the plate.

$$\text{for } b/a = \frac{13}{4.658} = 2.79$$

Reference 4, pg. 202 shows negligible differences of moments and deflections for clamped plates with $b/a = 2$ and $b/a = \infty$. The maximum moment due to pressure,

$$(Mp)\max. = .0833\, \alpha\, a^2$$

$$(Mp)\max. = .0833(17)(4.658)^2 = 30.73 \text{ in. lb./in.}$$

$$\text{Max. } Sp = \frac{6(30.73)}{(.160)^2} = 7202 \text{ psi}$$

At the edges of the end wall, this stress is additive to that caused by M_{12}, and the maximum end wall stress is:

$$S = 3544 + 7202 = 10,746 \text{ psi}$$

2.6.2.1.7 Summary of Maximum Stress Values

Top Wall-Outer Skin

Transverse "Large Plate Stress"	7,149 psi
Transverse "Small Plate Stress"	7,019 psi
Total Transverse Stress	14,168 psi
Longitudinal "Large Plate Stress"	1,766 psi
Longitudinal "Small Plate Stress"	7,580 psi
Total Longitudinal Stress	9,346 psi

Stiffener Flanges

Transverse Stress	10,232 psi
Longitudinal Stress	8,000 psi
Side Wall Stress	10,660 psi
End Wall Stress	10,746 psi

2.6.2.1.8 Bibliography

1. MIL-HDBK-5A
2. Aerospace Structural Metals Handbook (AFML-TR-68-115)
3. "Magnesium Design", The Dow Chemical Company
4. "Theory of Plates and Shells", S. Timoshenko and S. Woinowsky-Krieger
5. "Formulas for Stress and Strain", R.J. Roark, 4th Edition

TO STEP 1.1^0

A	=	20
B	=	13
D1	=	38524.37
D2	=	88725
H	=	1072.746
G	=	0.137377
W(0)	=	0
W(1)	=	3.065936E-03
W(2)	=	6.123524E-03
W(3)	=	9.164561E-03
W(4)	=	0.012181
W(5)	=	0.015166
W(6)	=	0.018111
W(7)	=	0.021012
W(8)	=	0.023861
W(9)	=	0.026653
W(10)	=	0.029385
W(11)	=	0.032053
W(12)	=	0.034652
W(13)	=	0.037181
W(14)	=	0.039637
W(15)	=	0.042019
W(16)	=	0.044324
W(17)	=	0.046553
W(18)	=	0.048703
W(19)	=	0.050774
W(20)	=	0.052767
W(21)	=	0.054680
W(22)	=	0.056513
W(23)	=	0.058268
W(24)	=	0.059944
W(25)	=	0.061542
W(26)	=	0.063062
W(27)	=	0.064507
W(28)	=	0.065877
W(29)	=	0.067173
W(30)	=	0.068396
W(31)	=	0.069549
W(32)	=	0.070632
W(33)	=	0.071648
W(34)	=	0.072597
W(35)	=	0.073480
W(36)	=	0.074300
W(37)	=	0.075057
W(38)	=	0.075753
W(39)	=	0.076388
W(40)	=	0.076964
W841)	=	0.077482
W(42)	=	0.077942
W(43)	=	0.078346
W(44)	=	0.078693
W(45)	=	0.078986
W(46)	=	0.079225
W(47)	=	0.079410
W(48)	=	0.079541
W(49)	=	0.079620
W(50)	=	0.079647

$\frac{1}{2}$" Longitudinal Flange

Deflection at 0.2" Intervals

0(6)	=	-1.279509E-03
0(7)	=	-1.407438E-03
0(8)	=	-1.519092E-03
0(9)	=	-1.614896E-03
0(10)	=	-1.695938E-03
0(11)	=	-1.763680E-03
0(12)	=	-1.819688E-03
0(13)	=	-1.865043E-03
0(14)	=	-1.901749E-03
0(15)	=	-1.930573E-03
0(16)	=	-1.952588E-03
0(17)	=	-1.968513E-03
0(18)	=	-1.978863E-03
0(19)	=	-1.983601E-03
0(20)	=	-1.983100E-03
0(21)	=	-1.977175E-03
0(22)	=	-1.966103E-03
0(23)	=	-1.949910E-03
0(24)	=	-1.928839E-03
0(25)	=	-1.903251E-03
0(26)	=	-1.874426E-03
0(27)	=	-1.841830E-03
0(28)	=	-1.807371E-03
0(29)	=	-1.771608E-03
0(30)	=	-1.735147E-03
0(31)	=	-1.698965E-03
0(32)	=	-1.663528E-03
0(33)	=	-1.629721E-03
0(34)	=	-1.597009E-03
0(35)	=	-1.566415E-03
0(36)	=	-1.537451E-03
0(37)	=	-1.509860E-03
0(38)	=	-1.484179E-03
0(39)	=	-1.459452E-03
0(40)	=	-1.436030E-03
0(41)	=	-1.413818E-03
0(42)	=	-1.393282E-03
0(43)	=	-1.373957E-03
0(44)	=	-1.356797E-03
0(45)	=	-1.342036E-03
0(46)	=	-1.329766E-03
0(47)	=	-1.320755E-03
0(48)	=	-1.315423E-03

>

$\frac{1}{2}$" Longitudinal Flange

2nd Derivative at 0.2" Intervals

Incremental Calculation by

$$\frac{\left(\frac{\Delta w}{\Delta x}\right)_{n+1} - \left(\frac{\Delta w}{\Delta x}\right)_n}{\Delta x}$$

2.6.2.2 Leakage Discussion

2.6.2.2.1 Background. - A properly designed sealing system has but one source of leakage; diffusion of gases through the sealing medium. This diffusion rate is dependent upon the seal material, seal length, gases to be contained, ΔP, etc. More important, however, are the allowable flange deflections and the resulting leak rate improvement over theoretical that can be achieved by "overdesigning" the stiffness of the flanges against which the seal is made.

The ERTS enclosure represents an internal volume of 1200 cubic inches, approximately 765 cubic inches of which is gas (90% "air", 10% helium). The launch pressure is 17 psia, and no degradation of performance due to gas leakage is to occur for 15 months in orbit, following 9 months at sea level pressure. "Air" (79% N_2, 21% O_2) has been selected as the pressurizing gas since most of head/tape life data has been derived in this atmosphere.

2.6.2.2.2 Approach

a. Determine what pressure drop within the recorder is tolerable.

b. Design a seal using known diffusion rates to meet the requirements of "a" above as a minimum.

c. Determine from DSU experience the degree of flange stiffness "overdesign" to be incorporated, if any, as a reliability trade-off.

d. Define leak rate test parameters for qualification/acceptance test purposes.

2.6.2.2.3 Tolerable Pressure Drop. - The two causes of performance degradation at reduced pressures are loss of moisture (water vapor) from tape and loss of lubricant from bearings. At say 140°F, a temperature well above that which would cause permanent tape damage, the vapor pressure of water is 2.88 psia. Further, the bearing greases operating within prescribed temperature limits have vapor pressures some orders of magnitude below this pressure. It is therefore safe to set 7 psia as a low limit for safe operation, or, conversely, a pressure loss of 10 psi through the life of the recorder.

2.6.2.2.4 Seal Design by Diffusion Rates

a. From Parker Seal Handbook, diffusion rate for helium through Viton at 140°F:

$$Q_H = 21 \text{ atm cc/in./year}$$

$$Q_H = 1.28 \text{ atm in.}^3\text{/in./year}$$

b. Diffusion rate coefficients for helium and air at 140° F:

$$\lambda H = 7.0$$

$$\lambda a = 5.1$$

c. Diffusion rate for air, Q_a:

$$Q_a = Q_H \frac{\lambda a}{\lambda H}$$

$$Q_a = .932 \text{ atm in.}^3\text{/in./year}$$

d. Diffusion rates for ERTS recorder seal length:

$$L = 2(21 + 14) \times 2$$

$$L = 140 \text{ inches}$$

Total pressure differential, $\Delta P = \frac{17.0}{14.7} = 1.16$ atmospheres.

Time in orbit (15 mos.) $t = \frac{15}{12} = 1.25$ years.

Partial pressure due to air = 1.045 atmospheres.

Partial pressure due to He = .115 atmospheres.

$$Q_a = (.932)\ (140)\ (1.045)\ (1.25)$$

$$Q_a = 171 \text{ in.}^3 \text{ air/15 mos.}$$

$$Q_H = (1.28)\ (140)\ (.115)\ (1.25)$$

$$Q_H = 26.6 \text{ in.}^3 \text{ helium/15 mos.}$$

$$Q_{total} = 197.6 \text{ in.}^3 \text{ mixture/15 mos.}$$

e. Pressure drop:

$$P_2 = P_1 \frac{V_1 - Q_T}{V_1}$$

$$P_2 = 17.1\ \frac{765 - 197.6}{765}$$

$$P_2 = 12.6 \text{ psia or } \Delta P = 4.4 \text{ psi}$$

f. Flange Stiffness. - The diffusion rates used in paragraph 2.6.2.2.4 are based upon the provision that flange deflection be limited to .003". The flange stiffness required in the ERTS enclosure is, however, dictated by other considerations, such as side wall thickness required for containment of pressure and flange thickness sufficient to retain flatness and support screws. These things considered, the theoretically required bolt spacing is above 10". Based upon paragraph 2.6.2.2.5, the bolt spacing for the ERTS enclosure is nominally 2.06".

2.6.2.2.5 Actual vs. Calculated Leak Rates per DSU. - The calculated leak rate by diffusion through the DSU Viton seal material is 89.2 in.^{3}/year of the 90% N_2, 10% the gas mixture. The measured rate is 18.6 in.^{3}/year, better than 1/4 the calculated rate. Further investigation reveals that the degree of "overdesign" in the DSU flange stiffness is about 4 to 1.

2.6.2.2.6 Summary. - The leak rate based upon calculations of diffusion of gases through a Viton seal with .003" flange deflection reflect a pressure drop of 4.4 psi vs. a tolerable drop of 10 psi within the pressurized enclosure. These drops and leak rates are summarized below along with other factors as an aid in determining a realistic qualification/acceptance test criteria. The terms used are: a) calculated leakage, b) tolerable leakage - as defined above, c) expected leakage - the leakage actually expected, based upon "overdesign" of the flanges, and d) test rate - the suggested leak test criteria. Dimensions are cubic inches or pounds per square inch per 15 months at orbit environment.

a)	Tolerable leakage	$\Delta V = 451$ in.^{3}
		$\Delta P = 10$ psi
b)	Calculated leakage	$\Delta V = 197.6$ in.^{3}
		$\Delta P = 4.4$ psi
c)	Expected leakage	$\Delta V = 99$ in.^{3}
		$\Delta P = 2.2$ psi
d)	Test rate	$\Delta V = 270$ in.^{3}
		$\Delta P = 6$ psi

2.7 Mechanical Design of Electronic Subsystems

2.7.1 Circuit Board Design Parameters. - The printed circuit boards are designed according to MIL-STD-275B which covers such items as copper trace thickness and width, trace spacing for various voltages and the temperature requirements of the base material. All boards are double-sided; none use plated through holes.

2.7.2 Connectors and Harness. - The basic interconnection system used within the Transport Unit consists of a hard-wired harness and, with three exceptions, plug-in sub-assemblies. Further, as directed by GSFC, the harness contains as few (solder) connections as possible and connects the enclosure-mounted hermetic input-output connectors directly to the motor-board-mounted sub-assembly interface connectors. The selection of connectors and design of the harness incorporate the current derating requirements. Ferrules are used wherever coax conductors are broken out as protection against damage due to vibration.

2.7.2.1 Connectors. - Three basic connector types are used to interconnect the Transport Unit. These are the Deutsch DM5605 series hermetic connectors for input-output, the Continental SM and MM series for general sub-assembly interface, and the Sealectro 50 (screw lock) series for coax interfaces. All connectors in the Transport Unit are solder types, except where coax shields are secured to RF connectors.

2.7.2.2 Harness. - The harness layout, while taking careful cognizance of lead length and routing requirement, is being developed during the Engineering Model build cycle.

2.7.2.3 Wired-In Sub-assemblies. - The three hard wired parts are the pressure and temperature transducers and the Motor/Solenoid Switch assembly. As the name implies, this sub-chassis contains the start/run and run relays for the headwheel, IW, and capstan motors plus the switching circuitry associated with the headwheel solenoid. Due to the large number of high current leads required, connector interfacing of this sub-assembly is impractical. The components mounted on this sub-assembly are replaceable individually.

2.8 Thermal Considerations

Throughout the thermal analysis of the Transport Unit, convective heat transfer is assumed to be zero. Although such "blowers" as the headwheel panel, headwheel panel momentum compensator and reel momentum compensator are operating periodically, there is no assurance that any effective convective transfer will result.

2.8.1 Printed Circuit Boards. - There are six printed circuit boards within the Transport Unit enclosure. Radiation is assumed to be the only cooling means available except where provisions are specifically made for conductive cooling. These six printed circuit boards and the dissipation requirements are as follows:

1)	Video Playback Amplifier	0.5 watts
2)	Aux/Search Preamp	2.6 watts
3)	Control Track/Tach Preamp	1.0 watts
4)	Video Recorder/Preamp (2 @ 8 w)	16.0 watts
5)	Motor/Solenoid Switch	1.7 watts

2.8.1.1 Video Record/Preamp (Item 4, previous paragraph). - The four record/play preamplifier channels are packaged on two identical printed circuit boards. When installed in the Transport Unit, these two boards are "stacked" one on top of the other. Dissipation is 8 watts per board, 95% of which is due to six components (4 IC's and 2 transistors). A one channel breadboard record/preamp was subjected to temperature tests simulating the installation to determine cooling requirements.

Transistor cooling (0.6 watt/transistor) is accomplished by radiation from a relatively large area dissipator. Conductive cooling is not feasible since dc or capacitive coupling to the motor board (signal ground) creates insurmountable electrical problems.

The bulk of the board dissipation is from 4 IC's (1.6 watts/IC). Here, capacitive coupling to the motor board is not an electrical problem, and a thermally conductive path is provided directly to the motor board.

2.8.1.2 Other Electronics - The remainder of the printed circuitry in the Transport Unit (items 1,2,3,5) depends upon radiation to the Transport Unit case for heat removal. The thermal density, view factor and sink area are particularly favorable in this instance. Where individual components on these borads were found lacking in sufficient radiant area, these areas were increased by enlarging the printed copper pad upon which the component mounts and transferring heat from the component to the pad by conductive cements, screws, etc.

2.8.2 System Wattage Profile. - This section defines the thermal dissipation load of the Transport Unit. To accomplish this, the following data was accumulated:

1) Power consumption for each sub-assembly during transient and steady state operation, and Ne modes in which sub-assemblies are operative. . . . . See Table 2-3

2) Steady state power consumption by recorder modes . . . . See Table 2-4

3) Definition of the various transient time sequences as allowed by the system control logic. These data are by time, mode and occurrence . . . . See Table 2-5

4) Definition of the average power consumption during each of the transient conditions per Tables 2-3, 2-4 & 2-5 . . . . . . See Table 2-6

TABLE 2-3. POWER CONSUMPTION - BY SUB-ASSEMBLY
(IN WATTS & SECONDS)

SUB-ASSEMBLY	START	START TIME	RUN	STANDBY	RECORD	PLAY	WIND
1. HWP Motor	135	4.0	12.0				
2. Shoe Solenoid	120	0.10	2.5				
3. Iw Motor	55	4.0	6.0				
4. Capstan (L.S.)	14	0.6	8.0				
5. Capstan (H.S)	92	1.5	13.0				
6. Capstan Brake	7	1.4					
7. Video Playback Amp						1.0	
8. Aux/Search Preamp				1.3	2.6	1.3	1.3
9. Video Rec/Preamp				0.8	16.0	0.8	
10. Control Trk/Tack Preamp				0.25	0.25	0.8	0.25
11. Motor/Solenoid Sw. (normal)				0.1	0.1	0.1	0.1
12. Erase Head					1.0		
				2.45	19.95	4.0	1.65

TABLE 2-4. POWER CONSUMPTION - STEADY STATE (BY MODE)

1. Standby - continuous

HWP	-	12.0 W
Iw	-	6.0 W
Electronics	-	2.4 W
		20.4 W continuous

2. Record - 30 minutes maximum

HWP	-	12.0 W
HWP Solenoid	-	2.5 W
Capstan	-	8.0 W
Iw	-	6.0 W
Electronics	-	20.0 W
		50.8 W continuous

3. Play - 30 minutes maximum

Same as Record except:

Electronics	-	4.0 W
Other	-	28.5 W
		32.5 W continuous

4. Wind/Forward

Capstan	-	13.0 W continuous
Electronics	-	1.7 W
		14.7 W

D

TABLE 2-5. TRANSIENT TIME SEQUENCES

1/ Data Storage/Readout Modes

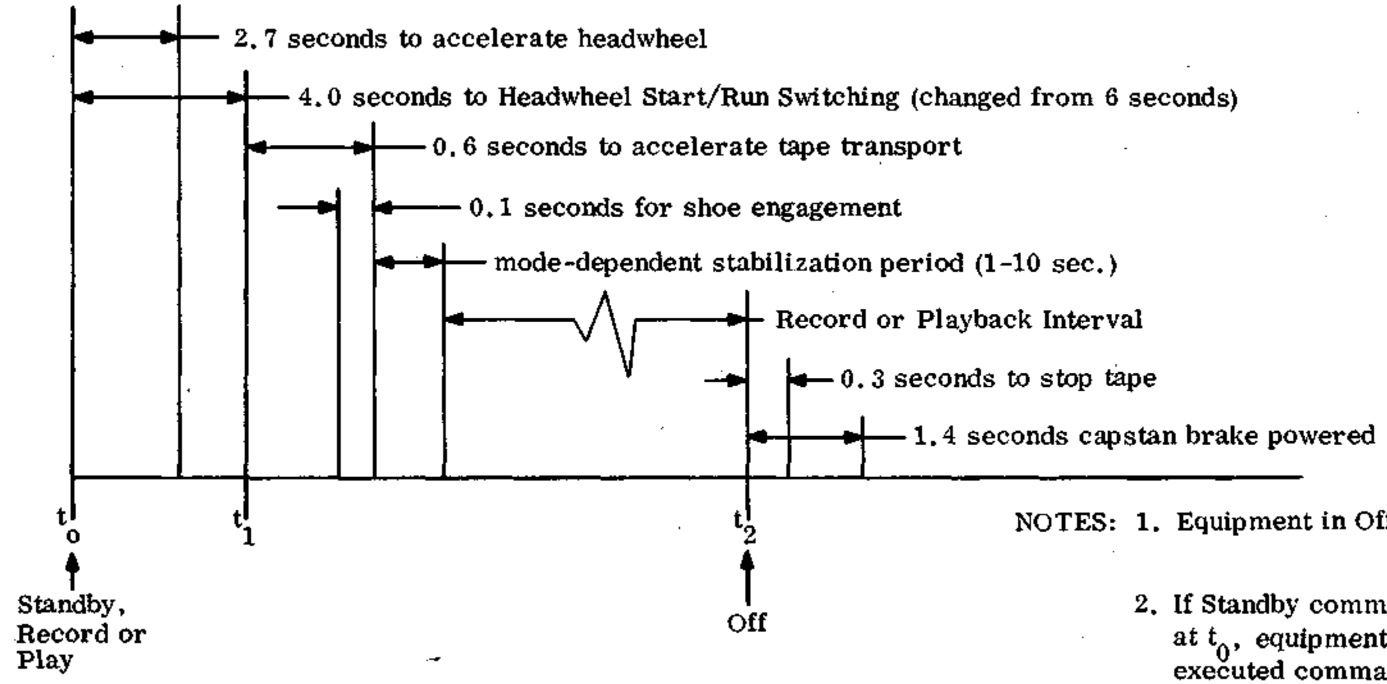

2/ Tape Shuttle Modes

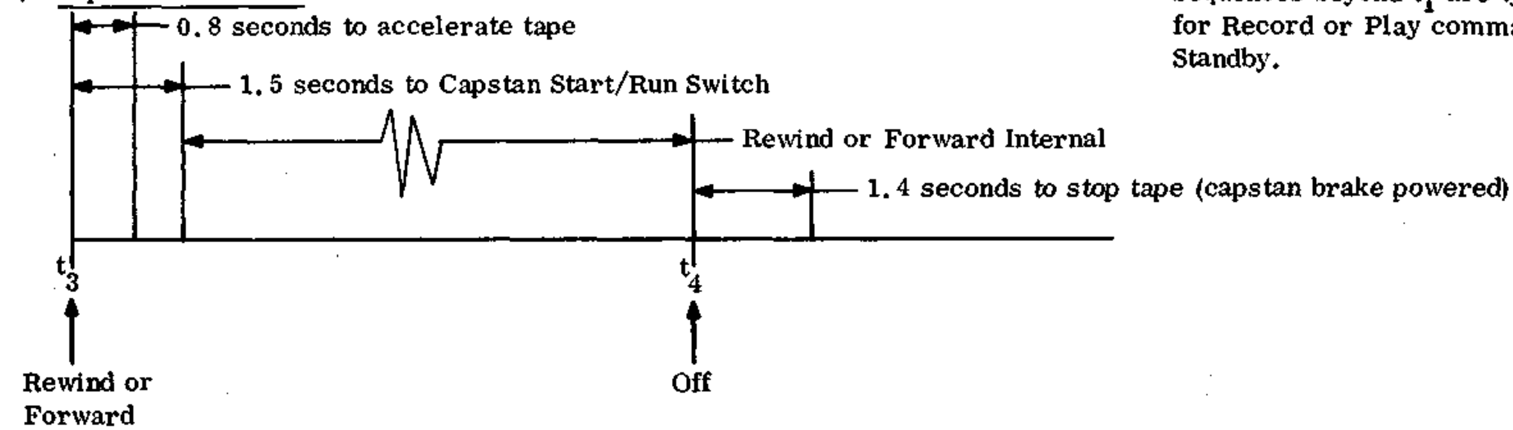

NOTES: 1. Equipment in Off at t_0, t_3

2. If Standby command is given at t_0, equipment will have executed command at t_1. Sequences beyond t_1 are typical for Record or Play command from Standby.

TABLE 2-6. DISSIPATIONS - TRANSIENT POWER
(WATTS & SECONDS)

1. Off to Standby - 5 sec. (by timer)

HWP	- Start	-	135 W for 3 sec.:	135 X 3/5 = 81.0
	Run	-	12 W for 2 sec.:	12 X 2/5 = 4.8
Iw	- Start	-	55 W for 4 sec.:	55 X 4/5 = 44.0
	Run	-	6 W for 1 sec.:	6 X 1/5 = 1.2
Electronics		-	2.4 W for 5 sec.:	2.4 X 5/5 = 2.4
				133.4 for 5 sec.

2. Standby to Record - 1.1 sec. minimum (Sense Capstan W + .5 sec. delay + .1 sec. Shoe Closure)

Capstan	- Start	-	32 W for .5 sec.:	32 X .5/1.1 = 14.5
	Run	-	8 W for .6 sec.:	8 X .6/1.1 = 4.4
HWP	- Run		12 W for 1.1 sec.:	12 X 1 = 12.0
Shoe Solenoid (Close)		-	120 W for .1 sec.:	120 X .1/1.1 = 10.9
(Hold)		-	4.8 W for 1.0 sec.:	4.8 X 1.0/1.1 = 4.4
Iw	Run	-	6 W for 1.1 sec.:	6 X 1 = 6.0
Electronics (Shoe Close)		-	22 W for .1 sec.:	22 X .1/1.1 = 2.0
(Run)		-	20 W for 1.0 sec.:	20 X 1.0/1.1 = 18.2
				72.4 for 1.1 sec.

3. Standby to Play - same as 2 above except "Electronics Run" is 4.0 W.
58.2 for 1.1 sec.

4. Record or Play to Standby - 1.4 sec. (timer)

Capstan Brake		-	7.0 W for 1.4 sec.:	= 7.0
Electronics		-	2.4 W for 1.4 sec.:	= 2.4
				9.4 for 1.4 sec.

5. Off to Forward or Wind - .8 sec. (Capstan Start Time + .5 delay)

Capstan	- Start	-	92 W for .3 sec.:	92 X .3/.8 = 35.0
	Run	-	13 W for .5 sec.:	13 X .5/.8 = 8.0
Electronics		-	1.7 W for .8 sec.:	1.7 X 1 = 1.7
				44.7 for .8 sec.

2.8.2.2 Duty Cycle. - A duty cycle of 60 seconds is thought to be a practical beginning. The definition of "off" in this discussion will be taken to be "OFF" mode. Additionally, the term "on" is defined as the mode under analysis. The purpose of this discussion is to allow comparison of transient conditions on a common basis. Therefore, the 60 second on-off cycle is defined as the time between the initiation of an electrical function by command and the completion of whatever sequence of electrical functions of control logic provides, all within the 60 second time period.

2.8.2.3 Worst Case Definition (60 second cycle). - The worst transient case is that of OFF to STANDBY to OFF. Here, the average dissipation is:

OFF-STANDBY:	(Table 2-6, Item 1)	192.4 W for 4 sec.: 192.4 X 4/60 =	12.8
STANDBY-RUN:	(Table 2-4, Item 1)	20.4 W for 54.6 sec.: 20.4 X 54.6/60 =	18.6
STANDBY-OFF:	(Table 2-3, Item 6)	7.0 W for 1.4 sec.: 7.0 X 1.4/60 =	0.2
			31.6 W

The worst case steady state condition (Table 2-4, Item 2) is that of the RECORD mode where the average dissipation is 48.5 watts.

2.8.2.4 Discussion of Results. - The worst case transient condition, based upon a 60 second on-off cycle, is 31.6 watts average for the OFF-STANDBY-OFF sequence. The likelihood of such a cycle being repeated with sufficient frequency to even approach the full 50 watt dissipation is minimal.

The worst case steady state dissipation is 48.5 watts in the RECORD modes. This condition is inescapable, and, if the T.U. is designed for 48.5 watts dissipation, the transient cycle frequencies can be shortened from the assumed 60 second limit.

2.8.3 Transport Unit Temperature Gradient. - At the start of an analysis such as this, certain objectives and assumptions must be stated. Such statements, or ground rules, are controlled by the input information available, the depth to which the analysis should be taken from a practical viewpoint, and the degree of detail required or desired in the results.

2.8.3.1 Ground Rules.

1) Internal heat originates from a constant temperature "Motor Board", i.e., no temperature gradient across the heat source. This is considered to be a conservative approach since many areas (such as PC boards and motors) will rise to an average temperature somewhat above that allowed for the motor board).

2) Radiant heat transfer occurs under the following conditions in all cases:

   a) View factor, $F_A = 1$

   b) Emmissivity, absorptivity, $F_e = 0.9$

   c) Area = inside area of T.U. enclosure.

3) There is no heat transferred through the gas mixture in the Transport Unit enclosure, either by conduction or convection.

4) A temperature gradient of zero exists across both the top and bottom halves of the T.U. enclosure, each taken individually, except as specifically stated. This is considered to be a reasonable assumption since thermal conduction through the magnesium enclosure is large compared to other thermal transfer media available (para. 2.8.3.3.2.3).

5) The sink temperature (spacecraft) is constant throughout, whether absorbing heat from the Transport Unit by conduction or radiation.

6) The analysis covers the long term steady state condition with no consideration given to the heat absorbing characteristics of the metallic elements of the Transport Unit.

2.8.3.2 Analysis.

1) Define the form factor and thermal transfer paths available - See Figure 2-31.

2) Develop an equivalent electrical circuit for steady state conditions - See Figure 2-32.

3) Define the constants required to analyze the circuit (summarized and indexed in Figure 2-32).

4) Analyze the electrical circuit, defining temperature drops, transfer paths, etc. (Figure 2-33).

5) Relate Δ t's to sink temperatures to determine adequacy of the design (paragraph 2.8.3.2.1).

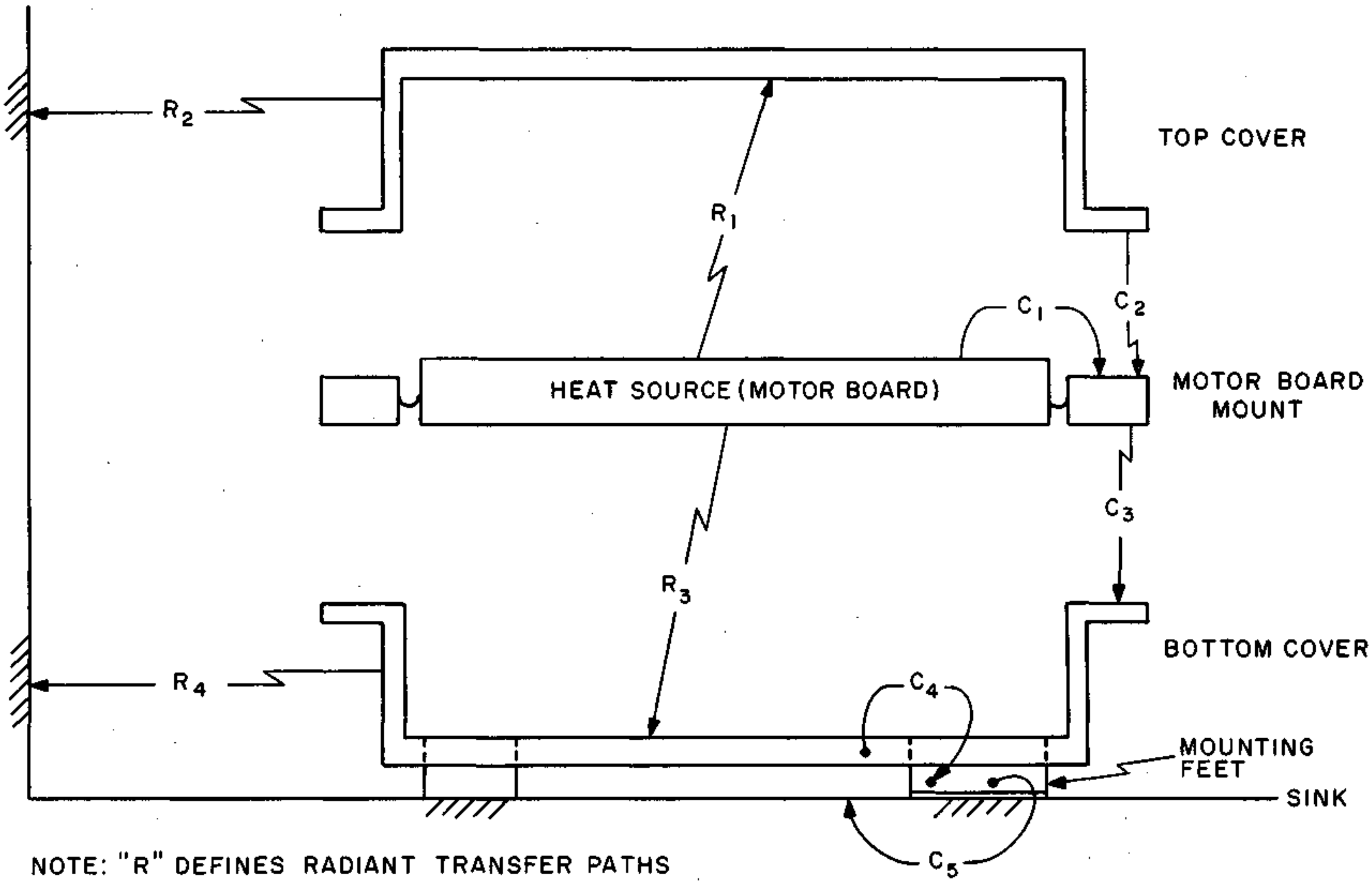

NOTE: "R" DEFINES RADIANT TRANSFER PATHS
"C" DEFINES CONDUCTIVE TRANSFER PATHS

Figure 2-31 THERMAL TRANSFER PATHS

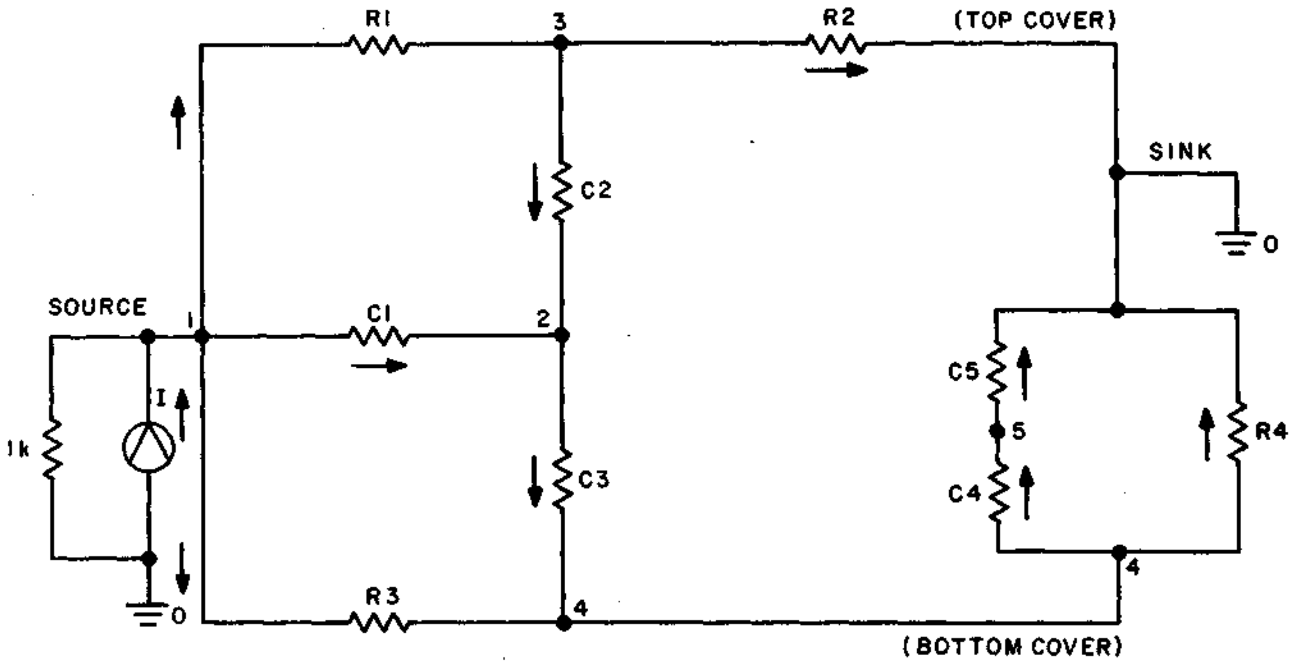

Constant	Value °F/BTU/Hr.	Ref. Paragraph	Path
R_1	.22	2.8.3.3.1.1	Rad - MB to Top Cover
R_2	.22	2.8.3.3.1.1	Rad - Top Cover to Sink
R_3	.27	2.8.3.3.1.2	Rad - MB to Bottom Cover
R_4	.27	2.8.3.3.1.2	Rad - Bottom Cover to Sink
C_1	.066	2.8.3.3.2.1	Cond - MB to MB Support
C_2	.047	2.8.3.3.2.1	Cond - MB Support to Top Cover
C_3	.047	2.8.3.3.2.2	Cond - MB Support to Bottom Cover
C_4	.037	2.8.3.3.2.4	Cond - Bottom Cover to Mtg. Feet
C_5	.036	2.8.3.3.2.5	Cond - Mtg. Feet to Sink

$I = Q =$ heat load

$Q = 50.8$ watts

$Q = 173$ BTU/Hr.

Figure 2-32 EQUIVALENT CIRCUIT & CONSTANTS

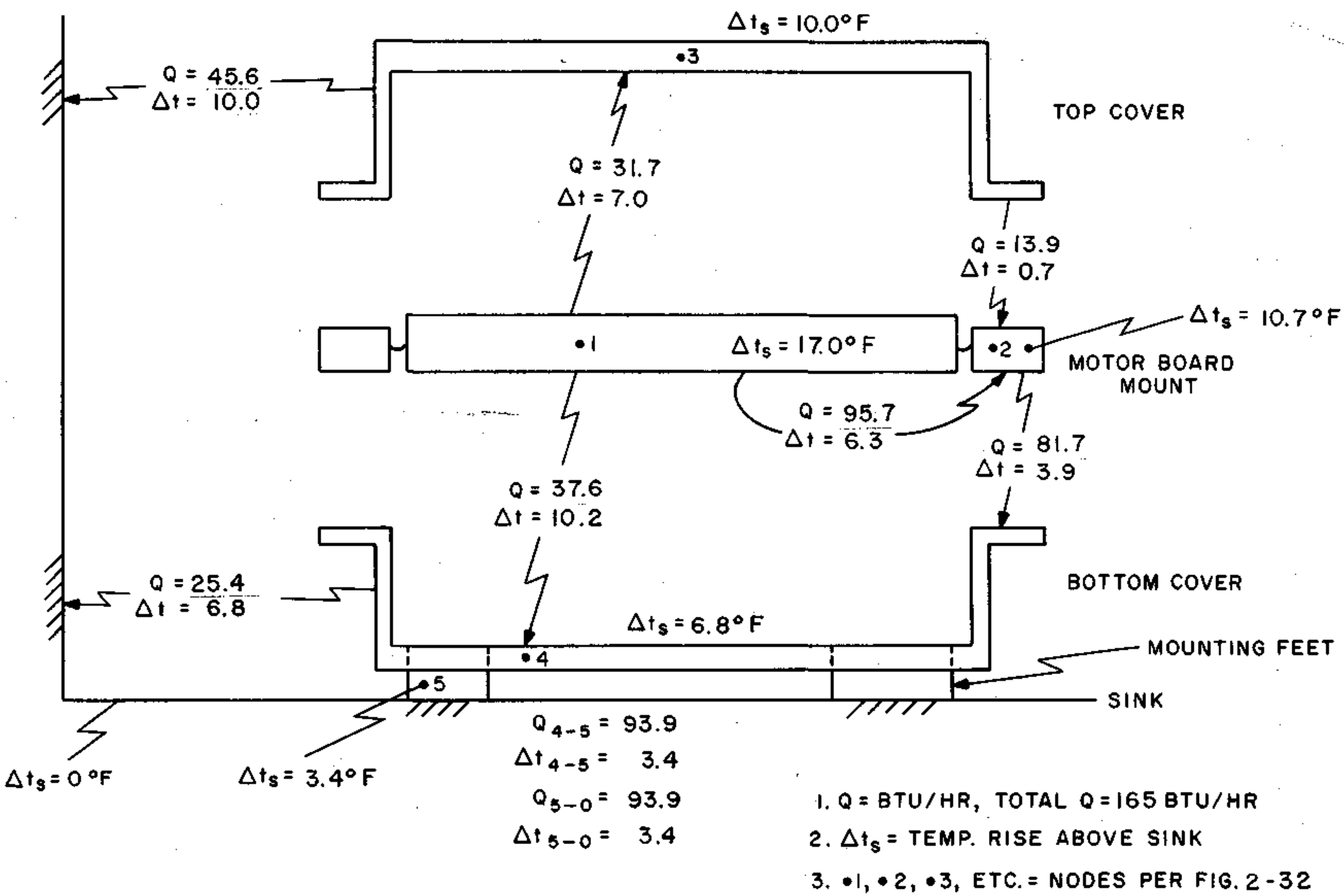

Figure 2-33. Temperature Gradient, Heat Flow

2.8.3.2.1 <u>Discussion of Results.</u> - This analysis is a "first cut" at the worst case with no allowances made for thermal absorbtivity of the metallic parts of the Transport Unit. This is considered to be a conservative approach. More detailed analysis will be undertaken as time and updated inputs become available.

The present analysis shows a maximum rise above sink of 17.0° F at the motor board. Applied to the Nimbus thermal-vacuum qualification temperature maximum of 45°C (113°F), this results in a maximum temperature at the motor board of 130° F.

Considering the assumptions, this figure is considered satisfactory.

2.8.3.3 <u>Definition of Transfer Constants.</u> - In order to make use of dc circuit equations and the equivalent circuit of Figure 2-31, transfer constants in the form of °F per BTU per hour are derived or stated below, and summarized in Figure 2-32.

2.8.3.3.1 <u>Radiation Constants R_1, R_2, R_3, R_4</u>

from: $$Q = .173\ F_e\ F_A\ A \left[\left(\frac{T1}{100}\right)^4 - \left(\frac{T2}{100}\right)^4 \right]$$

2.8.3.3.1.1 <u>Define R_1 = R_2</u>

$$\left(\frac{T2}{100}\right)^4 = \left(\frac{T1}{100}\right)^4 - \frac{Q}{.179\ F_A\ \ F_e\ \ A}$$

T_1 = 119°F: Motor board temperature assumed maximum value to permit maximum internal gas temperature of 125°F.

A = 3.56 ft.^{2}: enclosure area

Q = 10 BTU/Hr.

T_2 = Resultant wall temperature

$$\left(\frac{T2}{100}\right)^4 = \left(\frac{579}{100}\right)^4 - \frac{10}{(.179\ (1)\ (.9)\ (3.56)}$$

T_2 = 116.8°F

Δt = 2.2°F for 10 BTU/Hr.

Δt = .22°F/BTU/Hr.

R_1 = R_2 = Δt = .22°F/BTU/Hr.

2.8.3.3.1.2 Define $R_3 = R_4$. - (same as R_1 except A = 3.00, bottom cover area)

T_2 = 116.3°F

Δt = 2.7°F for 10 BTU/Hr.

Δt = .27°F/BTU/Hr.

$R_3 = R_4 = \Delta t =$ .27°F/BTU/Hr.

2.8.3.3.2 Conduction Constants - C_1 through C_5

2.8.3.3.2.1 C_1 - Motor Board to MB Support. - This path is via 8 mounting points which provide electrical isolation of the motor board (signal ground) from spacecraft ground. The insulating material is silicone rubber with a thermal conduction coefficient of 23 BTU/Hr./ft.^{2}/in./°F. Experimental determination of the overall transfer constant for the mounting point assembly is as yet incomplete. However, sufficient confidence has been achieved to introduce the stated conduction coefficient into this analysis.

$$Q = \frac{kA\Delta t}{L}$$

k = 23 BTU/Hr./ft.^{2}/in./°F

A = .47 in.^{2}/pad

L = .04"

$$Q = \frac{(23)\ (.47 \text{ X } 8)\ (1)}{(.04)\ (144)}$$

Q = 15.1 BUT/Hr./°F

$$C_1 = \frac{1}{15.1} = .066°\text{F/BTU/Hr.}$$

2.8.3.3.2.2 C_2, C_3 - Motor Board Mount to Top and Bottom Covers

$$Q = kA\Delta t$$

k = transfer constant = .3 watts/in.^{2}/°C based upon RCA Hightstown test work and experience for dry aluminum to magnesium interface at 100 to 200 psi interface pressure.

$k = .3 \text{ watts/in.}^2/°C = .68 \text{ BTU/Hr./°F}$

A = interface area = 31.52 in.^2/side

$\Delta t = 1°F$

$Q = (.68)\ (31.52)\ (1)$

$Q = 21.4$ BTU/Hr./°F per side

$$C_2 = C_3 = \frac{1}{21.4} = .047°F/BTU/Hr.$$

2.8.3.3.2.3 C_{-} - Down Side Walls of Cover

$$Q = \frac{kA\Delta t}{L}$$

$A = \text{area} = (.140)(19.8)\ (13)\ (2)$

$A = 72 \text{ in.}^2$

$k = 1100 \text{ BTU/Hr./ft.}^2/°F/in.$ (magnesium)

L = 2.5" maximum

$\Delta t = 1°F$

$$Q = \frac{(1100)\ (72)\ (1)}{(2.5)\ (144)}$$

$Q = 220$ BTU/Hr./°F

$C = \frac{1}{220} = .0045°F/BTU/Hr.$ - This value is roughtly one order of magnitude below all other conduction constants and was therefore not used in the final analysis.

2.8.3.3.2.4 C_4 - Bottom Cover to Mounting Pad

$$Q = \frac{kA\Delta t}{L}$$

A = area through which thermal conduction can occur between the side and bottom walls of the cover and the mounting pad.

$A = .915 \text{ in.}^2/\text{pad}$

$k = 1100 \text{ BTU/Hr./ft.}^2/°F/\text{in.}$ (magnesium)

$$Q = \frac{(1100)\ (.915)\ (4)\ \Delta t}{(144)\ (1)}$$

$Q = 28 \text{ BTU/Hr./°F}$ for 4 mounting pads.

$C4 = \frac{1}{28} = .037°F/\text{BTU/Hr.}$

2.8.3.3.2.5 C_5 - Mounting Pad to Sink

$Q = kA \Delta t$

k = transfer constant = 3 to 5 watts/in.^{2}/°C, 200 psi interface pressure with thin coating of DC4 or RTV material.

$k = 6.8 \text{ BTU/Hr./in.}^2/°F$

$A = 1 \text{ in.}^2$ per pad

$A = 4 \text{ in.}^2$

$Q = (6.8)\ (4)\ (1)$

$Q = 27.2 \text{ BTU/Hr./°F}$

$C_5 = \frac{1}{27.5} = .036°F/\text{BTU/Hr.}$

2.9 Weight and Power Consumption Summaries

Table 2-7 contains the most recent summary of the Transport Unit weight. The current tabulation for this unit, when combined with the estimated Electronic Unit weight of 27.2 lbs., yields a projected recording system weight of 69.93 lbs. exclusive of interconnecting cables. The E.U. weight, however, is still based largely on estimates.

Figure 2-33 reflects the power profile for the total VTR. The power surges, exclusive of the spikes, are consumed largely in the Transport Unit during start-up of the varous motors. These surges have been considered in estimating power consumption of the Transport Unit for the T.U. thermal analysis, and, are discussed in paragraph 2.8.2.9.

TABLE 2-7. WEIGHT CONTROL REPORT, TRANSPORT UNIT

ASSEMBLY NAME	DRAWING NUMBER / SERIAL NUMBER	UNIT WHT TARGET	QTY PER EQUIP	TOTAL TARGET EQUIP WHT	ESTIMATED/ACTUAL WEIGHTS									
					7 AUG 69	10 SEPT 69	15 NOV 69	2 FEB 70	14 May 70					
REEL ASSEMBLY			QTY	(2)	4.0 E	4.0 A	4.0 A	4.00 A	4.00 A					
DIA SENSING			QTY	(2)	.60 E	.60 A	.60	.60 A	.60 A					
TAPE GUIDES			QTY	(5)	.90 E	.80 A	.80 A	.80 A	.80 A					
ERASE HEAD					.25 E	.25 E	.25 E	.25 E	.20 A					
H.W. PANEL					2.60 E	2.60 E	2.35 A	2.35 A	2.35 A					
AUX HD					.25 E	.25 E	.25 E	.25 E	.25 E					
CAPSTAN					.50 E	.47 A	.47 A	.47 A	.47 A					
CAPSTAN MTR					1.80 E	1.40 A	1.40 A	1.40 A	1.40 A					
DIFF/NEG ASSY.					5.00 E	5.00 E	4.35 A	4.35 A	4.35 A					
H.W. IW					2.60 E	2.00 A	2.00 A	2.00 A	2.00 A					
REEL IW					1.50 E	1.70 A	1.70 A	1.70 A	1.70 A					
TAPE DECK					4.60 E	ALUMIN 8.50 A	ALUMIN 8.50 A	MAG. 6.00 E	MAG 4.80 A					
TAPE					2.90 E	2.90 E	2.90 E	2.90 E	2.90 E					
CASE & FRAME					10.3 E	10.3 E	10.9 E	11.10 E	11.71 A					
CONNECTORS					.50 E	.50 E	.50 E	.50 E	.50 E					
MODULES, WIRING					3.70 E	3.70 E	3.70 E	3.70 E	3.70 E					
MISC					1.0 E	1.0 E	1.0 E	1.00 E	1.00 E					
TOTAL WEIGHT					43.00	45.97	45.67	43.37	42.73					

AED-873 9/64

FOLDOUT FRAME -1

FOLDOUT FRAME 2

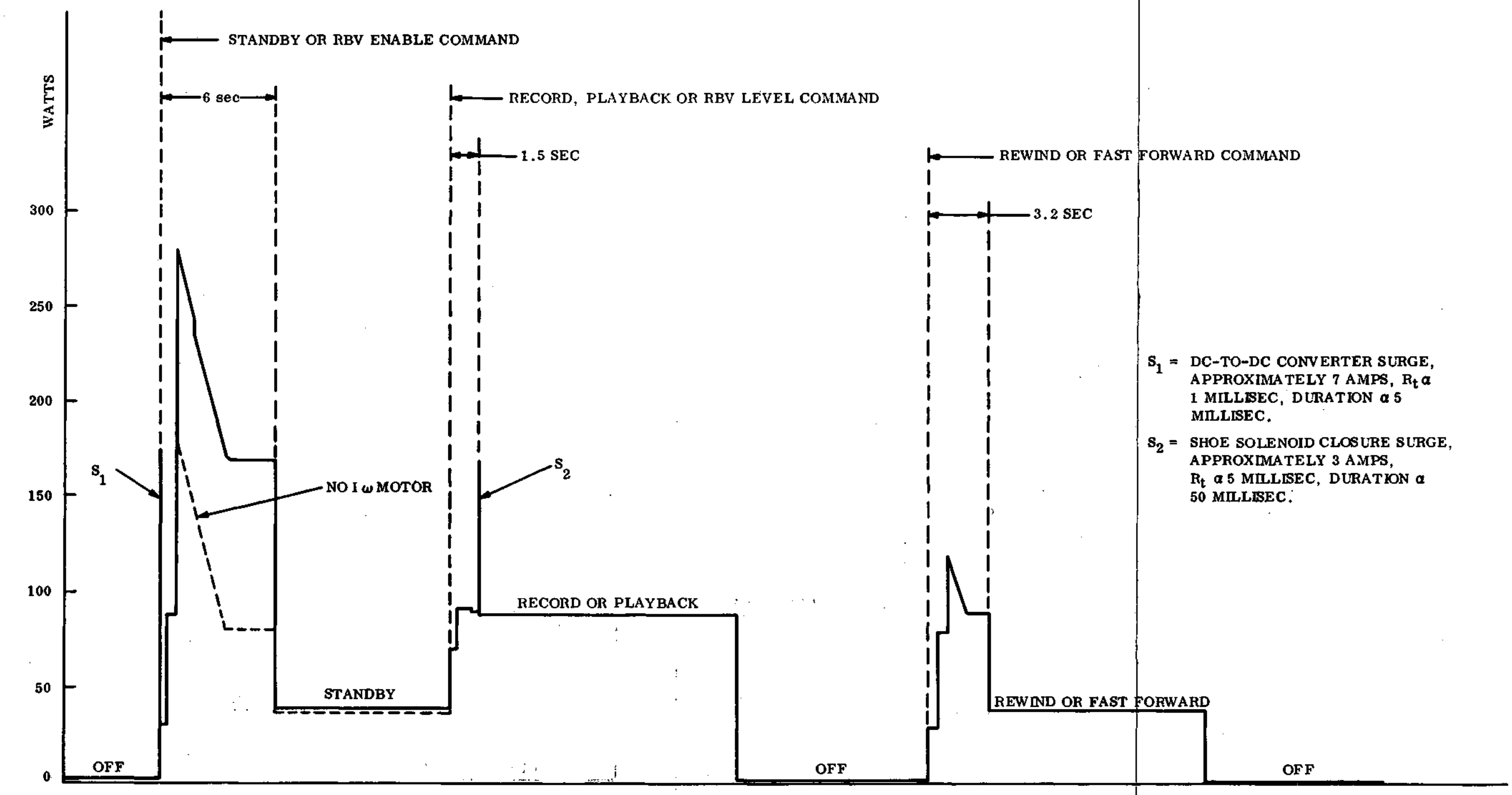

Figure 2-34. UTR Power Profile

FOLDOUT FRAME - 1

FOLDOUT FRAME - 2

E

3.0 RELIABILITY OF CIRCUITS WITHIN THE TRANSPORT UNIT

The majority of the electronic circuits for the ERTS recorder system are housed in the Electronics Unit. However, some circuits must be placed on the Transport unit to optimize equipment performance and to minimize cabling between the two units. For this reason, the circuits housed in the Transport unit are an aggregate of miscellaneous functions. Figure 3-1 and 3-2 show in block diagram form the various circuit functions performed: Two video record/preamplifier boards and a dual channel, video playback amplifier board comprise the circuitry required for the wideband channel. A control track/tach preamplifier and an aux/search preamplifier comprise the electronic circuitry required for the longitudinal tracks. A motor/solenoid switch assembly performs switching functions required for proper operation of the motors and the shoe solenoid. This module also contains circuits required for the pressure, temperature and tape footage telemetry monitors.

3.1 Introduction

Reliability of these circuits is presented as an analytical evaluation of circuit and component performance and failure mode effect and criticality. The analysis provides an estimate of reliability based on statistical data and probability theory for electronic components given in MIL-HDBK-217 (RCA DEP Stds. Vol. 14). Components are either JAN TX or MIL-ER (High Reliability) parts with established reliability of class (P) or higher, or they are MIL-Std level parts which have been screened to accomplish the same high reliability.

All parts have been derated to achieve an increased reliability in accordance with a conservative derating plan. A component ambient temperature of 60°C has been used in arriving at failure rates from RCA DEP Std., Volume 14.

3.1.1 Worst Case Analysis. - The Worst Case Analysis shows the performance of the circuit under a maximum cumulative tolerances of the various components. In general, the values of drift due to stress and aging are based upon MIL-HDBK-217 as interpreted by the appropriate RCA Defense Standard books. Significant deviations from this procedure are drift figures for RNR type resistors which are based on special data obtained from our Standards Department. This information is summarized in Appendix 3A.

The Worst Case Analyses made for the ERTS circuits have concentrated on those parameters most likely to affect the significant performance parameters for the circuit under consideration. Calculations have been performed by using the Electronic Circuit Analysis Program (ECAP), the Spectra 70/45 Computer, or the slide rule method. The calculations shown in the report are detailed enough so that the reader should be able to follow the computations.

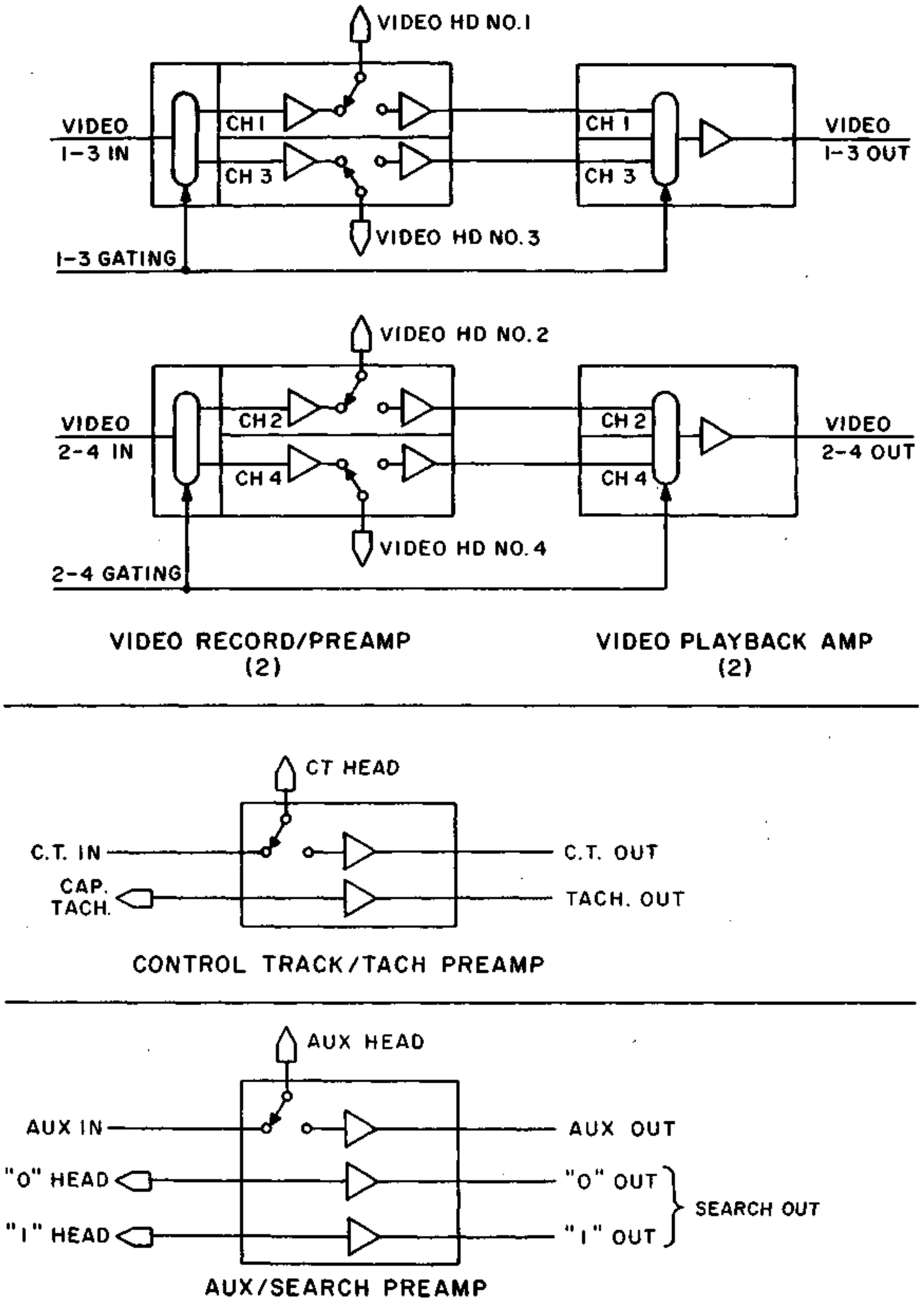

Figure 3-1 TRANSPORT SIGNAL ELECTRONICS

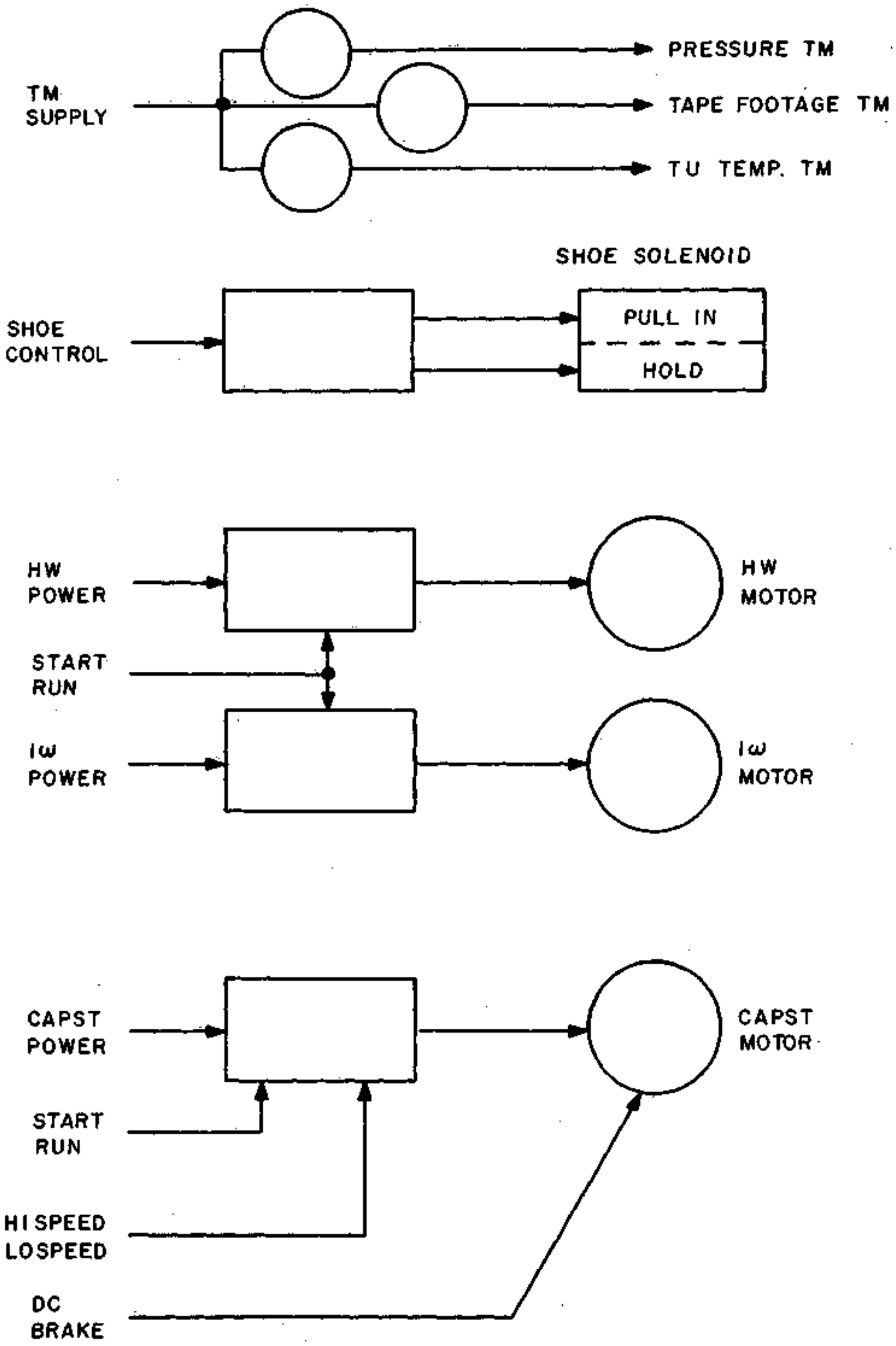

Figure 3-2. MOTOR/SOLENOID SWITCH

By definition, a Worst Case Analysis based upon maximum cumulative drift of the performance parameters gives circuit performance limits that are extreme. Such deviations from normal performance will not occur under normal circumstances since the drift of individual drift components will most likely be random rather than reinforcing. Thus the performance of a typical circuit will remain much nearer nominal values than those indicated in the Worst Case Analyses.

3.1.2 Stress Analysis. - In the Stress Analysis, the stress levels of individual components were measured and/or calculated for operating conditions at the Transport Unit maximum ambient temperature of 46°C and component ambient temperature of 60°C For those components where initial calculations indicated that performance was near the maximum derated stress, further calculations were made to ascertain that the derated limit stress levels were not exceeded. Data was recorded on Parts Application Data Sheets. Results of the calculation showing stress values and resulting failure rate were tabulated for each component on Reliability Data Worksheets presented as a part of this report. (See Appendix 3B.) Final failure rates for the modules are indicated on the block diagram in the Summary Section. For high-reliability components, a factor of 1/10 was applied to the failure rate from the tables in MIL-HDBK-217 as a one level upgrading typical in Established Reliability (ER) specifications.

3.1.3 Failure Mode, Effects and Criticality Analysis. - The primary objective of this analysis was to discover critical failure areas and to minimize susceptibility. The analysis considered the effect of each component failure on other components and circuits. In particular, the analysis shows which function of the recorder system is affected when the component under consideration opens, shorts or degrades in performance.

The analysis was conducted by consulting a functional or block diagram of each circuit and assuming the different failure modes of each part. The cause, symptoms and consequences of each failure on the next higher level and the effect on the capability of the recorder was then derived.

A classification of the failures and the resulting effects on performance is given in the summary. The Reliability Data Worksheets include the data and the documentation of the analysis. Block diagrams and schematics that were consulted are included in the appropriate sections of the report.

3.1.4 Reliability Summary

3.1.4.1 Worst Case Analysis. - The Worst Case Analysis performed on the circuits in the Transport Unit have been useful in isolating some design weaknesses. Wherever potential performance limitations were found, remedial action was taken by slight modification of the original circuit design. In general, modifications of this type are pointed out in the detailed circuit reviews.

3.1.4.2 Stress Analysis. - The Stress Analysis has specifically identified the components with a comparative high stress. These components are listed below for each of the Transport Unit modules. Although the stress for these parts is higher than on other components, it is still within the derated levels, and an adjustment to the next larger size was not required. Such an adjustment could be made for these components, but the advantage in reduced failure rate is soon offset by increased size, weight, component space, etc.

3.1.4.2.1 Failure Rate. - Total Failure Rate for electronic components in the Transport Unit for record, playback and standby is given as a summary.

	(Failures per 10^6 hours)		
	Record	Playback	Standby
Video Record/Preamp	2.188	.954	
Video Record/Preamp	2.188	.954	
Video Playback Amp		.611	
Control Track/Tach Preamp		.484	
Aux Search Preamp	.835	.835	.835
Motor Solenoid Switch	.693	.693	.693
TOTAL	= 5.904	4.531	1.528

Neither the MTBF nor the Reliability (Ps) estimate for the record, playback or standby mode of operation for the Transport Unit will significantly influence the total recorder reliability because of the small part of the total system electronics being considered. However, for the above failure rates and a mission time of 1,000 hours, the Ps for record and playback is in excess of 99% for the Transport Unit electronics. Composite failure rates for the total recording system will be included in Volume II.

3.1.4.2.2 Stressed Components (above average). - The following components are listed as those with a stress ratio above the average value but within that permitted by the Derating Plan.

a) Video Record/Preamp (Preamp)

Circuit Symbol	Component	Stress Ratio	Failure Rate ($x10^{-6}$)
	Resistor (Average)	.05	.002
R29	RNR55C3011FP	.172	.0025
R44	RNR55C3011FP	.172	.0025
R59	RNR55C3011FP	.172	.0025
	Solid Tantalum Capacitors (Ave.)	.33	.02
C5	8150547	.5	.04
C12	8150547	.5	.04
C19	8150547	.5	.04
C26	8150547	.5	.04
Video Record/Preamp (Record)			
	Resistor (Average)	.05	.002
R14	RNR55C2001FP	.2	.003
R18	RLR20C3001JP	.30	.003
R17	RCR200G202JP	.4	.002
R22	RCR20G201JP	.45	.003
R25	RCR20G101JP	.5	.004
R28	RCR20G101JP	.5	.004
R32	RCR07G100JP	.4	.002
	Solid Tantalum Capacitor (Ave.)	.33	.02
C18	8150547	.4	.025

Circuit Symbol	Component	Stress Ratio	Failure Rate ($x 10^{-6}$)
C19	8150547	.63	.125
	Transistor (Average)	.1	.02
Q1	JANTX2N3251A	.33	.04
Q2	JANTX2N3251A	.32	.04

b) Video Playback Amp

Circuit Symbol	Component	Stress Ratio	Failure Rate ($x 10^{-6}$)
	Solid Tantalum Capacitor (Ave.)	.33	.02
C1	8150547	.54	.05
C2	8150547	.53	.05

c) Control Track/Tach Preamp

Circuit Symbol	Component	Stress Ratio	Failure Rate ($x 10^{-6}$)
	Solid Tantalum Capacitor (Ave.)	.33	.02
C11	CSR13E156KP	.6	.07

d) Aux/Search Preamp

Circuit Symbol	Component	Stress Ratio	Failure Rate ($x 10^{-6}$)
	Solid Tantalum Capacitor (Ave.)	.33	.02
C22	CSR13C396KP	.6	.075
C11	CSR13E156KP	.6	.075
C33	CSR13E156KP	.6	.075
C34	CSR13C396KP	.6	.075

e) Motor Solenoid Switch

Circuit Symbol	Component	Stress Ratio	Failure Rate ($x10^{-6}$)
	Solid Tantalum Capacitor (Ave.)	.33	.02
C1	CSR13G475KP	.5	.04
C2	CSR13G106KP	.5	.04

3.1.4.3 Failure Mode and Effects Analysis. - The Failure Mode and Effects for the Transport Unit circuits has shown that a failure of any component (short or open) will cause the loss of some function of the recorder either directly or as a result of degradation. To determine which functions of the recorder remain, the schematics and functional diagrams were consulted and the resulting performance effects are indicated on the Reliability Data Worksheets. No further summary of this information can reasonably be made until the total systems electronics are considered to the same specific performance level. At that point, the estimates of performance modes for different failures will be undertaken.

3.2 Video Record Amplifier

3.2.1 Introduction. - The Transport Unit of the ERTS recorder contains four video record amplifiers and four video preamplifiers. These are located near the headwheel panel to minimize lead length between the electronic circuitry and the video heads. For mechanical reasons, two record amplifiers and two preamplifiers are mounted on one printed circuit board. For reasons of a clearer presentation, the record amplifier and preamplifier have been separated in the Reliability Analysis.

Since the four record amplifiers are identical, the Worst Case Analysis covers only a single unit.

3.2.2 Worst Case Analysis. - The ERTS record amplifier has been analyzed to show that a satisfactory performance is assured at the end of three years which includes one year of orbital life and two years shelf life. In order to prove the soundness of the design, a philosophical discussion is presented in the design analysis and augmented the computer ECAP analysis. A complete schematic diagram of the record amplifier is shown in Figure 3-3.

As a result of the ECAP worst case dc analysis, all of the fixed carbon "RC" type 5% initial tolerance resistors, which deviate ±25% under the worst case end of

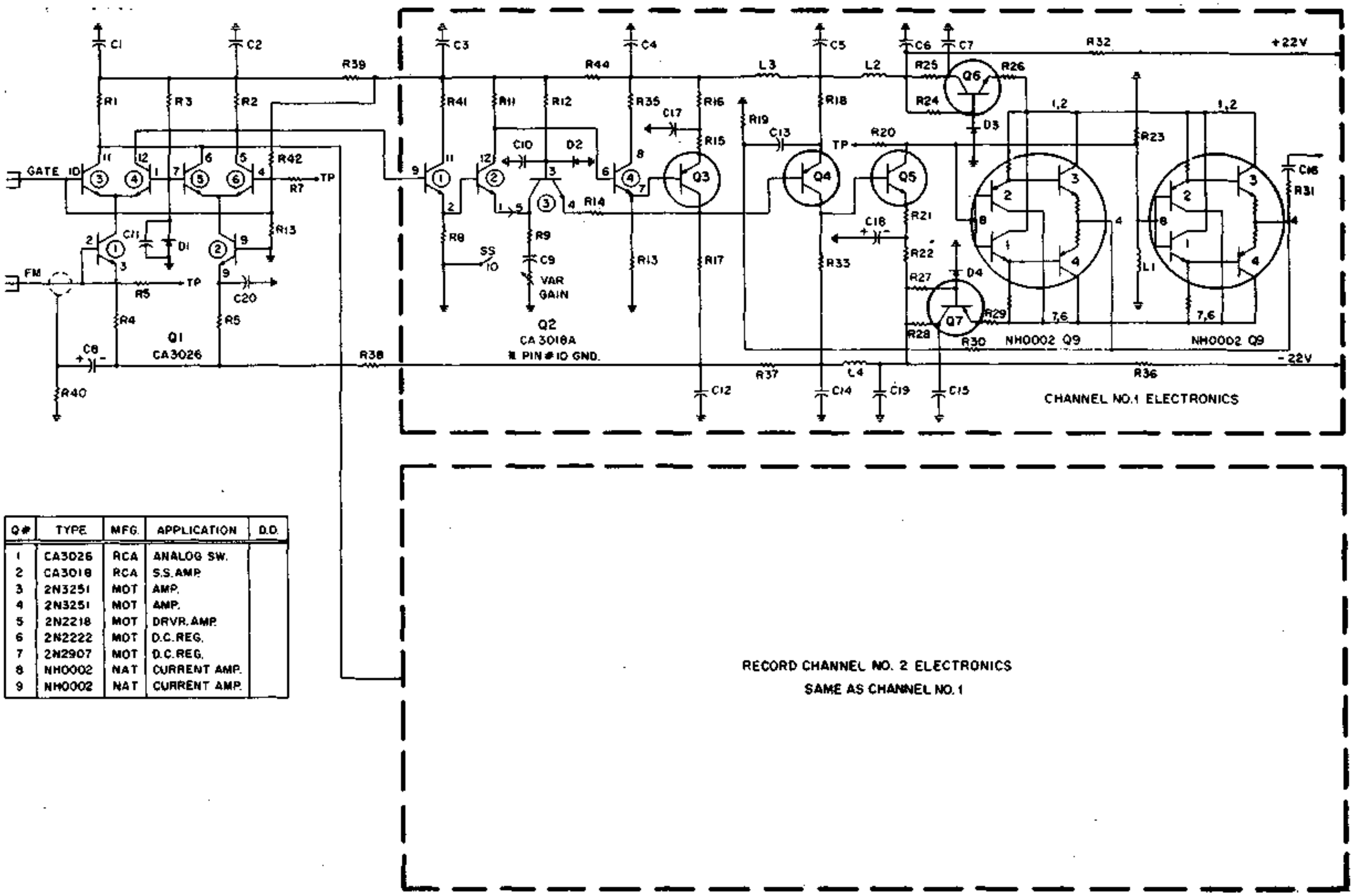

Q#	TYPE	MFG.	APPLICATION	D.D.
1	CA3026	RCA	ANALOG SW.	
2	CA3018	RCA	S.S.AMP.	
3	2N3251	MOT	AMP.	
4	2N3251	MOT	AMP.	
5	2N2218	MOT	DRVR.AMP.	
6	2N2222	MOT	D.C.REG.	
7	2N2907	MOT	D.C.REG.	
8	NH0002	NAT	CURRENT AMP.	
9	NH0002	NAT	CURRENT AMP.	

Figure 3-3 RECORD AMPLIFIER

three years life, have been replaced by the "RL" type with an initial 5% tolerance and themaximum deviation of $\pm 11.2\%$ in the $-35^\circ C$ to $+70^\circ C$ environment at the end of three years.

Ac and dc analyses of the record amplifier were made using ECAP. The summary of these results is shown in Figure 3-4 and indicates that all stages are capable of handling the required dynamic range.

Results of the ECAP dc analysis (Appendix 3C) are translated from the nodes of ECAP equivalent circuit to the schematic diagrams of Figures 3-5 and 3-6, which represent sections of the actual module. This, at a glance, permits an assessment of the bias variations under the worst case circuit components degradation.

An ac analysis (Appendix 3D) was made to ascertain the phase and the magnitude of the head current under the simulated heat equivalent impedance. From these analyses, it became evident that linearity of the head current phase depends on the resonances between the wiring capacity and the effective inductance of the head amplifier and rotary transformers. Some degree of adjustment upon the output current phase can be achieved by selection of a capacitor in parallel with R18. Depending on the wiring conditions between the heads and the record amplifier, the value of this capacitor may be between 40 and 120 picofarads. The final value of this capacitor will be established during Engineering Model tests.

3.2.2.1 Design Analysis. - In order to simplify the circuit analysis, the record amplifier is divided into four basic stages. For each stage of the amplifier, the analysis will attempt to show that a sufficient amount of negative feedback has been employed in the design to minimize A.C. and D.C. gain variations and to achieve a sufficient dynamic range stability in spite of the passive component variations.

3.2.2.1.1 Stage #1 Analog Switch - Q1. - Q1 consists of two independent monolytic integrated circuits operating in a transient mode differential amplifier configuration, and a steady state cascode amplifier configuration.

3.2.2.1.1.1 Transient Mode Consideration. - During the transient mode of operation, consider Q1 as two differential amplifiers biased so that one transistor of each differential pair is conducting (with the base zener biased to 1.4 VDC) while the second transistor of each pair is essentially biased at cut-off.

As a second condition, let the off transistor (refer to Figure 3-7) of each differential pair share a common load resistor (R_1 or R_2) with the (on) transistor of the alternate differential pair. Under the conditions stated above, a positive gate pulse of amplitude $V_G \geqq (V_1 + V_{bE})$ will reverse the quiescent state of the conducting and non-conducting transistors. The gate pulse V_G will not appear in the collector load resistor (R_1 or R_2) since alternate polarity and amplitude collector pulses share a common RC time constant.

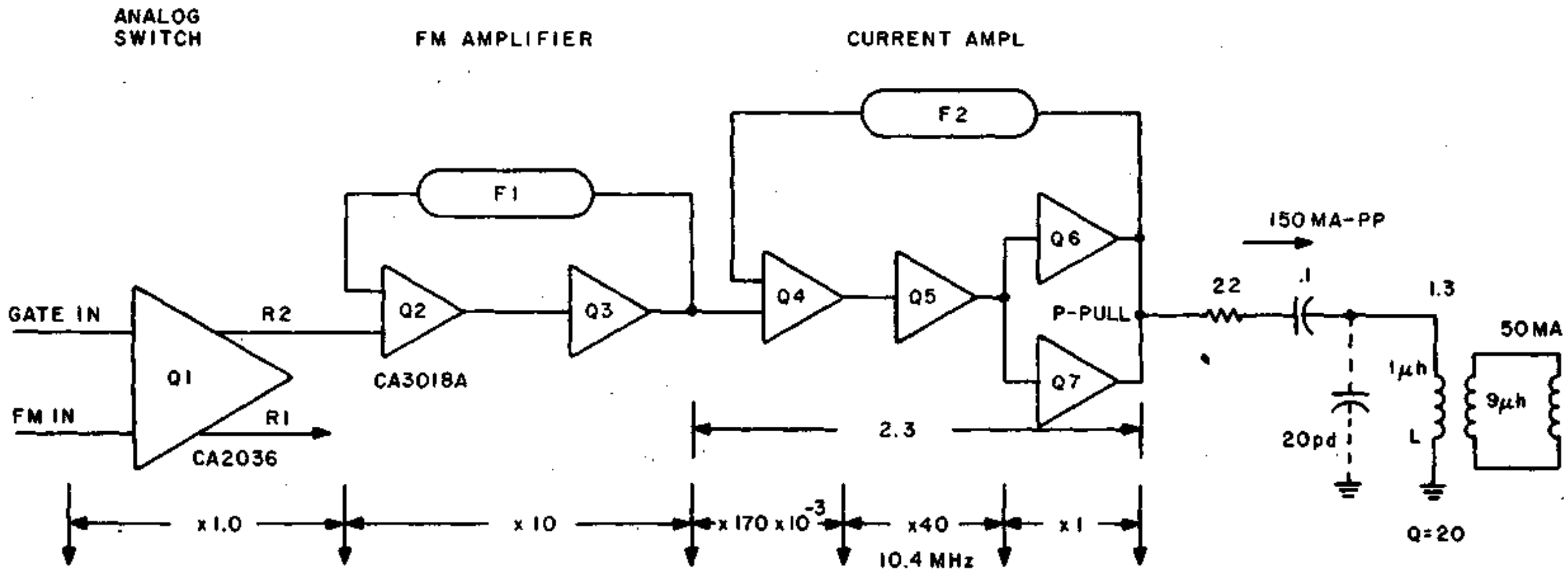

WORST CASE	Q2-I	Q3-C	Q4-C	Q5-C	Vo-PP
REQUIRED V-(P.P)	.5	5.05	.286	11.6	11.6
AVAILABLE V-(P.P)	10.0	26.0	1.2	20.2	20.0

Figure 3-4 ERTS RECORD AMP DYNAMIC RANGE SUMMARY

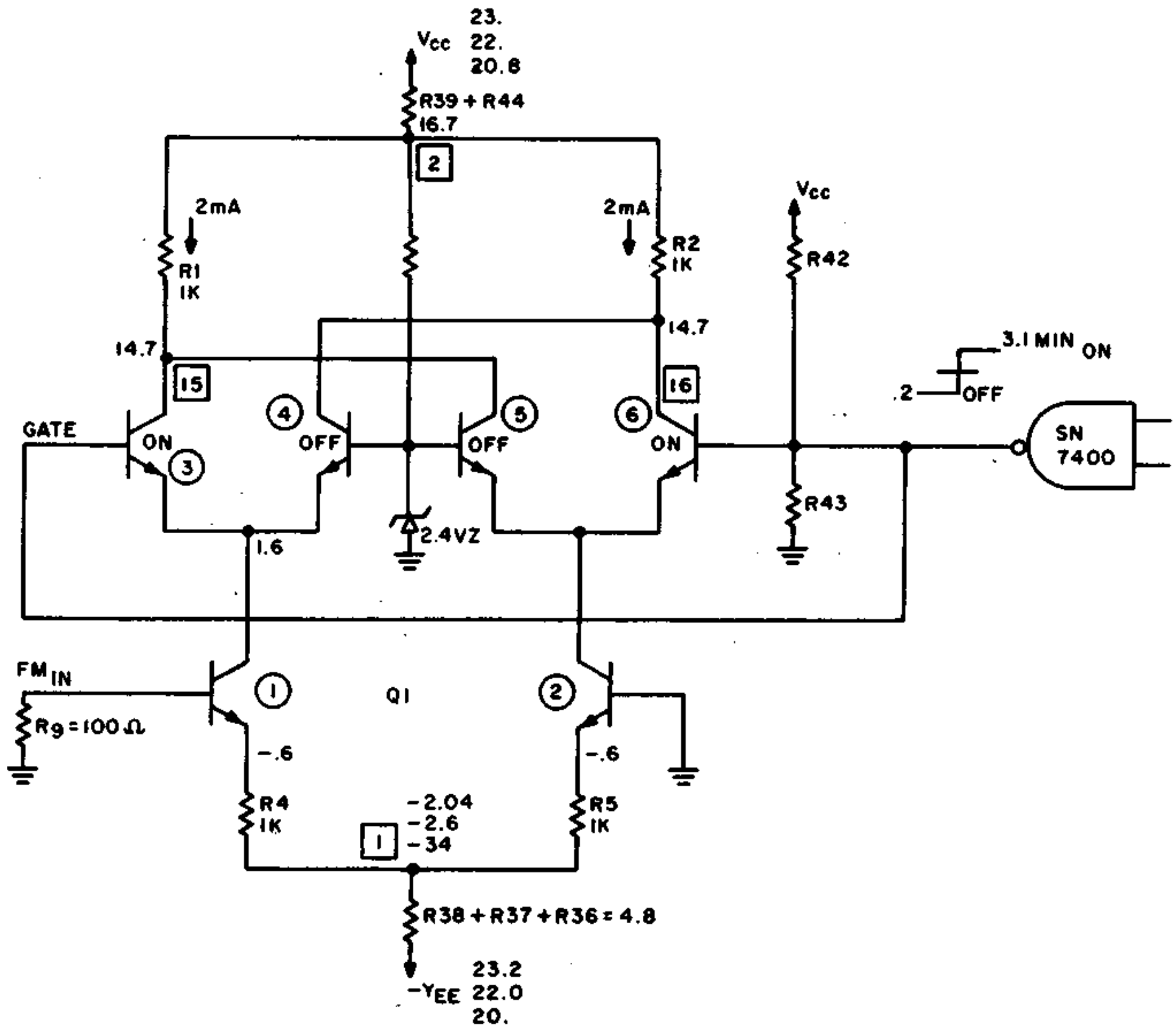

Figure 3-5 RECORD AMP DYNAMIC ANALYSIS SUMMARY

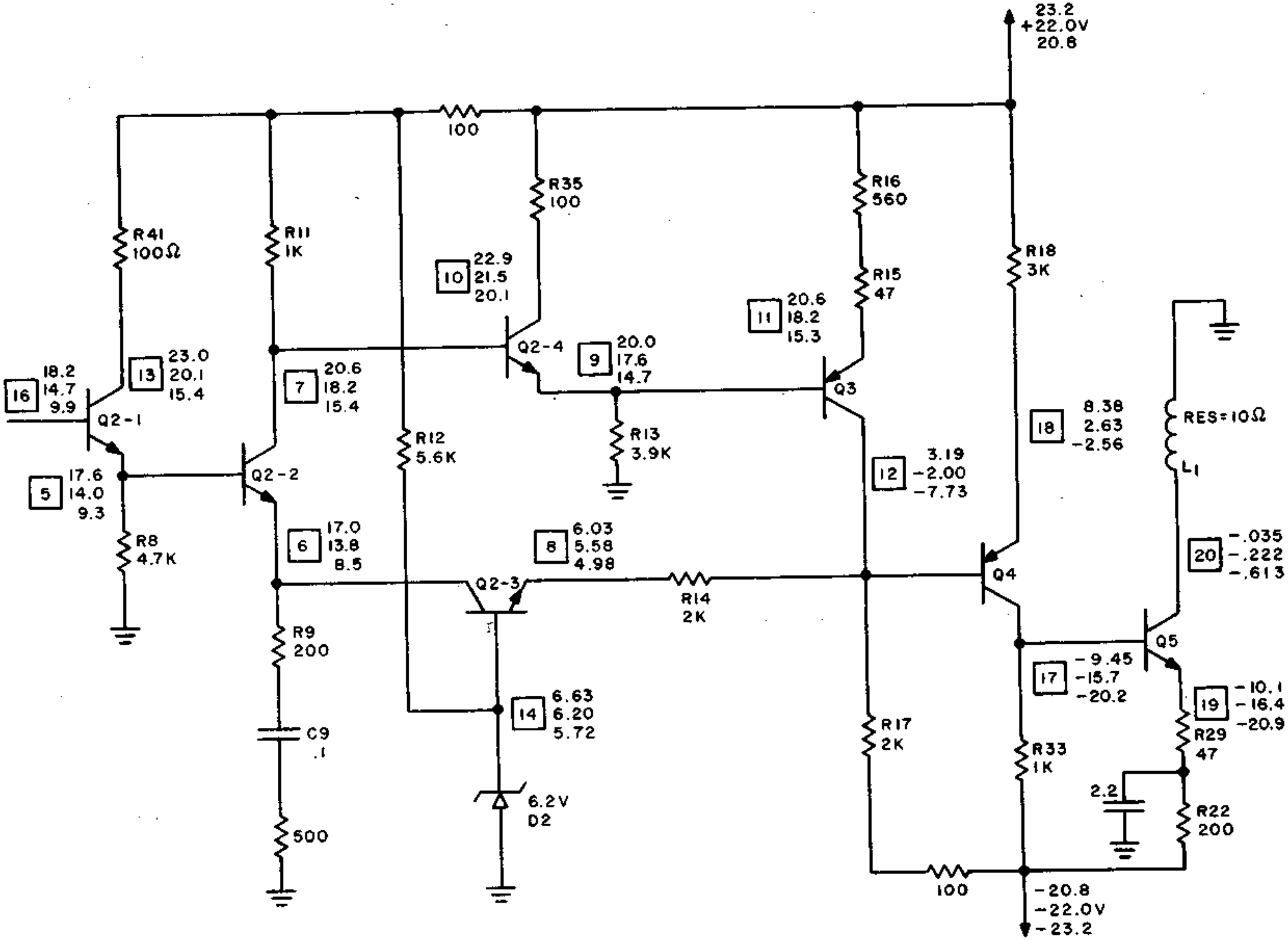

Figure 3-6 RECORD AMPLIFIER SECTION. WORST CASE ECAP SUMMARY

F

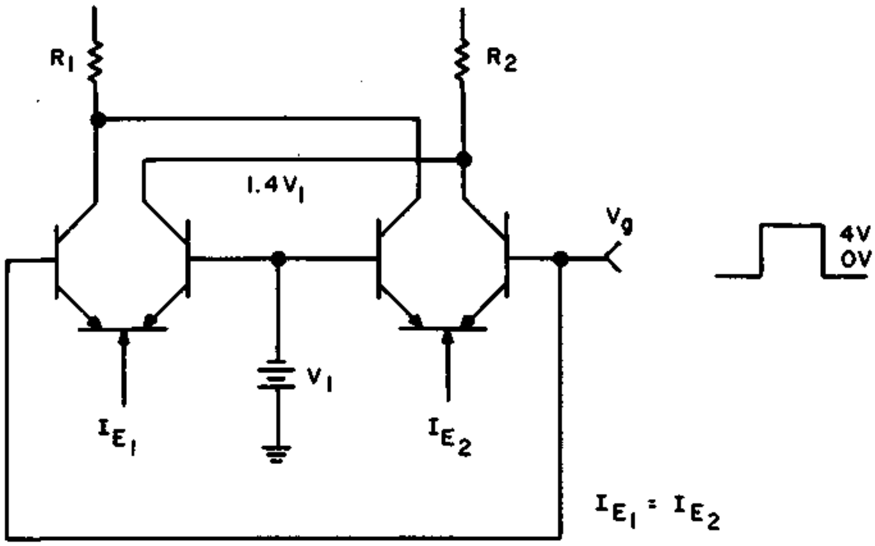

Figure 3-7 TRANSIENT MODE CIRCUIT

For transistor switching $\boxed{\begin{array}{l} V_g > (V_1 + V_{BE}) \\ \quad < (V_1 - V_{BE}) \end{array}}$

Since the base drive impedance is low the operating point stability is not impared over the temperature range.

3.2.2.1.1.2 Steady State Cascode Mode Considerations. - The steady state analog mode of Q1 which is shown in Figure 3-8 is essentially a cascode amplifier consisting of the conducting transistor in the differential amplifier pair and its constant current source with the FM 1V p-p signal injected into the base of the current sink. The emitter impedance (R_4) is large compared to the active device parameters $r_e + r_b$ so that the AC

voltage gain is = $\boxed{\begin{array}{l} AV = R_1/R_4 = R_2/R_4 \\ AV = 1 \end{array}}$ where $R_1 = R_2 = R_4$

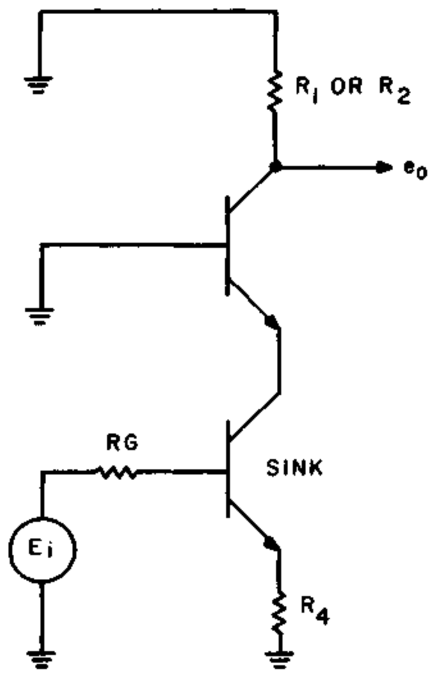

Figure 3-8 STEADY STATE ANALOG MODE CIRCUIT

The DC voltage gain equation (see Figure 3-3) is essentially given by

$$A_{VDC} = \frac{i\ (R_1 + R_{39})}{i\ (R_4 + R_{38}) + AV_{BE}}$$

Where AV_{BE} = incremental change in base emitter. Since the voltage of the current sink transistor, $i\ (R_4 + R_{38}) >> AV_{BE}$,

then

$$A_{VDC} = \boxed{\frac{(R_1 + R_{39})}{(R_4 + R_{38})}}$$

For the resistor values shown in the complete schematic diagram, the DC gain is less than unity. R_G is the FM input source impedance = 75 Ω << R_4 so that the DC bias point stability of the current sink transistor is excellent.

Because of the above dc considerations, Q1 can be dc coupled to the following amplifier stage.

3.2.2.1.2 Stage #2 dc Coupled Feedback Amplifier Q2 and Q3. - This dc coupled feedback amplifier consists of Q2 and Q3 in a modified feedback pair circuit. Q2 is an RCA 3018A four transistor monolytic array in which two of the four devices are simple dc coupled emitter followers employed to isolate miller capacity while the remaining two devices form a modified feedback amplifier together with a PNP transistor Q3. A simplified equivalent circuit configuration is shown in Figure 3-9. The following basic assumptions are made regarding the active device parameters.

1) r_e and r_b ignored due to degeneration

2) ic_o's ignored due to complementary pair 1st order cancellation effect.

3) Q3 current gain, $B_3 >>1$

The following basic equations may be derived from Figure 3-9.

$$V_{in} = R_E \ (if + ic_1)$$

$$if = ic_3 \left[\frac{R_L}{R_F + R_L}\right] = B_3\, ic_1 \left[\frac{R_L}{R_F + R_L}\right]$$

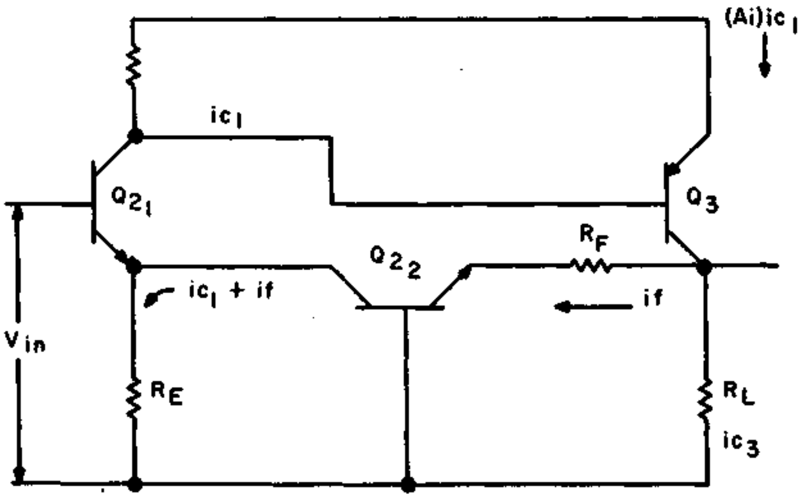

Figure 3-9 FEEDBACK AMPLIFIER

$$V_{in} = R_E ic_1 \left[1 + B_3 \left(\frac{R_L}{R_L + R_F} \right) \right]$$

$$V_o = B_3 ic_1 \quad \frac{R_F \; R_L}{R_F + R_L}$$

$$\text{Gain} = A_V = \frac{V_o}{V_{in}} = \frac{B_3 ic_1 \left(\frac{R_F \; R_L}{R_F + R_L} \right)}{B_3 ic_1 \left(\frac{R_L \; R_E}{R_F + R_L} \right)} \qquad \text{when } B_3 >> 1$$

$$= \boxed{R_F / R_E}$$

For $A_{AC} \rightarrow$ A.C. gain, $R_E = R_g + R_V$ = total AC emitter impedance of Q_{21}

$$A_{AC} \text{ max} = \boxed{R_{14} / R_E AC}$$

$$A_{DC} = R_F / Z_{022}$$

where Z_{022} is common base output impedance of Q_{22}

$$Z_{022} = r_c \left[\frac{1 + \frac{r_e + r_b (1 - \alpha)}{R_S}}{1 + \frac{r_e + r_b}{R_S}} \right]$$

r_c = incremental value of resistance of the collector junction.

but $R_S >> r_e + r_b = R_{14} = 2K$ so then

$$Zo_{22} \approx r_e > 10^6 = \text{ohms}$$

$$A_{DC} = R_F/Zo_{22} = \boxed{R_{14}/r_c} = 2X10^3/10^6 = -66db.$$

From the above analysis, it follows that the D.C. gain is attenuated drastically by the addition of the cascode amplifier inside the feedback loop which greatly enhances the amplifier operating point stability.

3.2.2.1.3 Stage #3 Complementary Feedback Pair, Q4 and Q5 - This amplifier stage is dc coupled to stage #2 and employs an ac feedback loop and choke decoupling in the collector of Q5 to prevent any dc offset voltage from developing in the output signal.

The equivalent circuit is shown in Figure 3-10. In this illustration the effects of re, r_b and ic_o are deleted from the circuit analysis due to feedback and the cancellation of the ic_o's. The following equations derived from Figure 3-10:

(1) $e_1 = i_1R_{19} = e_o + \text{if } R_{30} = e_i + V_{bE_4}$

(2) $E_1 - e_o = (B_5 ic_1 - \text{if})\ R_{23}$

(3) $E_1 - e_1 = (ic_1 + i_1 + \text{if})\ R_{18}$

(4) $e_2 - E_2 = B_5(i_{c_1})\ (R_{22})$

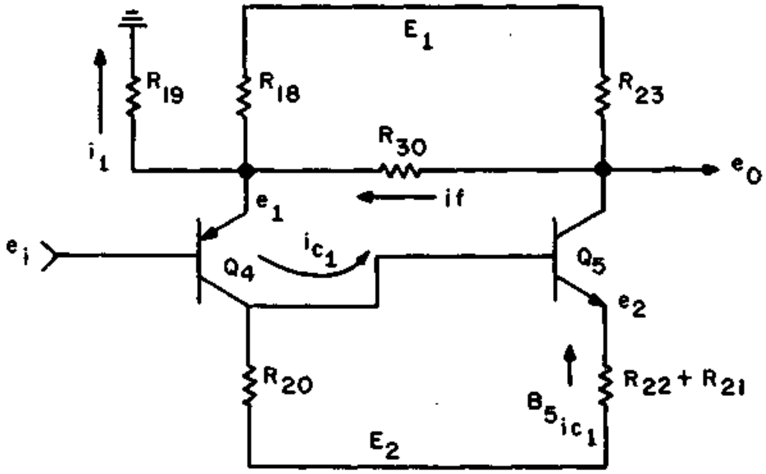

Figure 3-10 EQUIVALENT CIRCUIT OF FEEDBACK PAIR

Solving and substitution for voltage gain yields:

$$if = e_1/R_{30} \;\; -e_o/R_{30}$$

$$R_{18}(if) = e_1/R_{30}/R_{18} \;\; -e_o/R_{30}/R_{18}$$

$$E_1/R_{23} \;\; -e_o/R_{23} \; + \; if \; = \; B_5 \; ic_1$$

Let $\alpha_1 = R_F/R_{18}$, $\alpha_2 = R_F/R_{19}$, $\alpha_3 = R_F/R_{23}$, $R_F = R_{30}$

$$(R_{18} \; ic_1) \; B_5 = E_1 \; (R_{18}/R_{23}) \; +if \; R_{18}$$

$$= E_1 \; (\alpha_3/\alpha_1) \; -e_o \; (\alpha_3/\alpha_1) + e_1/\alpha_1 \; -e_o/\alpha_1$$

$$E_1 \; -e_1 \; = ic_1 \; R_{18} \; +i_1 \; R_{18} \; +if \; R_{18}$$

$$= \left[1/B_5 \left(\frac{E_3\alpha_3}{\alpha_1} - \frac{e_o \;\; \alpha_3}{\alpha_1} + \frac{e_1}{\alpha_1} - \frac{e_o}{\alpha_1} + e_1 \right) \right] + \frac{e_1 \;\; \alpha_2}{\alpha_1} + \frac{e_1}{\alpha_1} - \frac{e_o}{\alpha_1}$$

$$e_o \left[1 + \frac{1}{B_5} + \frac{\alpha_3}{B_5} \right] = e_1 \left[1 + \frac{1}{B_5} + \alpha_2 + \alpha_1 \right] + E_1 \left(\frac{\alpha_3}{B_5} - \alpha_1 \right)$$

When $\boxed{1/B_5 \; << \; 1}$

$$e_o \;\; (1 + \alpha_3/B_5) \; = \; e_i \; (1 + \alpha_1 + \alpha_2) + V_{bE} \; (1 + \alpha_1 + \alpha_2) + E_1 \; \frac{\alpha_3}{B_5} - \alpha_1$$

$$\text{Voltage Gain} = AV = \alpha e_o/\alpha e_i \; = (1 + \alpha_1 + \alpha_2) \Big/ 1 + \alpha_3/B_5$$

$$AV \approx 1 + \alpha_1 + \alpha_2$$

$$\text{Let } R_{18} \,/\!/\, R_{19} = R_E$$

$$AV = \boxed{\frac{R_F + R_E}{R_E}} = \frac{R_{30} + R_E}{R_E}$$

$$1/R_o = 1/R_{23} + B_5/R_{30} =$$

$$R_o = R_{30}/\alpha_3 B_5 = \boxed{R_{23}/B_5} \quad \text{if } B_5 > 10 \text{ and } R_{23} = 1K\Omega$$

$$R_o = 100\Omega$$

3.2.2.1.4 DC Stability considerations Stage #3 - Vin = d.c. input to Q4 considered to be constant voltage source due to case #2 d.c. gain equation. Q4 is d.c. coupled to Q5, but d.c. gain of Q4 = $R_{20}/R_{18} < 1$ so that d.c. input to Q5 base may also be considered to be a constant voltage source.

For Q5 $R_E = (R_{21} + R_{22}) << R_e$, and $R_L = 0$ (Choke decoupling so that the d.c. operating point of the feedback pair Q4 and Q5 will not drift with temperature appreciably.

3.2.2.1.5 Stage #4 NH0002 Current Amplifier in Series with Q4 and Q5 inside the feedback loop. - Consider a unity voltage gain current amplifier following Q5 with the current amplifier inside the feedback loop.

For NH0002 the integrated circuit comprising Q8 and Q9

$Z_o < 10\ \Omega$	Minimum Output Impedance
I_o ±100 mA	Max. Output Current
ΔV_o = 100 mV	Max. Output Offset
BW = 30 MHz	Min. Bandwidth

The voltage gain = AV = $(1 + \alpha_1 + \alpha_2)$ is unchanged by the current amplifier.

$R_o = R_L/B_5$ but now R_L becomes $Z_o < 10$ ohms

$= \boxed{Z_o/B_5} = 10/10 = 1$ ohm, thus greatly reducing the effective output impedance of the feedback pair.

3.2.2.1.6 Q6 to Q7 Class B Voltage Regulators - The dc supply voltages to the output current amplifiers Q8 and Q9 has been reduced to limit dissipation in these stages to the maximum required for the anticipated peak to peak ac voltage swing (see Figure 3-11).

A zener reference voltage V_R applied to the base of the regulator transistor determines the maximum dc voltage applied to Q8 and Q9, while to dc current is a function of the dynamic load impedance of Q8 and Q9, which is considered to be a

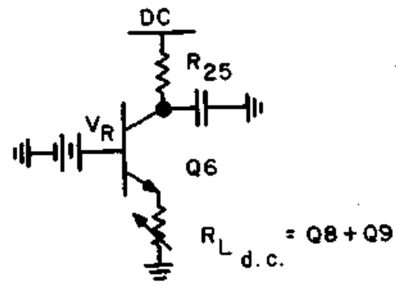

Figure 3-11 VOLTAGE REGULATOR

varying Class B impedance as a function of signal level. A collector load resistor, which is bypassed for ac signals, limits the maximum dissipation in Q6 and Q7 while also providing short circuit protection.

3.3 Video Preamplifier

3.3.1 Introduction - As stated in Section 3.2.1, the video preamplifier is physically mounted on the record/preamplifier board. This section covers the worst case analyses of the preamplifier circuit. Four identical preamplifiers are required for the recorder system. Again only one circuit is analyzed in detail.

3.3.2 Worst Case Analysis - The video preamplifier assembly contains four low noise preamplifiers (for schematic, see Figure 3-12). Since all of the preamps are to perform an identical function, only one is analyzed. Relevant analysis, in this case, is the frequency response characteristics which in the overall sense affect the S/N performance of the system, and the available dynamic range. To minimize circuit noise, low noise figure 2N3572 transistors were used by the designer in the first two stages of the preamp.

To ascertain dynamic performance of the preamp circuit, an ECAP ac equivalent of the preamp circuit was drawn from which an ac ECAP program was generated for SPECTRA 70/45 computer (see Appendix 3E). Resulting from the ac program is a printout of signal magnitude and phase at each of the (13) nodes of the circuit including the output. The results of this analysis are plotted in Figure 3-13 and indicates constant gain and linear phase from 40 KHz to 20 MHz. From the ac program, we see that if the FM signal from the magnetic head during the playback is 4 millivolts peak to peak, the required dynamic range of the preamp is (Vin) · G = 80 millivolts, p.p.

The object of the ECAP dc analysis program is to prove that the required dynamic output range is assured. In order to write a dc computer program, an ECAP dc equivalent circuit of the preamp was used (see Appendix 3F). In this case, the SPECTRA 70/45 computer was programmed to printout worst case tolerance solutions

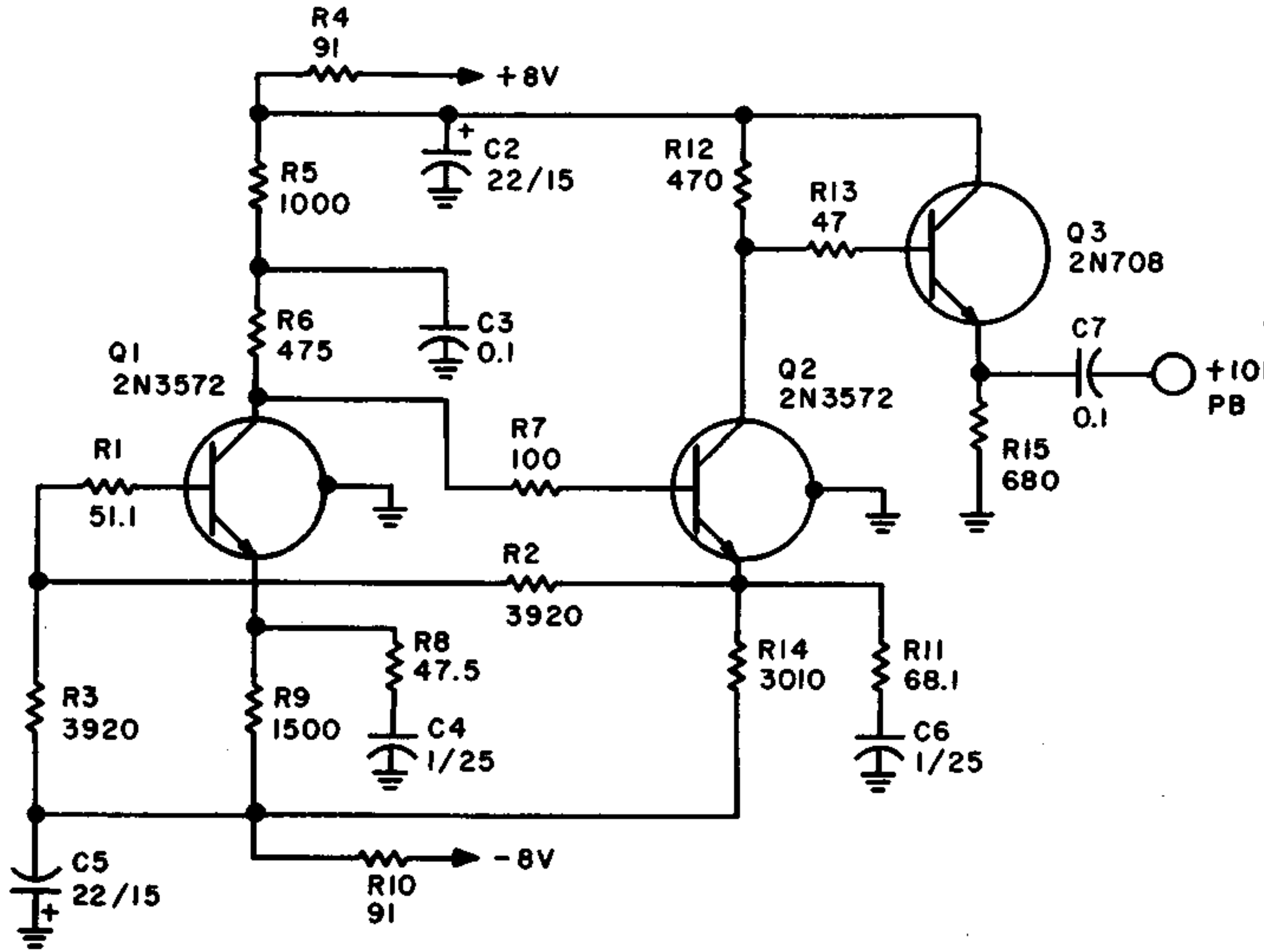

Figure 3-12 PLAYBACK PREAMP

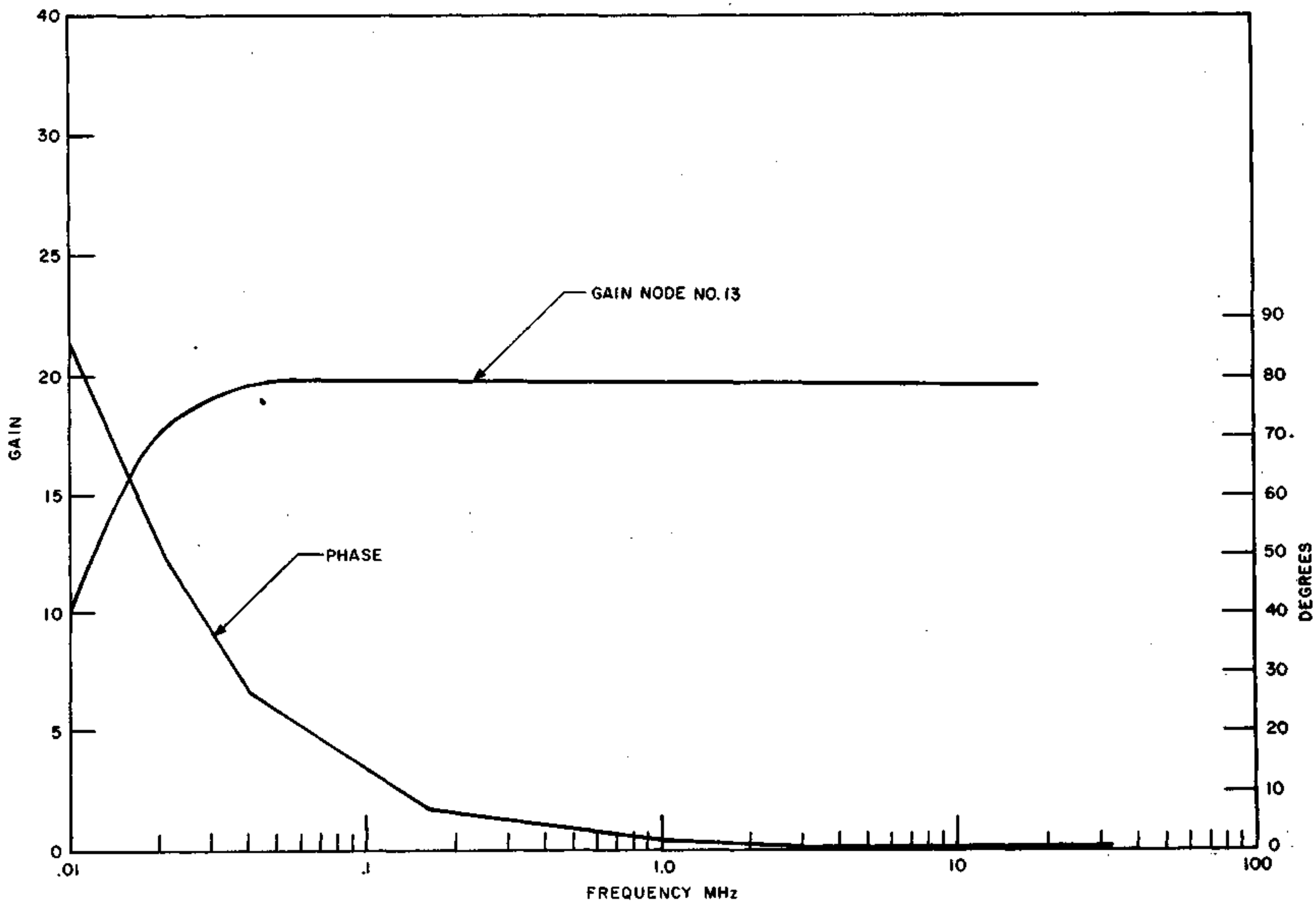

Figure 3-13 PLAYBACK PREAMP FREQUENCY RESPONSE

for the dc voltages at all of the circuit nodes of the preamp. The node potentials may be easily translated into a dynamic range of each of the three transistor stages of the preamplifier. For easy reference, maximum, nominal, and minimum dc potentials relative to ground are retabulated next to their designated nodes whose number appears within the square (see Figure 3-14). Under the worst-worst case conditions, for example, the output stage Q3 is assured to accommodate (7.46 - 5.46) = 2.58 volts peak and -2.64 volts peak unloaded. Therefore, $\approx$ 5.0 volt peak dynamic range is possible without load.

Modifying this number by the load factor of 90 ohm termination on coax, the dynamic range of $\approx$.60 volts peak to peak is adequate, for only .08 volts peak to peak is required.

3.4 Video Playback Amplifier

3.4.1 Introduction - The playback signal derived from the video preamplifier requires further amplification before the signal can be transmitted to the Electronics Unit. For this reason, a playback amplifier is provided in the Transport Unit. The four output signals from the preamplifiers are combined by suitable gating signals into two data channels; one handling the signals from heads 1 and 3, the other from heads 2 and 4. Since the playback amplifier channels are identical, only one channel is analyzed in detail.

3.4.2 Worst Case Analysis - The playback amplifier assembly contains two identical circuits to accommodate FM signals from heads (1-3) and heads (2-4), respectively. It is, therefore, sufficient to analyze only one of the two channels.

Head channels 1 and 3 (connector pins 7 and 5, respectively) are multiplexed (see Figure 3-15) in time by use of digital control signal appearing at Pin 1 via an integrated circuit analog switch Z1-MC1545. When digital gate signal is "high", Head 3 is "on", and when digital gate signal is "low", Head 1 is "on".

The switching mechanism, the gain of the stage, the frequency response, etc., are presented in the MC1545 specifications which are included in Appendix 3G. Referring to Figure 3-15, we shall prove that Z1-MC1545 is capable of driving the 100 ohms, impedance of the delay line, DL1, up to 15 MHz.

Since the gain of the MC1545 is 18 dB, e.g. x8 (see Figure 1 of Appendix 3G), the required dynamic swing at the input to DL1 is .125 volts peak to peak. From Figure 5 of Appendix 3G, the input impedance created by the shunt capacitance and shunt resistance of Z2 up to 15 MHz:

$$Z_{in} \geqq \frac{R_P \, X_P}{R_P + X_P} \simeq \frac{3.5\,(11.3)}{14.8} = 2.68 \text{ K-Ohms}$$

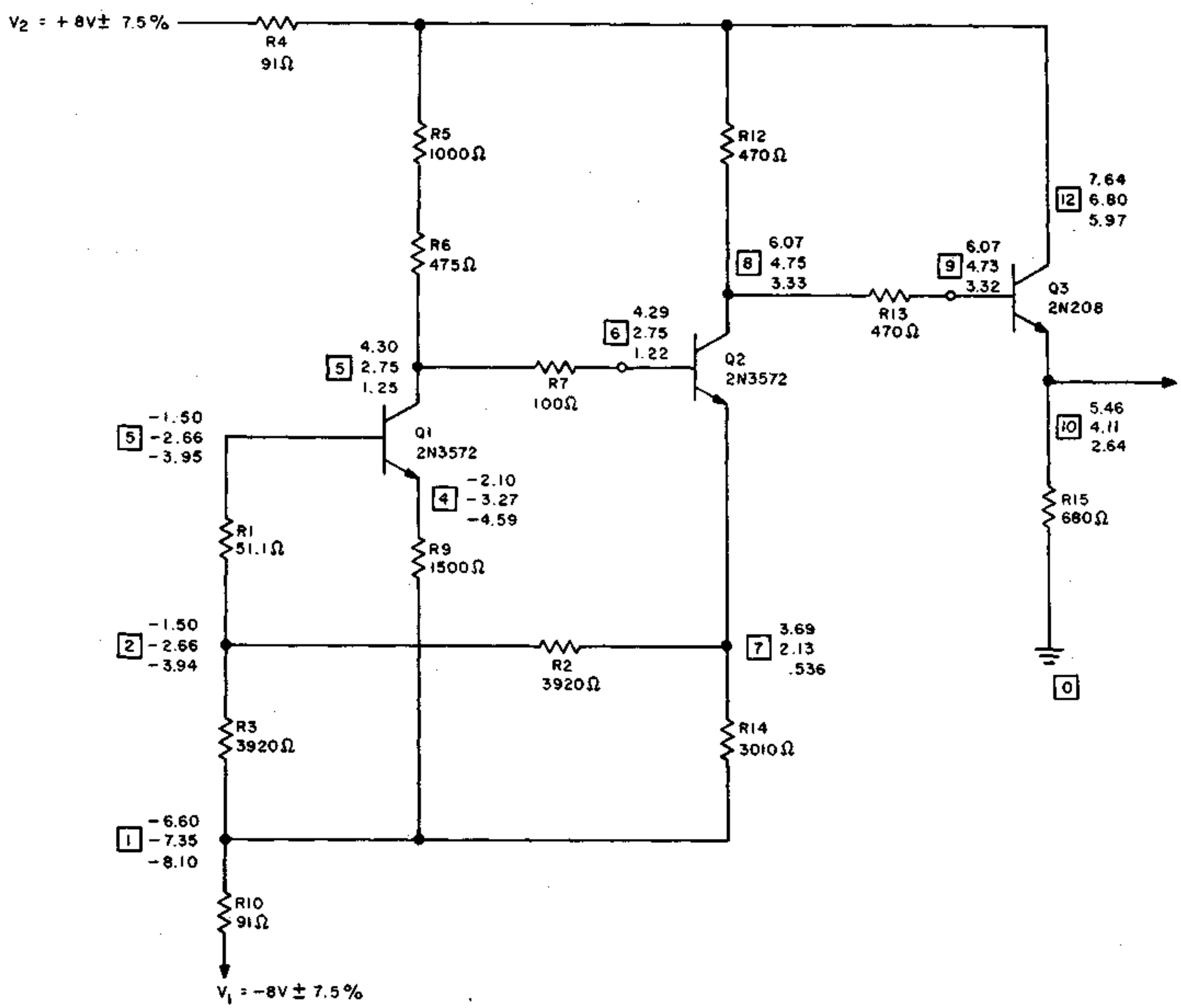

Figure 3-14 PREAMP. D.C. EQUIVALENT

The potentiometer R_X is nominally adjusted to 1/8 of its total from the ground, therefore, impedance looking into the DL1 is essentially:

$$Z_L = \frac{(7/8\ R_X)\ (Z_{in})}{(7/8\ R_X) + Z_{in}} \qquad \frac{.875\ (2.68)}{3.55} = .660\ \text{K-Ohms}$$

This means that Z1 has to drive not less than (R13 + ZL) = 75 + 660 = 735 ohms. Referring to Figure 4 of Appendix 3G, we find that MC1545 can drive more than 1.5 volts peak to peak into a load of 700 ohms. This is more than sufficient for the .125 volts peak to peak requirement.

In conclusion, therefore, the design satisfies a frequency range up to 15 MHz. In a new design, however, in order to accommodate the requirements of the MSS, an emitter follower Q1 (see Figure 3-15) has been added to drive a 75 ohm delay line (DL1) and to satisfy a 22 MHz frequency response. The performance of the new design has been checked experimentally. No special calculations in the area of Q1 were found necessary.

Next in the signal path is the FM cosine equalizer (apperture corrector). It consists of an unterminated delay line DL1 and a differential signal amplifier Z2-MC1545. The frequency response of the equalizer including the equalization adjustment range has been measured in lab. under the worst case environment and has been found to be stable.

The FM equalizer stage MC1545 feeds a discrete component circuit Z3, which is a dual 2N2807. The purpose of this circuit is to match a 75 ohm coax line and to provide 1.0 volts - p.p. signal drive to the "fill-in" switch of the main equalizer board. Both the AC and DC computer analyses have been programmed and exercised on SPECTRA 70/45 computer.

The results of the computer program, after a minor change of few resistor values, indicate that the line driver circuit meets all of the specified requirements under the worst case tolerance deviation.

As previously, the ECAP AC program was generated from the AC ECAP equivalent circuit which is shown in Appendix 3H. The results of AC analysis are plotted in terms of gain and phase vs. frequency in Figure 3-16 which shows a constant gain from 10KHz to 20MHz, and a linear phase in the same frequency range. This means that the line driver circuit meets a criteria of constant group delay.

To show that the line driver circuit will be capable to accommodate 1.0 volt p.p. at its output, a DC computer program was derived from the DC equivalent circuit shown in Appendix 3I. The first computer run using the original circuit component values showed a dynamic range deficiency on the negative signal excursion. Changing

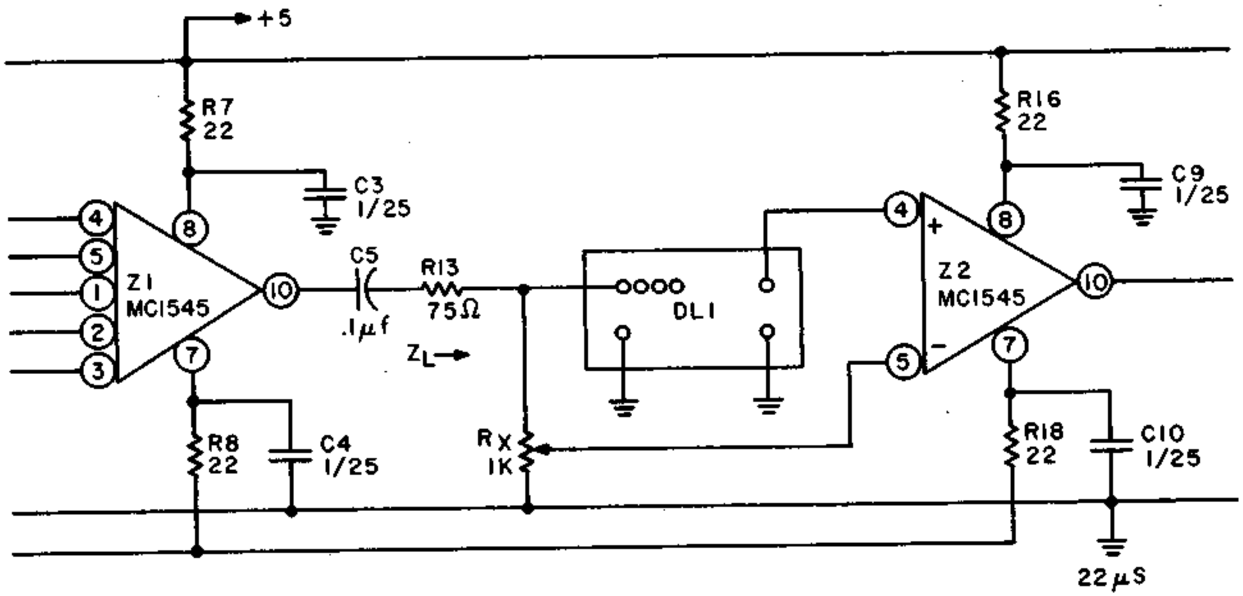

Figure 3-15 PLAYBACK AMPLIFIER

The potentiometer R_X is nominally adjusted to 1/8 of its total from the ground, therefore, impedance looking into the DL1 is essentially:

$$Z_L = \frac{(7/8\ R_X)\ (Z_{in})}{(7/8\ R_X) + Z_{in}} = \frac{.875\ (2.68)}{3.55} = .660 \text{ K-OHMS}$$

This means that Z1 has to drive not less than (R13 + ZL) = 75 + 660 = 735 ohms. Referring to Figure 4 of Appendix 3G, we find that MC1545 can drive more than 1.5 volts peak to peak into a load of 700 ohms. This is more than sufficient for the .125 volts peak to peak requirement.

In conclusion, therefore, the design satisfies a frequency range up to 15 MHz. In a new design, however, in order to accommodate the requirements of the MSS, an emitter follower Q1 (see Figure 3-15) has been added to drive a 75 ohm delay line (DL1) and to satisfy a 22 MHz frequency response. The performance of the new design has been checked experimentally. No special calculations in the area of Q1 were found necessary.

Next in the signal path is the FM cosine equalizer (apperture corrector). It consists of an unterminated delay line DL1 and a differential signal amplifier Z2-MC1545. The frequency response of the equalizer including the equalization adjustment range has been measured in lab. under the worst case environment and has been found to be stable.

The FM equalizer stage MC1545 feeds a discrete component circuit Z3, which is a dual 2N2807. The purpose of this circuit is to match a 75 ohm coax line and to provide 1.0 volts - p.p. signal drive to the "fill-in" switch of the main equalizer board. Both the AC and DC computer analyses have been programmed and exercised on SPECTRA 70/45 computer.

The results of the computer program, after a minor change of few resistor values, indicate that the line driver circuit meets all of the specified requirements under the worst case tolerance deviation.

As previously, the ECAP AC program was generated from the AC ECAP equivalent circuit which is shown in Appendix 3H. The results of AC analysis are plotted in terms of gain and phase vs. frequency in Figure 3-16 which shows a constant gain from 10KHz to 20KHz, and a linear phase in the same frequency range. This means that the line driver circuit meets a criteria of constant group delay.

To show that the line driver circuit will be capable to accommodate 1.0 volt p.p. at its output, a DC computer program was derived from the DC equivalent circuit shown in Appendix 3I. The first computer run using the original circuit component values showed a dynamic range deficiency on the negative signal excursion. Changing

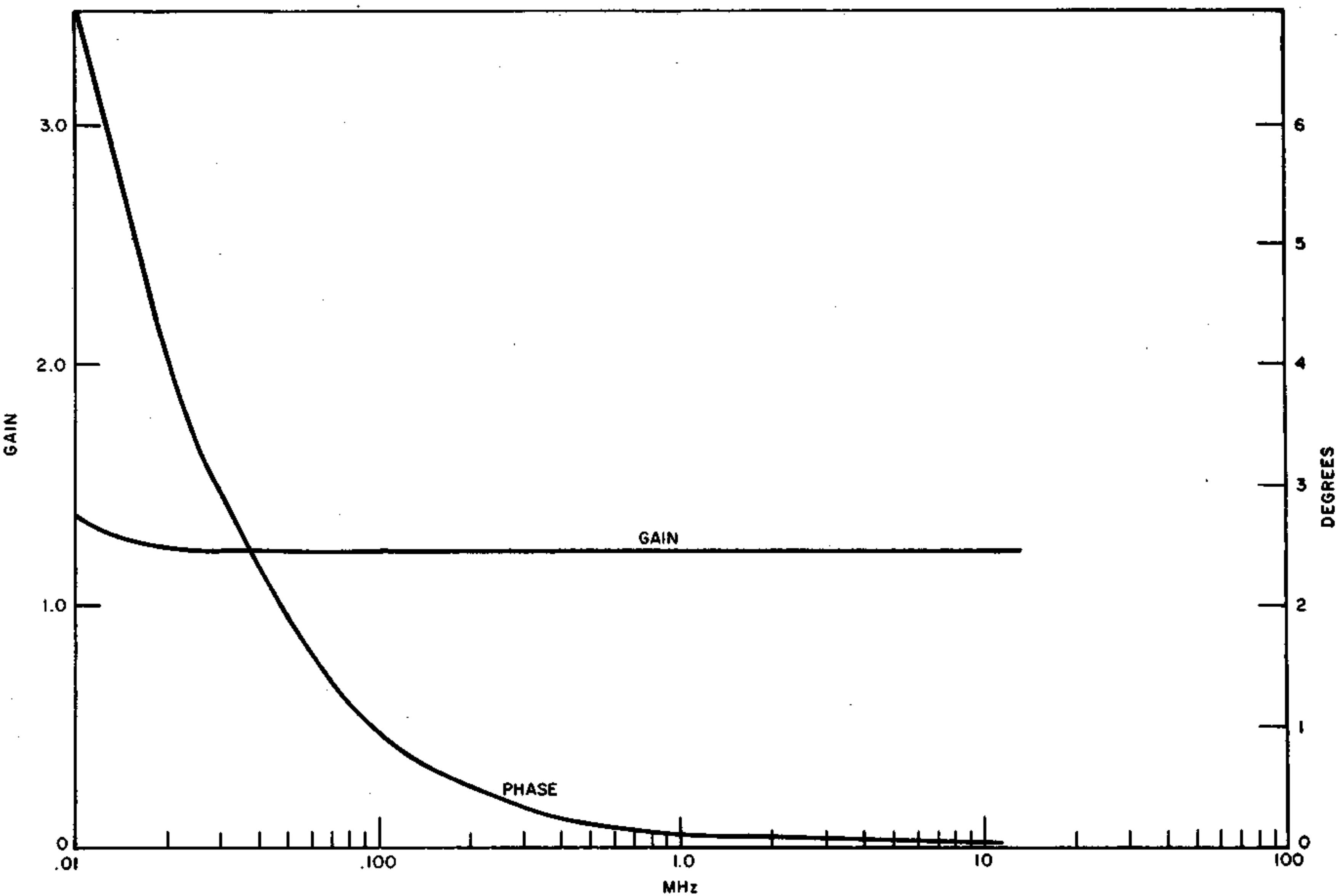

Figure 3-16 ERTS PLAYBACK LINE DRIVER RESPONSE

R24 from 1.0KΩ ± 10% (initial tol.), to 750 ohms, and changing the R25 from 75 ohms ± 10% to 75 ohms ± 1% (initial tol.) resulted in a sufficient dynamic range (see modified DC program pgs. C6 and Figure 3-17 which recapitulates the results of the worst case DC node potentials.)

3.5 Control Track/Tach Preamplifier

3.5.1 Introduction - The purpose of the control track preamplifier is to switch the control track head to its record amplifier (in the Transport Unit) during the record mode and to the preamplifier during the playback mode. The purpose of the tachometer preamplifier is to process the low level signal derived from the capstan tachometer pick-up. All signals will be amplified to a sufficient level for transmittal to the Electronic Unit.

3.5.2 - Worst Case Analysis - The circuit and performance requirements of the control track/tach preamplifier are essentially identical to the search track preamplifiers. For this reason, a single Worst Case Analysis has been made which is covered in Section 3.6.2.

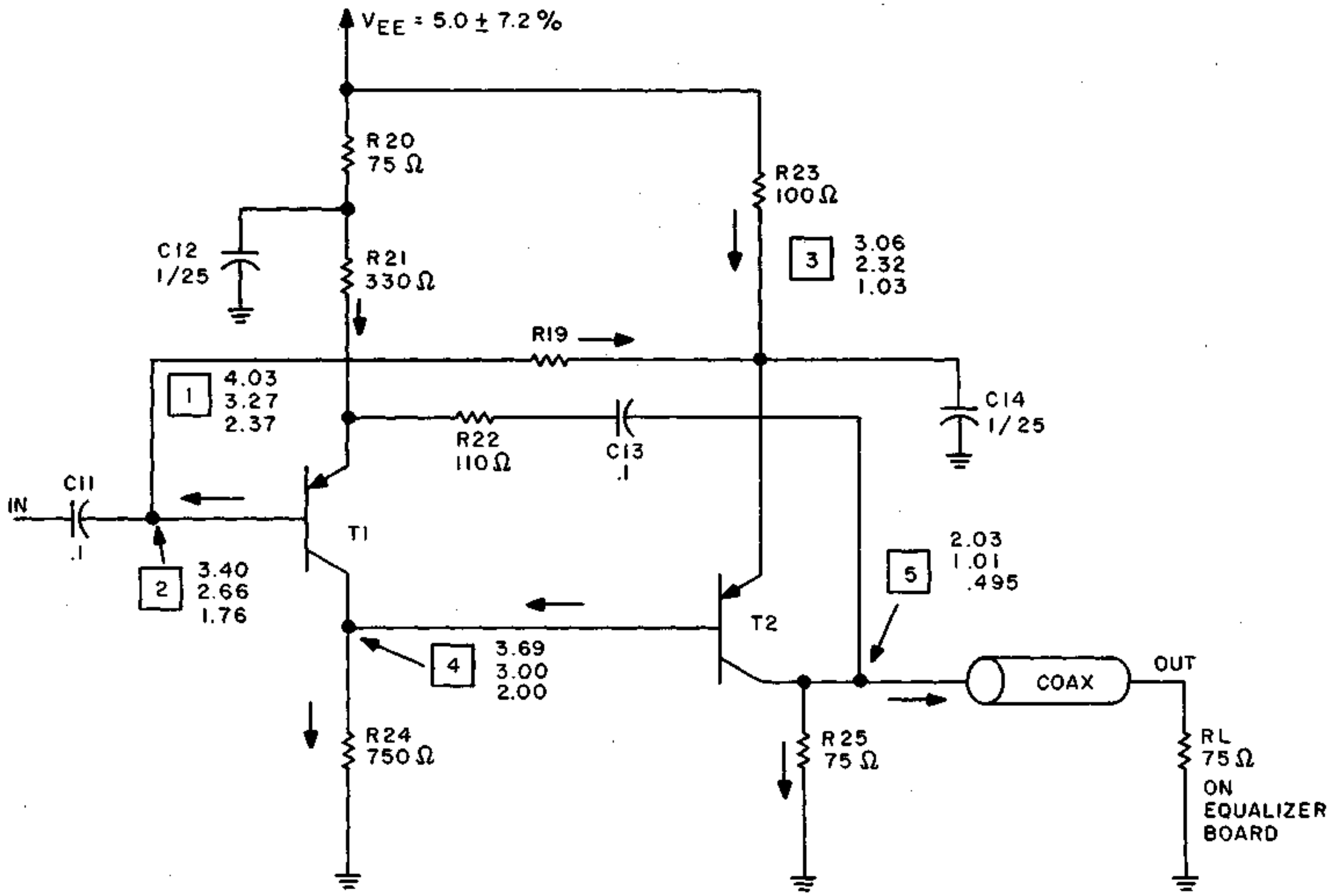

$$\begin{pmatrix}\text{P DERATED}\\ \text{BOTH SIDES}\end{pmatrix} = 500 - 2.86\,(60°C - 25°C) = 500 - 100 = 400$$

Figure 3-17 PLAYBACK LINE DRIVER

3.6 Auxiliary/Search Preamplifier

3.6.1 Introduction. - The purpose of the auxiliary channel preamplifier is to switch the auxiliary head to its record amplifier (in the Transport Unit) when the circuit is in the record mode, and to the preamplifier when in the playback mode. The purpose of the search track preamplifiers is to amplify the playback signals derived from the two search track playback heads. In all cases, the signal levels must be amplified to a sufficient level for transmittal to the Electronic Unit.

3.6.2 Worst Case Analysis. - The Worst Case Analysis for the auxiliary track and the search track preamplifiers are shown in the subsequent sections. Since the control track/tachometer preamplifiers are essentially similar to the search track preamp, the following analysis also covers these circuits.

3.6.2.1 Auxiliary Track Preamplifier. - The playback preamplifier is to be capable of processing FM voltage signal from the pick-up head and to amplify it sufficiently prior to FM limiting in the subsequent limiter; First, the frequency restricting parameters of the design are checked (see Figure 3-18 Aux Preamp Schematic).

3.6.2.1.1 Low Frequency Poles

$$f_1 = \frac{1}{2\pi \; C23 \; R28} = 320 \text{ Hz}$$

$$f_2 = \frac{1}{2\pi \; C28 \; R33} = 1.59 \text{ kHz}$$

3.6.2.1.2 High Frequency Poles

$$f_1 = \frac{1}{2\pi \; C27 \; R31} = \frac{1}{2\pi \, (51) \, 10^{-12} \, (21.5) \, 10^{-3}} = 143 \text{ kHz}$$

$$f_2 = \frac{1}{2\pi \; C32 \; R36} = \frac{}{2\pi \, (10^{-10}) \, (2.15 \times 10^{-5})} = 74 \text{ kHz}$$

The open loop lag compensation of the Z5 is at:

$$f_{Lo} = \frac{1}{2\pi \, (10^{-8}) \, (3.4 \times 10^{-3})} = 4.7 \text{ kHz}$$

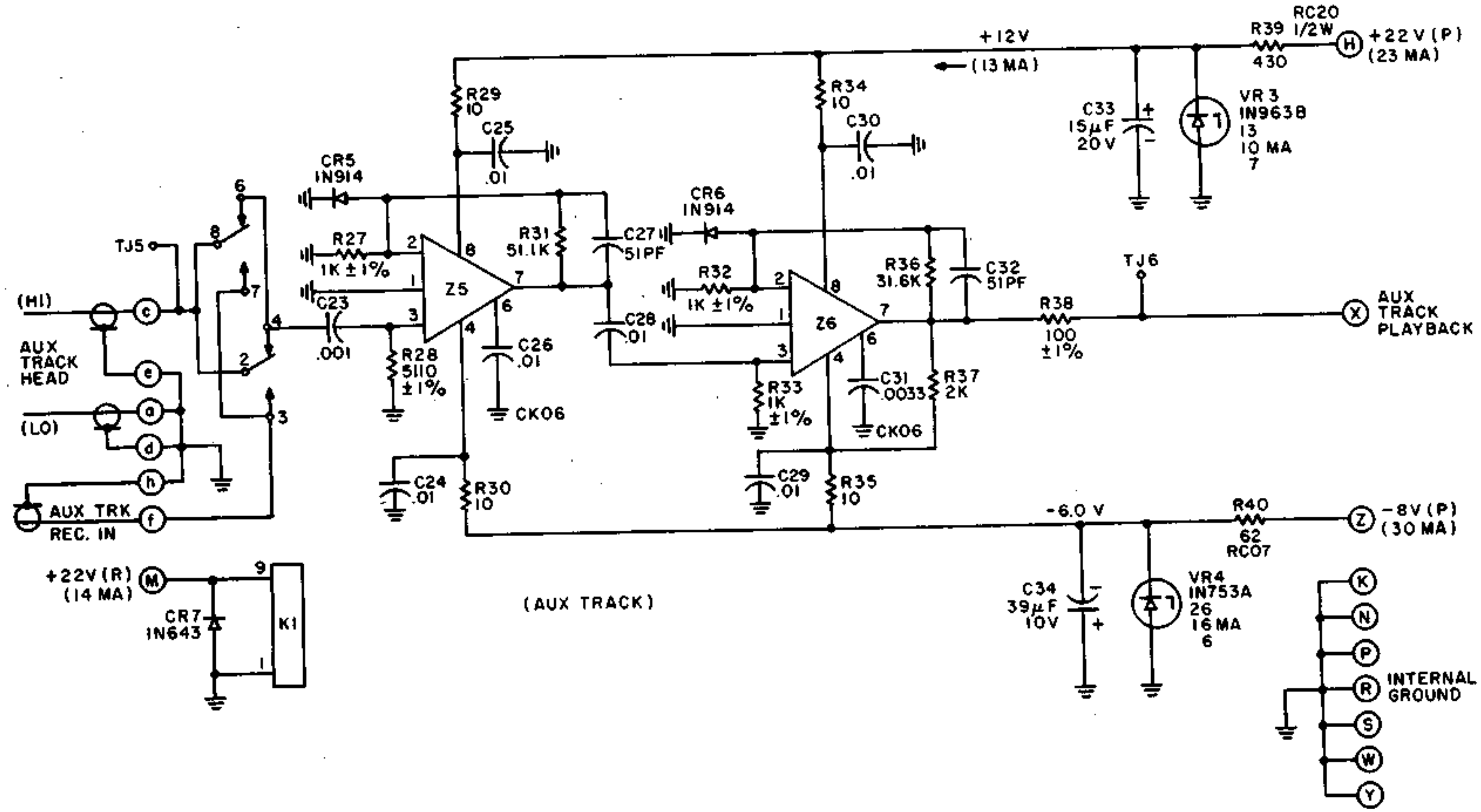

Figure 3-18 AUX PREAMPS

The closed loop gain of each Z5 and Z6 (see Figure 3-8) is:

$$G = 1 + \left(\frac{R31}{R27}\right) = 22.5 \quad = > 27 \text{ dB}$$

Projecting to 27 dB at the rate of 20 dB/decade the f_{Lo} = 470 kHz. A similar consideration is applicable to Z6. Thus the high frequency cutoff is primarily due to a pole at 74 kHz and 144 kHz. The 2.8 kHz to 34 kHz bandwidth of the playback subsystem is considered to be more than sufficient for a faithful discrimination of the auxiliary track frequency modulated signal assuming that the phase equalization and its linearity is not a factor. With a maximum signal input of 4 millivolts peak to peak and with the overall preamp gain of 54 dB, the output delivered to the limiter is 4X(505) or 2.0 volts peak to peak. The output of Z6 with R37 = 2K ohms is capable of delivering 3.5 volts peak to peak into 500 ohms load. Therefore, a sufficient undistorted signal drive capability is provided.

3.6.2.2 Search Track Preamplifier. - The search track signal preamplifier is used to amplify and band limit the pre-recorded search track signal representing digital information about a position of the tape. This circuit is located in the Transport Unit and thus is also used to prepare this signal for transmission to the Electronics Unit. The preamplifier consists of two pairs of integrated circuits. Each pair is used to accommodate an output originating from the two magnetic heads, one for search track "1", the other for search track "0". Since both systems are similar, only one of the preamp pairs (Z1 and Z2) shall be discussed. A schematic diagram of the preamplifier is shown in Figure 3-19.

3.6.2.2.1 AC Considerations. - The high frequency response is limited by two poles. Number one pole which is associated with the Z1 is located at:

$$f_1 = \frac{1}{2\pi \text{ R5 C5}} = \frac{1}{2\pi\,(21.5)\,(51)\,10^{-9}} = 145 \text{ KHz}$$

and the pole number two associated with Z2 is located at:

$$f_2 = \frac{1}{2\pi\,(R_{10})\,C_{10}} = \frac{1}{2\pi\,(21.5)\,(100)\,10^{-9}} = 74 \text{ KHz}$$

Thus the bandwidth of the input preamp is sufficient to accommodate the 10 kbs search track signal which will be present during the high speed tape winding. Reducing the high frequency cutoff point may be desirable in consideration of the tape signal to noise ratio.

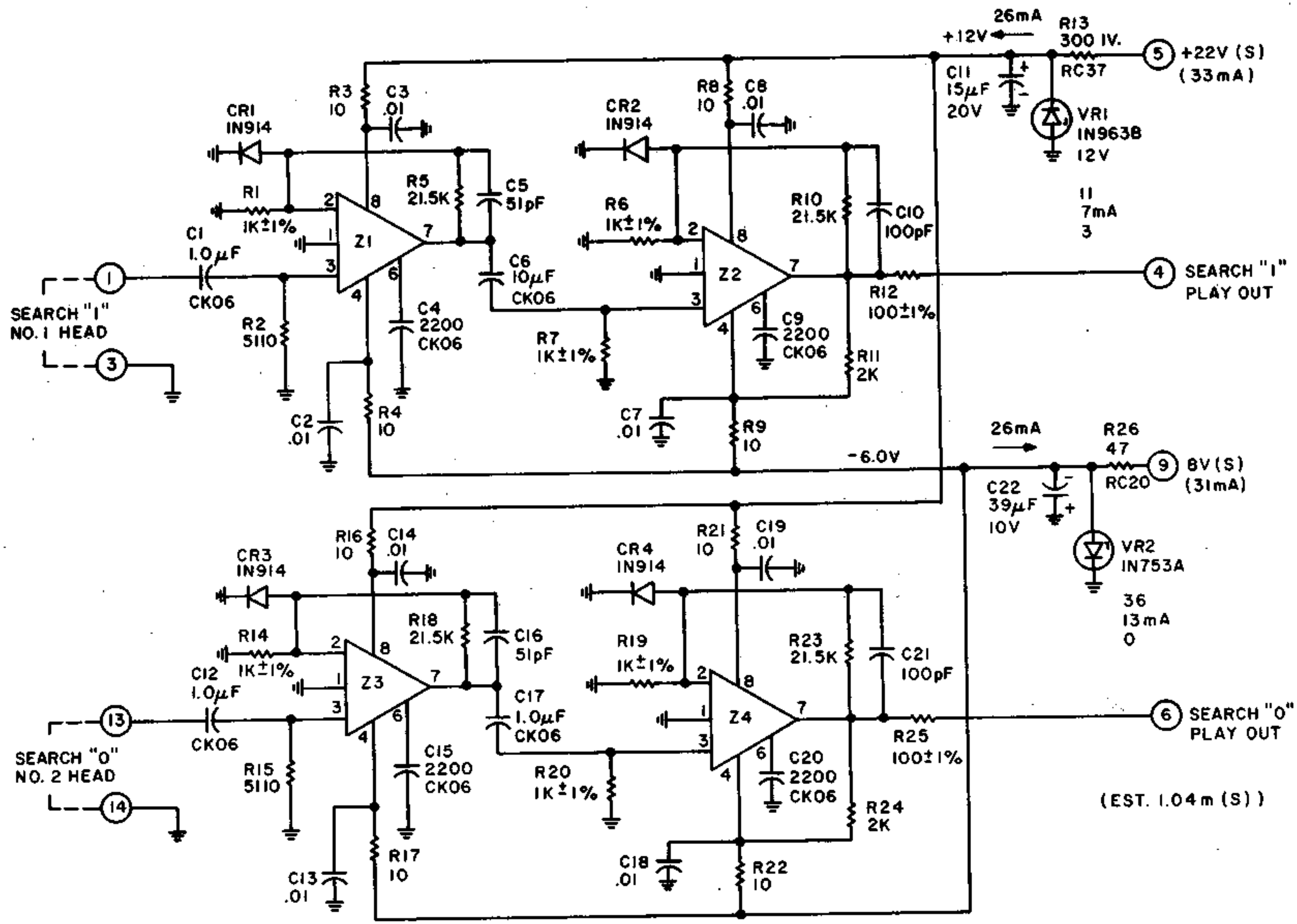

Figure 3-19 SEARCH TRACK PREAMP

The low frequency rolloff is primarily at:

$$f_1 = \frac{1}{2\pi R7\ C6} = \frac{1}{2\pi (10^{3})(10^{6})} = 160\ \text{Hz}$$

The ac coupling in this case may be appropriate since it tends to reduce low frequency drift. The inband gain of the two integrated circuits Z1 and Z2 is:

$$G = \left[1 + \frac{21.5}{1.0}\right]^2 = 40 \log 22.5 = 54\ \text{db}$$

Since the threshold detector which will be analyzed subsequently is responsive to a rather small input signal differential, it may be desirable to reduce the gain of the preamplifier in order to improve the output signals to noise performance.

3.6.2.2.2 <u>DC Considerations.</u> - The low frequency drift in the output stage of the preamplifier may cause a false decision by the threshold detector which is located on the search track playback module. Since there is no provisions for the preflight adjustment of either the threshold level or the output dc levels worst case output bias shall be computed from the equivalent circuit shown in Figure 3-20.

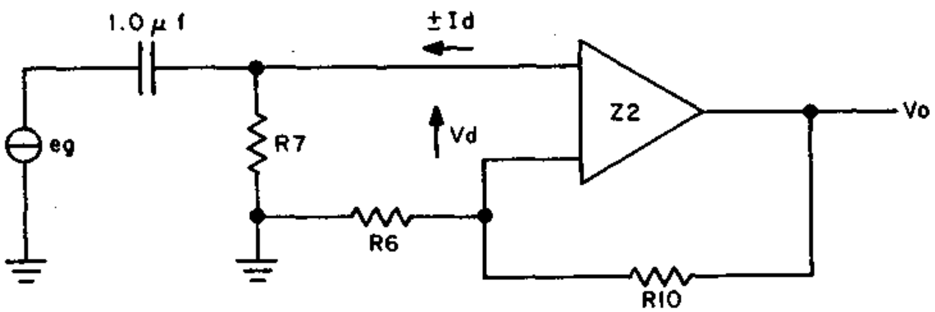

Figure 3-20 OUTPUT BIAS EQUIVALENT CIRCUIT

$$\Delta Vo = \Delta Vd \left[1 + \frac{R10}{R6}\right] \pm \Delta Id \ R10$$

$$\Delta Vd = \Delta Vd \text{ (initial)} + \Delta Vd \text{ (temp.)}$$

$$\Delta Vd = \pm 2.0 \text{ mv} + .02 \text{ mV/}^\circ\text{C } (\pm 35^\circ \text{C}) = \pm 2.7 \text{ mV}$$

$$\Delta Id = \Delta Id \text{ (initial)} + \Delta Id \text{ (temp.)}$$

$$\overline{\Delta Id} = \pm 2.0 \, \mu a + 20 \text{ NA/}^\circ\text{C } (\pm 35^\circ \text{C}) = \pm 2.7 \, \mu a$$

$$\Delta R_{10} = \Delta R_6 = \pm .05 \text{ (EOL + TEMP)}$$

Thus:

$$\overline{\Delta Vo} = \pm 2.7 \left[1 + \frac{21.5 \ (1 + .05)}{1.0 \ (1 - .05)}\right] \pm 2.7 \ (21.5) \ (1 + .05) = \pm 127 \text{ mV}$$

The calculated worst case offset may or may not be of any serious consequences. Its effects upon duty cycle of the recombined search track output signal shall be evaluated in conjunction with other worst case causes in the analysis of the Electronic Unit.

3.7 Motor/Solenoid Switch

3.7.1 Introduction. - The purpose of the motor switch circuitry is to switch the output of the motor bridge circuits to the start/run and high speed/low speed windings of the various motors in the Transport Unit. These switches are located in the Transport Unit so that the number of interconnecting wires between the two units can be held to a minimum.

The purpose of the solenoid switch circuitry is to control the pull-in/hold coils of the shoe solenoid. All of the above circuits are housed on a separate subassembly that is hard wired into the Transport Unit. Several resistors are also provided to process the telemetry signals for the temperature, pressure and footage transducers. The Worst Case Analysis for this subassembly is divided into two sections; the first covering the solenoid switch circuit, the second covering the motor switches.

3.7.2 Description of Operation.

3.7.2.1 Solenoid Switch. - The solenoid switch circuit controls a solenoid which in turn is mechanically coupled to a concave shoe that holds the magnetic tape against the headwheel during recording and playback. A spring automatically releases the solenoid in the event of power failure, and a number of auxiliary circuits provide additional protection against tape damage by continuously monitoring the capstan speed.

Referring to Figure 3-20, the solenoid switch circuit may be separated into three distinct functions: one; the relay timer, which consists of relay K7, represented by inductor L1 and its normally open (NO) and normally closed (NC) contacts and R1, C1; two; the solenoid driver consisting of transistors Q1, Q2 and Q3 and the solenoid L2 and its transient suppression diode CR15; and three; the solenoid hold circuit, shown as L3 and its transient suppression diodes CR14 and CR17. The relay timer is used to establish the solenoid pull-in duty cycle by turning off the transistor driver when the voltage across K1 decreases below the relay drop-out voltage. Activation of the solenoid pull-in driver and hold coils is initiated by the shoe control signal, V_1. As shown in Figure 3-20, hold coil L3 is immediately energized, while the turn-on of Q1, Q2, and Q3 is dependent upon charging of R2 and C2. This RC delay (which incidentally avoids the inductive loading effects of Q3) is included in the circuit design primarily to comply with system power supply current step requirements. Therefore, the voltage across the pull-in coil, V_{E3}, essentially follows the output of Q1 up until Q1 saturates. Clearly, whether or not Q1 saturates, depends on the driver gain and the relay timer drop-out time.

3.7.2.2 Motor Control. - The motor control circuit consists of relays K1, K2, K3, K4, and K6, which are used to switch power between the start/run windings of the capstan, headwheel, and Iω motors. The relays also select the high speed/low speed windings of the capstan motor. K1 controls the Iω motor, K2 and K3 the headwheel motor, and K4 and K6 control the capstan motor.

3.7.2.3 Telemetry. - In addition to the solenoid driver and motor control relays, the Transport Unit contains several resistor divider networks, R9 through R15, for various Telemetry (TM) functions.

3.7.3 Solenoid Switch Analysis. - To guarantee reliable shoe control, the relay timer and solenoid driver operating requirements must be defined.

3.7.3.1 Relay Timer. - The relay timer should be designed to provide sufficient time to energize the pull-in coil while simultaneously limiting unnecessary power dissipation and possible complete destruction of the solenoid coil. The minimum ON time must be equal to or greater than the worst case maximum time required to achieve minimum allowable pull-in force. Conversely, the maximum ON time must be equal to or less than the pull-in coil's maximum allowable period of continuous operation. Also of interest to the designer is the power dissipated by the solenoid driver transistor Q3.

3.7.3.2 Solenoid Driver. - Since the solenoid pull-in force varies with temperature, the worst case minimum current gain of the drive circuit must be adequate to energize the pull-in coil under the coil maximum current requirement condition.

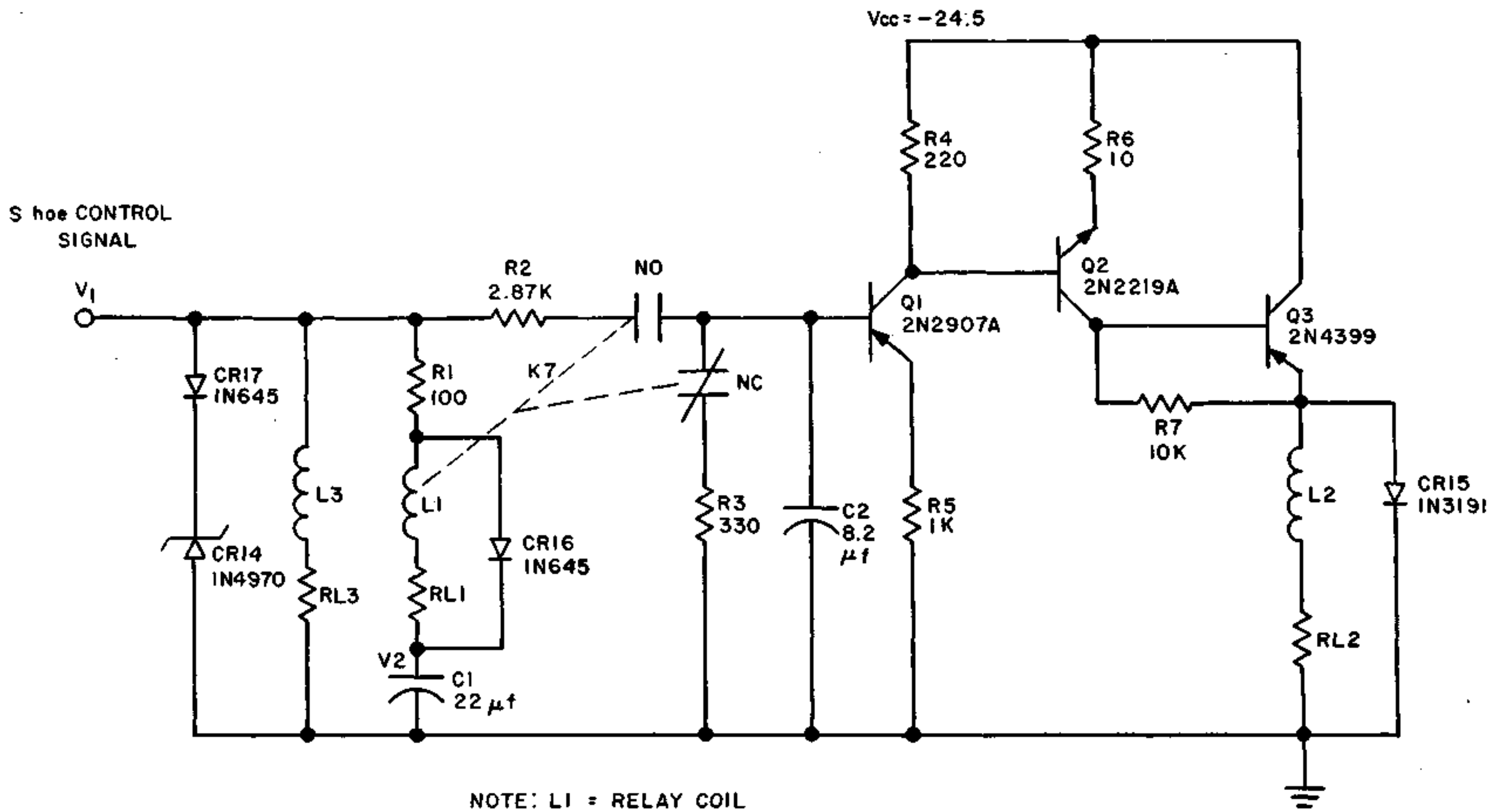

NOTE: L1 = RELAY COIL
L2 = SOLENOID PULL-IN COIL
L3 = SOLENOID HOLD COIL

Figure 3-21 SOLENOID SWITCH SCHEMATIC WITH REVISED NOMINAL COMPONENT VALUES SHOWN

In order not to exceed the power supply current step limitations, the pull-in, turn-on time must be delayed. However, this delay should be kept at a minimum in order to reduce the time the transistor is in an active region thereby minimizing power dissipation. Transistors which exhibit low leakage characteristics must be selected to eliminate the possibility of thermal runaway.

3.7.3.3 Summary, Solenoid Switch. - An initial Worst Case Analysis of the solenoid switch resulted in a number of recommendations which were incorporated into the revised network.

3.7.3.3.1 Preliminary Analysis. - Initial Worst Case Analysis of the solenoid switch revealed several points of weakness in the preliminary design. The circuit did not contain sufficient drive capability to provide the required pull-in force under worst case conditions. In addition, the driver turn-on time was excessive, compared to the relay timer minimum ON time, permitting the possibility of driver cut-off before the minimum required pull-in force has been achieved.

3.7.3.3.2 Revised Network Analysis. - Worst Case Analysis of the solenoid switch circuit containing the recommended component changes has shown that reliable operation will be achieved for worst case temperature and ageing conditions. The calculated minimum h_{FE} requirement of Q3 at 0°C is 33 as compared to the minimum available gain of $h_{FE} = 35$. Also, the minimum h_{FE}'s of Q1 and Q2 exceed the worst case circuit requirements. The minimum developed solenoid pull-in force is 4.75 lbs. vs a required minimum of 4.5 lbs. The minimum solenoid turn-on time is 4.5 ms vs a minimum requirement of 3 ms, and the maximum turn-on time is 33 ms which is well within the relay timer minimum ON time of 41.5 ms. The maximum average power dissipation of Q3 is 1.7 watts, resulting in a junction temperature of 90.7°C vs an allowable junction temperature of 110°C. The junction temperatures of Q1 and Q2 are also well within permissible limits. The thermal dissipation of Q3 is 2.5 mW/°C which is much less than its thermal dissipation factor of 28 mW/°C, thus ensuring considerable stability against possible thermal runaway. Over the temperature range of operation, the thermal currents of Q1 and Q2 are negligible. Worst case minimum holding force is 4.8 lbs. vs the specified 4.5 lbs. minimum. In addition, the maximum continuous hold voltage is 27V vs a maximum allowable of 30V.

3.7.3.4 Detailed Network Analysis. - The solenoid switch schematic showing the recommended values of R2, R6 and C2 is shown in Figure 3-20. The following analysis is based on these values and also on an assumed minimum h_{FE}=35 for Q3. Minimum h_{FE} for Q3 will be assured by specifying this parameter in the specification Control Drawing.

3.7.3.4.1 List of Symbols.

Transistor Parameters

V_C, V_E, V_B	- dc voltages at collector, emitter and base, respectively.
V_{BE}	- Base to emitter voltage.
V_{CB}	- Collector to base voltage.
V_{CE}	- Collector to emitter voltage.
I_{CBO}	- Collector cutoff current, emitter open.
I_C, I_E, I_B	- dc currents in collector, emitter and base leads, respectively.
h_{FE}	- Static value of the forward current transfer ratio (common emitter).
α N	- Small signal common base forward current transfer ratio from emitter to collector.

Diodes

i_D	- Forward current.

Coils

R_L	- Winding resistance.

Notes

a. Symbols including an n refer to specific part numbers.

b. An overline indicates a maximum value.

c. An underline indicates a minimum value.

3.7.3.4.2 Analysis Criteria. - An ambient temperature range of 0° C to 60° C over a 10,000 hour lifetime was used for component and parameter derating. The power supply and shoe control signal are -24.5±2% Vdc, with current step and transient limitations given in system specifications. For purposes of duty cycle

C3

computations, a minimun period of 2 seconds was used. This is approximately the minimum recycling time and is dependent upon the limitations of a series of system protection circuits. Coil resistance variations as a function of temperature were determined linearly using the temperature coefficient of copper. When derated transistor parameters were not defined in manufacturer's specifications, the derating factors shown in Appendix 3J were applied. These parameter derating rules are considered to be conservative and have been generally accepted for worst case circuit design. Appendix 3J also contains a summary of resistor and capacitor derating factors and the computed limits for all the components used in the solenoid switch circuit. Appendix 3K contains detailed worst case calculations.

3.7.3.4.3 Relay Timer Analysis. - As shown in Figure 3-20, the relay timer consists of R1, C1 and relay K7. When the shoe control signal, V_1, is applied, the relay is initially energized and remains ON until the charge on C1 reduces the voltage across the relay coil below its minimum drop-out voltage.

To compute the relay drop-out time, let V_2 equal the charge on C1. Then the voltage across the coil may be written as:

$$V_{L1} = \frac{R_{L1}}{R_1 + R_{L1}} (V_1 - V_2) \tag{1}$$

where

R_{L1} = relay coil resistance

Neglecting the inductive time constant, which is very small compared to the RC time constant, and also neglecting the capacitor low leakage current, then when equation 1 is substituted in the exponential function for a charging capacitor, and solved for time, the relay ON time is given by:

$$T_{ON} = (R_1 + R_{L1}) C_1 L_n \frac{V_1 R_{L1}}{V_{L1} R_1 + R_{L1})} \tag{2}$$

Since the relay drop-out voltage is extremely sensitive to changes in temperature, the worst case ON times will occur at 0° C and 60° C, where V_{L1} is given as 1.07V and 4.9V, respectively. Therefore at 60° C minimum T_{ON} is given by:

$$\underline{T_{ON}} = (R_{\underline{1}} + R_{\underline{L1}}) \underline{C1} \text{ Ln } \frac{V_{\underline{1}} R_{\underline{L1}}}{\overline{V}_{L1} (R_{\underline{1}} + R_{\underline{L1}})} \tag{3}$$

Using the values of Appendix 3J, minimum T_{ON} = 41.5 ms. Similarly for maximum T_{ON}, equation 2 is:

$$\overline{T_{ON}} = (\overline{R_1} + \overline{R_{L1}})\ \overline{C_1}\ L_n\ \frac{\overline{V_1}\ \overline{R_{L1}}}{\underline{V_{L1}}\ (\overline{R_1} + \overline{R_{L1}})} \tag{4}$$

and substituting the worst case component values in equation 4, maximum T_{ON} = 141 ms.

3.7.3.4.4 Solenoid Driver Analysis. - The solenoid driver, shown in Figure 3-20, is a three-stage transistor amplifier. When the shoe control signal (V1) is applied to the circuit, the solenoid hold coil is immediately energized. However, the solenoid pull-in current increases proportionately to the charge on capacitor C2 until the operatingpoint of Q1 reaches the saturation region. Once Q1 saturates, the pull-in current is constant throughout the relay timer ON time. Driver turn-off occurs when relay K7 de-energizes, shorting the base of Q1 to ground through R3. The turn-off time, essentially R3C2, is negligible compared to the turn-on time R2C2. Once the solenoid is pulled-in, it is kept energized by a small holding current in coil L3 until the shoe control signal is interrupted. In general, transistor and diode leakage currents may be neglected in the bulk of the following analysis due to the fact that silicon components have been specified.

3.7.3.4.4.1 Region of Operation. - In order to determine the regions of transistor linear and nonlinear operation, the time required for Q1 to saturate must be calculated. Neglecting capacitor leakage current and transistor base current, which are very small compared to the instantaneous charging current, the rise time of Q1 takes the form of:

$$T = R_2C_2\ \mathrm{Ln}\ \frac{V_1}{V_1 - V_{B1}} \tag{5}$$

From Equation 5, the minimum turn-on time is:

$$T = \underline{R_2}\,\underline{C_2}\ \mathrm{Ln}\ \frac{\underline{V_1}}{\underline{V_1} - \underline{V_{B1}}} \tag{6}$$

where:

$$\overline{V_{B1}} = \overline{I_{E1}}\ \overline{R_5} + \overline{V_{BE1}} \tag{7}$$

Using component values at 60° C, for comparison to the relay timer minimum ON time, and solving the above equations, the minimum rise time of Q1 is $\underline{T}$=24.5 ms. Similarly, for the maximum turn-on time of Q1, Equation 5 becomes:

$$\overline{T} = \overline{R}_2\,\overline{C}_2\,\mathrm{Ln}\,\frac{\overline{V}_1}{\overline{V}_1 - \overline{V}_{B1}} \tag{8}$$

where:

$$V_{\underline{B1}} = I_{\underline{E1}}\,R_{\underline{5}} + V_{\underline{BE}1} \tag{9}$$

Using component values at 0° C, for comparison to the relay timer maximum ON time, and solving the above equations, the maximum rise time of Q1 is: $\overline{T}$ = 63 ms. When the above turn-on times are compared to the relay timer ON times of $\underline{T}$=41.5 ms and $\overline{T}$=141 ms, it is apparent that the timer ON time is sufficient to permit transistor operation in the saturation region. Therefore, in the Worst Case Analysis, Q1 and Q2 may be considered to saturate during pull-in.

3.7.3.4.4.2 Drive Requirements. - To ensure that worst case pull-in force will be adequate, the transistor minimum allowable h_{FE}'s must be established. Beginning with Q3, from Figure 3-20, the current gain may be determined from:

$$V_{cc} = I_{E2}\,R_6 + V_{CE2} + V_{BE3} + \left(I_{E3} + I_{R7}\right) R_{L2} \tag{10}$$

substituting for I_{E2} and solving for h_{FE3}, the result is:

$$h_{FE3} = \frac{\alpha_{N3}\,I_{E3} + I_{CBO3}\;\; R_6}{\alpha_{N2}\left[V_{cc} + \left(\frac{I_{cbo3}}{\alpha_{N3}\alpha_{N2}} - \frac{V_{BE3}}{R_7\alpha_{N2}} + \frac{I_{CBO2}}{\alpha_{N2}}\right) R_6 - V_{CE2} - V\left(_{BE3} - I_{E3}\right) + I_{R7}\right] R_{L2}} \tag{11}$$

Now, for the h_{FE3} required, let

$$\overline{h}_{FE3} = \frac{\alpha_{N3}\,\overline{I}_{E3}}{\underline{I}_{B3}} \tag{12}$$

Or, calculate the h_{FE} required when I_E is maximum and I_B available is minimum, which is equivalent to specifying the minimum allowable h_{FE} for Q3. Since the coil resistance decreases with temperature, I_{E3} will be maximum at 0°C. By specifying the solenoid voltage requirement, maximum Q3 emitter current may be written as:

$$\overline{I_{E3}} = \frac{\overline{V_{E3}}}{\underline{R_{L2}}} - \frac{\overline{V_{BE3}}}{\underline{R7}} \qquad (13)$$

where

V_{E3} = solenoid voltage.

Neglecting I_{CBO} at 0°C, and substituting worst case parameters into Equation 11, results in a maximum h_{FE3} requirement of 33 compared to the specified $h_{FE3} = 35$ at 0°C.

In a similar manner, the h_{FE} requirements of Q1 and Q2 may be determined. From Figure 3-20, for Q2, the emitter current is given by:

$$V_{cc} = I_{E2}R_6 + V_{CE} + I_{R7} R_7 + I_{RL2}\, RL2 \qquad (14)$$

and, maximum $\underline{I_{B2}}$ required is:

$$\overline{I_{B2}} = \frac{I_{E2}}{\underline{h_{FE2}}} \qquad (15)$$

However, for the required pull-in, maximum I_{E2} = 162 mA. Using the minimum h_{FE2} specified at 0°C, or $\underline{h_{FE2}} = 53$, maximum required I_{B2} = 3 mA. To determine if Q1 is capable of delivering $\overline{I_{B2}}$, Q1 currents may be computed from:

$$V_{cc} = I_{E1}R_5 + V_{CE1} + (I_{C1} - I_{B2})\, R_4 \qquad (16)$$

Now solving for minimum available I_{E1}:

$$\underline{I_{E1}} = \frac{\underline{V_{cc}} - (I_{cbo1} - \overline{I_{B2}})\ \overline{R_4} - \overline{V_{CE1}}}{\overline{R_5} + \alpha_{N1}\, \overline{R_4}} \qquad (17)$$

Or, at 0°C, again neglecting I_{CBO}, and assuming I_{B2} = 3 mA, I_{E1} = 17.2 mA, from which:

$$\underline{I_{C1}} = \alpha_{N1}\, \underline{I_{E1}} = 17 \text{ mA} \qquad (18)$$

And, since:

$$I_{C1} = I_{R4} + I_{B2}$$

Clearly, $\underline{I_{C1}}$ is sufficient to drive Q2 for $\overline{I_{B2}} = 3$ mA.

For Q1, maximum I_{B1} required occurs at maximum I_{E1}, or

$$\overline{I_{B1}} = \frac{\overline{I_{E1}}}{\underline{h_{FE1}}} \tag{19}$$

Then using the above results for worst case pull-in, maximum required $\underline{I_{E1}} = 17.2$ mA. And since worst case specified $\underline{h_{FE1}} = 60$, then from Equation 19, $\overline{I_{B1}} = 0.29$ mA. Now, since:

$$I_{B1} = I_{R2} - I_{C2} \tag{20}$$

where:

I_{C2} = Capacitor charging current

and

$$I_{R2} = \frac{V_1 - V_{BE1} - V_{E1}}{R_2} \tag{21}$$

Then, for the above conditions, $\underline{I_{R2}} = 1.5$ mA, which is sufficient to drive the maximum possible requirement of $\overline{I_{B1}} = 0.29$ mA.

It is evident as a result of the above analysis that the revised solenoid driver is capable of supplying the required pull-in current under worst case transistor h_{FE} conditions.

3.7.3.4.5 Pull-In Force. - The solenoid pull-in force is directly proportional to the coil current, I_{L2}. Neglecting thermal current and bias resistor R7, $I_{L2} = I_{E3}$. Then Equation 10 may be written as:

$$V_{cc} = I_{E2} R_6 + V_{CE2} + V_{BE3} + I_{E3} R_{L2} \tag{22}$$

since:

$$I_{E2} \approx \frac{I_{E3}}{h_{FE3}} \tag{23}$$

Then solving the above equations for I_{E3}, and substituting worst case values at 60°C, where the coil resistance is maximum, minimum $I_{E3} = 3.6$ A. This current results in a minimum pull-in voltage of 21.4V. When translated to the manufacturer specifications, the pull-in voltage is:

$$V_{P-I} \text{ at } 25°C = \frac{V_{P-I \text{ at } T°C}}{R_c} \tag{24}$$

where:

R_c = Temperature correction factor

Or, for the above value, minimum pull-in voltage is 18.5V, which is equivalent to 4.75 lbs. force. This exceeds the minimum allowable pull-in of 4.5 lbs.

Since the maximum pull-in voltage is limited by $V_{CC} = 27V$, it is not possible to exceed the maximum allowable solenoid voltage of 30V.

3.7.3.4.6 Switching Time. - Since the L2 inductive time constant is less than 1 ms, the solenoid current rise time and fall time are dependent mainly on the charging and discharging of capacitor C2.

3.7.3.4.6.1 Minimum Turn-On. - The minimum rise time for the maximum current step must be determined for comparison to system minimum allowable limits. Neglecting the Q1 base current, which is small compared to the C2 charging current, the circuit minimum turn-on time is given by:

$$\underline{T} = \underline{R_2}\,\underline{C_2}\,\text{Ln}\,\frac{\underline{V_1}}{\underline{V_1} - \underline{V_{B1}}} \tag{25}$$

V_{B1} will be a minimum for I_{E1} minimum, and I_{E1} will be minimum when all h_{FE}'s are maximum, thus requiring minimum drive. Since h_{FE}'s are maximum at 60°C, drive currents will be computed at 60°C. Neglecting thermal currents, I_{E3} = 3.8 A and $V_{B1} = 5.47V$. Now, from Equation 25, $\underline{T}$ = 4.5 ms which clearly exceeds the 3 ms system rise time requirement for a 3.8 A step.

3.7.3.4.6.2 Maximum Turn-On. - The maximum turn-on time required must be calculated to insure that the solenoid switches to its hold condition before the relay timer drops out, cutting off the drive circuit. Maximum turn-on is given by:

$$\overline{T} = \overline{R}_2\,\overline{C}_2\,L_n\,\frac{\overline{V}_1}{\overline{V}_1 - \overline{V}_{B1}} \tag{26}$$

V_{B1} will be maximum when I_{E1} is maximum, which occurs during the maximum drive condition, or at 0°C. When the current drive equations are evaluated for maximum pull-in, I_{E3} = 5.7 A and from Equation 26, $\overline{T}$ = 54.5 ms, which is greater than the minimum relay timer ON time of 41.5 ms, resulting in drive circuit cut-off before the solenoid is fully energized. Therefore, to insure sufficient pull-in force, the time to reach the minimum allowable pull-in force of 4.5 lbs. must be considered. The alternate, but less desirable solution, would be to increase the minimum relay timer ON time. Using the former approach from the manufacturer's specifications, 4.5 lbs. pull-in at 25°C is equivalent to a coil voltage of V_{E3} = 18V, and correcting for 0°C, required V_{E3} = 16.2V. Using this condition, I_{E3} = 4.1 A and V_{B1} = 16.64V. Solving Equation 26, $\overline{T}$ = 33 ms, which is well within the minimum relay timer ON time to provide the required pull-in force.

3.7.3.4.6.3 Turn-Off. - Driver turn-off is primarily of interest in the calculation of transistor power dissipation during switching. Neglecting the small transistor emitter and collector capacitances and storage times, the driver turn-off may be written as:

$$T = R_3 C_2 \ln \frac{V_{B1}}{E_c} \tag{27}$$

where:

E_c = Capacitor charge at time = T

Solving Equation 27 for one time constant at 60°C, $\overline{T}$ = 4.27 ms and at 0°C $\underline{T}$ = 1.49 ms.

3.7.3.4.7 Transistor Power Dissipation. - Maximum power dissipation will be calculated to determine whether the transistors are operating within their specified maximum ratings and to estimate their maximum junction temperature for purposes of reliability evaluation.

3.7.3.4.7.1 Junction Dissipation. - In general, power dissipation during transistor switching takes the form of:

$$P = P(t_{off}) + P(t_{on}) + P(t_{sw1}) + P(t_{sw2}) \tag{28}$$

where:

t_{off} = OFF time

t_{ON} = ON time

t_{sw1} = Turn-on time

t_{sw2} = Turn-off time

Assuming a linear rise time, the energy dissipated during a switching interval is:

$$W_{(t_{sw})} = \frac{I_c \; V_{CE} \; (OFF) \; t_{sw}}{6} \tag{29}$$

Neglecting t_{sw} OFF, which is small compared to the maximum turn-on time, and storage and delay times, then combining Equations 28 and 29, the average power over a complete cycle is:

$$P_{avg} = \frac{V_{CE} \; (ON) \; I_c \, t_{ON} + V_{CE} \; (OFF) \; I_{CBO} \, t_{OFF}}{T} + \frac{V_{CE} \; (OFF) \; I_c \, t_{sw}}{6T} \tag{30}$$

where:

T = Switching Period

Due to system protection and recycle requirements, the minimum switching period is given as T=2s.* Since the relay timer maximum ON time is 141 ms, the driver maximum operating period is given by:

$$\bar{t}_{on} + \bar{t}_{sw} = 141 \text{ ms} \tag{31}$$

From Equation 30, it is clear that maximum dissipation occurs for $\bar{t}_{sw}$, $\bar{t}_{on}$, $\bar{I}_c$, $V_{\overline{CE}(ON)}$, $I_{\overline{CBO}}$, $V_{\overline{CE}(OFF)}$. Moreover, the worst case mode of operation is at 60°C, and maximum P_{avg} will be computed at 60°C.

3.7.3.4.7.1.1 Q3 Dissipation. - Assuming maximum $V_{CE3\,(ON)}$ results for $\bar{V}_{cc}$, $\bar{V}_{BE3}$, $\overline{V_{CE2}}$, $h_{\underline{FE3}}$ (equivalent to $\bar{I}_{E2}$) and $\bar{I}_{C3}$ results for RL2, then when Equation 11 is solved for $\bar{I}_{E3}$, the result is:

$$\bar{I}_{E3} = \frac{\bar{V}_{cc} + \left(\frac{\bar{I}_{CBO3}}{\alpha N_3 \, \alpha N_2} - \frac{\bar{V}_{BE3}}{R_7 \, \alpha N_2} + \frac{\bar{I}_{CBO2}}{\alpha N_2} \right) R_6 - \bar{V}_{LE2} - \bar{V}_{BE3}}{R_{L2} + \dfrac{\alpha N_3 \, R_6}{h_{FE3} \, \alpha N_2}} \tag{32}$$

* Typical operating cycle is 25 sec resulting in a corresponding reduction in average power and junction temperature.

substituting worst case parameters and component values, at 60°C, $\bar{I}_{E3} = 4.72$ A, $\bar{I}_{C3} = 4.62$ A, $V_{E3} = 22.5$V and $\bar{V}_{CE3} = 2.5$V. From Equation 26, the maximum turn-on time at 60°C is $\bar{t}_{SW} = 39$ ms. Then, substituting $\bar{t}_{SW}$ into Equation 31, $\bar{t}_{ON} =$ 102 ms, and since:

$$t_{OFF} = T - (t_{ON} + t_{sw}) \tag{33}$$

then,

$$\bar{t}_{OFF} = 2 - .144 = 1.86 \text{ S}$$

When the above values are substituted into Equation 30, $\bar{P}_{Q3} = 1.7$W.

3.7.3.4.7.1.2 Q2 Dissipation. - Following the above procedure for Q2, $\bar{V}_{CE2}$ ON = .41, and $\bar{I}_{C2}$ ON = 110 mA. Then, evaluating Equation 30, $\bar{P}_{Q2} = 11.3$ mw.

3.7.3.4.7.1.3 Q1 Dissipation. - Similarly for Q1, $\bar{V}_{CE}$ ON = 8V, and $\bar{I}_{C1}$ ON = 12 mA. When Equation 30 is evaluated, $\bar{P}_{Q1} = 5.9$ mw.

To determine the maximum allowable transistor power dissipation, the maximum junction temperature must be calculated.

3.7.3.4.7.2 Junction Temperature. - Transistor operating junction temperature without a heat sink is given by:

$$T_J = T_A + \theta_{J-A} P_T \tag{34}$$

where:

$$\theta_{J-A} = \theta_{J-C} + \theta_{C-A}$$

and:

θ_{J-A} = Thermal resistance from junction to free air (°C/W)

θ_{J-C} = Thermal resistance from junction to case (°C/W)

θ_{C-A} = Thermal resistance from case to free air (°C /W)

T_A = Ambient temperature (°C)

T_J = Junction temperature (°C)

P_T = Transistor average power dissipation (W)

Since the duty cycle of Q3 involves pulses of power dissipation occurring over a period of time much less than the transistor typical thermal time constant (T_{JC} = 165 sec), then the junction temperature rise is governed by the average, rather than the instantaneous power dissipation. Thus, for Q3, at $T_A = 60°C$, using nominal thermal resistances and P_T = 1.7 watts, the maximum junction temperature is $\overline{T_j}$ = 119.2°C.

Similarly, for Q2, $\underline{T_j}$ + 62.12° C, and for Q1, $\underline{T_j}$ = 62.58° C. Since the ERTS system maximum allowable transistor junction temperature is 110° C, a heat sink was required to reduce the junction temperature of Q3.

The Q3 heat sink is 6.6 sq. in. of copper clad circuit board. If the effects of heat convection are neglected due to zero gravity and the heat sink is isolated, preventing conduction, then heat transfer from the heat sink is entirely due to radiation. When the area of the heat sink is much smaller than the area of the surrounding surface, the radiant heat transfer in BTU/hr. is given by:

$$Q = A_1 e_1 \sigma (T_1^4 - T_2^4)$$

where

A_1 = heat sink area (ft^2)

e_1 = emissivity (approximately 0.8 for unpolished copper)

σ = Stefan-Boltzman constant (0.173×10^{-8} BTU/hr.-ft^2-R4)

T_1 = temperature of last sink (°Rankine)

T_2 = temperature of surrounding surface (°Rankine)

Since the heat sink is copper, which has a high conductivity, it may be assumed that the temperature of the heat sink is uniform, and that its temperature may be calculated for a given heat transfer. Then solving the above equation for T_1:

$$T_1 = \left(\frac{Q + A_1 e_1 \sigma T_2^4}{A_1 e_1 \sigma} \right)^{1/4} \tag{35}$$

Substituting worst case values into Equation 35, T_1 = 650°R or 87.5°C. Now, for a heat sink mounted transistor, the junction temperature is:

$$T_J = T_C + (\theta_{J-C} + \theta_{C-S}) P_T$$

where

θ_{C-S} = thermal resistance from case to heat sink

For a mica insulator, $\theta_{C-S} = 0.5$, and evaluating the above equation, $\overline{T}_J$ = 90.7°C. For the above temperatures, the power ratings are as follows:

	DISSIPATION	JUNCTION TEMPERATURE	MAXIMUM RATED POWER	MAXIMUM ALLOWABLE POWER
Q1	5.9 mw	62.58°C	200 mw	210 mw
Q2	11.3 mw	62.12°C	550 mw	330 mw
Q3	1.7 W	90.7°C	125 W	87 W

Comparing the above values indicates all the transistors are operating within their allowable power ratings.

3.7.3.4.7.3 Thermal Stability. - To avoid thermal runaway due to thermal regeneration, the rate at which junction heat is released as the junction temperature increases must not exceed the rate at which power can be dissipated. This may be expressed as follows:

$$\frac{\Delta P_T}{\Delta T_j} \leq \frac{1}{\theta_{J-A}} \qquad (36)$$

where P_T, T_j and θ J-A are defined in Paragraph 3.7.3.4.7.2. Assuming current flow in the cut-off region is primarily due to thermal current, this rate of change of power dissipation is:

$$\frac{\Delta P_T}{\Delta T_J} = V_{cc} \, \Delta I_{CBO} \qquad (37)$$

assuming:

$$\Delta I_{cbo} = \frac{10\%}{°C} \qquad (38)$$

Then, for Q3, maximum

$$\Delta I_{cbo} = \frac{0.1 \text{ MA}}{°C}$$

And substituting into Equation 36, the result for Q3 is:

$$2.5 \text{ MW} \leq 28.8 \text{ MW}$$

In a similar manner, for Q2,

$\overline{\Delta I}_{cbo}$ = .032 μA, and θ_{J-A} = 188,

and from Equation 36,

.0007 MW $\leq$ 5.3 MW

Also, for Q1,

$\overline{\Delta I}_{cbo}$ = .032 μA, and θ_{J-A} = 438

and from Equation 36,

.0007 MW $\leq$ 2.3 MW

Clearly, from the above inequalities, the temperature stability of transistors Q1, Q2 and Q3 is sufficient to prevent thermal runaway.

3.7.3.4.8 Hold Circuit. - The hold circuit consists of inductor L3 and clamping diodes CR14 and CR17. Of primary interest in the hold circuit analysis is the minimum available holding force, maximum turn-on time and maximum power dissipation.

3.7.3.4.8.1 Holding Force. - Since holding force varies inversely with temperature, minimum force will be developed at 60°C. Using the manufacturer's specifications, holding force at 25°C for minimum V_{cc} = 24V is 6 ±10% lbs. Dividing by the temperature correction factor, R_c = 1.13.

$\underline{\text{Force}}$ = 4.8 lbs.

Maximum holding force occurs at V_{cc} = 25V, 0°C. Again, from the manufacturer's specification, at 25°C, the holding force = 6.4 ±10% lbs. Correcting for temperature, for R_c = .9.

$\overline{\text{Force}}$ = 7.8 lbs.

Since the minimum allowable holding force is 4.5 lbs. vs the minimum developed force of 4.8 lbs., the worst case holding requirement will be satisfied.

3.7.3.4.8.2 Rise Time. - The build up of holding force is limited by the inductive time constant, expressed as

$$T = L/R$$

Or, the maximum time required to achieve 63.2% of the maximum holding force of approximately 4.9 lbs. at 0°C is:

$$\overline{T} = \frac{L}{\underline{R}_{L3}} = 0.27 \text{ MS}$$

To calculate the minimum pull-in time available at 0°C, let

$$\underline{T}\text{ (Pull-In ON)} = \underline{T}\text{(Relay Timer ON)} - \bar{T}\text{ (Pull-In Turn-ON)} \qquad (40)$$

which yields the minimum pull-in ON time of 8.5 ms. Or, the quiescent pull-in force can be considered to be present long enough for the hold coil to energize under worst case conditions.

3.7.3.4.8.3 Power Dissipation. - Maximum hold coil power dissipation occurs at 0°C, where coil resistance is minimum, resulting in maximum holding current. Thus,

$$\bar{P} = \frac{\bar{V}^2}{\underline{R}_L} \qquad (41)$$

Substituting worst case parameters, $\bar{P}_{0°C} = 6.3W$. For purposes of evaluating equipment temperature rise, the maximum power dissipation at 60°C is $\tilde{P}_{60°} = 5.1W$. Since the coil is rated at 30V, and $\tilde{V}1$ is 27V, there is no possibility of coil damage due to overload.

3.7.4 Motor Control. - Of primary interest in the motor control system design is whether the minimum available relay turn-on voltage is sufficient to activate the relays under worst case conditions, the maximum contact current and reverse voltage transient suppression. Since the peak suppression and contact currents are covered in the Stress Analysis Section of this report, only the turn-on voltage is discussed below.

The motor control relays, one side of which are connected to the primary power, are energized by grounding the control line through another relay contact. Thus, the voltage available at the coil is limited only by the relay contact resistance and may be expressed as:

$$V_{coil} = V_{cc} - I_{coil} R_c \qquad (42)$$

where:

R_c = contact resistance

V_{cc} = primary power

and for the motor control relay:

$$I_{coil} = \frac{V_{coil}}{R_{coil}} \qquad (43)$$

Combining the above equations, and solving for minimum coil voltage:

$$\underline{V_{coil}} = \frac{\underline{V_{cc}}}{1 + \frac{\underline{R_c}}{\underline{R_{coil}}}} \tag{44}$$

Substituting worst case value into Equation 44, the minimum available coil voltage is 23.9 volts, which is much greater than the maximum required pick-up voltage of 18V. Since the maximum available coil voltage is $\bar{V}_{cc} = 27V$, and the maximum allowable voltage is 29V, there is no possibility of coil overload.

Relay contact bounce, operate and release times are insignificant in the motor control circuit operation because the motor start sequence typically lasts several seconds.

3.7.5 Conclusions and Recommendations. - With the recommended values of R2, R6 and C2, and a minimum h_{FE} 2N4399 incorporated into the solenoid switch design, the Worst Case Analysis has shown that all operating requirements will be satisfied over the temperature range of 0°C-60°C for a lifetime of 10,000 hours. However, overall system efficiency and circuit reliability may be increased through several suggested improvements in future designs.

The maximum holding coil power dissipation (6.3 watts) is substantial, considering it to be more or less continuous. Conceivably, if size is not a major obstacle, this power consumption may be reduced considerably by a redesign of the coil winding. By using smaller wire size with an increased number of turns, the coil resistance would be increased, while at the same time providing the required holding force.*

---

* Since the writing of this report, the manufacturer of the solenoid has agreed to build the holding coil with an increased winding resistance of approximately 240 ohm while maintaining a minimum of 5 to 6 lbs. force at room temperature. The resulting nominal power dissipation will be 2.5 watts.

APPENDIX 1A

PRELIMINARY PART LIST

FOR

TRANSPORT UNIT

TRANSPORT ASSEMBLY
PL 8358497

ITEM	QTY (501)	FINAL RCA NUMBER	INTERIM NUMBER	DESCRIPTION
1	1	8777186-501	JL PL6907261-502	Reel Assembly, Supply
2	1	8777186-502	JL PL6907261-501	Reel Assembly, Take-Up
3	1	8658182-501	JL PL6907262-502	Dia. Sensing, Supply
4	1	8658182-502	JL PL6907262-501	Dia. Sensing, Take-Up
5	2	8656729-501	JL PL6907263-501	Tape Guide (2.00)
6	3	8656729-502	JL PL6907263-502	Tape Guide (2.04)
7	1	8777187-501	JL PL6907264-501	Erase Head
8	1	8359742-501	JL PL6907265-501	Headwheel Panel
9	1	8777181-501	JL PL6907266-501	Auxiliary Head
10	1	8777122-501	JL PL6907267-501	Capstan Assembly
11	1	8777183-501	JL PL6907268-501	Capstan Motor Assembly
12	1	8656730-501	JL PL6907269-501	Negator/Diff. Assembly
13	1	8777182-501	JL PL6907271-501	Momentum Comp. (HW)
14	1	8777123-501	JL PL6907272-501	Momentum Comp. (Reel)
15	1	8359765-1		Deck, Tape Transport
16	1	8778740-501		Cover, Negator
17	1	8656774-501		Gasket, Enclosure
18	1	8370328-501		Enclosure, Bottom
19	1	8370333-501		Enclosure, Top
20	1	8151213-1		Connector, Power, J51
21	1	8151213-2		Connector, Motor Power, J52
22	1	8151213-3		Connector, Signal, J53
23	1	8151213-4		Connector, Auxiliary, J54
24	1	8504636-1		Pressure Transducer
25	1	8151205-1		Probe, Thermistor
26	1	8505035-1		Support, Temperature Sensor
27	1	8805220-1		Case, Temperature Sensor

ITEM	QTY (501)	FINAL RCA NUMBER	INTERIM NUMBER	DESCRIPTION
28				
29				
30				
31	2	8359708-501		Video Rec/Preamp
32	1	8359709-501		Video Playback Amp
33	1	8359687-501		Control/Tach Preamp
34	1	8359750-501		Aux/Search Preamp
35	1	8359688-501		Motor/Solenoid Switch

REEL ASSEMBLY
JL PL6907261

ITEM	QTY 502	QTY 501	PART NUMBER	DESCRIPTION
1	1	1	8777189-1	Reel
2	1	1	8777188-1	Hub, Reel
3	-	1	8509260-501	Drive Shaft, Reel
4	1	-	8509260-502	Drive Shaft, Reel
5	1	-	8150516-1	Spanner, Reel Brg
6	1	1	8509261-1	Spacer } Matched Pair
7	1	1	8509261-2	Spacer } Matched Pair
8	1	1	SR8FFW5DB10CG-6	Barden Brg, Matched Pr.
9	1	1	8509259-1	Retainer, Reel Brg
10	1	-	8778705-501	Pulley Assembly, Take-Up
11	1	-	8509261-13	Spacer } Matched Pair
12	1	-	8509261-14	Spacer } Matched Pair
13	1	-	SFR1810SSW5DB2CG-6	Barden Brg, Matched Pr.
14	1	-	8150518-1	Lock, Reel Shaft
15	1	-	8150517-1	Lock, Reel Pulley
16	1	-	8509293-1	Spacer
17	1	-	MS28775-011	"O" Ring
18	1	-	8509296-1	Retainer Brg
19	1	1	8150511-1	Spacer, Shaft
20	-	1	8778743-501	Pulley Ass'y, Supply
21	-	1	8509299-2	Clamp

DIA SENSING ASSEMBLY
JL PL6907262

ITEM	QTY 502	QTY 501	PART NUMBER	DESCRIPTION
1	-	1	8778708-1	Plate, Bottom
2	1	-	8778708-2	Plate, Bottom
3	-	1	8656722-1	Plate, Top
4	1	-	8656722-2	Plate, Top
5	3	3	8150500-1	Spacer, Post
6	1	1	8150503-1	Shaft
7	1	1	8150504-1	Bushing
8	-	1	8150502-2	Spring
9	1	-	8150502-1	Spring
10	1	1	8509200-1	Cam
11	1	1	8509200-2	Cam
12	1	1	8778706-1	Bracket, Adjustable
13	2	2	11SM423	Micro-Switch
14	2	2	JS-5	Switch Actuator, Micro-Switch
15	x	1	8761443-1	Potentiometer
16	x	1	8778738-1	Gear, Spur
17	1	1	8150646-1	Bushing, Pot
18	1	1	JL PL 6908031	Arm Assembly
19	1	1	8505275-23	Connector
20	1	1	8509286-1	Spring Retainer
21	1	1	8151207-1	Spacer, Conn. Mtg.
22	1	1	8151208-1	Plate, Conn. Mtg.
23	1	1	8150647-1	Insulator, Micro-Switch
			8489878-1	Cleat

ARM ASSEMBLY, DIA SENSING
JL PL6908031

ITEM	QTY 502	QTY 501	PART NUMBER	DESCRIPTION
1	1	1	8778709-1	Arm
2	1	1	8778765-1	Post, Flexure
3	-	1	8778738-3	Gear, Spur
4	1	1	8151204-501	Roller
5	1	1	8150645-1	Retainer, Brg
6	1	1	8150643-1	Retainer, Brg
7	1	1	8150644-1	Retainer, Brg
8	2	2	SR166SSW3G-6	Bearing, Barden

TAPE GUIDE ASSEMBLY
JL PL6907263

ITEM	QTY 502	QTY 501	PART NUMBER	DESCRIPTION
1	1	1	8509292-1	Washer
2	1	1	8509295-1	Cap
3	1	1	MS28775-011	"O" Ring
4	-	1	8509293-1	Spacer
5	1	-	8509293-2	Spacer
6	-	1	8778737-3	Roller (2.000)
7	1	-	8778737-4	Roller (2.040)
8	1	1	SFR1810SSW5DB2CG-6	Barden Brg, Matched Pr.
9	1	1	8509296-1	Retainer, Brg
10	1	1	8151209-1	Spacer } Matched Pair
11	1	1	8151209-2	Spacer } Matched Pair
12	-	1	8656728-503	Guide Post
13	1	-	8656728-504	Guide Post
14	1	1	38031K-96C-6	Scr, But.Hd. 6-32x.38
15	6	6	28711N-94C-3	Scr, Set, 4-40x.18
16	AR	AR	8151210-2	Shim .002 Thick
17	AR	AR	8151210-3	Shim .003 Thick
18	AR	AR	8151210-4	Shim .005 Thick
19	AR	AR	8151210-5	Shim .010 Thick

ERASE HEAD ASSEMBLY
JL PL6907264

ITEM	QTY 502	QTY 501	PART NUMBER	DESCRIPTION
1	-	2	3315105-1	Cores
2	-	1	3315113-1	Mount
3	-	1	3313535-1	Base
4	-	1	3313536-1	Cover
5	-	1	8508097-1	Clamp
6	-	1	8722717-2	Connector

HEADWHEEL PANEL ASSEMBLY
JL PL6907265

ITEM	QTY 502	QTY 501	PART NUMBER	DESCRIPTION
1		1	JL PL6908032-501	Motor Headwheel Assembly
2		1	3314528-501	Shoe Assembly
3		1	3312369-1	Flex (Vertical)
4		1	JL 6907252-1	Level (Shoe Actuator)
5		1	3310983-2	Knob (Shoe Stop)
6		1	3310984-2	Nut (Special)
7		1	3310980-1	Scr, Hex Soc Special
8		1	3312718-2	Stabilizer Arm
9		2	3311348-1	Wedge
10		1	3313527-1	Bracket, Spring
11		1	3311447-1	Spring, Shoe Disengage
12		1	3311588-1	Clamp, Solenoid
13		1	3311589-1	Clamp, Solenoid
14		1	3313525-1	Clamp, Shoe Stop
15		1	3313528-1	Lug, Engage Solenoid
16		1	3313526-1	Mount, Engage Solenoid
17		1	8656766-2	Mount, Tonewheel Head
18		1	3314335-501	Tone Head
19		1	8505275-31	Connector
20		1	Drawings not Available until later date	Transformer Assembly
21		1	JL 6907312-1	Scr, #6-64x.38
22		1	3315116-1	Mount, Solenoid

MOTOR HEADWHEEL ASSEMBLY
JL PL6908032

ITEM	QTY 502	QTY 501	PART NUMBER	DESCRIPTION
1		1	8359743-501	Motor Assembly
2		1	8778790-1	Shaft, HW
3		1	SR6STA5DF2ER2CV26CG-6	Barden Matched Pair
4		1	3313546-1	End Cap
5		1	SR4STA5DB2ER2CV26CG-6	Barden Matched Pair
6		1	3313520-1	Mount, H.W. Tonewheel
7		1	3315103-1	Tonewheel
8		1	3313518-1	Interlock
9		1		HW Assembly
10		4		Rotary Transformer

AUXILIARY HEAD ASSEMBLY
JL PL6907266

ITEM	QTY 502	QTY 501	PART NUMBER	DESCRIPTION
1	-	x	3315247-501	Mount & Head Assembly
2	-	1	3317315-501	Head Assembly
3	-	1	3317307-1	Block
4	-	2	3313704-501	Core Assembly
5	-	2	3313704-502	Core Assembly
6	-	2	3313704-503	Core Assembly
7	-	90	3312552-1	Lamination
8	-	4	3313705-501	Terminal Board Assembly
9	-	4	3312420-2	Board Terminal
10	-	8	3312539-1	Terminal
11	-	2	3331409-1	Shield
12	-	1	3331404-1	Shield
13	-	4	8722717-2	Connector
14	-	1	3317301-1	Mount
15	-	1	3331406-1	Clamp, Plate
16	-	1	3331405-1	Cover, Plate

CAPSTAN ASSEMBLY
JL PL6907267

ITEM	QTY 502	QTY 501	PART NUMBER	DESCRIPTION
1		1	8509292-2	Washer
2		1	SR4SW5DB2ER2CG-6	Barden Brg, Match Pr.
3		1	8509248-1	Shaft
4		1	8509247-501	Housing
5		1	SR6SW5DF2ER2CG-6	Barden Brg, Matched Pr.
6		1	8150508-1	Ring
7		1	8777121-1	Pulley
8		1	8509299-1	Clamp
9		2	38031K-96C-6	Scr, But.Hd 6-32x.38

14

CAPSTAN MOTOR ASSEMBLY
JL PL6907268

ITEM	QTY 502	QTY 501	PART NUMBER	DESCRIPTION
1		1	8778735-501	Motor
2		1	8509255-1	Pulley
3		1	8150588-1	Tonewheel
4		1	8656766-1	Tone Head Mount
5		1	8505242-73	Connector
6		1	8150571-1	Ring, TW Lock
7		1	8150587-1	Spacer, TW
		1	3311053-1	Spring
14		1		
15		1	8778771-1	Clamp, Motor

NEGATOR/DIFFERENTIAL ASSEMBLY
JL PL6907269

ITEM	QTY 502	QTY 501	PART NUMBER	DESCRIPTION
1	-	1	8778741-1	Plate, Negator Mtg.
2	-	1	8509277-1	Shaft, Negator Take-Up
3	-	2	8150511-2	Spacer
4	-	2	8509278-501	Drum, Negator Take-Up
5	-	2	8509284-1	Ring, Negator Take-Up
6	-	2	8509261-6	Spacer
7	-	2	8509261-7	Spacer
8	-	1	8509261-8	Spacer, Drum
9	-	2	8509292-3	Washer
10	-	1	8778744-1	Shaft, Negator Output
11	-	1	8777199-501	Drum, Negator Output
12	-	1	8509261-9	Spacer } Match Pair
13	-	1	8509261-10	Spacer } Match Pair
14	-	1	8509285-1	Ring, Negator Output
15	-	1	8778700-1	Housing, Differential
16	-	1	8509276-1	End Plate, Top, Diff.
17	-	1	8509270-1	End Plate, Bottom, Diff.
18	-	1	8509246-1	Ring, Top
19	-	2	8509271-1	Ring, Bottom
20	-	1	8509245-1	Cap
21	-	1	8509261-3	Spacer
22	-	1	8778701-501	Pulley Assembly
23	-	1	8778702-501	Pulley Assembly
24	-	3	SFR6SSW5DB5-G6	Bearing, Barden Pair
25	-	1	8656765-501	Differential
26	-	1	8150639-1	Gear, Negator Drum
27	-	1	8509275-501	End Plate

ITEM	QTY 502	QTY 501	PART NUMBER	DESCRIPTION
28	-	1	SR4FW5DF2CG-6	Bearing, Barden Pair
29	-	1	SFR4FW5DB2CG-6	Bearing, Barden Pair
30	-	2		Spring, Negator

MOMENTUM COMPENSATION ASSEMBLY (H.W.)
JL PL6907271

ITEM	QTY 502	QTY 501	PART NUMBER	DESCRIPTION
1	-	1	8778734-501	Motor
2	-	1	8656763-501	Inertia Comp.
3	-	1	8656763-502	Inertia Comp.
4	-	1	8150520-1	Interlock

MOMENTUM COMPENSATOR (REEL)
JL PL6907272

ITEM	QTY 502	QTY 501	PART NUMBER	DESCRIPTION
1	-	1	8509254-1	Shaft
2	-	1	8150511-2	Spacer
3	-	1	8509261-4	Spacer } Matched Pair
4	-	1	8509261-5	Spacer
5	-	1	SFR6SSW5DB5G-6	Barden Brg, Matched Pr.
6	-	1	8509253-1	Ring
7	-	1	8509245-2	Cap
14	-	1	8151226-1	Clamp
15				

VIDEO RECORD/PREAMP
PL 8359708

ITEM	PART NUMBER	DESCRIPTION
A1	8150561-1	Current Probe (CT-2)
C1	CKR06BX104KP	Capacitor, CER, 0.1 UF, ±10%, 100V
C2	CKR06BX104KP	Capacitor, CER, 0.1 UF, ±10%, 100V
C3	CKR06BX104KP	Capacitor, CER, 0.1 UF, ±10%, 100V
C4	CKR06BX104KP	Capacitor, CER, 0.1 UF, ±10%, 100V
C5	8150547-41	Capacitor, Tant, 2.2 UF, ±10%, 35V
C6	CKR06BX104KP	Capacitor, CER, 0.1 UF, ±10%, 100V
C7	CKR06BX104KP	Capacitor, CER, 0.1 UF, ±10%, 100V
C8	CKR06BX104KP	Capacitor, CER, 0.1 UF, ±10%, 100V
C9	CKR06BX104KP	Capacitor, CER, 0.1 UF, ±10%, 100V
C10	CKR06BX104KP	Capacitor, CER, 0.1 UF, ±10%, 100V
C11	CKR06BX104KP	Capacitor, CER, 0.1 UF, ±10%, 100V
C12	CKR06BX104KP	Capacitor, CER, 0.1 UF, ±10%, 100V
C13	CKR06BX104KP	Capacitor, CER, 0.1 UF, ±10%, 100V
C14	CKR06BX104KP	Capacitor, CER, 0.1 UF, ±10%, 100V
C15	CM05CD102J03	Capacitor, Mica, 12 PF, ±5%, 500V
C16	8150547-41	Capacitor, Tant, 2.2 UF, ±10%, 35V
C17	8150547-41	Capacitor, Tant, 2.2 UF, ±10%, 35V
C18	CKR06BX104KP	Capacitor, CER, 0.1 UF, ±10%, 100V
C19	CKR06BX104KP	Capacitor, CER, 0.1 UF, ±10%, 100V
C20	CKR06BX104KP	Capacitor, CER, 0.1 UF, ±10%, 100V
C21	CKR06BX104KP	Capacitor, CER, 0.1 UF, ±10%, 100V
C22	CKR06BX104KP	Capacitor, CER, 0.1 UF, ±10%, 100V
C23	CKR06BX104KP	Capacitor, CER, 0.1 UF, ±10%, 100V
C24	CKR06BX104KP	Capacitor, CER, 0.1 UF, ±10%, 100V
C25	CKR06BX104KP	Capacitor, CER, 0.1 UF, ±10%, 100V
C26	CKR06BX104KP	Capacitor, CER, 0.1 UF, ±10%, 100V

ITEM	PART NUMBER	DESCRIPTION
C27	CKR06BX104KP	Capacitor, CER, 0.1 UF, ±10%, 100V
C28	CKR06BX104KP	Capacitor, CER, 0.1 UF, ±10%, 100V
C29	CKR06BX104KP	Capacitor, CER, 0.1 UF, ±10%, 100V
C30	CKR06BX104KP	Capacitor, CER, 0.1 UF, ±10%, 100V
C31	CM05CD120J03	Capacitor, Mica, 12 PF, ±5%, 500V
C32	8150547-41	Capacitor, Tant, 2.2 UF, ±10%, 35V
C33	8150547-41	Capacitor, Tant, 2.2 UF, ±10%, 35V
C34	CKR06BX104KP	Capacitor, CER, 0.1 UF, ±10%, 100V
C35	CKR06BX104KP	Capacitor, CER, 0.1 UF, ±10%, 100V
C36	CKR06BX104KP	Capacitor, CER, 0.1 UF, ±10%, 100V
C37	CKR06BX104KP	Capacitor, CER, 0.1 UF, ±10%, 100V
C38	CKR06BX104KP	Capacitor, CER, 0.1 UF, ±10%, 100V
C39	8150547-15	Capacitor, Tant, 22 UF, ±10%, 15V
C40	CKR06BX104KP	Capacitor, CER, 0.1 UF, ±10%, 100V
C41	CK06BX105K	Capacitor, CER, 1.0 UF, ±10%, 50V
C42	8150547-15	Capacitor, Tant, 22 UF, ±10%, 15V
C43	CK06BX105K	Capacitor, CER, 1.0 UF, ±10%, 50V
C44	CKR06BX104KP	Capacitor, CER, 0.1 UF, ±10%, 100V
C45	CKR06BX104KP	Capacitor, CER, 0.1 UF, ±10%, 100V
C46	8150547-15	Capacitor, Tant, 22 UF, ±10%, 15V
C47	CKR06BX104KP	Capacitor, CER, 0.1 UF, ±10%, 100V
C48	CK06BX105K	Capacitor, CER, 1.0 UF, ±10%, 50V
C49	8150547-15	Capacitor, Tant, 22 UF, ±10%, 15V
C50	CK06BX105K	Capacitor, CER, 1.0 UF, ±10%, 50V
C51	CKR06BX104KP	Capacitor, CER, 0.1 UF, ±10%, 100V
CR1	JANTX1N645	Diode
CR2	JANTX1N645	Diode
K1	M5757/40-010	Relay (412-26)

ITEM	PART NUMBER	DESCRIPTION
L1	8150567-26	Coil, 12 uH (SW-W-12)
L2	8150567-26	Coil, 12 uH (SW-W-12)
L3	8150567-26	Coil, 12 uH (SW-W-12)
L4	8150567-49	Coil, 1000 uH (SW-W-1000)
L5	8150567-26	Coil, 12 uH (SW-W-12)
L6	8150567-26	Coil, 12 uH (SW-W-12)
L7	8150567-26	Coil, 12 uH (SW-W-12)
L8	8150567-49	Coil, 1000 uH (SW-W-1000)
P80/86		Connector (Heads)
P81/87		Connector (Power)
P82/88		Connector (Output)
P83/89		Connector (Part of A1)
P84/90		Connector (Output)
Q1	JANTX2N3251A	Transistor, si, PNP
Q2	JANTX2N3251A	Transistor, si, PNP
Q3	JANTX2N2218A	Transistor, si, NPN
Q4	JANTX2N2222A	Transistor, si, NPN
Q5	JANTX2N2907A	Transistor, si, PNP
Q6	JANTX2N3251A	Transistor, si, PNP
Q7	JANTX2N3251A	Transistor, si, PNP
Q8	JANTX2N2218A	Transistor, si, NPN
Q9	JANTX2N2222A	Transistor, si, NPN
Q10	JANTX2N2907A	Transistor, si, PNP
Q11	8150548-1	Transistor, si, NPN (2N3572)
Q12	8150548-1	Transistor, si, NPN (2N3572)
Q13	JANTX2N2369A	Transistor, si, NPN (2N3572)
Q14	8150548-1	Transistor, si, NPN (2N3572)
Q15	8150548-1	Transistor, si, NPN (2N3572)

ITEM	PART NUMBER	DESCRIPTION
Q16	JANTX2N2369A	Transistor, si, NPN (2N3572)
R1	RCR07G151JP	Resistor, Comp, 150 ±5%, 1/4W
R2	RCR07G220JP	Resistor, Comp, 22, ±5%, 1/4W
R3	RNR55C1001FP	Resistor, Film, 1000, ±1%, 1/10W
R4	RNR55C1001FP	Resistor, Film, 1000, ±1%, 1/10W
R5	RCR07G302JP	Resistor, Comp, 3000, ±5%, 1/4W
R6	RCR07G122JP	Resistor, Comp, 1200, ±5%, 1/4W
R7	RNR55C1001FP	Resistor, Film, 1000, ±1%, 1/10W
R8	RNR55C1001FP	Resistor, Film, 1000, ±1%, 1/10W
R9	RCR07G432JP	Resistor, Comp, 4300, ±5%, 1/4W
R10	RCR07G272JP	Resistor, Comp, 2700, ±5%, 1/4W
R11	RCR07G102JP	Resistor, Comp, 1000, ±5%, 1/4W
R12	RCR07G122JP	Resistor, Comp, 1200, ±5%, 1/4W
R13	RCR07G472JP	Resistor, Comp, 4700, ±5%, 1/4W
R14	RCR07G101JP	Resistor, Comp, 100, ±5%, 1/4W
R15	RCR07G472JP	Resistor, Comp, 4700, ±5%, 1/4W
R16	RCR07G102JP	Resistor, Comp, 1000, ±5%, 1/4W
R17	RNR55C2000FP	Resistor, Film, 200, ±1%, 1/10W
R18	RJ24CX501	Resistor, Var, 500, ±10%, 1/2W
R19	RCR07G562JP	Resistor, Comp, 5600, ±5%, 1/4W
R20	RCR07G101JP	Resistor, Comp, 100, ±5%, 1/4W
R21	RNR55C2001FP	Resistor, Film, 2000, ±1%, 1/10W
R22	RCR07G101JP	Resistor, Comp, 100, ±5%, 1/4W
R23	RCR07G392JP	Resistor, Comp, 3900, ±5%, 1/4W
R24	RCR07G511JP	Resistor, Comp, 510, ±5%, 1/4W
R25	RCR07G820JP	Resistor, Comp, 82, ±5%, 1/4W
R26	RCR20G202JP	Resistor, Comp, 2000, ±5%, 1/2W
R27	RNR55C1001FP	Resistor, Film, 1000, ±1%, 1/10W

ITEM	PART NUMBER	DESCRIPTION
R28	RCR07G101JP	Resistor, Comp, 100, ±5%, 1/4W
R29	RNR60C3001FP	Resistor, Film, 3000, ±1%, 1/8W
R30	RCR07G221JP	Resistor, Comp, 220, ±5%, 1/4W
R31	RCR07G102JP	Resistor, Comp, 1000, ±5%, 1/4W
R32	RCR07G102JP	Resistor, Comp, 1000, ±5%, 1/4W
R33	RCR20G101JP	Resistor, Comp, 100, ±5%, 1/2W
R34	RCR07G202JP	Resistor, Comp, 2000, ±5%, 1/4W
R35	RCR07G470JP	Resistor, Comp, 47, ±5%, 1/4W
R36	RCR20G201JP	Resistor, Comp, 200, ±5%, 1/2W
R37	RCR07G202JP	Resistor, Comp, 2000, ±5%, 1/4W
R38	RCR20G101JP	Resistor, Comp, 100, ±5%, 1/2W
R39	RCR07G100JP	Resistor, Comp, 10, ±5%, 1/4W
R40	RCR07G100JP	Resistor, Comp, 10, ±5%, 1/4W
R41	RNR55C1001FP	Resistor, Film, 1000, ±1%, 1/10W
R42	RCR07G100JP	Resistor, Comp, 10, ±5%, 1/4W
R43	RNR55C1001FP	Resistor, Film, 1000, ±1%, 1/10W
R44	RCR07G100JP	Resistor, Comp, 10, ±5%, 1/4W
R45	RCR07G430JP	Resistor, Comp, 43, ±5%, 1/4W
R46	RCR07G101JP	Resistor, Comp, 100, ±5%, 1/4W
R47	RCR07G472JP	Resistor, Comp, 4700, ±5%, 1/4W
R48	RCR07G102JP	Resistor, Comp, 1000, ±5%, 1/4W
R49	RNR55C2000FP	Resistor, Film, 200, ±1%, 1/10W
R50	RJ24CX501	Resistor, Var, 500, ±10%, 1/2W
R51	RCR07G562JP	Resistor, Comp, 5600, ±5%, 1/4W
R52	RCR07G101JP	Resistor, Comp, 100, ±5%, 1/4W
R53	RNR55C2001FP	Resistor, Film, 2000, ±1%, 1/10W
R54	RCR07G101JP	Resistor, Comp, 100, ±5%, 1/4W
R55	RCR07G392JP	Resistor, Comp, 3900, ±5%, 1/4W

ITEM	PART NUMBER	DESCRIPTION
R56	RCR07G511JP	Resistor, Comp, 510, ±5%, 1/4W
R57	RCR07G820JP	Resistor, Comp, 82, ±5%, 1/4W
R58	RCR20G202JP	Resistor, Comp, 2000, ±5%, 1/2W
R59	RNR55C1001FP	Resistor, Film, 1000, ±1%, 1/10W
R60	RCR07G101JP	Resistor, Comp, 100, ±5%, 1/4W
R61	RNR60C3001FP	Resistor, Film, 3000, ±1%, 1/8W
R62	RCR07G221JP	Resistor, Comp, 220, ±5%, 1/4W
R63	RCR07G102JP	Resistor, Comp, 1000, ±5%, 1/4W
R64	RCR07G102JP	Resistor, Comp, 1000, ±5%, 1/4W
R65	RCR20G101JP	Resistor, Comp, 100, ±5%, 1/2W
R66	RCR07G202JP	Resistor, Comp, 2000, ±5%, 1/4W
R67	RCR07G470JP	Resistor, Comp, 47, ±5%, 1/4W
R68	RCR20G201JP	Resistor, Comp, 200, ±5%, 1/2W
R69	RCR07G202JP	Resistor, Comp, 2000, ±5%, 1/4W
R70	RCR20G101JP	Resistor, Comp, 100, ±5%, 1/2W
R71	RCR07G100JP	Resistor, Comp, 10, ±5%, 1/4W
R72	RCR07G100JP	Resistor, Comp, 10, ±5%, 1/4W
R73	RNR55C1001FP	Resistor, Film, 1000, ±1%, 1/10W
R74	RCR07G100JP	Resistor, Comp, 10, ±5%, 1/4W
R75	RNR55C1001FP	Resistor, Film, 1000, ±1%, 1/10W
R76	RCR07G100JP	Resistor, Comp, 10, ±5%, 1/4W
R77	RCR07G430JP	Resistor, Comp, 43, ±5%, 1/4W
R78	RNR55C51R1FP	Resistor, Film, 51.1, ±1%, 1/10W
R79	RNR55C3921FP	Resistor, Film, 3920, ±1%, 1/10W
R80	RNR55C3921FP	Resistor, Film, 3920, ±1%, 1/10W
R81	RCR07G910JP	Resistor, Comp, 91, ±5%, 1/4W
R82	RCR07G102JP	Resistor, Comp, 1000, ±5%, 1/4W
R83	RNR55C4750FP	Resistor, Film, 475, ±1%, 1/10W

ITEM	PART NUMBER	DESCRIPTION
R84	RNR55C1000FP	Resistor, Film, 100, ±1%, 1/10W
R85	RNR55C47R5FP	Resistor, Film, 47.5, ±1%, 1/10W
R86	RNR55C1501FP	Resistor, Film, 1500, ±1%, 1/10W
R87	RCR07G910JP	Resistor, Comp, 91, ±5%, 1/4W
R88	RNR55C68R1FP	Resistor, Film, 68.1, ±1%, 1/10W
R89	RCR07G471JP	Resistor, Comp, 470, ±5%, 1/4W
R90	RCR07G470JP	Resistor, Comp, 47, ±5%, 1/4W
R91	RNR55C3011FP	Resistor, Film, 3010, ±1%, 1/10W
R92	RCR07G681JP	Resistor, Comp, 680, ±5%, 1/4W
R93	RNR55C51R1FP	Resistor, Film, 51.1, ±1%, 1/10W
R94	RNR55C3921FP	Resistor, Film, 3920, ±1%, 1/10W
R95	RNR55C3921FP	Resistor, Film, 3920, ±1%, 1/10W
R96	RCR07G910JP	Resistor, Comp, 91, ±5%, 1/4W
R97	RCR07G102JP	Resistor, Comp, 1000, ±5%, 1/4W
R98	RNR55C4750FP	Resistor, Film, 475, ±1%, 1/10W
R99	RNR55C1000FP	Resistor, Film, 100, ±1%, 1/10W
R100	RNR55C47R5FP	Resistor, Film, 47.5, ±1%, 1/10W
R101	RNR55C1501FP	Resistor, Film, 1500, ±1%, 1/10W
R102	RCR07G910JP	Resistor, Comp, 91, ±5%, 1/4W
R103	RNR55C68R1FP	Resistor, Film, 68.1, ±1%, 1/10W
R104	RCR07G471JP	Resistor, Comp, 470, ±5%, 1/4W
R105	RCR07G470JP	Resistor, Comp, 47, ±5%, 1/4W
R106	RNR55C3011FP	Resistor, Film, 3010, ±1%, 1/10W
R107	RCR07G681JP	Resistor, Comp, 680, ±5%, 1/4W
T1		Transformer (Record)
T2		Transformer (Record)
TJ1		Test Jack
TJ2		Test Jack

ITEM	PART NUMBER	DESCRIPTION
TJ3		Test Jack
TJ4		Test Jack
U1	8150525-1	Integrated Circuit (CA3026)
U2	8150524-1	Integrated Circuit (CA3018A)
U3	8150524-1	Integrated Circuit (CA3018A)
U4	8150537-1	Integrated Circuit (NH0002)
U5	8150537-1	Integrated Circuit (NH0002)
U6	8150537-1	Integrated Circuit (NH0002)
U7	8150537-1	Integrated Circuit (NH0002)
VR1	JANTX1N4370A	Diode, Zener, 2.4V
VR2	JANTX1N753A	Diode, Zener, 6.2V
VR3	JANTX1N966B	Diode, Zener, 16V
VR4	JANTX1N966B	Diode, Zener, 16V
VR5	JANTX1N753A	Diode, Zener, 6.2V
VR6	JANTX1N966B	Diode, Zener, 16V
VR7	JANTX1N966B	Diode, Zener, 16V

VIDEO PLAYBACK AMP
PL 8359709

ITEM	PART NUMBER	DESCRIPTION
C1	8150547-20	Capacitor, Tant, 15 UF, ±10%, 25V
C2	8150547-15	Capacitor, Tant, 22 UF, ±10%, 15V
C3	CK06BX105K	Capacitor, CER, 1.0 UF, ±10%, 50V
C4	CK06BX105K	Capacitor, CER, 1.0 UF, ±10%, 50V
C5	CKR06BX104KP	Capacitor, CER, 0.1 UF, ±10%, 100V
C6	CK06BX105K	Capacitor, CER, 1.0 UF, ±10%, 50V
C7	CKR06BX104KP	Capacitor, CER, 0.1 UF, ±10%, 100V
C8	NOT USED	
C9	CK06BX105K	Capacitor, CER, 1.0 UF, ±10%, 50V
C10	CK06BX105K	Capacitor, CER, 1.0 UF, ±10%, 50V
C11	CKR06BX104KP	Capacitor, CER, 0.1 UF, ±10%, 100V
C12	CK06BX105K	Capacitor, CER, 1.0 UF, ±10%, 50V
C13	CKR06BX104KP	Capacitor, CER, 0.1 UF, ±10%, 100V
C14	CK06BX105K	Capacitor, CER, 1.0 UF, ±10%, 50V
C15	CK06BX105K	Capacitor, CER, 1.0 UF, ±10%, 50V
C16	CK06BX105K	Capacitor, CER, 1.0 UF, ±10%, 50V
C17	CKR06BX104KP	Capacitor, CER, 0.1 UF, ±10%, 100V
C18	CK06BX105K	Capacitor, CER, 1.0 UF, ±10%, 50V
C19	CKR06BX104KP	Capacitor, CER, 0.1 UF, ±10%, 100V
C20	NOT USED	
C21	CK06BX105K	Capacitor, CER, 1.0 UF, ±10%, 50V
C22	CK06BX105K	Capacitor, CER, 1.0 UF, ±10%, 50V
C23	CKR06BX104KP	Capacitor, CER, 0.1 UF, ±10%, 100V
C24	CK06BX105K	Capacitor, CER, 1.0 UF, ±10%, 50V

ITEM	PART NUMBER	DESCRIPTION
C25	CKR06BX104KP	Capacitor, CER, 0.1 UF, ±10%, 100V
C26	CK06BX105K	Capacitor, CER, 1.0 UF, ±10%, 50V
C27	CM05FD910J03	Capacitor, Mica, 91 PF, ±5%, 500V
C28	CM05FD910J03	Capacitor, Mica, 91 PF, ±5%, 500V
C29	CM05FD910J03	Capacitor, Mica, 91 PF, ±5%, 500V
C30	CM05FD910J03	Capacitor, Mica, 91 PF, ±5%, 500V
C31	CM05FD910J03	Capacitor, Mica, 91 PF, ±5%, 500V
DL1	8150544-2	Delay Line, 3 Sect.
DL2	8150544-2	Delay Line, 3 Sect.
Q1	JANTX2N2369A	Transistor, NPN
Q2	JAN 2N3810	Transistor, Dual PNP
Q3	JANTX2N2369A	Transistor, NPN
Q4	JAN 2N3810	Transistor, Dual PNP
R1	RCR07G3R3JP	Resistor, Comp, 3.3, ±5%, 1/4W
R2	RCR07G301JP	Resistor, Comp, 300, ±5%, 1/4W
R3	RCR07G301JP	Resistor, Comp, 300, ±5%, 1/4W
R4	RJ24CW101	Resistor, Var, 100, ±10%, 1/2W
R5	RJ24CW101	Resistor, Var, 100, ±10%, 1/2W
R6	RCR07G820JP	Resistor, Comp, 82, ±5%, 1/4W
R7	RCR07G220JP	Resistor, Comp, 22, ±5%, 1/4W
R8	RCR07G220JP	Resistor, Comp, 22, ±5%, 1/4W
R9	RCR07G220JP	Resistor, Comp, 22, ±5%, 1/4W
R10	RCR07G242JP	Resistor, Comp, 2400, ±5%, 1/4W
R11	RCR07G362JP	Resistor, Comp, 3600, ±5%, 1/4W
R12	RCR07G102JP	Resistor, Comp, 1000, ±5%, 1/4W
R13	RLR07C620JP	Resistor, Film, 62, ±5%, 1/4W
R14	RJ24CW501	Resistor, Var, 500, ±10%, 1/2W

D

ITEM	PART NUMBER	DESCRIPTION
R15	RCR07G471JP	Resistor, Comp, 470, ±5%, 1/4W
R16	RCR07G220JP	Resistor, Comp, 22, ±5%, 1/4W
R17	NOT USED	
R18	RCR07G220JP	Resistor, Comp, 22, ±5%, 1/4W
R19	RCR07G103JP	Resistor, Comp, 10K, ±5%,1/4W
R20	RCR07G750JP	Resistor, Comp, 75, ±5%, 1/4W
R21	RCR07G331JP	Resistor, Comp, 330, ±5%, 1/4W
R22	RCR07G111JP	Resistor, Comp, 110, ±5%, 1/4W
R23	RCR07G101JP	Resistor, Comp, 100, ±5%, 1/4W
R24	RCR07G102JP	Resistor, Comp, 1000, ±5%, 1/4W
R25	RCR07G750JP	Resistor, Comp, 75, ±5%, 1/4W
R26	RCR07G301JP	Resistor, Comp, 300, ±5%, 1/4W
R27	RCR07G301JP	Resistor, Comp, 300, ±5%, 1/4W
R28	RJ24CW101	Resistor, Var, 100, ±10%, 1/2W
R29	RJ24CW101	Resistor, Var, 100, ±10%, 1/2W
R30	RCR07G220JP	Resistor, Comp, 22, ±5%, 1/4W
R31	RCR07G220JP	Resistor, Comp, 22, ±5%, 1/4W
R32	RCR07G220JP	Resistor, Comp, 22, ±5%, 1/4W
R33	RCR07G242JP	Resistor, Comp, 2400, ±5%, 1/4W
R34	RCR07G362JP	Resistor, Comp, 3600, ±5%, 1/4W
R35	RCR07G102JP	Resistor, Comp, 1000, ±5%, 1/4W
R36	RLR07C620JP	Resistor, Film, 62, ±5%, 1/4W
R37	RJ24CW501	Resistor, Var, 500, ±10%, 1/2W
R38	RCR07G471JP	Resistor, Comp, 470, ±5%, 1/4W
R39	RCR07G220JP	Resistor, Comp, 22, ±5%, 1/4W
R40	NOT USED	
R41	RCR07G220JP	Resistor, Comp, 22, ±5%, 1/4W
R42	RCR07G103JP	Resistor, Comp, 10K, ±5%, 1/4W

ITEM	PART NUMBER	DESCRIPTION
R43	RCR07G750JP	Resistor, Comp, 75, ±5%, 1/4W
R44	RCR07G331JP	Resistor, Comp, 330, ±5%, 1/4W
R45	RCR07G111JP	Resistor, Comp, 110, ±5%, 1/4W
R46	RCR07G102JP	Resistor, Comp, 1000, ±5%, 1/4W
R47	RCR07G101JP	Resistor, Comp, 100, ±5%, 1/4W
R48	RCR07G750JP	Resistor, Comp, 75, ±5%, 1/4W
U1	8150536-1	Integrated Circuit
U2	8150536-1	Integrated Circuit
U3	8150536-1	Integrated Circuit
U4	8150536-1	Integrated Circuit

CONTROL TRACK/TACH PREAMP
PL 8359687

ITEM	PART NUMBER	DESCRIPTION
C1	CK06BX105K	Capacitor, Cer, 1 UF, ±10%, 50V
C2	CKR06BX103KP	Capacitor, Cer, 0.01 UF, ±10%, 200V
C3	CKR06BX103KP	Capacitor, Cer, 0.01 UF, ±10%, 200V
C4	CKR06BX103KP	Capacitor, Cer, 0.01 UF, ±10%, 200V
C5	CM05FD221J03	Capacitor, Mica, 220 PF, ±5%, 500V
C6	CK06BX105K	Capacitor, Cer, 1 UF, ±10%, 50V
C7	CKR06BX103KP	Capacitor, Cer, 0.01 UF, ±10%, 200V
C8	CKR06BX103KP	Capacitor, Cer, 0.01 UF, ±10%, 200V
C9	CKR06BX103KP	Capacitor, Cer, 0.01 UF, ±10%, 200V
C10	CM05FD221J03	Capacitor, Mica, 220 PF, ±5%, 500V
C11	CSR13E156KP	Capacitor, Tant, 15 UF, ±10%, 20V
C12	CSR13D226KP	Capacitor, Tant, 22 UF, ±10%, 15V
C13	CKR06BX103KP	Capacitor, Cer, 0.01 UF, ±10%, 200V
C14	CKR06BX103KP	Capacitor, Cer, 0.01 UF, ±10%, 200V
C15	CSR13E156KP	Capacitor, Tant, 15 UF, ±10%, 20V
C16	CSR13D226KP	Capacitor, Tant, 22 UF, ±10%, 15V
C17	CKR06BX103KP	Capacitor, Cer, 0.01 UF, ±10%, 200V
C18	CK06BX105K	Capacitor, Cer, 1.0 UF, ±10%, 50V
C19	CKR06BX152KP	Capacitor, Cer, 1500 PF, ±10%, 200V
C20	CKR06BX103KP	Capacitor, Cer, 0.01 UF, ±10%, 200V
CR1	JANTX1N914	Diode, si
CR2	JANTX1N914	Diode, si
CR3	JANTX1N645	Diode, si
K1	M5757/40-010	Relay, DPDT (412-26)
R1	RNR55C1001FP	Resistor, Film, 1K, ±1%, 1/10W
R2	RNR55C1001FP	Resistor, Film, 1K, ±1%, 1/10W
R3	RCR07G100JP	Resistor, Comp, 10, ±5%, 1/4W

ITEM	PART NUMBER	DESCRIPTION
R4	RCR07G100JP	Resistor, Comp, 10, ±5%, 1/4W
R5	RNR55C4642FP	Resistor, Film, 46.4K, ±1%, 1/10W
R6	RNR55C1001FP	Resistor, Film, 1K, ±1%, 1/10W
R7	RNR55C1001FP	Resistor, Film, 1K, ±1%, 1/10W
R8	RCR07G100JP	Resistor, Comp, 10, ±5%, 1/4W
R9	RCR07G100JP	Resistor, Comp, 10, ±5%, 1/4W
R10	RNR55C4642FP	Resistor, Film, 46.4K, ±1%, 1/10W
R11	RNR55C1000FP	Resistor, Film, 100, ±1%, 1/10W
R12	RCR20G511JP	Resistor, Comp, 510, ±5%, 1/2W
R13	RCR07G620JP	Resistor, Comp, 62, ±5%, 1/4W
R14	RNR55C1001FP	Resistor, Film, 1K, ±1%, 1/10W
R15	NOT USED	
R16	RNR55C1001FP	Resistor, Film, 1K, ±1%, 1/10W
R17	RCR07G100JP	Resistor, Comp, 10, ±5%, 1/4W
R18	RCR07G100JP	Resistor, Comp, 10, ±5%, 1/4W
R19	RNR55C5111FP	Resistor, Film, 5.11K, ±1%, 1/10W
R20	RCR07G101JP	Resistor, Comp, 100, ±5%, 1/4W
R21	RCR20G681JP	Resistor, Comp, 680, ±5%, 1/2W
R22	RCR07G750JP	Resistor, Comp, 75, ±5%, 1/4W
R23	RCR07G103JP	Resistor, Comp, 10K, ±5%, 1/4W
VR1	JANTX1N963B	Diode, Zener, 12V
VR2	JANTX1N753A	Diode, Zener, 6.2V
VR3	JANTX1N963B	Diode, Zener, 12V
VR4	JANTX1N753A	Diode, Zener, 6.2V
U1	8150533-20	Integrated Circuit, Op Amp (702A)
U2	8150533-20	Integrated Circuit, Op Amp (702A)
U3	8150533-20	Integrated Circuit, Op Amp (702A)

AUX/SEARCH PREAMPS
PL 8359757

ITEM	PART NUMBER	DESCRIPTION
C1	CK06BX105KP	Capacitor, 1.0 UF
C2	CKR06BX103KP	Capacitor, 0.01 UF
C3	CKR06BX103KP	Capacitor
C4	CKR06BX222KP	Capacitor, 2200 PF
C5	CM05ED510J03	Capacitor, 51 PF
C6	CK06PX105KP	
C7	CKR06BX103KP	Capacitor
C8	CKR06BX103KP	Capacitor
C9	CKR06BX222KP	Capacitor
C10	CM05FD101J03	Capacitor, 100 PF
C11	CSR13E156KP	Capacitor, 15 UF, 20V
C12	CK06BX105KP	Capacitor
C13	CKR06BX103KP	Capacitor
C14	CKR06BX103KP	Capacitor
C15	CKR06BX222KP	Capacitor
C16	CM05ED510J03	Capacitor
C17	CK06BX105KP	Capacitor
C18	CKR06BX103KP	Capacitor
C19	CKR06BX103KP	Capacitor
C20	CKR06BX222KP	Capacitor
C21	CM05FD101J03	Capacitor
C22	CSR13C396KP	Capacitor, 39 UF, 10V
C23	CKR05BX102KP	Capacitor, .001 UF
C24	CKR06BX103KP	Capacitor
C25	CKR06BX103KP	Capacitor
C26	CKR06BX103KP	Capacitor
C27	CM05ED510J03	Capacitor

ITEM	PART NUMBER	DESCRIPTION
C28	CKR06BX103KP	Capacitor
C29	CKR06BX103KP	Capacitor
C30	CKR06BX103KP	Capacitor
C31	CKR06BX332KP	Capacitor, .0033 UF
C32	CM05ED510J03	Capacitor
C33	CSR13E156KP	Capacitor
C34	CSR13C396KP	Capacitor
	8505806-4	Pad, Mtg., 8 Pin
	8505806-5	Pad, Mtg., 10 Pin
CR1	JANTX1N914	Diode
CR2	JANTX1N914	Diode
CR3	JANTX1N914	Diode
CR4	JANTX1N914	Diode
CR5	JANTX1N914	Diode
CR6	JANTX1N914	Diode
CR7	JANTX1N645	
E1 to E7		Terminal (Test Points)
K1	M5757/40-005	Relay
P1	8505242-73	Connector
R1	RNR55C1001FP	Resistor
R2	RNR55C5111FP	Resistor
R3	RCR07G100JP	Resistor
R4	RCR07G100JP	Resistor
R5	RNR55C2152FP	Resistor
R6	RNR55C1001FP	Resistor
R7	RNR55C1001FP	Resistor
R8	RCR07G100JP	Resistor
R9	RCR07G100JP	Resistor

ITEM	PART NUMBER	DESCRIPTION
R10	RNR55C2152FP	Resistor
R11	RCR07G202JP	Resistor
R12	RNR55C1000FP	Resistor
R13	RCR32G301JP	Resistor
R14	RNR55C1001FP	Resistor
R15	RNR55C5111FP	Resistor
R16	RCR07G100JP	Resistor
R17	RCR07G100JP	Resistor
R18	RNR55C2152FP	Resistor
R19	RNR55C1001FP	Resistor
R20	RNR55C1001FP	Resistor
R21	RCR07G100JP	Resistor
R22	RCR07G100JP	Resistor
R23	RNR55C2152FP	Resistor
R24	RCR07G202JP	Resistor
R25	RNR55C1000FP	Resistor
R26	RCR20G470JP	Resistor
R27	RNR55C1001FP	Resistor
R28	RNR55C5111FP	Resistor
R29	RCR07G100JP	Resistor
R30	RCR07G100JP	Resistor
R31	RNR55C5112FP	Resistor
R32	RNR55C1001FP	Resistor
R33	RNR55C1001FP	Resistor
R34	RCR07G100JP	Resistor
R35	RCR07G100JP	Resistor
R36	RNR55C3162FP	Resistor

ITEM	PART NUMBER	DESCRIPTION
R37	RCR07G202JP	Resistor
R38	RNR55C1000FP	Resistor
R39	RCR20G431JP	Resistor
R40	RCR07G620JP	Resistor
VR1	JANTX1N963B	Diode, Zener, 12V
VR2	JANTX1N753A	Diode, Zener, 6.2V
VR3	JANTX1N963B	Diode, Zener
VR4	JANTX1N753A	Diode, Zener
Z1	8150533-10	Integrated Circuit, Op Amp
Z2	8150533-10	Integrated Circuit, Op Amp
Z3	8150533-10	Integrated Circuit, Op Amp
Z4	8150533-10	Integrated Circuit, Op Amp
Z5	8150533-10	Integrated Circuit, Op Amp
Z6	8150533-10	Integrated Circuit, Op Amp

MOTOR SOLENOID SWITCH
PL 8359688

ITEM	PART NUMBER	DESCRIPTION
C1	CSR13G226KP	Capacitor, Tant, 22 UF, ±10%, 50V
C2	CSR13G825KP	Capacitor, Tant, 8.2 UF, ±10%, 50V
CR1	NOT USED	
CR2	NOT USED	
CR3	JANTX1N645	Diode
CR4	JANTX1N4970	Diode, Zener, 33V
CR5	JANTX1N645	Diode
CR6	JANTX1N4970	Diode, Zener, 33V
CR7	JANTX1N645	Diode
CR8	JANTX1N4958	Diode, Zener, 10V
CR9	JANTX1N4958	Diode, Zener, 10V
CR10	JANTX1N4958	Diode, Zener, 10V
CR11	JANTX1N4958	Diode, Zener, 10V
CR12	JANTX1N4970	Diode, Zener, 33V
CR13	JANTX1N645	Diode
CR14	JANTX1N4970	Diode, Zener, 33V
CR15	JANTX1N3191	Diode
CR16	JANTX1N645	Diode
CR17	JANTX1N645	Diode
K1	8150555-1	Relay, DPDT, 10A (J-J2A)
K2	8150555-1	Relay, DPDT, 10A (J-J2A)
K3	8150555-1	Relay, DPDT, 10A (J-J2A)
K4	8150555-1	Relay, DPDT, 10A (J-J2A)
K5	NOT USED	
K6	8150555-1	Relay, DPDT, 10A (J-J2A)
K7	M5757/40-005	Relay, DPDT, 1A (412-26)
J1	8413691-45	Test Point, Brown

ITEM	PART NUMBER	DESCRIPTION
R1	RCR07G101JP	Resistor, CC, 100, ±5%, 1/4W
R2	RNR55C2871FP	Resistor, Film, 2.87K, ±1%, 1/10W
R3	RCR07G331JP	Resistor, CC, 330, ±5%, 1/4W
R4	RCR07G221JP	Resistor, CC, 220, ±5%, 1/4W
R5	RCR07G102JP	Resistor, CC, 1000, ±5%, 1/4W
R6	RWR69G10R0SFP	Resistor, WW, 10, ±1%, 2.5W
R7	RCR07G103JP	Resistor, CC, 10K, ±5%, 1/4W
R8	RCR07G103JP	Resistor, CC, 10K, ±5%, 1/4W
R9	RNR55C1332FP	Resistor, Film, 13.3K, ±1%, 1/10W
R10	RNR55C4641FP	Resistor, Film, 4640, ±1%, 1/10W
R11	RCR07G392JP	Resistor, CC, 3900, ±5%, 1/4W
R12	RNR55C1472FP	Resistor, Film, 14.7K, ±1%, 1/10W
R13	RNR55C2872FP	Resistor, Film, 28.7K, ±1%, 1/10W
R14	RCR07G392JP	Resistor, CC, 3900, ±5%, 1/4W
R15	RCR07G102JP	Resistor, CC, 1000, ±5%, 1/4W
Q1	JANTX2N2907A	Transistor
Q2	JANTX2N2219A	Transistor
Q3	8150549-1	Transistor, Power
E1	8505806-5	Relay, Pad, 10 Pin

SPECIFICATION ERTS-564-2
VIDEO RECORDING TAPE

This tape is to be prepared using a mylar backing thickness of 0.00092" and is to receive the same exclusive backing treatment as "Scotch" Video Tape No. 400. The magnetic coating, however, is to be of the same formulation and thickness (0.00021) as MT24070.

To facilitate performance comparison with the double-face coated, MT24070 tape, the manufacture of this tape shall be arranged to include a "long" cycle between the application and the surface treatment of the magnetic coating.

Surface roughness measurements are to be taken for each reel and are to be included with the tape upon delivery.

Thickness		
Mylar Backing	-	0.00092"
Magnetic Coating	-	0.00021
Total	-	0.00113
Magnetic Coating	-	Same formulation as MT24070
Backing Treatment	-	Same as "Scotch" No. 400
Manufacturing Technique	-	Long-cycle between coating and surface treating

APPENDIX 3A

RNR RESISTOR DRIFT DATA

To	C. Russell	Location	10-5	Date	October 13, 1969
From	A. Siegel	Location	1-6-5	Telephone	PC 3915

Subject Variation in Mepco Fixed Film Resistors (RNR Type) with Time

Mr. A. Ringel, Manager of Quality Assurance at Mepco, supplied me with curves on their RNR Type Resistors. Their graphical analysis falls into two categories; up to 10,000 hours with power applied continuously and up to 50,000 hours of Shelf Life. The variations noted for the first group of curves would approximate those for resistors where their "on" time is quite large when compared to their "off" time. The second group of graphs would indicate the trend that could be expected for resistors with very low duty cycles.

Analyzing the data, we find the following using the comparisons described above:

(A) For Mepco Model FH10, 1/10 Watt (RNR55C) -

1. After 50,000 hours of Shelf Life, units within the resistance range from 49.9 to 20,000 ohms always indicated a positive average increased value ($\bar{x}$ of 0.3%). For units between 20.1K and 51K the average was also positive but at a value of 0.42% at 50,000 hours. In the 51.1K to 100K range the average change was also always positive and again was 0.42% at 50,000 hours.

2. The Load Life Test for this resistor model resulted in an average negative change in values with the average change being 0.24% at 10,000 hours.

(B) For Mepco Model FH11, 1/8 Watt (RNR57C)

1. Only a Load Life Test Curve was supplied and it indicated that the average change was negative with the average change being 0.06% at 10,000 hours.

(C) For Mepco Model FH12, 1/8 Watt (RNR60C) -

1. After 50,000 hours of Shelf Life units within the resistance range from 49.9 to 80,000 ohms always indicated a positive average increased value ($\bar{x}$ of 0.12%). For units between 80.1K and 300K ohms the average was also positive but at a value of 0.1% at 50,000 hours. In the 301K to 499K ohm range the average change was also always positive and increased up to 0.17%.

2. Load Life Test Data was run on two groups. Both indicated as average negative change with average changes after 10,000 hours of 0.08 and 0.12%.

(D) For Mepco Model FH25, 1/4 Watt (RNR65C) -

1. After 50,000 hours of Shelf Life, units within the resistance range from 49.9 to 300,000 ohms always indicated a positive average increased value

($\bar{x}$ of 0.09%). For units between 301K ohms and 1 megohm the average was also positive but at a value of 0.08% at 50,000 hours.

2. Load Life Test Date indicated that the average change was positive with the value being 0.06% at 10,000 hours.

(E) For Mepco Model FH50, 1/2 Watt (RNR70C) -

1. After 50,000 hours of Shelf Life, units within the resistance range from 49.9 to 400,000 ohms indicated a basic positive average increase of insignificant value. However, in the range from 401K ohms to 1 megohm the average value was also consistently positive but with an average value of 0.08% at 50,000 hours.

2. Load Life Test Data was run on two groups. Both indicated an average positive change with average changes after 10,000 hours of 0.08 and 0.1%.

All units undergoing examination were of the 1% tolerance category and were supplied with maximum temperature coefficients of ±50 PPM/°C.

Please advise me of any additional information you may require or of any other way that I can be of service.

A. Siegel
A. Siegel
Central Engineering

AS:jmp

APPENDIX 3B

RELIABILITY DATA WORKSHEETS

RELIABILITY DATA WORKSHEETS

NAME Record/Preamp
DRAWING NO. 8359708
SCHEMATIC NO.
NEXT ASSEM.

Temp:
Ambient = 46°C
Part = 60°C

(X) Failure
(D) Degraded
(0) No Effect

SYSTEM ERTS/TU
MODULE Record/Preamp (4)
SUB-MODULE Record

ITEM	NUMBER RCA OR MILITARY	CIRCUIT SYMBOL	QTY PER UNIT	RATED STRESS	APPLIED STRESS	FAIL. RATE $x10^{-6}$	STRESS RATIO	MODULE FAILURE EFFECT OPEN	MODULE FAILURE EFFECT SHORT	MODULE FAILURE EFFECT DEGRAD.	FAILURE MODE NON PERFORMANCE RECORD RBV	RECORD MSS	AUX. REC.	AUX. P.B.	SEARCH P.B.
5.1	RNR55C1001FP	R1		.1W	4 mw	.002	.04		X		X	X			
								X			X	X			
5.2	RNR55C1001FP	R2		.1W	4 mw	.002	.04		X		X	X			
								X			X	X			
5.3	RCR07G302JP	R3		0.25W	34 mw	.001	.13		X		X	X			
								X			X	X			
5.4	RNR55C1001FP	R4		0.1W	4 mw	.002	.04		X		X	X			
								X			X	X			
5.5	RNR55C1001FP	R5		0.1W	4 mw	.002	.04		X		X	X			
								X			X	X			
5.6	RCR07G122JP	R6		0.25W	T.P.N/A	.001	N/A		X		0	0			
								X			0	0			
5.7	RCR07G272JP	R7		0.25W	T.P.N/A	.001	N/A		X		0	0			
								X			0	0			
5.8	RCR07G472JP	R8		0.25W	42 mw	.001	.17		X		X	X			
								X			X	X			
5.9	RNR55C7000FP	R9		0.1W	1 mw	.002	<.1		X		D	D			
								X			D	D			
5.10	RJ24CW501	R10		0.25W	<.1 mw	.012	<.1		X		D	D			
								X			D	D			
5.11	RCR07G102JP	R11		0.25W	9 mw	.001	<.1		X		X	X			
								X			X	X			
5.12	RCR07G562JP	R12		0.25W	29 mw	.001	.16		X		X	X			
								X			X	X			
5.13	RCR07G392JP	R13		0.25W	35 mw	.001	.14		X		X	X			
								X			X	X			
5.14	RNR55C2001FP	R14		0.1W	20 mw	.002	.2		X		X	X			
								X			X	X			
5.15	RCR07G470JP	R15		0.25W	1.9 mw	.001	<.1		X		X	X			
								X			X	X			
5.16	RCR07G511JP	R16		0.25W	26 mw	.001	.1		X		X	X			
								X			X	X			
5.17	RCR200G202JP	R17		0.5W	200 mw	.002	.40		X		X	X			
								X			X	X			
5.18	RLR20C3001JP	R18		0.50W	135 mw	.003	.30		X		X	X			
								X			X	X			

CIRCUIT ANALYSIS RELIABILITY ________ ENGINEERING ________ TOTAL ________

(A) MIL-HDBK-217
(B) EST. DATA

DATE ________ SHEET 1 OF 5

RELIABILITY DATA WORKSHEETS

NAME Record/Preamp
DRAWING NO. 8359708
SCHEMATIC NO.
NEXT ASSEM.

Temp:
Ambient = 46°C
Part = 60°C

(X) Failure
(D) Degraded
(0) No Effect

SYSTEM ERTS/TU
MODULE Record/Preamp (4)
SUB-MODULE Record

ITEM	NUMBER RCA OR MILITARY	CIRCUIT SYMBOL	QTY PER UNIT	RATED STRESS	APPLIED STRESS	FAIL. RATE x10^-6	STRESS RATIO	MODULE FAILURE EFFECT: OPEN	MODULE FAILURE EFFECT: SHORT	MODULE FAILURE EFFECT: DEGRAD.	FAILURE MODE NON PERFORMANCE: RECORD RBV	RECORD MSS	AUX. REC.	AUX. P.B.	SEARCH P.B.
5.19	RNR55C1001FP	R19		0.1W	10 mw	.002	.10		X		X	X			
								X			X	X			
5.20	RCR07G102JP	R20		0.25W	T.P.N/A	.001	N/A		X		0	0			
								X			0	0			
5.21	RCR07G470FP	R21		0.25W	30 mw	.001	.12		X		X	X			
								X			X	X			
5.22	RCR20G201J P	R22		0.5W	225 mw	.003	.45		X		X	X			
								X			X	X			
5.23	RNR55C1001FP	R23		0.1W	-	.002	-		X		X	X			
								X			X	X			
5.24	RCR07G2025P	R24		0.25W	12.5mw	.001	<.1		X		X	X			
								X			X	X			
5.25	RCR20G101JP	R25		0.5W	250 mw	.004	.50		X		D	D			
								X			X	X			
5.26	RCR07G100JP	R26		0.25W	25 mw	.001	.1		X		X	X			
								X			X	X			
5.27	RCR07G202JP	R27		0.25W	25 mw	.001	.1		X		X	X			
								X			X	X			
5.28	RCR20G101JP	R28		0.5W	250 mw	.004	.5		X		X	X			
								X			X	X			
5.29	RCR07G100JP	R29		0.25W	20 mw	.001	<.1		X		D	D			
								X			X	X			
5.30	RNR55C1001FP	R30		0.1W	-	.002	-		X		X	X			
								X			X	X			
5.31	RCR07G220JP	R31		0.25W	20 mw	.001	<.1		X		D	D			
								X			X	X			
5.32	RCR07G100JP	R32		0.25W	100 mw	.002	.4		X		X	X			
								X			X	X			
5.33	RCR07G102JP	R33		0.25W	19 mw	.001	.19				X	X			
											X	X			
5.34	DELETED	R34	FROM CIRCUIT												
5.35	RCR07G101JP	R35		0.25W	< 1 mw	.001	<.1		X		X	X			
								X			X	X			
5.36	RCR07G100JP	R36		0.25W	100 mw	.003	.4		X		X	X			
								X			X	X			

CIRCUIT ANALYSIS
RELIABILITY
ENGINEERING
TOTAL

(A) MIL-HDBK-217
(B) EST. DATA

DATE
SHEET 2 OF 5

RELIABILITY DATA WORKSHEETS

NAME Record/Preamp
DRAWING NO. 8359708
SCHEMATIC NO.
NEXT ASSEM.

Temp:
Ambient = 46°C
Part = 60°C

(X) Failure
(D) Degraded
(O) No Effect

SYSTEM ERTS/TL
MODULE Record/Preamp (4)
SUB-MODULE Record

ITEM	NUMBER RCA OR MILITARY	CIRCUIT SYMBOL	QTY PER UNIT	RATED STRESS	APPLIED STRESS	FAIL. RATE $\times 10^{-6}$	STRESS RATIO	MODULE FAILURE EFFECT			FAILURE MODE NON PERFORMANCE				
								OPEN	SHORT	DEGRAD.	RECORD		AUX.		SEARCH
											RBV	MSS	REC.	P.B.	P.B.
5.37	RCR07G101JP	R37		0.25W	2.5 mw	.001	<.1	X	X		D X	D X			
5.38	RCR07G472JP	R38		0.25W	75 mw	.002	.30	X	X		X X	X X			
5.39	RCR07G122JP	R39		0.25W	19 mw	.001	<.1	X	X		X X	X X			
5.40	RCR07G220JP	R40		0.25W	20 mw	.001	<.1	X	X		D D	D D			
5.41	RCR07G101JP	R41		0.25W	2 mw	.001	<.1	X	X		X X	X X			
5.42	RCR06G432 JP	R42		0.25W	78 mw	.002	.31	X	X		X X	X X			
5.43	RCR06G102JP	R43		0.25W	17 mw	.001	<.1	X	X		X X	X X			
5.44	RCR07G101JP	R44		0.25W	19 mw	.001	<.1	X	X		D X	D X			
5.45	CKR06BX104KP	C1		100V	8V	.001	<.1	X	X		X D	X D			
5.46	CKR06BX104KP	C2		100V	8V	.001	<.1	X	X		X D	X D			
5.47	CKR06BX104KP	C3		100V	20V	.001	.20	X	X		X D	X D			
5.48	CKR06BX104KP	C4		100V	21V	.001	.21	X	X		X D	X D			
5.49	CKR06BX104KP	C5		100V	21V	.001	.21	X	X		X D	X D			
5.50	CKR06BX104KP	C6		100V	21V	.001	.21	X	X		X D	X D			
5.51	CKR06BX104KP	C7		100V	16V	.001	.16	X	X		X D	X D			
5.52	CKR06BX104KP	C8		100V	1V	.001	<.1	X	X		X D	X D			
5.53	CKR06BX104KP	C9		100V	< 1V	.001	<.1	X	X		X X	X X			
5.54	CKR06BX104KP	C10		100V	6.2V	.001	<.1	X	X		X D	X D			

CIRCUIT ANALYSIS ____ ENGINEERING ____ TOTAL ____
RELIABILITY
(A) MIL-HDBK-217
(B) EST. DATA
DATE ____ SHEET 3 OF 5

RELIABILITY DATA WORKSHEETS

NAME Record/Preamp
DRAWING NO. 8359708
SCHEMATIC NO.
NEXT ASSEM.

Temp:
Ambient = 46°C
Part = 60°C

(X) Failure
(D) Degraded
(0) No Effect

SYSTEM ERTS/TU
MODULE Record/Preamp (4)
SUB-MODULE Record

ITEM	NUMBER RCA OR MILITARY	CIRCUIT SYMBOL	QTY PER UNIT	RATED STRESS	APPLIED STRESS	FAIL. RATE $x10^{-6}$	STRESS RATIO	MODULE FAILURE EFFECT: OPEN	MODULE FAILURE EFFECT: SHORT	MODULE FAILURE EFFECT: DEGRAD.	FAILURE MODE NON PERFORMANCE: RECORD RBV	RECORD MSS	AUX. REC.	AUX. P.B.	SEARCH P.B.
5.55	CKR06BX104KP	C11		100V	2.4V	.001	<.1		X		X	X			
								X			D	D			
5.56	CKR06BX104KP	C12		100V	20V	.001	0.20		X		X	X			
								X			D	D			
5.57	CKR06BX104KP	C13		100V	2V	.001	<.10		X		X	X			
								X			X	X			
5.58	CKR06BX104KP	C14		100V	21V	.001	.21		X		X	X			
								X			D	D			
5.59	CKR06BX104KP	C15		100V	16V	.001	.16		X		X	X			
								X			D	D			
5.60	CKR06BX104KP	C16		100V	6V	.001	<.10		X		X	X			
								X			X	X			
5.61	CKR06BX104KP	C17		100V	17V	.001	.17		X		X	X			
								X			D	D			
5.62	8150547	C18		35V	14V	.025	.40		X		X	X			
								X			X	X			
5.63	8150547	C19		35V	22V	.125	.63		X		X	X			
								X			D	D			
5.64	8150547	C20		35V	2V	.006	<.1		X		X	X			
								X			D	D			
5.65	8150567	L1				.05			X		X	X			
								X			X	X			
5.66	8150567	L2				.05			X		D	D			
								X			X	X			
5.67	8150567	L3				.05			X		D	D			
								X			X	X			
5.68	8150567	L4				.05			X		D	D			
								X			X	X			
5.69	JAN TX1N4370A	VR1		400mw	8 mw	.020			X		X	X			
							P_D=.02	X			X	X			
5.70	JAN TX1N753A	VR2		400mw	20 mw	.020			X		X	X			
							P_D=.05	X			X	X			
5.71	JAN TX1N966B	VR3		400mw	48 mw	.020			X		X	X			
							P_D=.12	X			X	X			
5.72	JAN TX1N966B	VR4		400mw	48 mw	.020			X		X	X			
							P_D=.12	X			X	X			

CIRCUIT ANALYSIS ________ ENGINEERING ________ TOTAL ________
RELIABILITY

(A) MIL-HDBK-217
(B) EST. DATA

DATE ________ SHEET 4 OF 5

RELIABILITY DATA WORKSHEETS

NAME Record/Preamp
DRAWING NO. 8359708
SCHEMATIC NO.
NEXT ASSEM.

Temp:
Ambient = 46°C
Part = 60°C

(X) Failure
(D) Degraded
(0) No Effect

SYSTEM ERTS/TU
MODULE Record/Preamp (4)
SUB-MODULE Record

ITEM	NUMBER RCA OR MILITARY	CIRCUIT SYMBOL	QTY PER UNIT	RATED STRESS	APPLIED STRESS	FAIL. RATE $x10^{-6}$	STRESS RATIO	MODULE FAILURE EFFECT			FAILURE MODE NON PERFORMANCE				
								OPEN	SHORT	DEGRAD.	RECORD RBV	RECORD MSS	AUX. REC.	AUX. P.B.	SEARCH P.B.
5.73	8150525	Z1		N.A.	N.A.	.040	N.A.		X		X	X			
								X			X	X			
5.74	8150524	Z2		N.A.	N.A.	.040	N.A.		X		X	X			
								X			X	X			
5.75	JAN TX2N3251A	Q1		360mw	120mw	.04			X		X	X			
							P_D=.33	X			X	X			
5.76	JAN TX2N3251A	Q2		360mw	115mw	.04			X		X	X			
							P_D=.32	X			X	X			
5.77	JAN TX2N2218	Q3		3W	420mw	.026			X		X	X			
	(Heat Sink)						P_D=.20	X			X	X			
5.78	JAN TX 2N2222	Q4		500mw	100 mw	.026			X		X	X			
							P_D=.20	X			X	X			
5.79	JAN TX 2N2907	Q5		400mw	100 mw	.065			X		X	X			
							P_D=.30	X			X	X			
5.80	8150537	Z3		N.A.	N.A.	.040	N.A.		X		X	X			
								X			X	X			
5.81	8150537	Z4		N.A.	N.A.	.040	N.A.		X		X	X			
								X			X	X			

CIRCUIT ANALYSIS RELIABILITY ______ ENGINEERING ______ TOTAL ______

(A) MIL-HDBK-217
(B) EST. DATA

DATE ______ SHEET 5 OF 5

RELIABILITY DATA WORKSHEETS

NAME Record/Preamp
DRAWING NO. 8359708
SCHEMATIC NO.
NEXT ASSEM.

Temp:
Ambient = 46°C
Part = 60°C

(X) Failure
(D) Degraded
(0) No Effect

SYSTEM ERTS/TU
MODULE Record/Preamp (4)
SUB-MODULE Preamp

ITEM	NUMBER RCA OR MILITARY	CIRCUIT SYMBOL	QTY PER UNIT	RATED STRESS	APPLIED STRESS	FAIL. RATE $x10^{-6}$	STRESS RATIO	MODULE FAILURE EFFECT			FAILURE MODE NON PERFORMANCE				
								OPEN	SHORT	DEGRAD.	RECORD		PLAYBACK		SEARCH
											RBV	MSS	RBV	MSS	P.B.
4.1	CKR06BX104KP	C1		100V	4.5V	.001	.045	X					X	X	
									X				X	X	
4.2	8150547	C2		15V	5.0V	.01	.33	X					D	D	
									X				X	X	
4.3	CKR0BX104KP	C3		100V	3.0V	.001	.03	X					D	D	
									X				X	X	
4.4	8150546	C4		50V	4.2V	.001	.084	X					D	D	
									X				X	X	
4.5	8150547	C5		15V	7.5V	.04	.50	X					D	D	
									X				X	X	
4.6	8150546	C6		50V	1.0V	.001	.02	X					D	D	
									X				D	D	
4.7	CKR06BX104KP	C7		100V	2.0V	.001	.02	X					X	X	
									X				X	X	
4.8	CKR06BX104KP	C8		100V	4.5V	.001	.045	X					X	X	
									X				X	X	
4.9	8150547	C9		15V	5.0V	.02	.33	X					D	D	
									X				X	X	
4.10	CKR0BX104KP	C10		100V	3.0V	.001	.03	X					D	D	
									X				X	X	
4.11	8150546	C11		50V	4.2V	.001	.084	X					D	D	
									X				X	X	
4.12	8150547	C12		15V	7.5V	.04	.5	X					D	D	
									X				X	X	
4.13	8150546	C13		50V	1.0V	.001	.02	X					D	D	
									X				D	D	
4.14	CKR06BX104KP	C14		100V	2.0V	.001	.02	X					X	X	
									X				X	X	
4.15	CKR06BX104KP	C15		100V	4.5V	.001	.045	X					X	X	
									X				X	X	
4.16	8150547	C16		15V	5.0V	.02	.33	X					D	D	
									X				X	X	
4.17	CKR06BX104KP	C17		100V	3.0V	.001	.03	X					D	D	
									X				X	X	
4.18	8150546	C18		50V	4.2V	.001	.084	X					D	D	
									X				X	X	

CIRCUIT ANALYSIS RELIABILITY ________ ENGINEERING ________ TOTAL ________

(A) MIL-HDBK-217
(B) EST. DATA

DATE ________ SHEET 1 OF 6

RELIABILITY DATA WORKSHEETS

NAME Record/Preamp
DRAWING NO. 8359708
SCHEMATIC NO.
NEXT ASSEM.

Temp:
Ambient = 46°C
Part = 60°C

(X) Failure
(D) Degraded
(O) No Effect

SYSTEM ERTS/TU
MODULE Record/Preamp (4)
SUB-MODULE Preamp

ITEM	NUMBER RCA OR MILITARY	CIRCUIT SYMBOL	QTY PER UNIT	RATED STRESS	APPLIED STRESS	FAIL. RATE $x10^{-6}$	STRESS RATIO	MODULE FAILURE EFFECT			FAILURE MODE NON PERFORMANCE				
								OPEN	SHORT	DEGRAD.	RECORD RBV	RECORD MSS	PLAYBACK RBV	PLAYBACK MSS	SEARCH P.B.
4.19	8150547	C19		15V	7.5V	.04	.50	X					D	D	
									X				X	X	
4.20	8150546	C20		50V	1.0V	.001	.02	X					D	D	
													X	X	
4.21	CKR06BX104KP	C21		100V	2.0V	.001	.02	X					X	X	
									X				D	D	
4.22	CKR06BX104KP	C22		100V	4.5V	.001	.045	X					X	X	
									X				X	X	
4.23	8150547	C23		15V	5.0V	.02	.33	X					D	D	
									X				X	X	
4.24	CKR06BX104KP	C24		100V	3.0V	.001	.03	X					D	D	
									X				X	X	
4.25	8150546	C25		50V	4.2V	.001	.084	X					D	D	
									X				X	X	
4.26	8150547	C26		15V	7.5V	.04	.50	X					D	D	
									X				X	X	
4.27	8150546	C27		50V	1.0V	.001	.02	X					D	D	
									X				D	D	
4.28	CKR06BX104KP	C28		100V	2.0V	.001	.02	X					X	X	
									X				X	X	
4.29	412-26	K1		1 amp	.2 amp	.05	.2								
4.30	412-26	K2		1 amp	.2 amp	.05	.2								
4.31	8150560	T1				.05	26V(sec)								
4.32	8150560	T2				.05	26V(sec)								
4.33	8150560	T3				.05	26V(sec)								
4.34	8150560	T4				.05	26V(sec)								
4.35	8150561	T5				.05									
4.36	8150548	Q1		200mw	12mw	.02	.06	X					X	X	
									X				X	X	
4.37	8150548	Q2		200mw	8.4mw	.02	.042	X					X	X	
									X				X	X	
4.38	JAN TX2N918	Q3		360mw	8.1mw	.02	.023	X					X	X	
									X				X	X	

CIRCUIT ANALYSIS ______ ENGINEERING ______ TOTAL ______
RELIABILITY

(A) MIL-HDBK-217
(B) EST. DATA

DATE ______ SHEET 2 OF 6

RELIABILITY DATA WORKSHEETS

NAME Record/Preamp
DRAWING NO. 8359708
SCHEMATIC NO.
NEXT ASSEM.

Temp:
Ambient = 46°C
Part = 60°C

(X) Failure
(D) Degraded
(0) No Effect

SYSTEM ERTS/TU
MODULE Record/Preamp (4)
SUB-MODULE Preamp

ITEM	NUMBER RCA OR MILITARY	CIRCUIT SYMBOL	QTY PER UNIT	RATED STRESS	APPLIED STRESS	FAIL RATE x10^-6	STRESS RATIO	MODULE FAILURE EFFECT: OPEN	MODULE FAILURE EFFECT: SHORT	MODULE FAILURE EFFECT: DEGRAD.	FAILURE MODE NON PERFORMANCE: RECORD RBV	RECORD MSS	PLAYBACK RBV	PLAYBACK MSS	SEARCH P.B.
4.39	8150548	Q4		200mw	12mw	.02	.06	X					X	X	
									X				X	X	
4.40	8150548	Q5		200mw	8.4mw	.02	.042	X					X	X	
									X				X	X	
4.41	JAN TX2N918	Q6		360mw	8.1mw	.02	.023	X					X	X	
									X				X	X	
4.42	8150548	Q7		200mw	12mw	.02	.06	X					X	X	
									X				X	X	
4.43	8150548	Q8		200mw	8.4mw	.02	.042	X					X	X	
									X				X	X	
4.44	JAN TX2N918	Q9		360mw	8.1mw	.02	.023	X					X	X	
									X				X	X	
4.45	8150548	Q10		200mw	12 mw	.02	.06	X					X	X	
									X				X	X	
4.46	8150548	Q11		200mw	8.4mw	.02	.042	X					X	X	
									X				X	X	
4.47	JAN TX2N918	Q12		360mw	8.1mw	.02	.023	X					X	X	
									X				X	X	
4.48	RNR55G51R1FP	R1		1/10W	6.0mw	.002	.06	X					X	X	
									X				D	D	
4.49	RNR55C3921FP	R2		1/10W	7.5mw	.002	.075	X					X	X	
									X				X	X	
4.50	RNR55C3921FP	R3		1/10W	6.0mw	.002	.06	X					X	X	
									X				X	X	
4.51	RCR07G910JP	R4		1/10W	7.2mw	.001	.028	X					X	X	
									X				D	D	
4.52	RCR07G102JP	R5		1/10W	4.8mw	.001	.012	X					X	X	
									X				D	D	
4.53	RNR55C4750FP	R6		1/10W	2.4mw	.002	.024	X					X	X	
									X				X	X	
4.54	RNR55C1000FP	R7		1/10W	6.0mw	.002	.06	X					X	X	
									X				D	D	
4.55	RNR55C47R5FP	R8		1/10W	6.0mw	.002	.06	X					D	D	
									X				D	D	
4.56	RNR55C1501FP	R9		1/10W	7.3mw	.002	.073	X					X	X	
									X				X	X	

CIRCUIT ANALYSIS ______ ENGINEERING ______ TOTAL ______
RELIABILITY

(A) MIL-HDBK-217
(B) EST. DATA

DATE ______ SHEET 3 OF 6

RELIABILITY DATA WORKSHEETS

NAME Record/Preamp
DRAWING NO. 8359708
SCHEMATIC NO. ______
NEXT ASSEM. ______

Temp:
Ambient = 46°C
Part = 60°C

(X) Failure
(D) Degraded
(0) No Effect

SYSTEM ERTS/TU
MODULE Record/Preamp (4)
SUB-MODULE Preamp

ITEM	NUMBER RCA OR MILITARY	CIRCUIT SYMBOL	QTY PER UNIT	RATED STRESS	APPLIED STRESS	FAIL. RATE $x10^{-6}$	STRESS RATIO	MODULE FAILURE EFFECT			FAILURE MODE NON PERFORMANCE				
								OPEN	SHORT	DEGRAD.	RECORD RBV	RECORD MSS	PLAYBACK RBV	PLAYBACK MSS	SEARCH P.B.
4.57	RCR07G910JP	R10		1/10W	16mw	.001	.064	X					X	X	
									X				D	D	
4.58	RNR55C68R1FP	R11		1/10W	6.0mw	.002	.06	X					D	D	
									X				D	D	
4.59	RCR07G471JP	R12		1/10W	7.6mw	.001	.03	X					X	X	
									X				X	X	
4.60	RCR07G470JP	R13		1/10W	6.0mw	.001	.06	X					X	X	
									X				D	D	
4.61	RNR55C3011FP	R14		1/10W	17.2mw	.002	.172	X					X	X	
									X				X	X	
4.62	RCR07G681JP	R15		1/10W	3.3mw	.001	.013	X					X	X	
									X				X	X	
4.63	RNR55C51R1FP	R16		1/10W	5.0mw	.002	.02	X					X	X	
									X				D	D	
4.64	RNR55C3921FP	R17		1/10W	7.5mw	.002	.075	X					X	X	
									X				X	X	
4.65	RNR55C3921FP	R18		1/10W	6.0mw	.002	.06	X					X	X	
									X				X	X	
4.66	RCR07G910JP	R19		1/10W	7.2mw	.001	.028	X					X	X	
									X				D	D	
4.67	RCR07G102JP	R20		1/10W	4.8mw	.001	.012	X					X	X	
									X				D	D	
4.68	RNR55C4750FP	R21		1/10W	2.4mw	.002	.024	X					X	X	
									X				X	X	
4.69	RNR55C1000FP	R22		1/10W	5.0mw	.002	.02	X					X	X	
									X				D	D	
4.70	RNR55C47R5FP	R23		1/10W	5.0mw	.002	.02	X					D	D	
									X				D	D	
4.71	RNR55C1501FP	R24		1/10W	7.3mw	.002	.073	X					X	X	
									X				X	X	
4.72	RCR07GF910JP	R25		1/10W	16mw	.0015	.064	X					X	X	
									X				D	D	
4.73	RNR55C68R1FP	R26		1/10W	5.0mw	.002	.02	X					D	D	
									X				D	D	
4.74	RCR07G471JP	R27		1/10W	7.6mw	.001	.03	X					X	X	
									X				X	X	

CIRCUIT ANALYSIS ______ ENGINEERING ______ TOTAL ______
RELIABILITY

(A) MIL-HDBK-217
(B) EST. DATA

DATE ______ SHEET 4 OF 6

RELIABILITY DATA WORKSHEETS

NAME Record/Preamp
DRAWING NO. 8359708
SCHEMATIC NO.
NEXT ASSEM.

Temp:
Ambient = 46°C
Part = 60°C

(X) Failure
(D) Degraded
(0) No Effect

SYSTEM ERTS/TU
MODULE Record/Preamp (4)
SUB-MODULE Preamp

ITEM	NUMBER RCA OR MILITARY	CIRCUIT SYMBOL	QTY PER UNIT	RATED STRESS	APPLIED STRESS	FAIL. RATE $x10^{-6}$	STRESS RATIO	MODULE FAILURE EFFECT: OPEN	MODULE FAILURE EFFECT: SHORT	MODULE FAILURE EFFECT: DEGRAD.	FAILURE MODE NON PERFORMANCE: RECORD RBV	RECORD MSS	PLAYBACK RBV	PLAYBACK MSS	SEARCH P.B.
4.75	RCR079470JP	R28		1/10W	2.0mw	.001	.01	X					X	X	
									X				D	D	
4.76	RNR55C3011FP	R29		1/10W	17.2mw	.0025	.172	X					X	X	
									X				X	X	
4.77	RCR07G681JP	R30		1/10W	3.3mw	.001	.013	X					X	X	
									X				X	X	
4.78	RNR55C51R1FP	R31		1/10W	2.0mw	.001	.01	X					X	X	
									X				D	D	
4.79	RNR55C3921FP	R32		1/10W	7.5mw	.002	.075	X					X	X	
									X				X	X	
4.80	RNR55C3921FP	R33		1/10W	6.0mw	.001	.06	X					X	X	
									X				X	X	
4.81	RCR07G910JP	R34		1/10W	7.2mw	.001	.028	X					X	X	
									X				D	D	
4.82	RCR07G102JP	R35		1/10W	4.8mw	.001	.012	X					X	X	
									X				D	D	
4.83	RNR55C4750FP	R36		1/10W	2.4mw	.002	.024	X					X	X	
									X				X	X	
4.84	RNR55C1000FP	R37		1/10W	5.0mw	.002	.02	X					X	X	
									X				D	D	
4.85	RNR55C47R5FP	R38		1/10W	5.0mw	.002	.02	X					D	D	
									X				D	D	
4.86	RNR55C1501FP	R39		1/10W	7.3mw	.002	.073	X					X	X	
									X				X	X	
4.87	RCR07GF910JP	R40		1/10W	16mw	.001	.064	X					X	X	
									X				D	D	
4.88	RNR55C68R1FP	R41		1/10W	5.0mw	.002	.02	X					D	D	
									X				D	D	
4.89	RCR07G471JP	R42		1/10W	7.6mw	.001	.03	X					X	X	
									X				X	X	
4.90	RCR07G470JP	R43		1/10W	2.0mw	.001	.01	X					X	X	
									X				D	D	
4.91	RNR55C3011FP	R44		1/10W	17.2mw	.0025	.172	X					X	X	
									X				X	X	
4.92	RCR07G681JP	R45		1/10W	3.3mw	.001	.013	X					X	X	
									X				X	X	

CIRCUIT ANALYSIS ____ ENGINEERING ____ TOTAL ____
RELIABILITY

(A) MIL-HDBK-217
(B) EST. DATA

DATE ____ SHEET 5 OF 6

RELIABILITY DATA WORKSHEETS

NAME Record/Preamp
DRAWING NO. 8359708
SCHEMATIC NO.
NEXT ASSEM.

Temp:
Ambient = 46°C
Part = 60°C

(X) Failure
(D) Degraded
(0) No Effect

SYSTEM ERTS/TU
MODULE Record/Preamp (4)
SUB-MODULE Preamp

ITEM	NUMBER RCA OR MILITARY	CIRCUIT SYMBOL	QTY PER UNIT	RATED STRESS	APPLIED STRESS	FAIL. RATE $x10^{-6}$	STRESS RATIO	MODULE FAILURE EFFECT			FAILURE MODE NON PERFORMANCE				
								OPEN	SHORT	DEGRAD.	RECORD RBV	RECORD MSS	PLAYBACK RBV	PLAYBACK MSS	SEARCH P.B.
4.93	RNR55C51R1FP	R46		1/10W	5.0mw	.002	.02	X					X	X	
									X				D	D	
4.94	RNR55C3921FP	R47		1/10W	7.5mw	.0015	.075	X					X	X	
									X				X	X	
4.95	RNR55C3921FP	R48		1/10W	6.0mw	.002	.06	X					X	X	
									X				X	X	
4.96	RCR07G910JP	R49		1/10W	7.2mw	.001	.028	X					X	X	
									X				D	D	
4.97	RCR07G102JP	R50		1/10W	4.8mw	.001	.012	X					X	X	
									X				D	D	
4.98	RNR55C4750FP	R51		1/10W	2.4mw	.002	.024	X					X	X	
									X				X	X	
4.99	RNR55C1000FP	R52		1/10W	5.0mw	.002	.02	X					X	X	
									X				D	D	
4.100	RNR55C47R5FP	R53		1/10W	5.0mw	.002	.02	X					D	D	
									X				D	D	
4.101	RNR55C1501FP	R54		1/10W	7.3mw	.002	.073	X					X	X	
									X				X	X	
4.102	RCR07GF910JP	R55		1/10W	16mw	.001	.064	X					X	X	
									X				D	D	
4.103	RNR55C68R1FP	R56		1/10W	5.0mw	.002	.02	X					D	D	
									X				D	D	
4.104	RCR07G471JP	R57		1/10W	7.6mw	.001	.03	X					X	X	
									X				X	X	
4.105	RCR07G470JP	R58		1/10W	1.0mw	.0005	.01	X					X	X	
									X				D	D	
4.106	RNR55C3011FP	R59		1/10W	17.2mw	.0025	.172	X					X	X	
									X				X	X	
4.107	RCR07G681JP	R60		1/10W	3.3mw	.001	.013	X					X	X	
									X				X	X	
4.108	JANTXIN645	CR1		400mw	40mw	.01	.1	X							
									X						

CIRCUIT ANALYSIS ______ ENGINEERING ______ TOTAL ______
RELIABILITY

(A) MIL-HDBK-217
(B) EST. DATA

DATE ______ SHEET 6 OF 6

RELIABILITY DATA WORKSHEETS

NAME Video Playback Amp
DRAWING NO. 8359692
SCHEMATIC NO.
NEXT ASSEM.

Temp:
Ambient = 46°C
Part = 60°C

(X) Failure
(D) Degraded
(N) No Effect

SYSTEM ERTS/TU
MODULE Playback Amplifier, Video
SUB-MODULE 3

ITEM	NUMBER RCA OR MILITARY	CIRCUIT SYMBOL	QTY PER UNIT	RATED STRESS	APPLIED STRESS	FAIL. RATE x10⁻⁶	STRESS RATIO	MODULE FAILURE EFFECT: OPEN	SHORT	DEGRAD.	FAILURE MODE NON PERFORMANCE: RECORD RBV	RECORD MSS	PLAYBACK RBV	PLAYBACK MSS	SEARCH P.B.
3.1	8150547	C1		25V	13.5V	.05	0.54	X	X				X D	X D	
3.2	8150547	C2		15V	8V	.05	0.53	X	X				X D	X D	
3.3	8150546	C3		50V	5.5V	.001	0.11	X	X				X D	X D	
3.4	8150546	C4		50V	5.5V	.001	0.11	X	X				X D	X D	
3.5	CKR06BX104KP	C5		100V	5V	.001	0.05	X	X				X X	X X	
3.6	8150546	C6		50V	5.5V	.001	0.11	X	X				X D	X D	
3.7	CKR06BX104KP	C7		100V	5V	.001	0.05	X	X				X X	X X	
3.8										DELETED					
3.9	8150546	C9		50V	5.5V	.001	0.11	X	X				X D	X D	
3.10	8150546	C10		50V	5.5V	.001	0.11	X	X				X D	X D	
3.11	CKR06BX104KP	C11		100V	5V	.001	0.05	X	X				X X	X X	
3.12	8150546	C12		50V	5.5V	.001	0.11	X	X				X D	X D	
3.13	CKR06BX104KP	C13		100V	5V	.001	0.05	X	X				X X	X X	
3.14	8150546	C14		50V	5.5V	.001	0.11	X	X				X D	X D	
3.15	8150546	C15		50V	5.5V	.001	0.11	X	X				X D	X D	
3.16	8150546	C16		50V	5.5V	.001	0.11	X	X				X D	X D	
3.17	CKR06BX104KP	C17		100V	5V	.001	0.05	X	X				X X	X X	
3.18	8150546	C18		50V	5.5V	.001	0.11	X	X				X D	X D	

CIRCUIT ANALYSIS
RELIABILITY
ENGINEERING
(A) MIL-HDBK-217
(B) EST. DATA
TOTAL
DATE
SHEET 1 OF 5

F

RELIABILITY DATA WORKSHEETS

NAME Video Playback Amp
DRAWING NO. 8359692
SCHEMATIC NO. ____
NEXT ASSEM. ____

Temp:
Ambient = 46°C
Part = 60°C

(X) Failure
(D) Degraded
(0) No Effect

SYSTEM ERTS/TU
MODULE Playback Amplifier, Video
SUB-MODULE 3

ITEM	NUMBER RCA OR MILITARY	CIRCUIT SYMBOL	QTY PER UNIT	RATED STRESS	APPLIED STRESS	FAIL. RATE $x10^{-6}$	STRESS RATIO	MODULE FAILURE EFFECT: OPEN	SHORT	DEGRAD.	FAILURE MODE NON PERFORMANCE: RECORD RBV	RECORD MSS	PLAYBACK RBV	PLAYBACK MSS	SEARCH P.B.
3.19	CKR06BX104KP	C19		100V	2V	.001	0.02		X				X	X	
								X					X	X	
3.20										DELETED					
3.21	8150546	C21		50V	5.5V	.001	0.11		X				X	X	
								X					D	D	
3.22	8150546	C22		50V	5.5V	.001	0.11		X				X	X	
								X					D	D	
3.23	CKR06BX104KP	C23		100V	5V	.001	0.05		X				X	X	
								X					X	X	
3.24	8150546	C24		50V	5.5V	.001	0.11		X				X	X	
								X					D	D	
3.25	CKR06BX104KP	C25		100V	5V	.001	0.05		X				X	X	
								X					X	X	
3.26	8150546	C26		50V	5.5V	.001	0.11		X				X	X	
								X					D	D	
3.27	8150545	DL1		100V	< .1V	.05	< .1		X				X	X	
								X					X	X	
3.28	8150545	DL2		100V	< .1V	.05	< .1		X				X	X	
								X					X	X	
3.29	JAN TX2N2369A	Q1		360 mw	8 mw	.020	.022		X				X	X	
				T_M=0.4	T_N=0.14			X					X	X	
3.30	JAN TX2N2369A	Q3		360 mw	8 mw	.020	.022		X				X	X	
				T_M=0.4	T_M=0.14			X					X	X	
3.31	8150536	U1		680 mw	80 mw	.040	N/A		X				X	X	
								X					X	X	
3.32	8150536	U2		680 mw	80 mw	.040	N/A		X				X	X	
								X					X	X	
3.32	8150553	U3		680 mw	80 mw	.040	N/A		X				X	X	
								X					X	X	
3.33	8150536	U4		680 mw	80 mw	.040	N/A		X				X	X	
								X					X	X	
3.34	JAN2N3810	Q2		600 mw	6 mw	.03	.2		X				X	X	
					60 mw			X					X	X	
3.35	JAN2N3810	Q4		600 mw	6 mw	.03	.2		X				X	X	
					60 mw			X					X	X	

CIRCUIT ANALYSIS ____ ENGINEERING ____ TOTAL ____
RELIABILITY
(A) MIL-HDBK-217
(B) EST. DATA
DATE ____ SHEET 2 OF 5

NAME Video Playback Amp
DRAWING NO. 8359692
SCHEMATIC NO.
NEXT ASSEM.

Temp:
Ambient = 46°C
Part = 60°C

(X) Failure
(D) Degraded
(0) No Effect

SYSTEM ERTS/TU
MODULE Playback Amplifier, Video
SUB-MODULE 3

ITEM	NUMBER RCA OR MILITARY	CIRCUIT SYMBOL	QTY PER UNIT	RATED STRESS	APPLIED STRESS	FAIL. RATE $x10^{-6}$	STRESS RATIO	MODULE FAILURE EFFECT: OPEN	MODULE FAILURE EFFECT: SHORT	MODULE FAILURE EFFECT: DEGRAD.	FAILURE MODE NON PERFORMANCE: RECORD RBV	RECORD MSS	PLAYBACK RBV	PLAYBACK MSS	SEARCH P.B.
3.36	RCR07GF3R3JP	R1		1/4W	25 mw	.001	0.1		X				D	D	
								X					X	X	
3.37	RCR07GF301JP	R2		1/4W	<5 mw	.001	<.1		X				X	X	
								X					D	D	
3.38	RCR07GF301JP	R3		1/4W	<5 mw	.001	<.1		X				X	X	
								X					D	D	
3.39	RJ24CW101JP	R4		1/2W	<5 mw	.011	<.1		X				X	X	
								X					X	X	
3.40	RJ24CW101JP	R5		1/2W	<5 mw	.011	<.1		X				X	X	
								X					X	X	
3.41	RCR07GF820JP	R6		1/4W	80 mw	.002	0.33		X				X	X	
								X					X	X	
3.42	RCR07GF220JP	R7		1/4W	<5 mw	.001	<.1		X				X	X	
								X					X	X	
3.43	RCR07GF220JP	R8		1/4W	<5 mw	.001	<.02		X				X	X	
								X					X	X	
3.44	RCR07GF220JP	R9		1/4W	<5 mw	.001	<.02		X				X	X	
								X					X	X	
3.45	RCR07GF242JP	R10		1/4W	2.6 mw	.001	0.01		X				X	X	
								X					X	X	
3.46	RCR07GF362JP	R11		1/4W	3 mw	.001	0.01		X				X	X	
								X					X	X	
3.47	RCR07GF102JP	R12		1/4W	8 mw	.001	0.03		X				X	X	
								X					X	X	
3.48	RNR55C1000FP	R13		1/10W	<1 mw	.032	<.01		X				X	X	
								X					X	X	
3.49	RJ24CW501	R14		1/2W	<1 mw	.011	<.01		X				X	X	
								X					X	X	
3.50	RCR07G471JP	R15		1/4W	10 mw	.001	.10		X				X	X	
								X					X	X	
3.51	RCR07GF220JP	R16		1/4W	<5 mw	.001	<.02		X				X	X	
								X					X	X	
3.52	NOT USED														
3.53	RCR07GF220JP	R18		1/4W	<5 mw	.001	<.02		X				X	X	
								X					X	X	

CIRCUIT ANALYSIS ________ ENGINEERING ________ TOTAL ________
RELIABILITY

(A) MIL-HDBK-217
(B) EST. DATA

DATE ________ SHEET 3 OF 5

RELIABILITY DATA WORKSHEETS

NAME Video Playback Amp
DRAWING NO. 8359692
SCHEMATIC NO.
NEXT ASSEM.

Temp:
Ambient = 46°C
Part = 60°C

(X) Failure
(D) Degraded
(0) No Effect

SYSTEM ERTS/TU
MODULE Playback Amplifier, Video
SUB-MODULE 3

ITEM	NUMBER RCA OR MILITARY	CIRCUIT SYMBOL	QTY PER UNIT	RATED STRESS	APPLIED STRESS	FAIL. RATE x10^{-6}	STRESS RATIO	MODULE FAILURE EFFECT			FAILURE MODE NON PERFORMANCE				
								OPEN	SHORT	DEGRAD.	RECORD RBV	RECORD MSS	PLAYBACK RBV	PLAYBACK MSS	SEARCH P.B.
3.54	RCR07GF103JP	R19		1/4W	<5 mw	.001	<.02		X				X	X	
								X					X	X	
3.55	RCR07GF750JP	R20		1/4W	< 5 mw	.001	<.02		X				X	X	
								X					X	X	
3.56	RCR07GF331JP	R21		1/4W	3 mw	.001	.01		X				X	X	
								X					X	X	
3.57	RCR07GF111JP	R22		1/4W	<5 mw	.001	<.02		X				D	D	
								X					X	X	
3.58	RCR07GF101JP	R23		1/4W	40 mw	.001	.16		X				X	X	
								X					X	X	
3.59	RCR07GF102JP	R24		1/4W	8 mw	.001	.03		X				X	X	
								X					X	X	
3.60	RCR07GF750JP	R25		1/4W	14 mw	.001	.06		X				X	X	
								X					X	X	
3.61	RCR07GF301JP	R26		1/4W	5 mw	.001	.02		X				D	D	
								X					X	X	
3.62	RCR07GF301JP	R27		1/4W	5 mw	.001	.02		X				X	X	
								X					D	D	
3.63	RJ24CW101	R28		1/2W	5 mw	.011	.01		X				X	X	
								X					D	D	
3.64	RJ24CW101	R29		1/2W	5 mw	.011	.01		X				X	X	
								X					X	X	
3.65	RCR07GF220JP	R30		1/4W	5 mw	.001	.02		X				X	X	
								X					X	X	
3.66	RCR07GF220JP	R31		1/4W	5 mw	.001	.02		X				X	X	
								X					X	X	
3.67	RCR07GF220JP	R32		1/4W	5 mw	.001	.02		X				X	X	
								X					X	X	
3.68	RCR07GF242JP	R33		1/4W	2.6 mw	.001	.01		X				X	X	
								X					X	X	
3.69	RCR07GF362JP	R34		1/4W	3 mw	.001	.01		X				X	X	
								X					X	X	
3.70	RCR07GF102JP	R35		1/4W	8 mw	.001	.03		X				X	X	
								X					X	X	
3.71	RLR07C620JP	R36		1/4W	1 mw	.032	.01		X				D	D	
								X					X	X	

CIRCUIT ANALYSIS ENGINEERING TOTAL
RELIABILITY

(A) MIL-HDBK-217
(B) EST. DATA

DATE SHEET 4 OF 5

RELIABILITY DATA WORKSHEETS

NAME Video Playback Amp
DRAWING NO. 8359692
SCHEMATIC NO.
NEXT ASSEM.

Temp:
Ambient = 46°C
Part = 60°C

(X) Failure
(D) Degraded
(0) No Effect

SYSTEM ERTS/TT
MODULE Playback Amplifier, Video
SUB-MODULE 3

ITEM	NUMBER RCA OR MILITARY	CIRCUIT SYMBOL	QTY PER UNIT	RATED STRESS	APPLIED STRESS	FAIL. RATE $x10^{-6}$	STRESS RATIO	MODULE FAILURE EFFECT			FAILURE MODE NON PERFORMANCE				
								OPEN	SHORT	DEGRAD.	RECORD		PLAYBACK		SEARCH
											RBV	MSS	RBV	MSS	P.B.
3.72	RJ24CW501	R37		1/2W	1 mw	.011	.01		X				X	X	
								X					X	X	
3.73	RCR07G471JP	R38		1/4W	10 mw	.001	.1		X				X	X	
								X					X	X	
3.74	RCR07GF220JF	R39		1/4W	5 mw	.001	.02		X				X	X	
								X					X	X	
3.75	NOT USED	R40													
3.76	RCR07GF220JP	R41		1/4W	5 mw	.001	.02		X				X	X	
								X					X	X	
3.77	RCR07GF103JP	R42		1/4W	5 mw	.001	.02		X				X	X	
								X					X	X	
3.78	RCR07GF750JP	R43		1/4W	5 mw	.001	.02		X				X	X	
								X					X	X	
3.79	RCR07GF331JP	R44		1/4W	5 mw	.001	.02		X				X	X	
								X					X	X	
3.80	RCR07GF111JP	R45		1/4W	5 mw	.001	.02		X				D	D	
								X					X	X	
3.81	RCR07GF102JP	R46		1/4W	8 mw	.001	.03		X				X	X	
								X					X	X	
3.82	RCR07GF101JP	R47		1/4W	40 mw	.001	.16		X				X	X	
								X					X	X	
3.83	RCR07GF750JP	R48		1/4W	14 mw	.001	.06		X				X	X	
								X					X	X	

CIRCUIT ANALYSIS
RELIABILITY
ENGINEERING
(A) MIL-HDBK-217
(B) EST. DATA

TOTAL
DATE SHEET 5 OF 5

RELIABILITY DATA WORKSHEETS

NAME Control Track/Tach Preamp
DRAWING NO. 8359710
SCHEMATIC NO.
NEXT ASSEM.

Temp:
Ambient = 46°C
Part = 60°C

(X) Failure
(D) Degraded
(0) No Effect

SYSTEM ERTS/TU
MODULE Control Track/Tach Preamp
SUB-MODULE 16

ITEM	NUMBER RCA OR MILITARY	CIRCUIT SYMBOL	QTY PER UNIT	RATED STRESS	APPLIED STRESS	FAIL. RATE x10^-6	STRESS RATIO	MODULE FAILURE EFFECT: OPEN	SHORT	DEGRAD.	FAILURE MODE NON PERFORMANCE: RECORD RBV	RECORD MSS	PLAYBACK RBV	PLAYBACK MSS	SEARCH P.B.
16.1	CKR06BX103KP	C1		200V	1V	.001	<.1	X			0	0	X	X	
									X		0	0	D	D	
.2		C2			6.2V	.001	<.1	X			0	0	X	X	
									X		0	0	D	D	
.3	"	C3		"	12V	.001	<.1	X			0	0	D	D	
									X		0	0	X	X	
.4		C4			4V	.001	<.1	X			0	0	D	D	
									X		0	0	X	X	
16.5	CM05FD331J03	C5		500V	7V	.001	<.1	X			0	0	D	D	
									X		0	0	X	X	
.6	"	C10		"	7V	.001	<.1	X			0	0	D	D	
									X		0	0	X	X	
16.7	CKR06BX103KP	C6		200V	1V	.001	<.1	X			0	0	X	X	
									X		0	0	D	D	
.8		C7			6V	.001	<.1	X			0	0	D	D	
									X		0	0	X	X	
.9	"	C8		"	12V	.001	<.1	X			0	0	D	D	
									X		0	0	X	X	
.10		C9			4V	.001	<.1	X			0	0	D	D	
									X		0	0	X	X	
16.11	CSR13E156KP	C11		20V	12V	.07	.6	X			0	0	D	D	
									X		0	0	X	X	
.12	"	C15		"	"	.025	.4	X			0	0	D	D	
									X		0	0	X	X	
.13	CSR13D226KP	C12		15V	6.2V	.025	.4	X			0	0	D	D	
									X		0	0	X	X	
.14	"	C16		"	"	.025	.4	X			0	0	D	D	
									X		0	0	X	X	
16.15	CKR06CW103KP	C13		200V	11.3V	.001	<.1	X			0	0	D	D	
									X		0	0	X	X	
.16	"	C14		"	6.1V	.001	<.1	X			0	0	D	D	
									X		0	0	X	X	
16.17	RNR55C1001FP	R1		.1W	1 mw	.202 .002	<.1	X			0	0	D	D	
									X		0	0	X	X	
.18	"	R2		.1W	1 mw	.002	<.1	X			0	0	X	X	
									X		0	0	X	X	

CIRCUIT ANALYSIS ______ ENGINEERING ______ TOTAL ______
RELIABILITY

(A) MIL-HDBK-217
(B) EST. DATA

DATE ______ SHEET 1 OF 3

RELIABILITY DATA WORKSHEETS

NAME Control Track/Tach Preamp
DRAWING NO. 8359710
SCHEMATIC NO.
NEXT ASSEM.

Temp:
Ambient = 46°C
Part = 60°C

(X) Failure
(D) Degraded
(0) No Effect

SYSTEM ERTS/TU
MODULE Control Track/Tach Preamp
SUB-MODULE 16

ITEM	NUMBER RCA OR MILITARY	CIRCUIT SYMBOL	QTY PER UNIT	RATED STRESS	APPLIED STRESS	FAIL. RATE $x10^{-6}$	STRESS RATIO	MODULE FAILURE EFFECT			FAILURE MODE NON PERFORMANCE				
								OPEN	SHORT	DEGRAD.	RECORD RBV	RECORD MSS	PLAYBACK RBV	PLAYBACK MSS	SEARCH P.B.
.19		R6		.1W	1 mw	.002	<.1	X			0	0	X	X	
									X		0	0	X	X	
16.20	RNR55C1001FP	R7		.1W	1mw	.002	<.1	X			0	0	X	X	
									X		0	0	X	X	
.21	RCR07G100JP	R3		1/4W	1 mw	.001	<.1	X			0	0	X	X	
									X		0	0	D	D	
.22		R4			1 mw	.001	<.1	X			0	0	X	X	
									X		0	0	D	D	
.23		R8			1 mw	.001	<.1	X			0	0	X	X	
									X		0	0	D	D	
.24	"	R9		"	1 mw	.001	<.1	X			0	0	X	X	
									X		0	0	D	D	
.25		R17			1 mw	.001	<.1	X			0	0	X	X	
									X		0	0	D	D	
.26		R18			1 mw	.001	<.1	X			0	0	X	X	
									X		0	0	D	D	
16.27	RNR55C3162FP	R5		.1W	1 mw	.002	<.1	X			0	0	D	D	
									X		0	0	X	X	
.28	"	R10		.1W	1 mw	.002	<.1	X			0	0	D	D	
									X		0	0	X	X	
16.29	RNR55C1000FP	R11		.1W	1 mw	.002	<.1	X			0	0	X	X	
									X		0	0	D	D	
16.30	RCR20G511JP	R12		1/2W	.2W	.002	.4	X			0	0	X	X	
									X		0	0	D	D	
16.31	RCR07G620JP	R13		1/4W	54 mw	.001	.21	X			0	0	X	X	
									X		0	0	D	D	
16.32	RCR07G101JP	R14		1/4W	1 mw	.001	<.1	X			0	0	X	X	
									X		0	0	X	X	
.33	"	R16		"	1 mw	.001	<.1	X			0	0	X	X	
									X		0	0	X	X	
.34	"	R20		"	1 mw	.001	<.1	X			0	0	X	X	
									X		0	0	D	D	
16.35	RCR07G123JP	R15		1/4W	1 mw	.001	<.1	X			0	0	X	X	
									X		0	0	D	D	
16.36	RCR20G681JP	R21		1/2W	.147W	.002	.3	X			0	0	X	X	
									X		0	0	D	D	

CIRCUIT ANALYSIS ____ ENGINEERING ____ TOTAL ____
RELIABILITY

(A) MIL-HDBK-217
(B) EST. DATA

DATE ____ SHEET 2 OF 3

RELIABILITY DATA WORKSHEETS

NAME Control Track/Tach Preamp
DRAWING NO. 8359710
SCHEMATIC NO.
NEXT ASSEM.

Temp:
Ambient = 46°C
Part = 60°C

(X) Failure
(D) Degraded
(0) No Effect

SYSTEM ERTS/TU
MODULE Control Track/Tach Preamp
SUB-MODULE 16

ITEM	NUMBER RCA OR MILITARY	CIRCUIT SYMBOL	QTY PER UNIT	RATED STRESS	APPLIED STRESS	FAIL. RATE $x10^{-6}$	STRESS RATIO	MODULE FAILURE EFFECT			FAILURE MODE NON PERFORMANCE				
								OPEN	SHORT	DEGRAD.	RECORD RBV	RECORD MSS	PLAYBACK RBV	PLAYBACK MSS	SEARCH P.B.
16.37	RCR07G750JP	R22		1/4W	.043W	.001	.2	X			0	0	X	X	
									X		0	0	D	D	
16.38	RCR07G682JP	R19		1/4W	1 mw	.001	<.1	X			0	0	X	X	
									X		0	0	D	D	
						.031									
16.39	JANTX1N914	CR1		200mw	1 mw	.01	<.1	X			0	0	D	D	
									X		0	0	X	X	
.40	"	CR2		200mw	1 mw	.01	<.1	X			0	0	D	D	
									X		0	0	X	X	
16.41	JANTX1N645	CR3		400mw	1 mw	.01	<.1	X			0	0	0	0	
									X		D	D	X	X	
16.42	M5757/40-010	K1		400mw	1 mw	.05	<.1	X			0	0	0	0	
									X		D	D	X	X	
16.43	JANTX1N963B	VR1		300mw	84 mw	.018	.28	X			0	0	X	X	
									X		0	0	D	D	
.44	"	VR3		300mw	84 mw	.018	.28	X			0	0	X	X	
									X		0	0	D	D	
16.45	JANTX1N753A	VR2		400mw	78 mw	.015	.2	X			0	0	X	X	
									X		0	0	D	D	
16.46	8150533-20	Z1		400mw	78 mw	.94	.2	X			0	0	X	X	
									X		0	0	X	X	
.47	"	Z2		400mw	78 mw	.04	.2	X			0	0	X	X	
									X		0	0	X	X	
.48	"	Z3		400mw	78 mw	.04	.2	X	X		0	0	X	X	
									X		0	0	X	X	
						.251									
					TOTAL	.484									

CIRCUIT ANALYSIS ENGINEERING TOTAL 484
RELIABILITY

(A) MIL-HDBK-217
(B) EST. DATA

DATE SHEET 3 OF 3

RELIABILITY DATA WORKSHEETS

NAME Aux/Search Preamp
DRAWING NO. 8359710
SCHEMATIC NO.
NEXT ASSEM.

Temp:
Ambient = 46°C
Part = 60°C

(X) Failure
(D) Degraded
(0) No Effect

SYSTEM ERTS/TU
MODULE Aux/Search Preamp
SUB-MODULE 17

ITEM	NUMBER RCA OR MILITARY	CIRCUIT SYMBOL	QTY PER UNIT	RATED STRESS	APPLIED STRESS	FAIL. RATE $x10^{-6}$	STRESS RATIO	MODULE FAILURE EFFECT			FAILURE MODE NON PERFORMANCE				
								OPEN	SHORT	DEGRAD.	RECORD RBV	RECORD MSS	PLAYBACK RBV	PLAYBACK MSS	SEARCH P.B.
17.1	CK06BX105KP	C1		50V	1V	.001	<.1	X					0	0	X
									X				0	0	D
.2		C6		50V	1V	.001	<.1	X					0	0	X
									X				0	0	D
.3	"	C12		50V	1V	.001	<.1	X					0	0	X
									X				0	0	D
.4		C17		50V	1V	.001	<.1	X					0	0	X
									X				0	0	D
17.5	CK06BX103KP	C2		200V	12V	.001	<.1	X					0	0	D
									X				0	0	X
.6		C3		200V	12V	.001	<.1	X					0	0	D
									X				0	0	X
.7		C7		200V	12V	.001	<.1	X					0	0	D
									X				0	0	X
.8		C8		200V	12V	.001	<.1	X					0	0	D
									X				0	0	X
.9		C13		200V	12V	.001	<.1	X					0	0	D
									X				0	0	X
.10		C14		200V	12V	.001	<.1	X					0	0	D
									X				0	0	X
.11		C18		200V	12V	.001	<.1	X					0	0	D
									X				0	0	X
.12	"	C19		200V	12V	.001	<.1	X					0	0	D
									X				0	0	X
.13		C24		200V	12V	.001	<.1	X					0	D	0
									X				0	X	0
.14		C25		200V	12V	.001	<.1	X					0	D	0
									X				0	X	0
.15		C26		200V	12V	.001	<.1	X					0	D	0
									X				0	X	0
.16		C28		200V	12V	.001	<.1	X					0	X	0
									X				0	D	0
.17		C29		200V	12V	.001	<.1	X					0	X	0
									X				0	D	0
.18		C30		200V	12V	.001	<.1	X					0	X	0
									X				0	D	0

CIRCUIT ANALYSIS
RELIABILITY
ENGINEERING
(A) MIL-HDBK-217
(B) EST. DATA
TOTAL
DATE
SHEET 1 OF 6

RELIABILITY DATA WORKSHEETS

NAME Aux/Search Preamp
DRAWING NO. 8359710
SCHEMATIC NO.
NEXT ASSEM.

Temp:
Ambient = 46°C
Part = 60°C

(X) Failure
(D) Degraded
(0) No Effect

SYSTEM ERTS/TU
MODULE Aux/Search Preamp
SUB-MODULE 17

ITEM	NUMBER RCA OR MILITARY	CIRCUIT SYMBOL	QTY PER UNIT	RATED STRESS	APPLIED STRESS	FAIL. RATE $x10^{-6}$	STRESS RATIO	MODULE FAILURE EFFECT OPEN	SHORT	DEGRAD.	FAILURE MODE NON PERFORMANCE RECORD RBV	RECORD MSS	PLAYBACK RBV	PLAYBACK MSS	SEARCH P.B.
17.19	CKR06BX222KP	C4		200V	4V	.001	<.1	X					0	0	D
									X				0	0	X
.20	"	C7		200V	4V	.001	<.1	X					0	0	D
									X				0	0	X
17.21	CKR06BX222KP	C15		200V	4V	.001	<.1	X					0	0	X
									X				0	0	D
.22	"	C20		200V	4V	.001	<.1	X					0	0	X
									X				0	0	D
17.23	CM05ED510J03	C5		200V	1V	.001	<.1	X					0	0	D
									X				0	0	D
.24		C16		200V	1V	.001	<.1	X					0	0	D
									X				0	0	D
.25	"	C27		200V	1V	.001	<.1	X					0	D	0
									X				0	D	0
.26		C32		200V	1V	.001	<.1	X					0	D	0
									X				0	D	0
.27	CM05FD101J03	C10		500V	7V	.001	<.1	X					0	0	D
									X				0	0	D
17.28	"	C21		500V	7V	.001	<.1	X					0	0	D
									X				0	0	D
* .29	CSR13C396KP	C22		10V	6V	.075	.6	X					0	0	D
									X				0	0	X
.30	CKR05BX102KP	C23		200V	1V	.001	<.1	X					0	X	0
									X				0	D	0
.31	CKR06BX332KP	C31		200V	4V	.001	<.1	X					0	D	0
									X				0	X	0
* .32	CSR13E156KP	C11		20V	12V	.075	.6	X					0	0	X
									X				0	0	D
* .33	"	C33		20V	12V	.075	.6	X					0	X	0
									X				0	D	0
* .34	CSR13C396KP	C34		10V	6V	.075	.6	X					0	X	0
									X				0	D	0
17.35	RNR55C1001FP	R1		.1W	1 mw	.002	<.1	X					0	0	X
									X				0	0	X
.36		R6		.1W	1 mw	.002	<.1	X					0	0	X
									X				0	0	X

CIRCUIT ANALYSIS ____ ENGINEERING ____ TOTAL ____
RELIABILITY

(A) MIL-HDBK-217
(B) EST. DATA

DATE ____ SHEET 2 OF 6

* Critical Part, High Failure Rate.

RELIABILITY DATA WORKSHEETS

NAME Aux/Search Preamp
DRAWING NO. 8359710
SCHEMATIC NO.
NEXT ASSEM.

Temp:
Ambient = 46°C
Part = 60°C

(X) Failure
(D) Degraded
(0) No Effect

SYSTEM ERTS/TU
MODULE Aux/Search Preamp
SUB-MODULE 17

ITEM	NUMBER RCA OR MILITARY	CIRCUIT SYMBOL	QTY PER UNIT	RATED STRESS	APPLIED STRESS	FAIL. RATE $x10^{-6}$	STRESS RATIO	MODULE FAILURE EFFECT			FAILURE MODE NON PERFORMANCE				
								OPEN	SHORT	DEGRAD.	RECORD RBV	RECORD MSS	PLAYBACK RBV	PLAYBACK MSS	SEARCH P.B.
17.37		R7		.1W	1 mw	.002	<.1	X					0	0	X
									X				0	0	X
.38		R14		.1W	1 mw	.002	<.1	X					0	0	X
									X				0	0	X
.39		R19		.1W	1 mw	.002	<.1	X					0	0	X
									X				0	0	X
.40		R20		.1W	1 mw	.002	<.1	X					0	0	X
									X				0	0	X
.41		R27		.1W	1 mw	.002	<.1	X					0	X	0
									X				0	X	0
.42		R32		.1W	1 mw	.002	<.1	X					0	X	0
									X				0	X	0
.43		R33		.1W	25 mw	.003	.4	X					0	X	0
									X				0	X	0
17.44	RNR55C5111FP	R2		.1W	5 mw	.002	<.1	X					0	0	X
									X				0	0	X
.45	"	R15		.1W	5 mw	.002	<.1	X					0	0	X
									X				0	0	X
.46	"	R28		.1W	5 mw	.002	<.1	X					0	X	0
									X				0	X	0
17.47	RCR07G100JP	R3		1/4W	10 mw	.001	.1	X					0	0	X
									X				0	0	D
.48		R4		1/4W	10 mw	.001	.1	X					0	0	X
									X				0	0	D
.49		R8		1/4W	10 mw	.001	.1	X					0	0	X
									X				0	0	D
.50	"	R9		1/4W	10 mw	.001	.1	X					0	0	X
									X				0	0	D
.51		R21		1/4W	10 mw	.001	.1	X					0	0	X
									X				0	0	D
.52		R22		1/4W	10 mw	.001	.1	X					0	0	X
									X				0	0	D
17.53	RCR07G100JP	R29		.1W	10 mw	.001	.1	X					0	X	0
									X				0	D	0
.54		R30		.1W	10 mw	.001	.1	X					0	X	0
									X				0	D	0

CIRCUIT ANALYSIS ____ ENGINEERING ____ TOTAL ____
RELIABILITY

(A) MIL-HDBK-217
(B) EST. DATA

DATE ____ SHEET 3 OF 6

RELIABILITY DATA WORKSHEETS

NAME Aux/Search Preamp
DRAWING NO. 8359710
SCHEMATIC NO. ____
NEXT ASSEM. ____

Temp:
Ambient = 46°C
Part = 60°C

(X) Failure
(D) Degraded
(0) No Effect

SYSTEM ERTS/TU
MODULE Aux/Search Preamp
SUB-MODULE 17

ITEM	NUMBER RCA OR MILITARY	CIRCUIT SYMBOL	QTY PER UNIT	RATED STRESS	APPLIED STRESS	FAIL. RATE x10⁻⁶	STRESS RATIO	MODULE FAILURE EFFECT: OPEN	SHORT	DEGRAD.	FAILURE MODE NON PERFORMANCE: RECORD RBV	RECORD MSS	PLAYBACK RBV	PLAYBACK MSS	SEARCH P.B.
17.55	RCR07G100JP	R34		.1W	10 mw	.001	.1	X					0	X	0
									X				0	D	0
.56		R35		.1W	10 mw	.001	.1	X					0	X	0
									X				0	D	0
17.57	RNR55C2152FP	R5		.1W	0.8 mw	.002	<.1	X					0	0	D
									X				0	0	X
.58		R10		.1W	0.8 mw	.002	<.1	X					0	0	D
									X				0	0	0
.59	"	R18		.1W	0.8 mw	.002	<.1	X					0	0	D
									X				0	0	X
.60		R23		.1W	0.8 mw	.002	<.1	X					0	0	D
									X				0	0	X
17.61	RCR07G202JP	R11		1/4W	18 mw	.001	<.1	X					0	0	D
									X				0	0	X
.62	"	R24		1/4W	18 mw	.001	<.1	X					0	0	D
									X				0	0	X
.63	"	R37		1/4W	18 mw	.001	<.1	X					0	D	0
									X				0	X	0
17.64	RNR55C1000FP	R12		.1W	10 mw	.002	.1	X					0	0	X
									X				0	0	D
.65	"	R25		.1W	10 mw	.002	.1	X					0	0	X
									X				0	0	D
.66	"	R38		.1W	10 mw	.002	.1	X					0	X	0
									X				0	D	0
17.67	RCR07G100JP	R16		.1W	10 mw	.001	.1	X					0	0	X
									X				0	0	D
.68	"	R17		.1W	10 mw	.001	.1	X					0	0	X
									X				0	0	D
17.69	RCR32G301JP	R13		1W	330 mw	.002	.33	X					0	0	X
									X				0	0	D
17.70	RCR20G470JP	R26		1/2W	86 mw	.002	.2	X					0	0	X
									X				0	0	D
17.71	RNR55C5112FP	R31		.1W	.5 mw	.002	<.1	X					0	D	0
									X				0	X	0
17.72	RNR55C3162FP	R36		.1W	.5 mw	.002	<.1	X					0	D	0
									X				0	X	0

CIRCUIT ANALYSIS ____ ENGINEERING ____ TOTAL ____
RELIABILITY

(A) MIL-HDBK-217
(B) EST. DATA

DATE ____ SHEET 4 OF 6

RELIABILITY DATA WORKSHEETS

NAME Aux/Search Preamp
DRAWING NO. 8359710
SCHEMATIC NO.
NEXT ASSEM.

Temp:
Ambient = 46°C
Part = 60°C

(X) Failure
(D) Degraded
(0) No Effect

SYSTEM ERTS/TU
MODULE Aux/Search Preamp
SUB-MODULE 17

ITEM	NUMBER RCA OR MILITARY	CIRCUIT SYMBOL	QTY PER UNIT	RATED STRESS	APPLIED STRESS	FAIL. RATE $x10^{-6}$	STRESS RATIO	MODULE FAILURE EFFECT: OPEN	SHORT	DEGRAD.	FAILURE MODE NON PERFORMANCE: RECORD RBV	RECORD MSS	PLAYBACK RBV	PLAYBACK MSS	SEARCH P.B.
17.73	RCR20G431JP	R39		1/2W	230 mw	.003	.46	X					0	X	0
									X				0	D	0
17.74	RCR07G620JP	R40		1/4W	64 mw	.002	.25	X					0	X	0
									X				0	D	0
17.75	M5757/40-005	K1		1A	1.8 mA	.05	<.1	X					X	0	0
									X				X	0	0
17.76	JANTXIN914	CR1		100mw	1 mw	.01	<.1	X					0	0	D
									X				0	0	X
.77		CR2		100mw	1 mw	.01	<.1	X					0	0	D
									X				0	0	X
.78		CR3		100mw	1 mw	.01	<.1	X					0	0	D
									X				0	0	X
.79		CR4		100mw	1 mw	.01	<.1	X					0	0	D
									X				0	0	X
.80		CR5		100mw	1 mw	.01	<.1	X					0	D	0
									X				0	X	0
.81		CR6		100mw	1 mw	.01	<.1	X					0	D	0
									X				0	X	0
17.82	JANTXIN645	CR7		RELAY	COIL SUPP.	.01	<.1	X					0	D	0
									X				0	D	0
.83	JANTXIN963B	VR1		100mw	1 mw	.018	.28	X					0	0	D
									X				0	0	X
.84	"	VR3		100mw	1 mw	.025	.4	X					0	D	0
									X				0	X	0
.85	JANTXIN753A	VR2		100mw	1 mw	.015	.26	X					0	0	D
									X				0	0	X
.86	"	VR4		100mw	1 mw	.02	.3	X					0	D	0
									X				0	X	0
17.87	8150533-10	Z1		100mw	1 mw	.04	.4	X					0	0	X
									X				0	0	X
.88		Z2		100mw	1 mw	.04	.4	X					0	0	X
									X				0	0	X
.89		Z3		100mw	1 mw	.04	.4	X					0	0	X
									X				0	0	X
.90		Z4		100mw	1 mw	.04	.4	X					0	0	X
									X				0	0	X

CIRCUIT ANALYSIS RELIABILITY ____ ENGINEERING ____ TOTAL ____

(A) MIL-HDBK-217
(B) EST. DATA

DATE ____ SHEET 5 OF 6

RELIABILITY DATA WORKSHEETS

NAME Aux/Search Preamp
DRAWING NO. 8359710
SCHEMATIC NO.
NEXT ASSEM.

Temp:
Ambient = 46°C
Part = 60°C

(X) Failure
(D) Degraded
(0) No Effect

SYSTEM ERTS/TU
MODULE Aux/Search Preamp
SUB-MODULE 17

ITEM	NUMBER RCA OR MILITARY	CIRCUIT SYMBOL	QTY PER UNIT	RATED STRESS	APPLIED STRESS	FAIL. RATE $x10^{-6}$	STRESS RATIO	MODULE FAILURE EFFECT OPEN	SHORT	DEGRAD.	FAILURE MODE NON PERFORMANCE RECORD RBV	RECORD MSS	PLAYBACK RBV	PLAYBACK MSS	SEARCH P.B.
17.91	8150533-10	Z5		100 mw	1 mw	.04	.4	X					0	X	0
									X				0	X	0
.92	"	Z6		100 mw	1 mw	.04	.4	X					0	X	0
									X				0	X	0
						.08									
					TOTAL	.835									

CIRCUIT ANALYSIS RELIABILITY
ENGINEERING
(A) MIL-HDBK-217
(B) EST. DATA
TOTAL
DATE
SHEET 6 OF 6

RELIABILITY DATA WORKSHEETS

NAME Motor/Solenoid Switch
DRAWING NO.
SCHEMATIC NO.
NEXT ASSEM.

Temp:
Ambient = 46°C
Part = 60°C

(X) Failure
(D) Degraded
(0) No Effect

SYSTEM ERTS/TU
MODULE Motor/Solenoid Switch
SUB-MODULE 18

ITEM	NUMBER RCA OR MILITARY	CIRCUIT SYMBOL	QTY PER UNIT	RATED STRESS	APPLIED STRESS	FAIL. RATE $x10^{-6}$	STRESS RATIO	MODULE FAILURE EFFECT: OPEN	SHORT	DEGRAD.	FAILURE MODE NON PERFORMANCE: RECORD RBV	RECORD MSS	PLAYBACK REC.	PLAYBACK P.B.	AUX. REC.	AUX. P.B.	SEARCH P.B.
18.1	CSR13G475KP	C1		50V	24.5V	.04	.5	X			X	X	X	X	X	X	X
									X		X	X	X	X	X	X	X
.2	CSR13G106KP	C2		50V	20V	.04	.5	X			X	X	X	X	X	X	X
									X		X	X	X	X	X	X	X
18.3	RCR07G101JP	R1		1/4W	17 mw	.001	< .1	X			X	X	X	X	X	X	X
									X		D	D	D	D	D	D	D
.4	RNR55C2870FP	R2		1/10W	20 mw	.003	.2	X			X	X	X	X	X	X	X
									X		X	X	X	X	X	X	X
.5	RCR07G331JP	R3		1/2W	132 mw	.002	.3	X			X	X	X	X	X	X	X
									X		D	D	D	D	D	D	D
.6	RCR07G221JP	R4		1/4W	88 mw	.002	.35	X			X	X	X	X	X	X	X
									X		X	X	X	X	X	X	X
.7	RCR07G102JP	R5		1W	.44W	.003	.44	X			X	X	X	X	X	X	X
									X		X	X	X	X	X	X	X
.8	RCR20G220JP	R6		2-1/2W	.78	.002	.3	X			X	X	X	X	X	X	X
									X		X	X	X	X	X	X	X
.9	RCR07G103JP	R7		1/4W	25 mw	.001	.1	X			X	X	X	X	X	X	X
									X		X	X	X	X	X	X	X
.10	RCR07G103JP	R8		1/4W	-	.001	< .1	X			O	O	O	O	O	O	O
									X		O	O	O	O	O	O	O
.11	RCR07G392JP	R14		1/4W	2 mw	.001	< .1	X			X	X	X	X	X	X	X
									X		D	D	D	D	D	D	D
.12	RCR07G392JP	R15		1/4W	1 mw	.001	< .1	X			X	X	X	X	X	X	X
									X		D	D	D	D	D	D	D
.13	RCR07G392JP	R11		1/10W	2 mw	.001	< .1	X			X	X	X	X	X	X	X
									X		D	D	D	D	D	D	D
.14	RNR55C4641FP	R10		1/10W	1.2 mw	.002	< .1	X			X	X	X	X	X	X	X
									X		D	D	D	D	D	D	D
.15	RNR55C1332FP	R9		1/10W	36 mw	.003	.36	X			X	X	X	X	X	X	X
									X		X	X	X	X	X	X	X
.16	RNR55C1472FP	R12		1/10W	2.1 mw	.003	.2	X			X	X	X	X	X	X	X
									X		D	D	D	D	D	D	D
.17	RNR55C2872FP	R13		1/10W	7 mw	.002	< .1	X			X	X	X	X	X	X	X
									X		D	D	D	D	D	D	D
18.18	JANTXIN645	CR1			DELETED												
.19	JANTXIN645	CR3		400 mw	40 mw	.01	.1	X			D	D	D	D	D	D	D
									X		D	D	D	D	D	D	D
.20	JANTXIN645	CR5		400 mw	40 mw	.01	.1	X			D	D	D	D	D	D	D
									X		D	D	D	D	D	D	D
18.21	JANTXIN645	CR7		400 mw	40 mw	.01	.1	X			D	D	D	D	D	D	D
									X		X	X	X	X	X	X	X
.22		CR13		400 mw	40 mw	.01	.1	X			D	D	D	D	D	D	D
									X		D	D	D	D	D	D	D
.23	JANTXIN645	CR16		400 mw	40 mw	.01	< .1	X			D	D	D	D	D	D	D
									X		X	X	X	X	X	X	X
.24		CR17		400 mw	40 mw	.01	< .1	X			D	D	D	D	D	D	D
									X		D	D	D	D	D	D	D
18.25	JANTXIN4970	CR2			DELETED												
.26		CR4		500 mw	132 mw	.02	.3	X			D	D	D	D	D	D	D
									X		X	X	X	X	X	X	X
.27	JANTXIN4970	CR6		500 mw	132 mw	.02	.3	X			D	D	D	D	D	D	D
									X		X	X	X	X	X	X	X

CIRCUIT ANALYSIS
RELIABILITY
ENGINEERING

(A) MIL-HDBK-217
(B) EST. DATA

TOTAL .118

DATE SHEET 1 OF 2

RELIABILITY DATA WORKSHEETS

NAME Motor/Solenoid Switch
DRAWING NO.
SCHEMATIC NO.
NEXT ASSEM.

Temp:
Ambient = 46°C
Part = 60°C

(X) Failure
(D) Degraded
(0) No Effect

SYSTEM ERTS/TU
MODULE Motor/Solenoid Switch
SUB-MODULE 18

ITEM	NUMBER RCA OR MILITARY	CIRCUIT SYMBOL	QTY PER UNIT	RATED STRESS	APPLIED STRESS	FAIL RATE $x10^{-6}$	STRESS RATIO	MODULE FAILURE EFFECT OPEN	SHORT	DEGRAD.	FAILURE MODE NON PERFORMANCE RECORD RBV	MSS	PLAYBACK REC.	P.B.	AUX. REC.	P.B.	SEARCH P.B.
.28		CR12		500 mw	132 mw	.02	.3	X			D	D	D	D	D	D	D
									X		X	X	X	X	X	X	X
.29		CR14		500 mw	132 mw	.02	.3	X			D	D	D	D	D	D	D
									X		X	X	X	X	X	X	X
18.30	JANTX4958	CR8		1.5W	.34W	.02	.25	X			D	D	D	D	D	D	D
									X		D	D	D	D	D	D	D
.31		CR9		1.5W	.34W	.02	.25	X			D	D	D	D	D	D	D
									X		D	D	D	D	D	D	D
.32	JANTX4958	CR10		1.5W	.34W	.02	.25	X			D	D	D	D	D	D	D
									X		D	D	D	D	D	D	D
.33		CR11		1.5W	.34W	.02	.25	X			D	D	D	D	D	D	D
									X		D	D	D	D	D	D	D
.34	JANTXIN3191	CR15		750 mw	150 mw	.015	.2	X			D	D	D	D	D	D	D
									X		X	X	X	X	X	X	X
18.35	8150555-1	K1		750 mw	150 mw	.05	.2	X			X	X	X	X	X	X	X
									X		X	X	X	X	X	X	X
.36		K2		750 mw	150 mw	.05	.2	X			X	X	X	X	X	X	X
									X		X	X	X	X	X	X	X
.37		K3		750 mw	150 mw	.05	.2	X			X	X	X	X	X	X	X
									X		X	X	X	X	X	X	X
.38	8150555-1	K4		750 mw	150 mw	.05	.2	X			X	X	X	X	X	X	X
									X		X	X	X	X	X	X	X
.39		K6		750 mw	150 mw	.05	.2	X			X	X	X	X	X	X	X
									X		X	X	X	X	X	X	X
.40	M5757/40-005	K7		750 mw	150 mw	.05	.2	X			X	X	X	X	X	X	X
									X		X	X	X	X	X	X	X
18.41	JANTX2N2907A	Q1		1.8W	4 mw	.02	< .1	X			X	X	X	X	X	X	X
									X		X	X	X	X	X	X	X
.42	JANTX2N2219A	Q2		3.0W	2.2 mw	.02	< .1	X			X	X	X	X	X	X	X
									X		X	X	X	X	X	X	X
.43	8150549-1	Q3		5.0W	.22 mw	.02	< .1	X			X	X	X	X	X	X	X
									X		X	X	X	X	X	X	X
						.06											
					TOTAL	.693											

CIRCUIT ANALYSIS
RELIABILITY
ENGINEERING

(A) MIL-HDBK-217
(B) EST. DATA

TOTAL
DATE
SHEET 2 OF 2

APPENDIX 3C

RECORD AMPLIFIER

ECAP DC ANALYSIS

```
       DC ANALYSIS
C      SCHEM.EQUIV TO Q2 AND PARTIAL Q1
C      ERTS RECORD AMPLTF, N.MALY,AUG.19,1969
R1     N(0 ,3 ),     R=350(.1 ), E=-.6(-.5,-.7)
R2     N(15,3 ),     R=1E4(.1 )
R3     N(3 ,1 ),     R=1E3(.15)
R4     N(0 ,2 ),     R=1.3E3(.15),E=22(20.8,23.2)
R5     N(1 ,0 ),     R=4.81E3(.15),E=22(20.8,23.2)
R6     N(0 ,4 ),     R=350(.1 )  ,E=-.6(-.5,-.7)
R7     N(16,4 ),     R=1E4(.1 )
R8     N(4 ,1 ),     R=1E3(.15)
R9     N(16,5 ),     R=350(.1 )  , E=-.6(-.5,-.7)
R10    N(13,5 ),     R=1E4(.1 )
R11    N(5 ,0 ),     R=4.7E3(.15)
R12    N(0 ,13),     R=100(.15) , E=22(20.8,23.2)
R13    N(5 ,6 ),     R=350(.1 ) , E=-.6(-.5,-.7)
R14    N(7 ,6 ),     R=1E4(.1 )
R15    N(0 ,7 ),     R=1E3(.15) , E=22(20.8,23.2)
R16    N(14,8 ),     R=350(.1 ) , E=-.6(-.5,-.7)
R17    N(0 ,14),      R=100(.15)  ,  E=6.2(.07)
R18    N(8 ,12),      R=2E3(.06)
R19    N(7 ,9 ),      R=350(.1 )  ,  E=-.6(-.5,-.7)
R20    N(10,9 ),      R=1E4(.1 )
R21    N(9 ,0 ),      R=3.9E3(.15)
R22    N(11,9 ),      R=350(.1)   ,  E=-.6(-.5,-.7)
R23    N(0 ,11),      R=607(.15)  ,  E=22(20.8,23.2)
R24    N(11,12),      R=1E4(.1)
R25    N(2 ,15),      R=1E3(.15)
R26    N(2 ,16),      R=1E3(.15)
R27    N(12,0 ),      R=2E3(.15)  ,  E=22(20.8,23.2)
R28    N(6 ,8 ),      R=1E4(.1 )
R29    N(0 ,10),      R=100(.15)  ,  E=22(20.8,23.2)
T1     B(1 ,2 ),      BETA=70(15,210)
T2     B(6 ,7 ),      BETA=70(15,210)
T3     B(9 ,10),      BETA=70(15,210)
T4     B(13,14),      BETA=70(15,210)
T5     B(16,28),      BETA=70(15,210)
T6     B(19,20),      BETA=70(15,210)
T7     B(22,24),      BETA=200(100,300)
       WORST CASE
       PRINT,WORST CASE
       EXECUTE


WORST CASE SOLUTIONS FOR NODE VOLTAGES


NODE      WCMIN              NOMINAL              WCMAX


 1  PARTIAL W.R.T.  R  1  HAS CHANGED SIGN AT MAX


 1  PARTIAL W.R.T.  R  6  HAS CHANGED SIGN AT MAX


 1  PARTIAL W.R.T.  T  1  HAS CHANGED SIGN AT MAX


 1  PARTIAL W.R.T.  T  2  HAS CHANGED SIGN AT MAX
```

```
2  PARTIAL W.R.T.  R  1  HAS CHANGED SIGN AT MAX

2  PARTIAL W.R.T.  R  6  HAS CHANGED SIGN AT MAX

2  PARTIAL W.R.T.  T  1  HAS CHANGED SIGN AT MAX

2  PARTIAL W.R.T.  T  2  HAS CHANGED SIGN AT MAX
2       0.13165991E 02     0.16737320E 02     0.19591276D 02
3  PARTIAL W.R.T.  R  1  HAS CHANGED SIGN AT MAX

3  PARTIAL W.R.T.  R  6  HAS CHANGED SIGN AT MAX

3  PARTIAL W.R.T.  T  1  HAS CHANGED SIGN AT MAX

3  PARTIAL W.R.T.  T  2  HAS CHANGED SIGN AT MAX
3      -0.64388067E 00    -0.60237426E 00    -0.59900120D 00
4  PARTIAL W.R.T.  R  1  HAS CHANGED SIGN AT MAX

4  PARTIAL W.R.T.  R  6  HAS CHANGED SIGN AT MAX

4  PARTIAL W.R.T.  T  1  HAS CHANGED SIGN AT MAX

4  PARTIAL W.R.T.  T  2  HAS CHANGED SIGN AT MAX
4      -0.64406133E 00    -0.60238999E 00    -0.59900923D 00
5  PARTIAL W.R.T.  R  6  HAS CHANGED SIGN AT MAX

5  PARTIAL W.R.T.  T  2  HAS CHANGED SIGN AT MAX
5       0.92709570E 01     0.14085935E 02     0.17692472D 02
6  PARTIAL W.R.T.  R  6  HAS CHANGED SIGN AT MAX

6  PARTIAL W.R.T.  T  2  HAS CHANGED SIGN AT MAX
6       0.85400124E 01     0.13469787E 02     0.17030736D 02
7  PARTIAL W.R.T.  R  6  HAS CHANGED SIGN AT MIN

7  PARTIAL W.R.T.  R 14  HAS CHANGED SIGN AT MIN

7  PARTIAL W.R.T.  T  2  HAS CHANGED SIGN AT MIN
7       0.15404556E 02     0.18236069E 02     0.20654505D 02
8  PARTIAL W.R.T.  R  6  HAS CHANGED SIGN AT MAX
```

```
 8  PARTIAL W.R.T.  T  2  HAS CHANGED SIGN AT MAX
 8       0.49802313E 01     0.55809488E 01     0.60335258D 01
 9  PARTIAL W.R.T.  R  6  HAS CHANGED SIGN AT MIN

 9  PARTIAL W.R.T.  R 14  HAS CHANGED SIGN AT MIN

 9  PARTIAL W.R.T.  T  2  HAS CHANGED SIGN AT MIN
 9       0.14718895E 02     0.17615845E 02     0.20047718D 02
10  PARTIAL W.R.T.  R  6  HAS CHANGED SIGN AT MAX

10  PARTIAL W.R.T.  R 14  HAS CHANGED SIGN AT MAX

10  PARTIAL W.R.T.  T  2  HAS CHANGED SIGN AT MAX
10       0.20108932E 02     0.21556168E 02     0.22938014D 02
11  PARTIAL W.R.T.  R  6  HAS CHANGED SIGN AT MIN

11  PARTIAL W.R.T.  R 14  HAS CHANGED SIGN AT MIN

11  PARTIAL W.R.T.  T  2  HAS CHANGED SIGN AT MIN

11  PARTIAL W.R.T.  R 24  HAS CHANGED SIGN AT MAX

11  PARTIAL W.R.T.  T  7  HAS CHANGED SIGN AT MAX
11       0.15340083E 02     0.18223160E 02     0.20650593D 02
12  PARTIAL W.R.T.  R  6  HAS CHANGED SIGN AT MAX

12  PARTIAL W.R.T.  T  2  HAS CHANGED SIGN AT MAX
12      -0.77355003E 01    -0.20082846E 01     0.31969716D 01
13  PARTIAL W.R.T.  R  6  HAS CHANGED SIGN AT MIN

13  PARTIAL W.R.T.  T  2  HAS CHANGED SIGN AT MIN
13       0.20250717E 02     0.21698883E 02     0.23053553D 02
14  PARTIAL W.R.T.  R  6  HAS CHANGED SIGN AT MAX

14  PARTIAL W.R.T.  T  2  HAS CHANGED SIGN AT MAX
14       0.57232199E 01     0.61957655E 01     0.66338958D 01
15  PARTIAL W.R.T.  R  1  HAS CHANGED SIGN AT MAX
```

```
15  PARTIAL W.R.T.  T  1  HAS CHANGED SIGN AT MAX

15       0.99815989E 01      0.14729260E 02      0.18248685D 02

16  PARTIAL W.R.T.  R  6  HAS CHANGED SIGN AT MAX

16  PARTIAL W.R.T.  T  2  HAS CHANGED SIGN AT MAX

16       0.99100208E 01      0.14697183E 02      0.18236475D 02
```

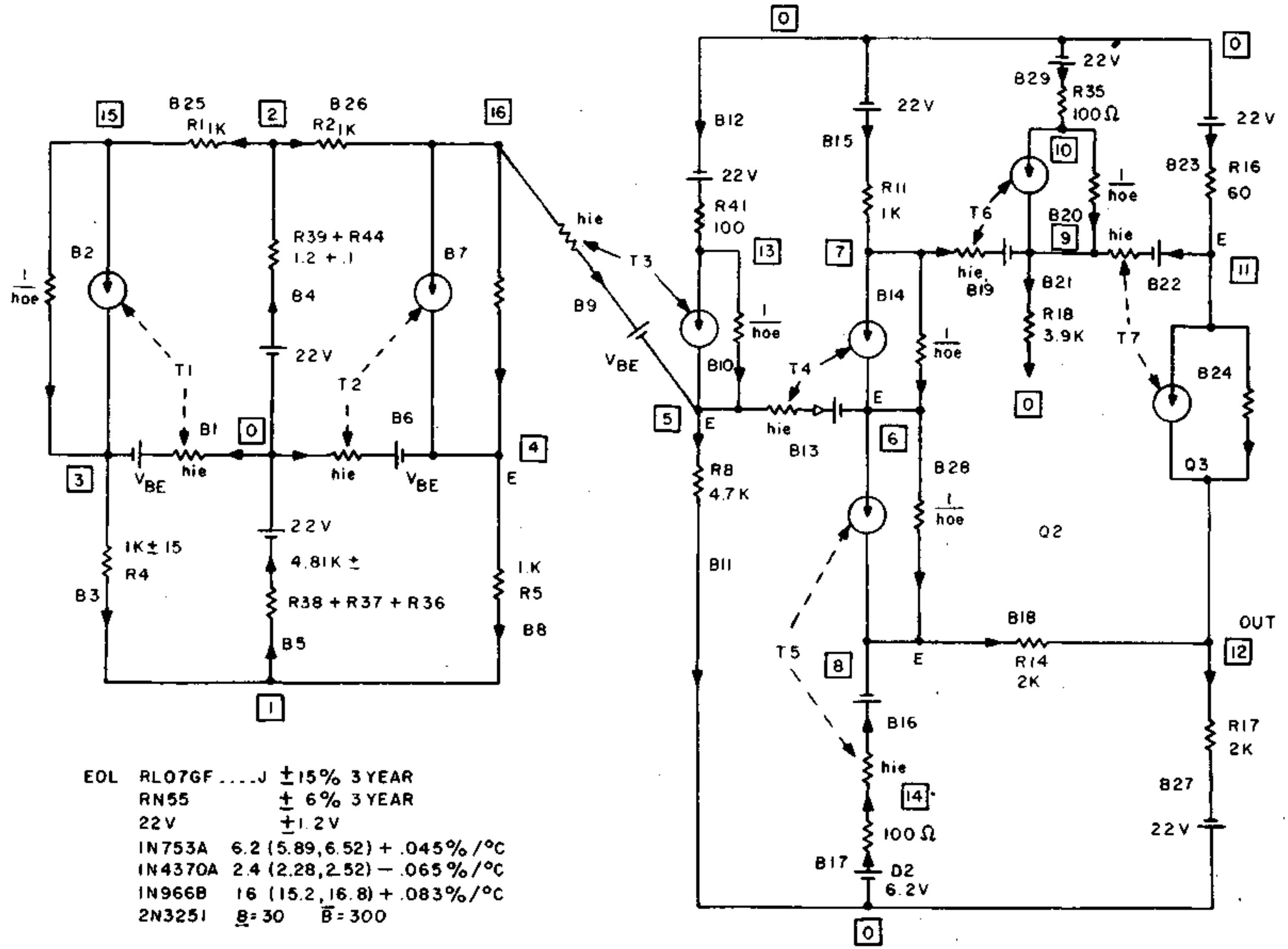

EOL	RL07GF ....J	±15% 3 YEAR
	RN55	± 6% 3 YEAR
	22V	±1.2V
	IN753A	6.2 (5.89, 6.52) + .045%/°C
	IN4370A	2.4 (2.28, 2.52) − .065%/°C
	IN966B	16 (15.2, 16.8) + .083%/°C
	2N3251	$\underline{B}$ = 30 $\bar{B}$ = 300

Figure 3C-1 RECORD AMPLIFIED THROUGH Q3 EPAT D.C. EQUIVALENT CKT.

```
      DC ANALYSIS
C     SCHEM.EQUIV TO Q3 AND Q4
C     ERTS RECORD AMPLIFIER
C     N.MALY, PC 2670, AUG.20,1969
B1    N(1 ,0 ),      R=1E3, E=-2.0(-7.73,3.19)
B2    N(2 ,1 ),      R=351(.1), E=-.6(-.5,-.7)
B3    N(2 ,3 ),      R=1E4(.1)
B4    N(3 ,0 ),      R=1E3(.15), E=22(20.8,23.2)
B5    N(0 ,2 ),      R=3E3(.15), E=22(20.8,23.2)
B6    N(3 ,4 ),      R=351(.1),  E=-.6(-.5,-.7)
B7    N(5 ,4 ),      R=1E4(.1)
B8    N(4 ,0 ),      R=247(.15), E=22(21.8,23.2)
B9    N(5 ,0 ),      R=10
T1    B(2 ,3 ),      BETA=200(100,300)
T2    B(6 ,7 ),      BETA=100(50,200)
      WORST CASE
      PRINT,WORST CASE
      EXECUTE
```

WORST CASE SOLUTIONS FOR NODE VOLTAGES

NODE	WCMIN	NOMINAL	WCMAX
1	-0.31731205E 01	0.20229626E 01	0.77671411D 01
2	-0.25677872E 01	0.26310234E 01	0.83814640D 01
3	-0.20287231E 02	-0.15773222E 02	-0.94521640D 01
4	-0.20953018E 02	-0.16445724E 02	-0.10115402D 02
5	-0.61310101E 00	-0.22280300E 00	-0.35541974D-01

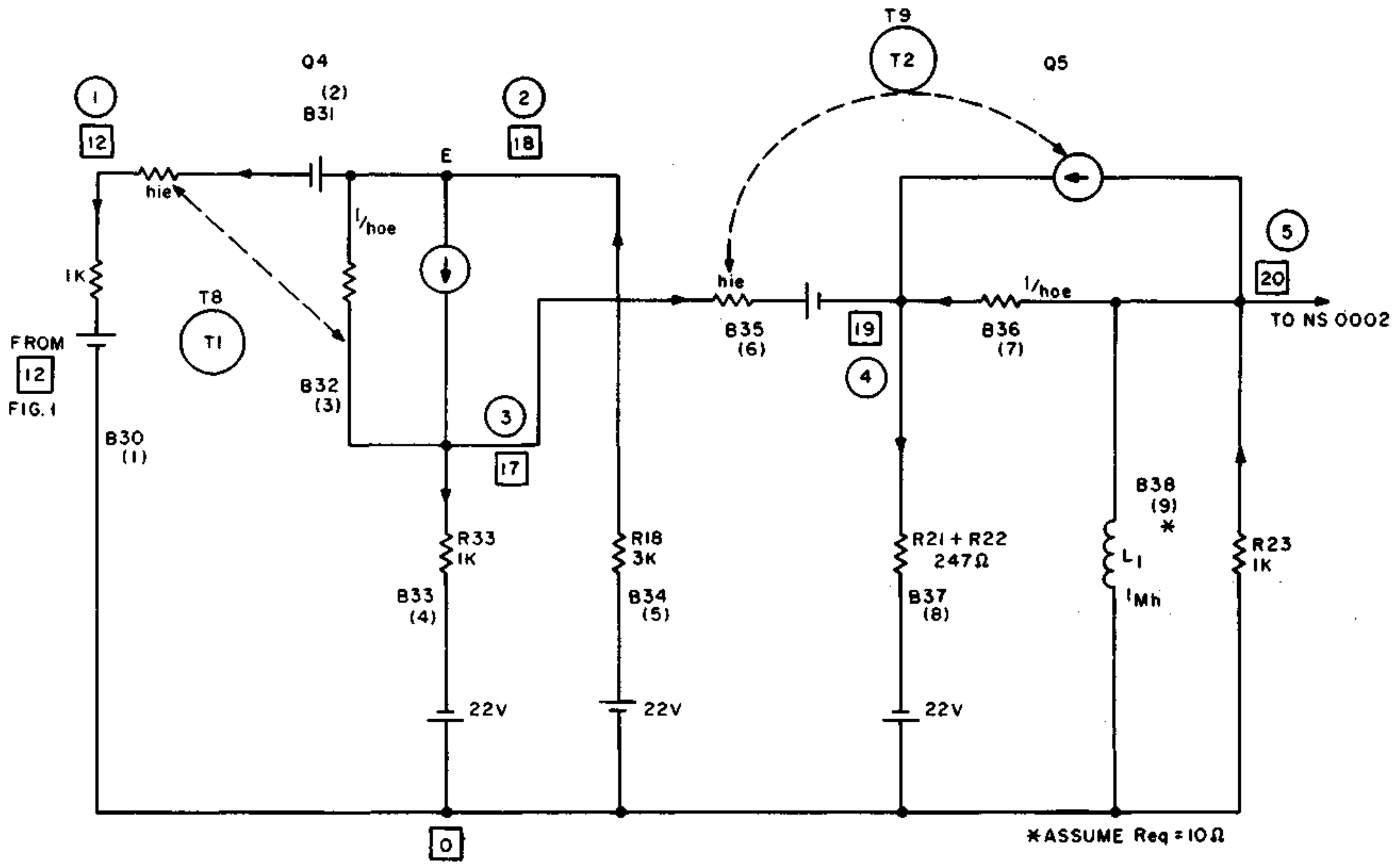

Figure 3C-2 RECORD AMP. Q4, Q5 ECAP D.C. EQUIVALENT

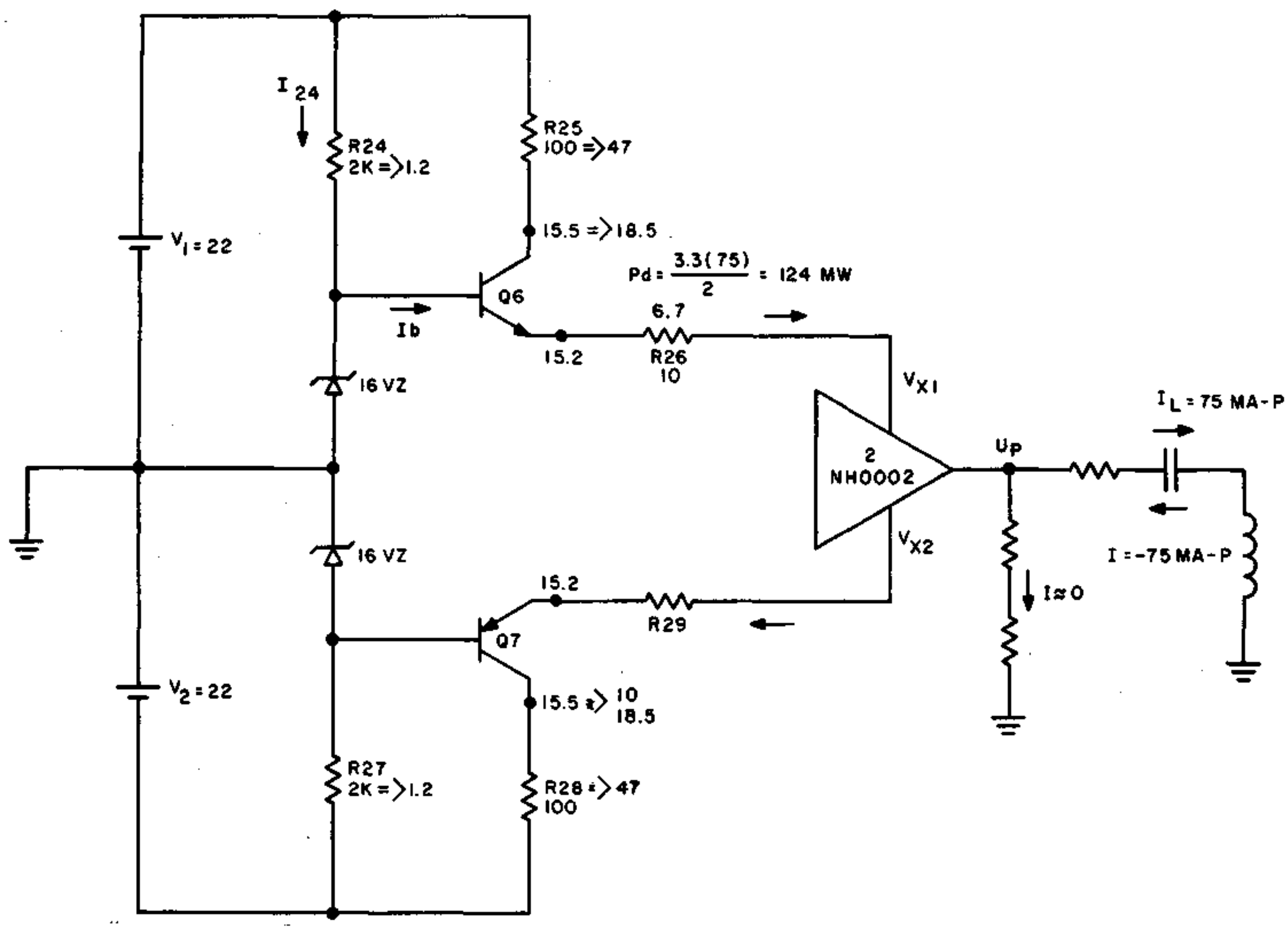

Figure 3C-3 RECORD AMP. REGULATORS

Required signal swing:

f	X_L	$\lvert Z \rvert$	$I_p \lvert Z \rvert (V-D)$
9 MHz	57	61	5.5
16 MHz	100	105	9.4
12 MHz	75	78	7.0

$$\lvert Z \rvert = \sqrt{X_L^2 - X_C^2 + R^2}$$

Worst Case Limiting due to V_2

$$\underline{V_2} = \underline{V_1} - 75\text{ma } (\overline{R_{25}}) = 20.8 - .075\,(115) = \underline{\underline{12.2\text{V}}}$$

		Pulsed	
For 2N2222	$\underline{\beta} =$	100 at I = 150 ma	10V
	$\underline{\beta} =$	75 at I = 10 ma	10V
Assume	$\underline{\beta} =$	75 at I = 100 ma	W.C. Temp.

$$\therefore \text{Required Base drive } \overline{I_B} = \frac{75\text{ ma}}{75} = \underline{1.0\text{ ma}}$$

$$\underline{I_{R24}} = \frac{20.8 - 16.8}{2.3\text{K}} = \frac{4.0}{2.3} = 1.75\text{ ma}$$

$$\underline{I_{R24}}_{\text{PEAK}} = \frac{20.8 - \left[12.2 - V_{CE} + V_{BE}\right]}{2.3} = \frac{8.0}{2.3} = 3.5\text{ ma}$$

Full FM
NO FM

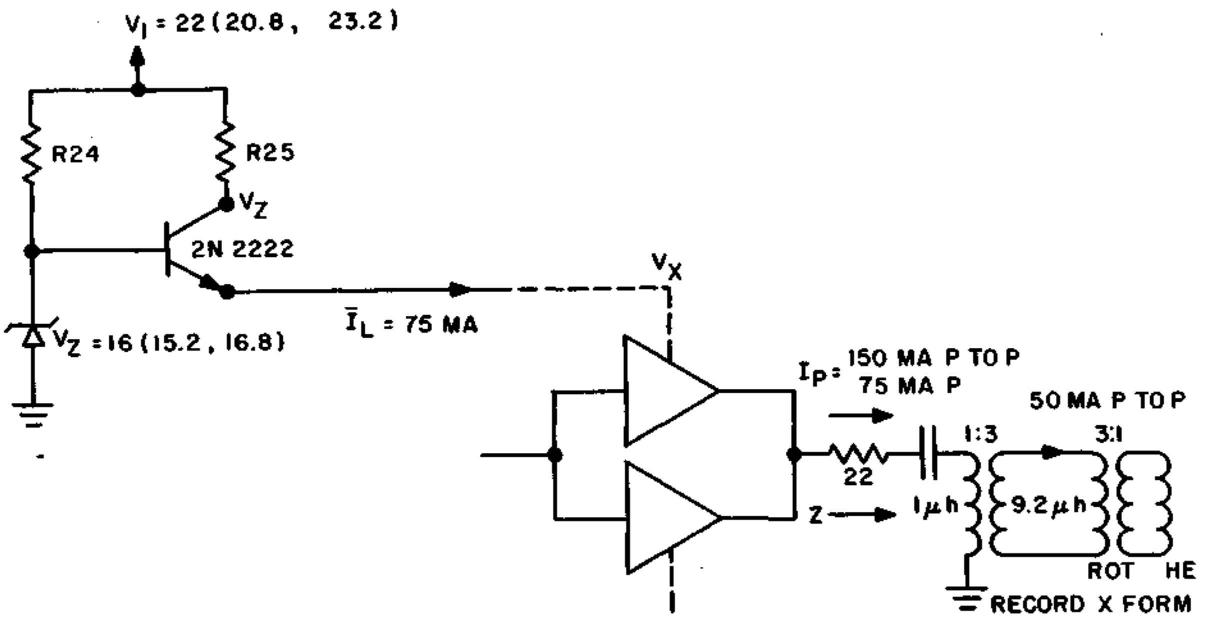

Figure 3C-4 RECORDING AMPLIFIER - REGULATORS Q6 OR Q7

APPENDIX 3D

RECORD AMPLIFIER ECAP AC ANALYSIS

An ac ECAP model (see Figure 3D-1) representing Q4 through Q8 and Q9 with a 1 microhenry load was used to analyze a gain and phase behavior of the main section of the record amplifier. The results representing the output at node 8 of the circuit D are shown in Figure 15.

Both gain and the phase of the record amplifier as per results of the ECAP ac analysis are considered proper for an optimum performance. However, in reality there is a stray and wiring capacity which exist at the load. These have been properly compensated by experimental means to achieve a maximum phase linearity.

```
        AC ANALYSIS
C       ERTS RECORD AMPLIFIER Q4 THROUGH LOAD
C       N.MALY,AUG.23,1969
R1      N(1 ,0 ),          R=1E3,   E=1.0/0
R2      N(2 ,1 ),          R=350
R3      N(2 ,3 ),          R=1E4
R4      N(0 ,2 ),          R=5E3
R5      N(3 ,0 ),          R=1E3
B6      N(3 ,4 ),          R=350
R7      N(4 ,6 ),          R=47
R8      N(5 ,4 ),          R=1E4
R9      N(6 ,0 ),          R=200
R10     N(6 ,0 ),          C=2.2E-6
B11     N(0 ,5 ),          L=1E-3
R12     N(5 ,7 ),          R=90
R13     N(0 ,7 ),          R=1E4
R14     N(7 ,8 ),          R=1.0
R15     N(8 ,11),          R=22
R16     N(9 ,0 ),          L=1E-6
R17     N(8 ,10),          R=1E3
R18     N(10,2 ),          C=.1E-6
R19     N(10,0 ),          R=1E3
B20     N(11,9 ),          C=.1E-6
T1      B(2,3),            BETA=50
T2      B(6,8),            BETA=50
T3      B(12,13),          BETA=60E3
        FREQUENCY=1E4
        PRINT,VOLTAGES
        EXECUTE
```

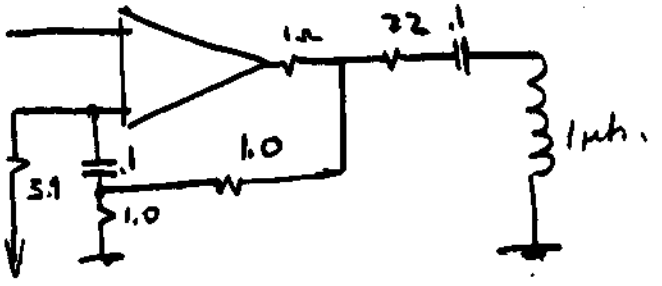


```
FREQ =  0.99999922F 04


      NODES              NODE VOLTAGES

MAG    1-  4  0.95961994E 00  0.94560468E 00  0.15157909E 01  0.13265371E 01
PHA          -0.17873080E 03 -0.17826109E 03 -0.30766846E 02 -0.31898392E 02

MAG    5-  8  0.17089872E 01  0.20059079E 00  0.17089834E 01  0.17064762E 01
PHA          -0.11321317E 03 -0.11113525E 03 -0.11321371E 03 -0.11359697E 03

MAG    9- 11  0.66760229E-03  0.11403542E 01  0.16903906E 01
PHA           0.58529800E 02 -0.16617740E 03 -0.12147015E 03
```

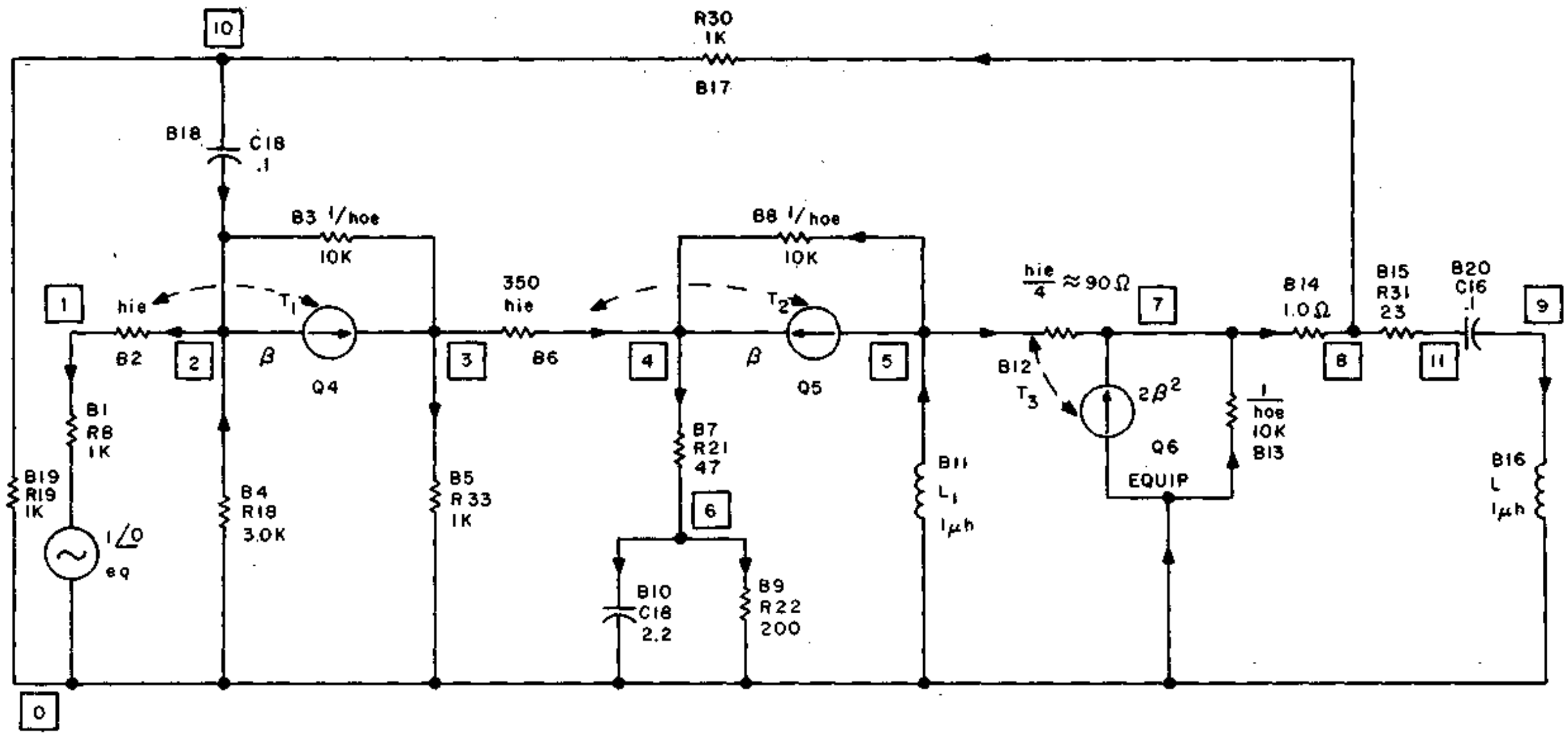

Figure 3D-1 ERTS RECORD AMPLIFIER Q4 THROUGH LOAD A.C. EQUIVALENT CKT. REV A

```
      MODIFY
      FREQUENCY=264(2)40.96E6
      EXECUTE

FREQ =  0.19999980E 05


      NODES              NODE VOLTAGES


MAG     1-  4  0.98329037E 00  0.97757053E 00  0.93636638E 00  0.81737339E 00
PHA           -0.17866763E 03 -0.17819067E 03 -0.57867432E 02 -0.58513779E 02


MAG     5-  8  0.21331434E 01  0.62623501E-01  0.21331310E 01  0.21248827E 01
PHA           -0.14413463E 03 -0.14308432E 03 -0.14413567E 03 -0.14481798E 03


MAG     9- 11  0.32389069E-02  0.10664358E 01  0.20478268E 01
PHA            0.19704712E 02 -0.17666158E 03 -0.16029524E 03

FREQ =  0.39999969E 05


      NODES              NODE VOLTAGES


MAG     1-  4  0.99355328E 00  0.99134320E 00  0.49962056E 00  0.43584114E 00
PHA           -0.17919995E 03 -0.17891751E 03 -0.72627853E 02 -0.73087555E 02


MAG     5-  8  0.22823982E 01  0.16752444E-01  0.22829582E 01  0.22564039E 01
PHA           -0.16091565E 03 -0.16036671E 03 -0.16091728E 03 -0.16201886E 03


MAG     9- 11  0.12533586E-01  0.10178423E 01  0.19717159E 01
PHA           -0.11111959E 02 -0.17919373E 03  0.16888800E 03

FREQ =  0.79999938E 05


      NODES              NODE VOLTAGES


MAG     1-  4  0.99662650E 00  0.99545896E 00  0.25783461E 00  0.22487879E 00
PHA           -0.17957430E 03 -0.17942464E 03 -0.80096909E 02 -0.80596664E 02


MAG     5-  8  0.23574314E 01  0.43254942E-02  0.23573389E 01  0.22967100E 01
PHA           -0.16956343E 03 -0.16923552E 03 -0.16956529E 03 -0.17082784E 03


MAG     9- 11  0.39365695E-01  0.10025129E 01  0.15186701E 01
PHA           -0.39433533E 02 -0.17972697E 03  0.14056644E 03
```

```
      NODES              NODE VOLTAGES

MAG    1-  4  0.99792641E 00  0.99666417E 00  0.13140243E 00  0.11459249E 00
PHA          -0.17978101E 03 -0.17970413E 03 -0.84079698E 02 -0.84864929E 02

MAG    5-  8  0.24032183E 01  0.11023143E-02  0.24030800E 01  0.23113184E 01
PHA          -0.17446356E 03 -0.17418423E 03 -0.17446483E 03 -0.17534052E 03

MAG    9- 11  0.97844481E-01  0.99847907E 00  0.87029368E 00
PHA          -0.63221268E 02 -0.17987975E 03  0.11677863E 03

FREQ =  0.31999969E 06

      NODES              NODE VOLTAGES

MAG    1-  4  0.99778128E 00  0.99700570E 00  0.66213846E-01  0.57723161E-01
PHA          -0.17988936E 03 -0.17985051E 03 -0.85816681E 02 -0.87289642E 02

MAG    5-  8  0.24210711E 01  0.27764658E-03  0.24209137E 01  0.23161497E 01
PHA          -0.17732329E 03 -0.17694933E 03 -0.17732378E 03 -0.17765431E 03

MAG    9- 11  0.20978272E 00  0.99746424E 00  0.30914992E 00
PHA          -0.79983795E 02 -0.17994182E 03  0.10001614E 03

FREQ =  0.63999950E 06

      NODES              NODE VOLTAGES

MAG    1-  4  0.99784839E 00  0.99709564E 00  0.33202887E-01  0.28906122E-01
PHA          -0.17994449E 03 -0.17992499E 03 -0.85625702E 02 -0.88514771E 02

MAG    5-  8  0.24238157E 01  0.69519680E-04  0.24236565E 01  0.23174944E 01
PHA          -0.17899718E 03 -0.17834459E 03 -0.17899690E 03 -0.17882457E 03

MAG    9- 11  0.42257303E 00  0.99721068E 00  0.16124696E 00
PHA          -0.92814285E 02 -0.17997110E 03 -0.92814285E 02

FREQ =  0.12799990E 07

      NODES              NODE VOLTAGES

MAG    1-  4  0.99786550E 00  0.99711859E 00  0.16659282E-01  0.14426820E-01
PHA          -0.17997220E 03 -0.17996242E 03 -0.83254257E 02 -0.88972992E 02
```

```
MAG     5-  8  0.24156675E 01  0.17348415E-04  0.24155207E 01  0.23178453E 01
PHA            0.17988258E 03 -0.17888789E 03  0.17988398E 03 -0.17941158E 03

MAG     9- 11  0.80954921E 00  0.99714738E 00  0.68438965E 00
PHA           -0.10658525E 03 -0.17998553E 03 -0.10658525E 03

FREQ =  0.25599980E 07

     NODES             NODE VOLTAGES

MAG     1-  4  0.99787003E 00  0.99712467E 00  0.84455784E-02  0.71691163E-02
PHA           -0.17998608E 03 -0.17998116E 03 -0.77469696E 02 -0.88666122E 02

MAG     5-  8  0.23904142E 01  0.43104783E-05  0.23909046E 01  0.23179483E 01
PHA            0.17910487E 03 -0.17862360E 03  0.17910663E 03 -0.17970522E 03

MAG     9- 11  0.13865023E 01  0.99713188E 00  0.13329124E 01
PHA           -0.12480766E 03 -0.17999274E 03 -0.12480766E 03

FREQ =  0.51199950E 07

     NODES             NODE VOLTAGES

MAG     1-  4  0.99787146E 00  0.99712658E 00  0.44899210E-02  0.35557491E-02
PHA           -0.17999301E 03 -0.17999055E 03 -0.65995192E 02 -0.87030106E 02

MAG     5-  8  0.23539038E 01  0.10689591E-05  0.23538485E 01  0.23179922E 01
PHA            0.17894675E 03 -0.17700882E 03  0.17894849E 03 -0.17985220E 03

MAG     9- 11  0.19260206E 01  0.99712837E 00  0.19074097E 01
PHA           -0.14522549E 03 -0.17999635E 03 -0.14522549E 03

FREQ =  0.10239992E 08

     NODES             NODE VOLTAGES

MAG     1-  4  0.99787194E 00  0.99712723E 00  0.27483029E-02  0.17773181E-02
PHA           -0.17999646E 03 -0.17999525E 03 -0.48060150E 02 -0.83309387E 02

MAG     5-  8  0.23306592E 01  0.26719605E-06  0.23306341E 01  0.23180113E 01
PHA            0.17927824E 03 -0.17329878E 03  0.17927945E 03 -0.17992596E 03

MAG     9- 11  0.21980867E 01  0.99712765E 00  0.21927767E 01
PHA           -0.16100618E 03 -0.17999815E 03 -0.16100618E 03
```

```
      NODES              NODE VOLTAGES

MAG     1-  4  0.99787211E 00  0.99712741E 00  0.21055066E-02  0.90687722E-03
PHA           -0.17999821E 03 -0.17999760E 03 -0.29007679E 02 -0.76225784E 02

MAG     5-  8  0.23224077E 01  0.68158215E-07  0.23224001E 01  0.23180180E 01
PHA            0.17960429E 03 -0.16622046E 03  0.17960495E 03 -0.17996297E 03

MAG     9- 11  0.22862062E 01  0.99712753E 00  0.22848253E 01
PHA           -0.17025529E 03 -0.17999902E 03 -0.17025529E 03

FREQ =  0.40959968E 08

      NODES              NODE VOLTAGES

MAG     1-  4  0.99787211E 00  0.99712747E 00  0.19120651E-02  0.49136300E-03
PHA           -0.17999908E 03 -0.17999881E 03 -0.15480490E 02 -0.63607468E 02

MAG     5-  8  0.23201256E 01  0.18464711E-07  0.23201218E 01  0.23180189E 01
PHA            0.17979729E 03 -0.15360483E 03  0.17979762E 03 -0.17998143E 03

MAG     9- 11  0.23099422E 01  0.99712747E 00  0.23095932E 01
PHA           -0.17509473E 03 -0.17999951E 03 -0.17509473E 03
```

```
      MODIFY
      FREQUENCY=.5E6
      EXECUTE

FREQ =  0.49999969E 06


      NODES            NODE VOLTAGES


MAG    1- 4  0.99783397E 00  0.99707633E 00  0.42464089E-01  0.36994729E-01
PHA         -0.17992897E 03 -0.17990407E 03 -0.85914536E 02 -0.88182098E 02

MAG    5- 8  0.24240093E 01  0.11388499E-03  0.24238491E 01  0.23172016E 01
PHA         -0.17849092E 03 -0.17796429E 03 -0.17849092E 03 -0.17849622E 03

MAG    9- 11 0.33089495E 00  0.99726462E 00  0.43721162E-02
PHA         -0.88388153E 02 -0.17996297E 03  0.91611786E 02
```

SUMMARY NODE #9

Freq	Gain x 10^{-3}	$\approx 20 \log \frac{A_o}{A}$	Phase
.01	.667		58°
.02	3.2	- 56 db	19
.04	12.5	- 45	-11
.08	39.3	- 35	-39
.16	97.8	- 27	-63
.32	209	- 20	-79
.64	422	- 14	-93
1.28	809	- 8	-106
2.56	1.386	- 4	-124
5.12	1.926	- 1.0	-145
10.24	2.198 =>	0	-161
20.48	2.286	.4	-170

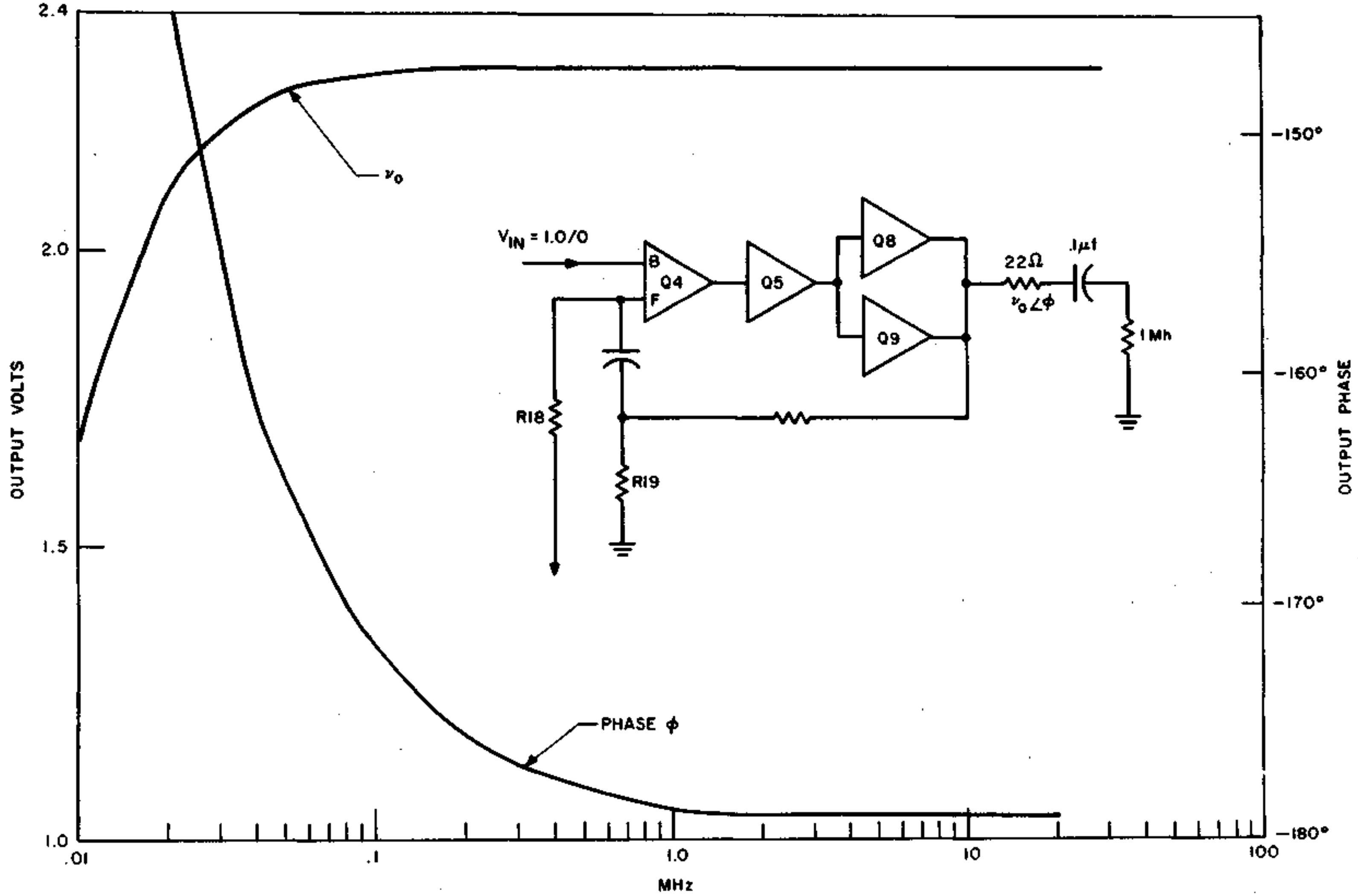

Figure 3D-2 RECORD AMPLIFIER SIGNAL RESPONSE NODE #8 (NO STRAY CAPACITY)

APPENDIX 3E

VIDEO PREAMPLIFIER,

ECAP AC ANALYSIS

3E-1

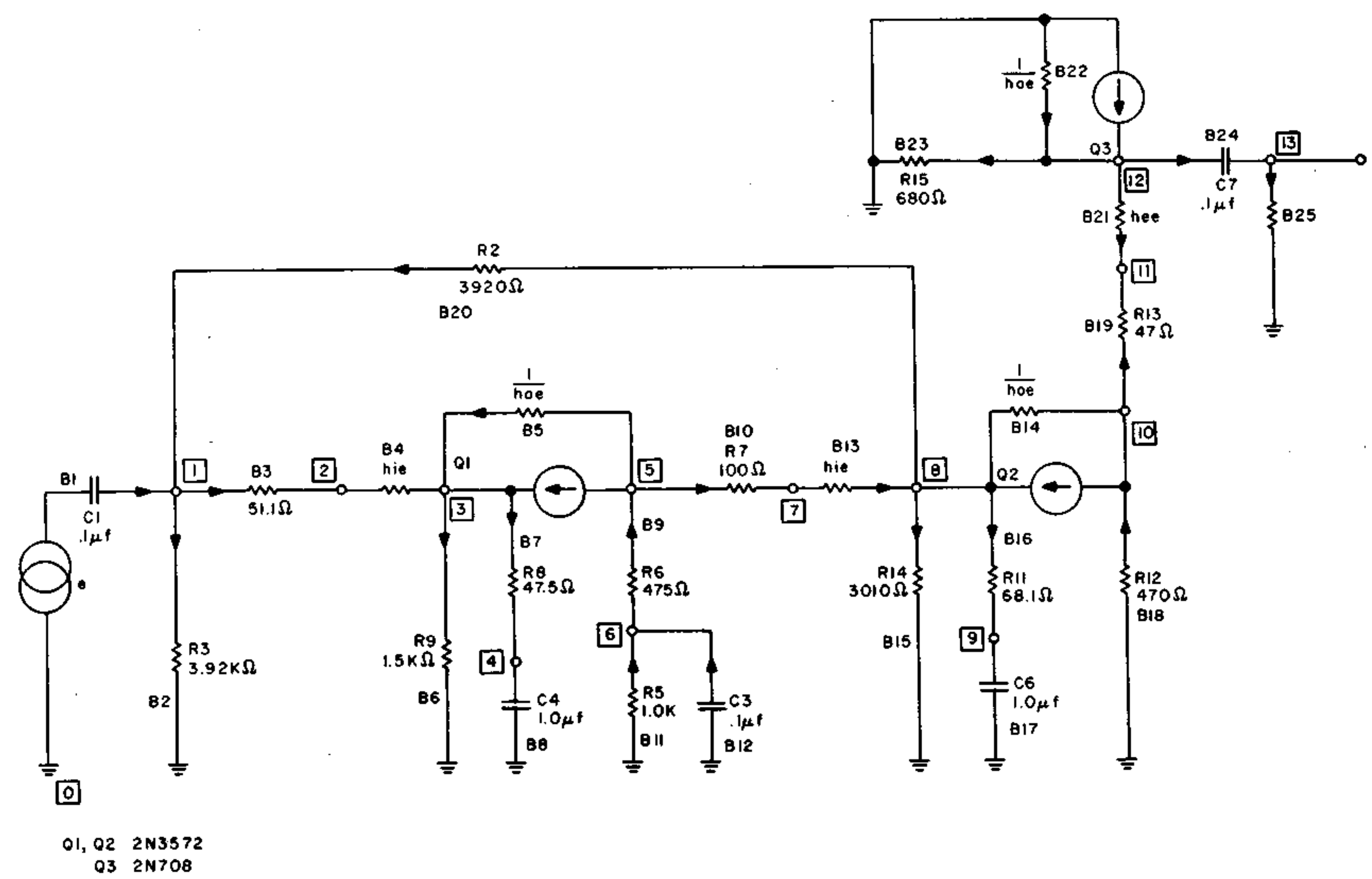

Figure 3E-1 ERTS PREAMP. A.C. EQUIVALENT

```
        AC ANALYSIS
C       ERTS PREAMP. FREQ.RESPONSE / MIN.GAIN
C       N.MALY,JULY 10, 1969
R1      N(0 ,1 )       , C=.1E-6 , F=1.0/0
R2      N(1 ,0 )       , R=3920
R3      N(1 ,2 )       , R=51.1
R4      N(2 ,3 )       , R=300
R5      N(5 ,3 )       , R=1E4
R6      N(3 ,0 )       , R=1500
R7      N(3 ,4 )       , R=47.5
R8      N(4 ,0 )       , C=1E-6
R9      N(6 ,5 )       , R=475
R10     N(5 ,7 )       , R=100
R11     N(0 ,6 )       , R=1E3
R12     N(0 ,6 )       , C=.1E-6
R13     N(7 ,8 )       , R=300
R14     N(10,8 )       , R=1E4
R15     N(8 ,0 )       , R=3010
R16     N(8 ,9 )       , R=68.1
R17     N(9 ,0 )       , C=1E-6
R18     N(0 ,10)       , R=470
R19     N(10,11)       , R=47
R20     N(8 ,1 )       , R=3920
R21     N(11,12)       , R=300
R22     N(0 ,12)       , R=1E4
R23     N(12,0 )       , R=680
R24     N(12,13)       , C=.1E-6
R25     N(13,0 )       , R=75
T1      B(4 ,5 )       , BETA=20
T2      B(13,14)       , BETA=20
T3      B(21,22)       , BETA=25
        FREQUENCY=5E3
        PRINT,VOLTAGES
        EXECUTE

FREQ =  0.49999961E 04          5KHZ


        NODES                NODE VOLTAGES


MAG     1-  4  0.76288778E 00  0.73797911E 00  0.59611750E 00  0.33185178E 00
PHA            0.36146439E 02  0.35279877E 02  0.28755325E 02 -0.27417557E 02


MAG     5-  8  0.48264971E 01  0.23003006E 01  0.45752153E 01  0.38332739E 01
PHA           -0.14336293E 03  0.17130382E 03 -0.14442538E 03 -0.14844176E 03


MAG     9- 12  0.16231718E 01  0.22785141E 02  0.22690170E 02  0.22098190E 02
PHA            0.14661034E 03  0.52744049E 02  0.52452881E 02  0.50536163E 02

                X5
MAG    13- 13  0.50679836E 01
PHA            0.12727794E 03
```

13 is the output node
1 is the input node

```
MODIFY
FREQUENCY=10E3(2)20.48E6
EXECUTE

FREQ =  0.99999922E 04


NODES               NODE VOLTAGES


MAG    1-  4  0.92519504E 00  0.89025301E 00  0.68702817E 00  0.21827155E 00
PHA           0.20704208E 02  0.20194748E 02  0.16163727E 02 -0.55312134E 02


MAG    5-  8  0.54152012E 01  0.16266241E 01  0.31077213E 01  0.41893349E 01
PHA          -0.16133606E 03  0.13496327E 03 -0.16191553E 03 -0.16416304E 03


MAG    9- 12  0.95339090E 00  0.25923645E 02  0.25732803E 02  0.24559845E 02
PHA           0.11899129E 03  0.24019028E 02  0.23537506E 02  0.20291672E 02


MAG   13- 13  0.10469338E 02
PHA           0.85060059E 02

FREQ =  0.19999980E 05


NODES               NODE VOLTAGES


MAG    1-  4  0.98011738E 00  0.94156045E 00  0.71576160E 00  0.11826462E 00
PHA           0.10725511E 02  0.10459017E 02  0.83161478E 01 -0.72173294E 02


MAG    5-  8  0.55386324E 01  0.90080112E 00  0.52172709E 01  0.42542505E 01
PHA          -0.17076527E 03  0.11311491E 03 -0.17105771E 03 -0.17219987E 03


MAG    9- 12  0.49376667E 00  0.25368439E 02  0.25024174E 02  0.22890839E 02
PHA           0.10446512E 03  0.92787704E 01  0.87098227E 01  0.46819267E 01


MAG   13- 13  0.15700064E 02
PHA           0.51378143E 02

FREQ =  0.39999969E 05


NODES               NODE VOLTAGES


MAG    1-  4  0.99494690E 00  0.95539278E 00  0.72332376E 00  0.60378384E-01
PHA           0.54108887E 01  0.52760820E 01  0.41879837E 01 -0.81024338E 02


MAG    5-  8  0.55645609E 01  0.46260244E 00  0.52401934E 01  0.42673559E 01
PHA          -0.17540067E 03  0.10164272E 03 -0.17554607E 03 -0.17611484E 03
```

```
MAG     9- 12  0.69376667E 00  0.25368439E 02  0.25024124E 02  0.22890839E 02
PHA            0.10446512E 03  0.92787704E 01  0.87098227E 01  0.46819267E 01

MAG    13- 13  0.15700064E 02
PHA            0.51378143E 02

FREQ =  0.39999969E 05


      NODES             NODE VOLTAGES

MAG     1-  4  0.99494690E 00  0.95539278E 00  0.72332376E 00  0.60378384E-01
PHA            0.54108887E 01  0.52760820E 01  0.41878857E 01 -0.81024358E 02

MAG     5-  8  0.55645609E 01  0.46260244E 00  0.52401934E 01  0.42673559E 01
PHA           -0.17540067E 03  0.10164272E 03 -0.17556607E 03 -0.17611484E 03

MAG     9- 12  0.24890429E 00  0.24438828E 02  0.23971893E 02  0.21028732E 02
PHA            0.97228882E 02  0.35527153E 01  0.31211693E 01 -0.81741452E-01

MAG    13- 13  0.18576491E 02
PHA            0.27864960E 02

FREQ =  0.79999938E 05


      NODES             NODE VOLTAGES

MAG     1-  4  0.99873114E 00  0.95892119E 00  0.72924071E 00  0.30348595E-01
PHA            0.27115755E 01  0.26439743E 01  0.20974188E 01 -0.85504242E 02

MAG     5-  8  0.55707541E 01  0.23287541E 00  0.52457027E 01  0.42706156E 01
PHA           -0.17770256E 03  0.95832458E 02 -0.17777501E 03 -0.17805865E 03

MAG     9- 12  0.12470639E 00  0.24041229E 02  0.23524185E 02  0.20236191E 02
PHA            0.93614624E 02  0.15569910E 01  0.13087854E 01 -0.57070410E 00

MAG    13- 13  0.19559769E 02
PHA            0.14285354E 02

FREQ =  0.15999988E 06


      NODES             NODE VOLTAGES

MAG     1-  4  0.99968183E 00  0.95980757E 00  0.72572136E 00  0.15194365E-01
PHA            0.13565598E 01  0.13227339E 01  0.10491791E 01 -0.87751099E 02
```


B

```
MAG     5-  8  0.55726719E 01  0.58342990E-01  0.52474155E 01  0.42716484E 01
PHA           -0.17942578E 03  0.91458954E 02 -0.17944386E 03 -0.17951468E 03

MAG     9- 12  0.31196691E-01  0.23894913E 02  0.23359467E 02  0.19942535E 02
PHA            0.90903687E 02  0.36905962E 00  0.30409491E 00 -0.19276768E 00

MAG    13- 13  0.19898819E 02
PHA            0.36012239E 01

FREQ =  0.63999950E 06

      NODES            NODE VOLTAGES

MAG     1-  4  0.99997997E 00  0.96008551E 00  0.72587222E 00  0.38001549E-02
PHA            0.33920098E 00  0.33074206E 00  0.26233155E 00 -0.89437653E 02

MAG     5-  8  0.55727692E 01  0.29174604E-01  0.52475014E 01  0.42717009E 01
PHA           -0.17971288E 03  0.90729492E 02 -0.17972194E 03 -0.17975735E 03

MAG     9- 12  0.15598811E-01  0.23887283E 02  0.23350876E 02  0.19927170E 02
PHA            0.90451797E 02  0.18400604E 00  0.15144414E 00 -0.97702563E-01

MAG    13- 13  0.19916229E 02
PHA            0.18013744E 01

FREQ =  0.12799990E 07

      NODES            NODE VOLTAGES

MAG     1-  4  0.99999493E 00  0.96009946E 00  0.72587979E 00  0.19001167E-02
PHA            0.16960174E 00  0.16537243E 00  0.13116670E 00 -0.89718796E 02

MAG     5-  8  0.55727930E 01  0.14587689E-01  0.52475293E 01  0.42717142E 01
PHA           -0.17985641E 03  0.90364700E 02 -0.17986095E 03 -0.17987865E 03

MAG     9- 12  0.77994689E-02  0.23885376E 02  0.23348709E 02  0.19923325E 02
PHA            0.90225922E 02  0.91937363E-01  0.75646520E-01 -0.49016625E-01

MAG    13- 13  0.19920578E 02
PHA            0.90078282E 00

FREQ =  0.25599980E 07

      NODES            NODE VOLTAGES
```

```
      NODES              NODE VOLTAGES

MAG    1-  4  0.99999815E 00  0.96010244E 00  0.72588178E 00  0.95006311E-03
PHA           0.84801078E-01  0.82686424E-01  0.65589467E-01 -0.89859375E 02

MAG    5-  8  0.55727959E 01  0.72930912E-02  0.52478262E 01  0.42717152E 01
PHA          -0.17992821E 03  0.90182373E 02 -0.17993045E 03 -0.17993930E 03

MAG    9- 12  0.38997426E-02  0.23884872E 02  0.23348160E 02  0.19922348E 02
PHA           0.90112915E 02  0.45960527E-01  0.37813846E-01 -0.24928980E-01

MAG   13- 13  0.19921661E 02
PHA           0.45040397E 00

FREQ =  0.51199950E 07

      NODES              NODE VOLTAGES

MAG    1-  4  0.99999934E 00  0.96010363E 00  0.72588199E 00  0.47503226E-03
PHA           0.42400572E-01  0.41343238E-01  0.32791764E-01 -0.89929657E 02

MAG    5-  8  0.55727997E 01  0.36469533E-02  0.52478290E 01  0.42717180E 01
PHA          -0.17996405E 03  0.90091171E 02 -0.17996521E 03 -0.17996964E 03

MAG    9- 12  0.19498728E-02  0.23884766E 02  0.23348038E 02  0.19922119E 02
PHA           0.90056473E 02  0.22979237E-01  0.18909737E-01 -0.12267083E-01

MAG   13- 13  0.19921936E 02
PHA           0.22520328E 00

FREQ =  0.10239992E 08

      NODES              NODE VOLTAGES

MAG    1-  4  0.99999976E 00  0.96010399E 00  0.72588223E 00  0.23751620E-03
PHA           0.21200277E-01  0.20671617E-01  0.16398882E-01 -0.89964844E 02

MAG    5-  8  0.55728006E 01  0.18234774E-02  0.52478300E 01  0.42717180E 01
PHA          -0.17998204E 03  0.90045547E 02 -0.17998257E 03 -0.17998482E 03

MAG    9- 12  0.97493618E-03  0.23884735E 02  0.23348007E 02  0.19922058E 02
PHA           0.90028229E 02  0.11489481E-01  0.94527195E-02 -0.61938693E-02

MAG   13- 13  0.19922012E 02
PHA           0.11260176E 00

FRFO =  0.20479984E 08
```

```
      NODES            NODE VOLTAGES

MAG    1-  4  0.99999988E 00  0.96010411E 00  0.72588229E 00  0.11875809E-03
PHA           0.10600138E-01  0.10335807E-01  0.81979409E-02 -0.89982376E 02

MAG    5-  8  0.55728006E 01  0.91173849E-03  0.52479309E 01  0.42717190E 01
PHA          -0.17999100E 03  0.90022766E 02 -0.17999127E 03 -0.17999236E 03

MAG    9- 12  0.48746797E-03  0.23884735E 02  0.23348007E 02  0.19922043E 02
PHA           0.90014069E 02  0.57447217E-02  0.47263391E-02 -0.30669733E-02

MAG   13- 13  0.19922028E 02
PHA           0.56300916E-01
```

APPENDIX 3F

VIDEO PREAMPLIFIER,

ECAP DC ANALYSIS

3F-1

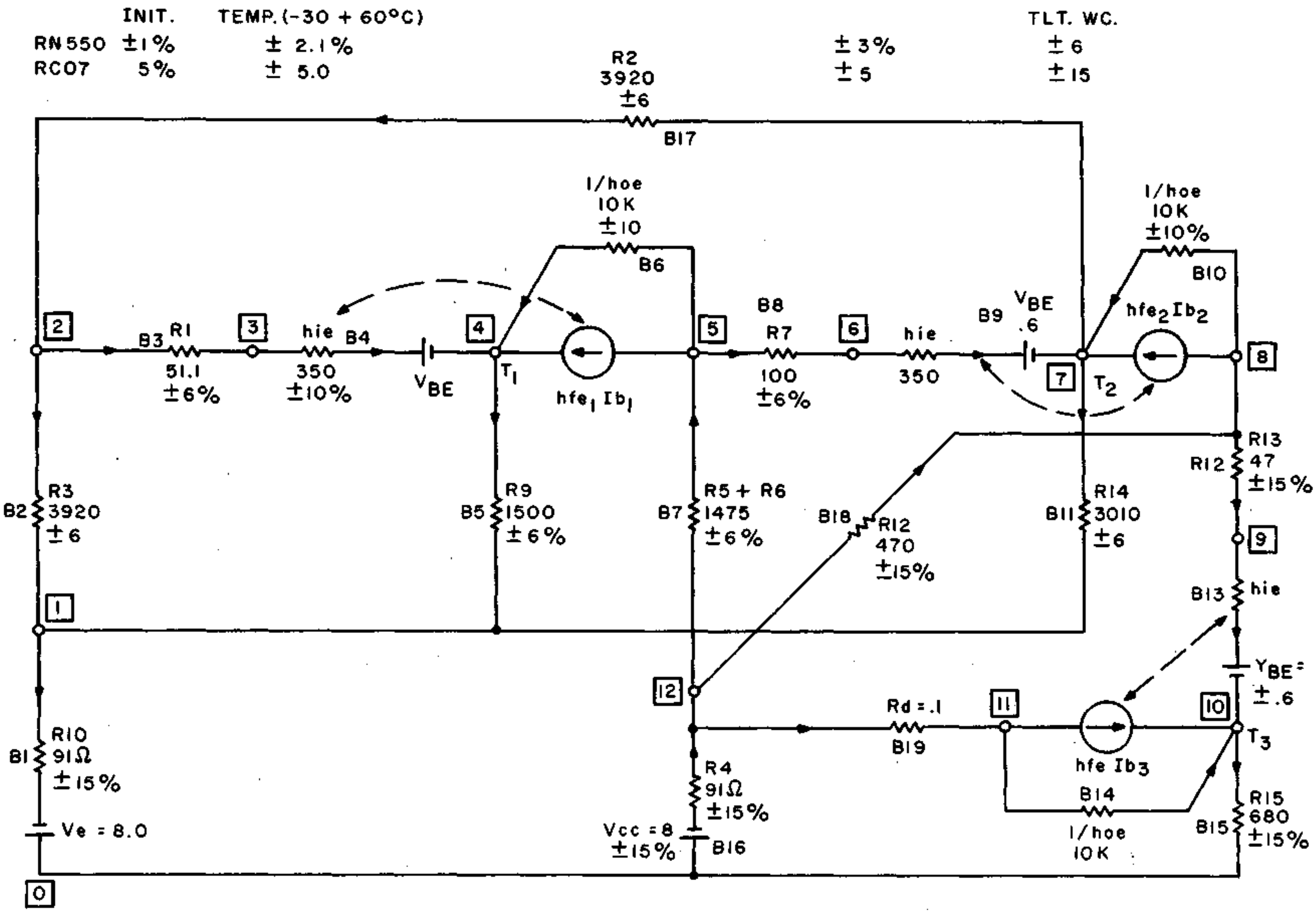

Figure 3F-1 PREAMP ECAP D.C. EQUIVALENT

```
      DC ANALYSIS
C     ERTS PREAMP
C     JUNE 25,1969, N.MALY
B1    N(1,0)  ,R=91(.15),      E=8.0(7.4,8.6)
B2    N(2,1)  ,R=3920(.06)
B3    N(2,3)  ,R=51.1(.06)
B4    N(3,4)  ,R=350(.10),     E=-.6(-.5,-.7)
B5    N(4,1)  ,R=1500(.06)
B6    N(5,4)  ,R=1E4(.10)
B7    N(12,5) ,R=1475(.06)
B8    N(5,6)  ,R=100(.06)
B9    N(6,7)  ,R=350(.10),     E=-.6(-.5,-.7)
B10   N(8,7)  ,R=1E4(.10)
B11   N(7,1)  ,R=3010(.06)
B12   N(8,9)  ,R=47(.15)
B13   N(9,10) ,R=350(.10),     E=-.6(-.5,-.7)
B14   N(11,10),R=1E4(.10)
B15   N(10,0) ,R=680(.15)
B16   N(0,12) ,R=91(.15),      E=8.0(7.4,8.6)
B17   N(7,2)  ,R=3920(.06)
B18   N(12,8) ,R=470(.15)
B19   N(12,11),R=.1
T1    B(4,6)  ,BETA=80(15,350)
T2    B(9,10) ,BETA=80(15,350)
T3    B(13,14),BETA=80(20,200)
      WORST CASE
      PRINT,WORST CASE
      EXECUTE
```

```
WORST CASE SOLUTIONS FOR NODE VOLTAGES


NODE      WCMIN               NOMINAL              WCMAX

  1       -0.81011238E 01     -0.73564892E 01      -0.66059917D 01
  2       -0.39462557E 01     -0.26633139E 01      -0.15037471D 01
  3       -0.39524040E 01     -0.26646509E 01      -0.15040598D 01
  4       -0.45948820E 01     -0.32738066E 01      -0.21061693D 01

  5  PARTIAL W.R.T.  R 11  HAS CHANGED SIGN AT MIN

  5        0.12594500E 01      0.27552662E 01       0.43019904D 01

  6  PARTIAL W.R.T.  R 11  HAS CHANGED SIGN AT MAX

  6        0.12212019E 01      0.27501850E 01       0.42978335D 01

  7  PARTIAL W.R.T.  R 11  HAS CHANGED SIGN AT MAX

  7        0.53655016E 00      0.21324043E 01       0.36935880D 01
  8        0.33324747E 01      0.47399597E 01       0.60735221D 01
  9        0.33218946E 01      0.47366076E 01       0.60721422D 01
 10        0.26460190E 01      0.41116447E 01       0.54613685D 01
 11        0.59695635E 01      0.68056564E 01       0.76400772D 01
 12        0.59702063E 01      0.68062544E 01       0.76406108D 01
```

APPENDIX 3G

SPECIFICATION
FOR
MC 1545
INTEGRATED CIRCUIT

3-6-1

MC1545

GATED DUAL-INPUT WIDEBAND-AMPLIFIER INTEGRATED CIRCUIT

MONOLITHIC SILICON EPITAXIAL PASSIVATED

JANUARY 1969 – DS 9117

GATE-CONTROLLED TWO-CHANNEL-INPUT WIDEBAND AMPLIFIER

. . . designed for use as a general-purpose gated wideband-amplifier, video switch, sense amplifier, multiplexer, modulator, FSK circuit, limiter, AGC circuit, or pulse amplifier.

GATE HI 4,5 ON
" LO 2,3 ON

- Large Bandwidth; 75 MHz typical
- Channel-Select Time of 20 ns typical
- Differential Inputs and Differential Output

G Suffix
CASE 602A
(Formerly CASE 71A)

F Suffix
CASE 607
(Formerly CASE 83)
(TO-86)

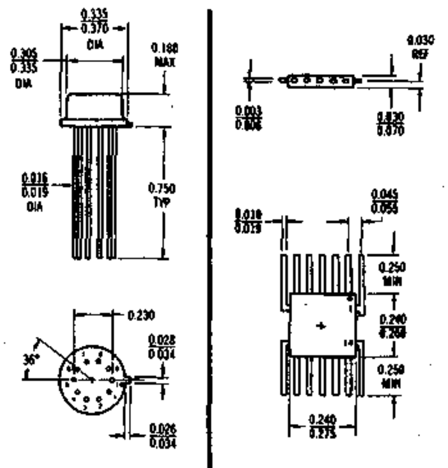

(Bottom View)

Pin 7 connected to case

Weight = 0.918 grams (approx.)

Lead 1 identified by color dot or by elbow or lead. All leads electrically isolated from package

Weight = 0.218 grams (approx.)

L Suffix
CASE 605C
(TO-116)
Ceramic

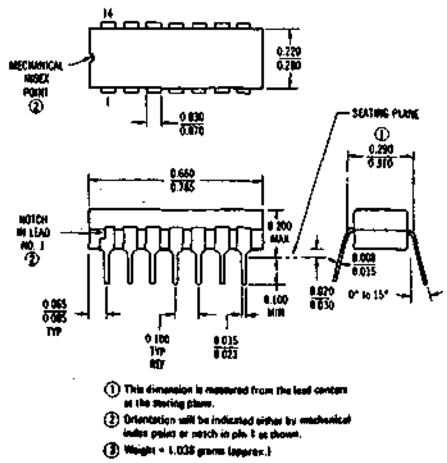

MAXIMUM RATINGS (T_A = 25°C unless otherwise noted)

Rating	Symbol	Value	Unit
Power Supply Voltage	V^+ V^-	+12 -12	Vdc Vdc
Differential Input Signal	V_{in}	±5.0	Volts
Load Current	I_L	25	mA
Power Dissipation (Package Limitation) Flat Package Derate above 25°C Ceramic Dual In-Line Package Derate above 25°C Metal Can Derate above 25°C	P_D	 500 3.3 625 5.0 680 4.6	 mW mW/°C mW mW/°C mW mW/°C
Operating Temperature Range	T_A	-55 to +125	°C
Storage Temperature Range	T_{stg}	-65 to +150	°C

CIRCUIT SCHEMATIC

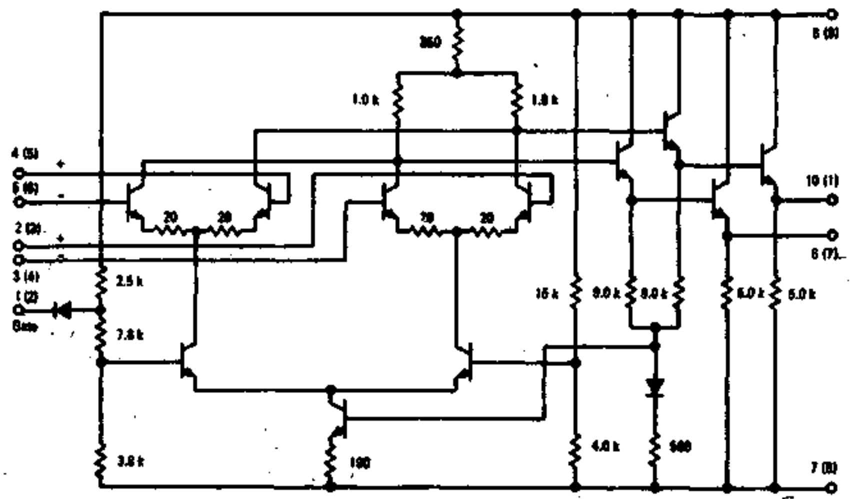

Number at end of terminal is pin number for G package.
Number in parenthesis is pin number for F and L packages.

ELECTRICAL CHARACTERISTICS

(V+ = +5.0 Vdc, V− = −5.0 Vdc, at T_A = 25°C, specifications apply to both input channels unless otherwise noted)

Characteristic	Fig. No.	Symbol	Min	Typ	Max	Unit
Single-Ended Voltage Gain	1,12	A_V	16	18	20	dB
Bandwidth	1,12	BW	50	75	-	MHz
Input Impedance (f = 50 kHz)	5,14	Z_{in}	4.0	10	-	k ohms
Output Impedance (f = 50 kHz)	6,15	Z_{out}	-	25	-	Ohms
Output Voltage Swing (R_L = 1.0 k ohm, f = 50 kHz)	4,13	V_{out}	1.5	2.0	-	V_{p-p}
Input Bias Current ($I_b = (I_1 + I_2)/2$)	16	I_b	-	15	25	µAdc
Input Offset Current	16	$\|I_{io}\|$	-	2.0	-	µAdc
Input Offset Voltage	17	$\|V_{io}\|$	-	1.0	5.0	mVdc
Quiescent Output dc Level	17	$V_{out}(dc)$	-	0.5	-	Vdc
Output dc Level Change (Gate Voltage Change: +5.0 V to 0 V)	17	$\|\Delta V_{out}(dc)\|$	-	15	-	mV
Common Mode Rejection Ratio (f = 50 kHz)	9,18	CM_{rej}	-	85	-	dB
Input Common Mode Voltage Swing	18	CMV_{in}	-	±2.5	-	V_p
Gate Current Low (Gate Voltage = 0 V)	18	I_{GOL}	-	-	2.5	mA
Gate Current High (Gate Voltage = +5.0 V)	18	I_{GOH}	-	-	2.0	µA
Step Response (e_{in} = 20 mV)	19	t_{pd+}	-	6.5	10	ns
		t_{pd-}	-	6.3	10	
		t_r	-	6.5	10	
		t_f	-	7.0	10	
Wideband Input Noise (5.0 Hz - 10 MHz, R_S = 50 ohms)	10,20	$V_{n(in)}$	-	25	-	µVrms
DC Power Dissipation	11,20	P_D	-	70	110	mW

TYPICAL CHARACTERISTICS

FIGURE 1 – SINGLE-ENDED VOLTAGE GAIN versus FREQUENCY

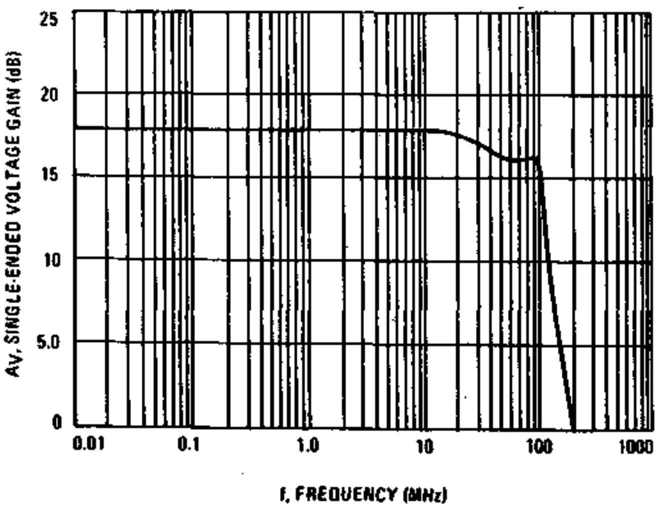

FIGURE 2 – SINGLE-ENDED VOLTAGE GAIN versus TEMPERATURE

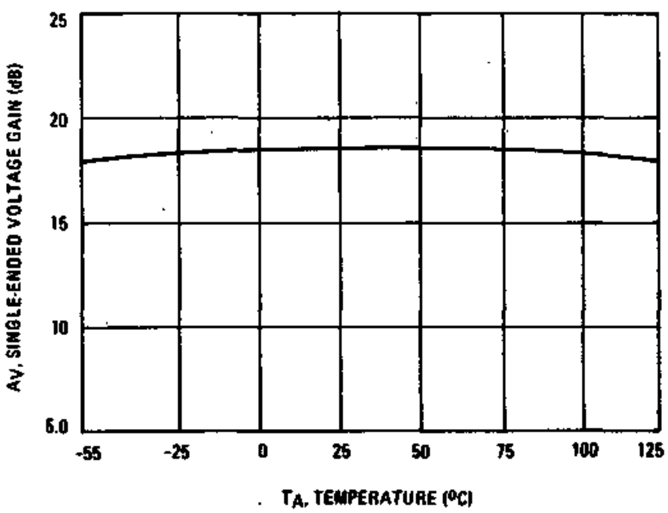

FIGURE 3 – VOLTAGE GAIN versus POWER SUPPLY VOLTAGES

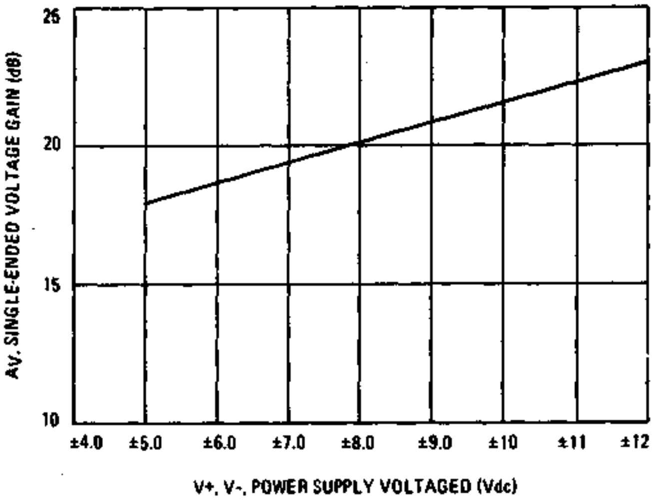

FIGURE 4 – OUTPUT VOLTAGE SWING versus LOAD RESISTANCE

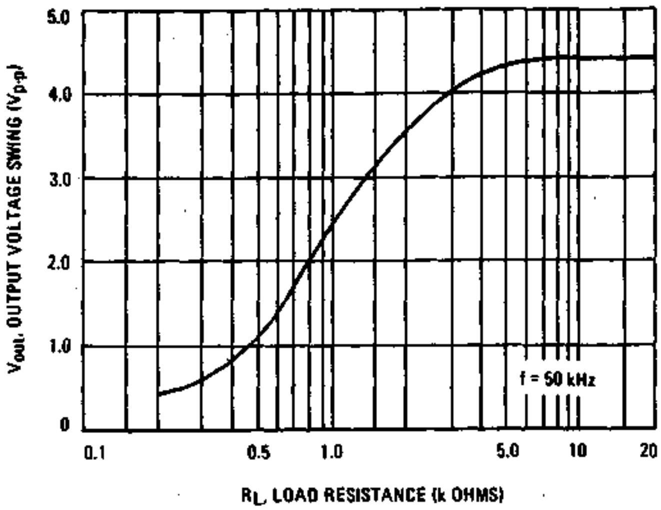

FIGURE 5 – INPUT Cp AND Rp versus FREQUENCY (BOTH CHANNELS)

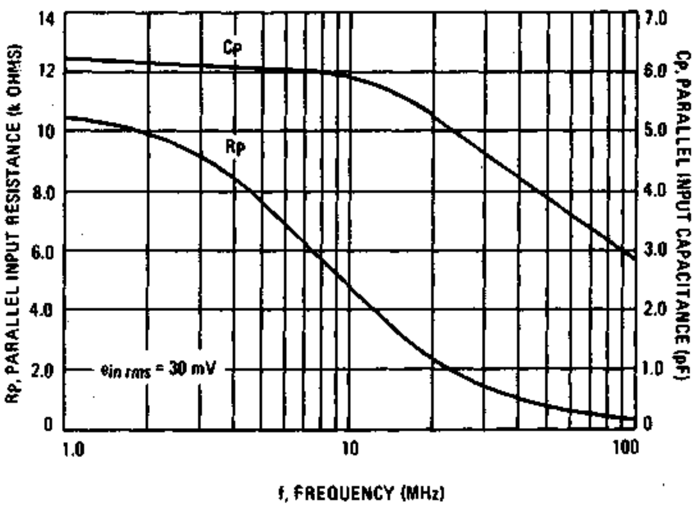

FIGURE 6 – OUTPUT IMPEDANCE versus FREQUENCY

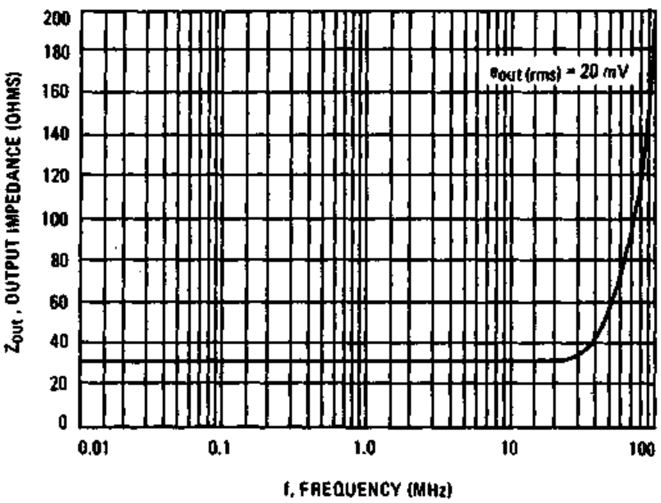

FIGURE 7 – CHANNEL SEPARATION versus FREQUENCY

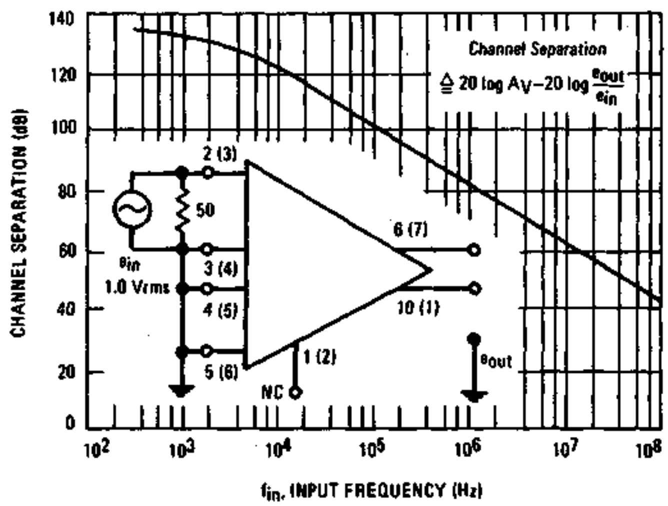

FIGURE 8 – GATE CHARACTERISTICS

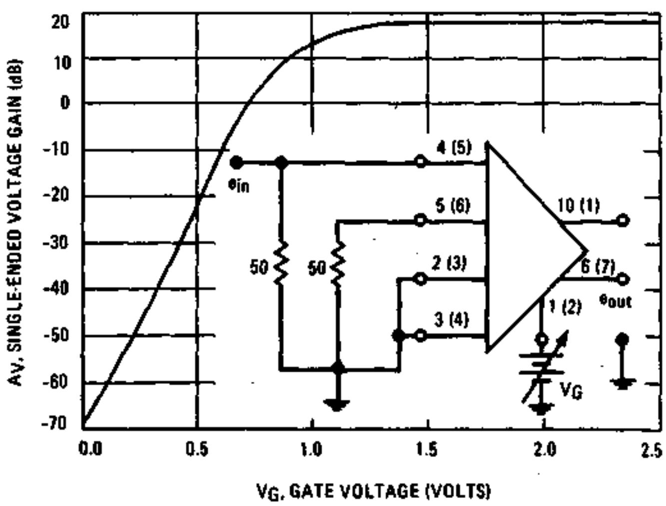

Number at end of terminal is pin number for G package. Number in parenthesis is pin number for F and L packages.

APPENDIX 3H

ECAP AC ANALYSES

FOR

PLAYBACK AMPLIFIER, LINE DRIVER

3H-1

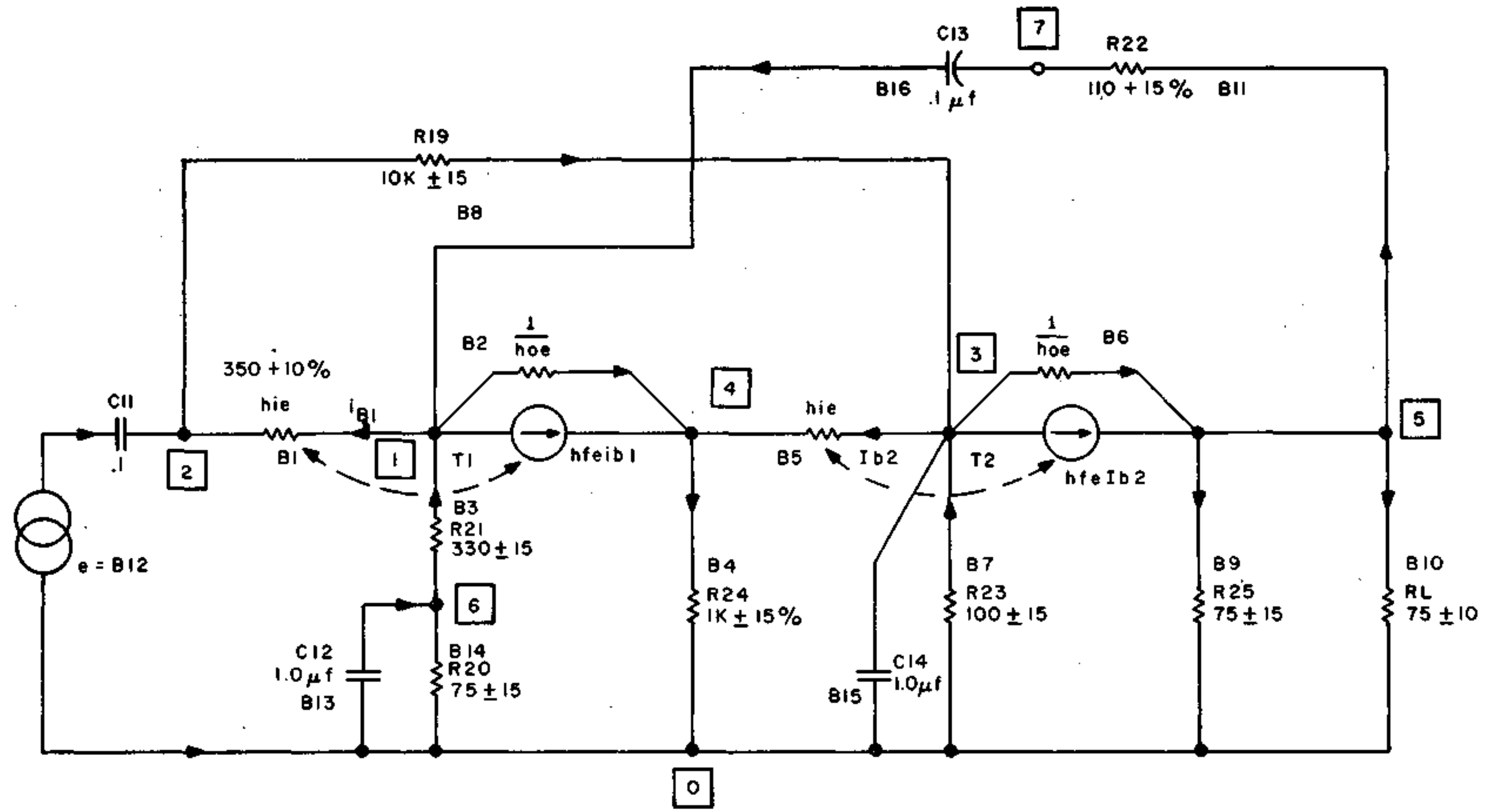

Figure 3H-1 AC EQUIVALENT ECAPS

```
        AC ANALYSIS
C       ERTS PB AMPL.LINE DRIVER (FREQ.RESP./MINIMUM GAIN)
C       JUNE 24,1969 N.HALY
R1      N(1,2)   ,R=350
R2      N(1,4)   ,R=1E4
R3      N(6,1)   ,R=330
R4      N(4,0)   ,R=1E3
R5      N(3,4)   ,R=350
R6      N(3,5)   ,R=1E4
R7      N(0,3)   ,R=100
R8      N(2,3)   ,R=1E4
R9      N(5,0)   ,R=75
R10     N(5,0)   ,R=75
R11     N(5,7)   ,R=110
R12     N(0,2)   ,C=.10E-6 ,E=0.1/0
R13     N(0,6)   ,C=1.0E-6
R14     N(0,6)   ,R=75
R15     N(0,3)   ,C=1.0E-6
R16     N(7,1)   ,C=.10E-6
T1      B(1,2)   ,BETA=50
T2      B(5,6)   ,BETA=50
        FREQUENCY=5E3
        PRINT, VOLTAGES
        EXECUTE

FREQ =  0.49999961E 04     .005


        NODES              NODE VOLTAGES

MAG     1-  4  0.10430437E 00  0.10559970E 00  0.15112066E 00  0.16504437E 00
PHA            0.39220514E 01  0.32634258E 01  0.10709835E 03  0.11850984E 03

MAG     5-  7  0.17945516E 00  0.89230649E-02  0.16886771E 00
PHA           -0.31002035E 01 -0.58564224E 02 -0.10613605E 02
```

FREQ = 0.99999922E 04 .01 MHZ

NODES NODE VOLTAGES

MAG	1- 4	0.10037875E 00	0.10121065E 00	0.61432216E-01	0.70949197E-01
PHA		0.14839516E 01	0.11643982E 01	0.93643906E 02	0.11570787E 03
MAG	5- 7	0.13739133E 00	0.46848767E-02	0.11865252E 00	
PHA		-0.72234507E 01	-0.73918427E 02	-0.13484637E 02	

FREQ = 0.19999980E 05 .02 MHZ

NODES NODE VOLTAGES

MAG	1- 4	0.99523544E-01	0.10028446E 00	0.28658148E-01	0.39488468E-01
PHA		0.71279830E 00	0.55774766E 00	0.91136566E 02	0.13017116E 03
MAG	5- 7	0.12575722E 00	0.23798600E-02	0.10424727E 00	
PHA		-0.44409513E 01	-0.81868011E 02	-0.81703129E 01	

FREQ = 0.39999969E 05 .04 MHZ

NODES NODE VOLTAGES

MAG	1- 4	0.99323690E-01	0.10006988E 00	0.14065672E-01	0.28681856E-01
PHA		0.35370004E 00	0.27685356E 00	0.90479401E 02	0.14881894E 03
MAG	5- 7	0.12280571E 00	0.11950361E-02	0.10051554E 00	
PHA		-0.23297119E 01	-0.85921036E 02	-0.42874565E 01	

FREQ = 0.79999938E 05 .08 MHZ

```
      NODES              NODE VOLTAGES

MAG    1-  4  0.99262476E-01  0.10000426E 00  0.34957237E-02  0.24556577E-01
PHA           0.88233173E-01  0.69076240E-01  0.90112808E 02  0.17134895E 03

MAG    5-  7  0.12187999E 00  0.29916735E-03  0.99337161E-01
PHA          -0.59109372E 00 -0.88979218E 02 -0.10882759E 01

FREQ =  0.31999969E 06


      NODES              NODE VOLTAGES

MAG    1-  4  0.99259436E-01  0.10000104E 00  0.17473439E-02  0.24334669E-01
PHA           0.44111922E-01  0.34534834E-01  0.90056198E 02  0.17564847E 03

MAG    5-  7  0.12183368E 00  0.14959408E-03  0.99278152E-01
PHA          -0.29576421E 00 -0.89489563E 02 -0.54455215E 00

FREQ =  0.63999950E 06


      NODES              NODE VOLTAGES

MAG    1-  4  0.99258661E-01  0.10000020E 00  0.87360688E-03  0.24278916E-01
PHA           0.22055358E-01  0.17266996E-01  0.90028061E 02  0.17782097E 03

MAG    5-  7  0.12182212E 00  0.74798285E-04  0.99263370E-01
PHA          -0.14790934E 00 -0.89744751E 02 -0.27232772E 00

FREQ =  0.12799990E 07
```

```
          NODES               NODE VOLTAGES

MAG       1-  4  0.99258423E-01  0.99999905E-01  0.21839672E-03  0.24261463E-01
PHA              0.55137984E-02  0.43167211E-02  0.90006973E 02  0.17945496E 03

MAG       5-  7  0.12181848E 00  0.18699677E-04  0.99258721E-01
PHA             -0.36979456E-01 -0.89936157E 02 -0.68086028E-01

FREQ =  0.51199950E 07

          NODES               NODE VOLTAGES

MAG       1-  4  0.99258423E-01  0.99999905E-01  0.10919824E-03  0.24260595E-01
PHA              0.27568976E-02  0.21583596E-02  0.90003479E 02  0.17972746E 03

MAG       5-  7  0.12181830E 00  0.93498438E-05  0.99258482E-01
PHA             -0.18489774E-01 -0.89968063E 02 -0.34043115E-01

FREQ =  0.10239992E 08

          NODES               NODE VOLTAGES

MAG       1-  4  0.99258423E-01  0.99999905E-01  0.54599077E-04  0.24260379E-01
PHA              0.13784482E-02  0.10791789E-02  0.90001724E 02  0.17986368E 03

MAG       5-  7  0.12181824E 00  0.46749201E-05  0.99258482E-01
PHA             -0.92449002E-02 -0.89984024E 02 -0.17021563E-01
```

```
C       MIN, GAIN
        MODIFY
R3      R=380
R4      R=850
R9      R=64.0
R10     R=67.5
R11     R=94
        FREQUENCY=80E3(2)640E3
        EXECUTE

FREQ =   0.79999938E 05


        NODES              NODE VOLTAGES


MAG     1-  4  0.99211216E-01  0.10001850E 00  0.73437579E-02  0.26664723E-01
PHA            0.18379307E 00  0.14035887E 00  0.90552078E 02  0.16340779E 03


MAG     5-  7  0.11411417E 00  0.51914528E-03  0.99491239E-01
PHA           -0.82384968E 00 -0.87996979E 02 -0.16025124E 01

FREQ =   0.15999988E 06


        NODES              NODE VOLTAGES


MAG     1-  4  0.99198639E-01  0.10000455E 00  0.36671546E-02  0.25748074E-01
PHA            0.91830552E-01  0.70126355E-01  0.90274384E 02  0.17150598E 03


MAG     5-  7  0.11393207E 00  0.25963783E-03  0.99268675E-01
PHA           -0.41385692E 00 -0.88998337E 02 -0.80428207E 00

FREQ =   0.31999969E 06


        NODES              NODE VOLTAGES


MAG     1-  4  0.99195540E-01  0.10000110E 00  0.18329865E-02  0.25514510E-01
PHA            0.45907073E-01  0.35056610E-01  0.90136963E 02  0.17572693E 03


MAG     5-  7  0.11388654E 00  0.12982720E-03  0.99219064E-01
PHA           -0.20717007E 00 -0.89499130E 02 -0.40251964E 00

FREQ =   0.63999950E 06


        NODES              NODE VOLTAGES
```

```
MAG     1-  4  0.99194765E-01  0.10000020E 00  0.91641885E-03  0.25455829E-01
PHA            0.22952501E-01  0.17527476E-01  0.90068436E 02  0.17786020E 03

MAG     5-  7  0.11387515E 00  0.64914595E-04  0.99199116E-01
PHA           -0.10361522E 00 -0.89749557E 02 -0.20130718E 00
```

APPENDIX 31

ECAP DC ANALYSIS
FOR
PLAYBACK AMPLIFIER, LINE DRIVER

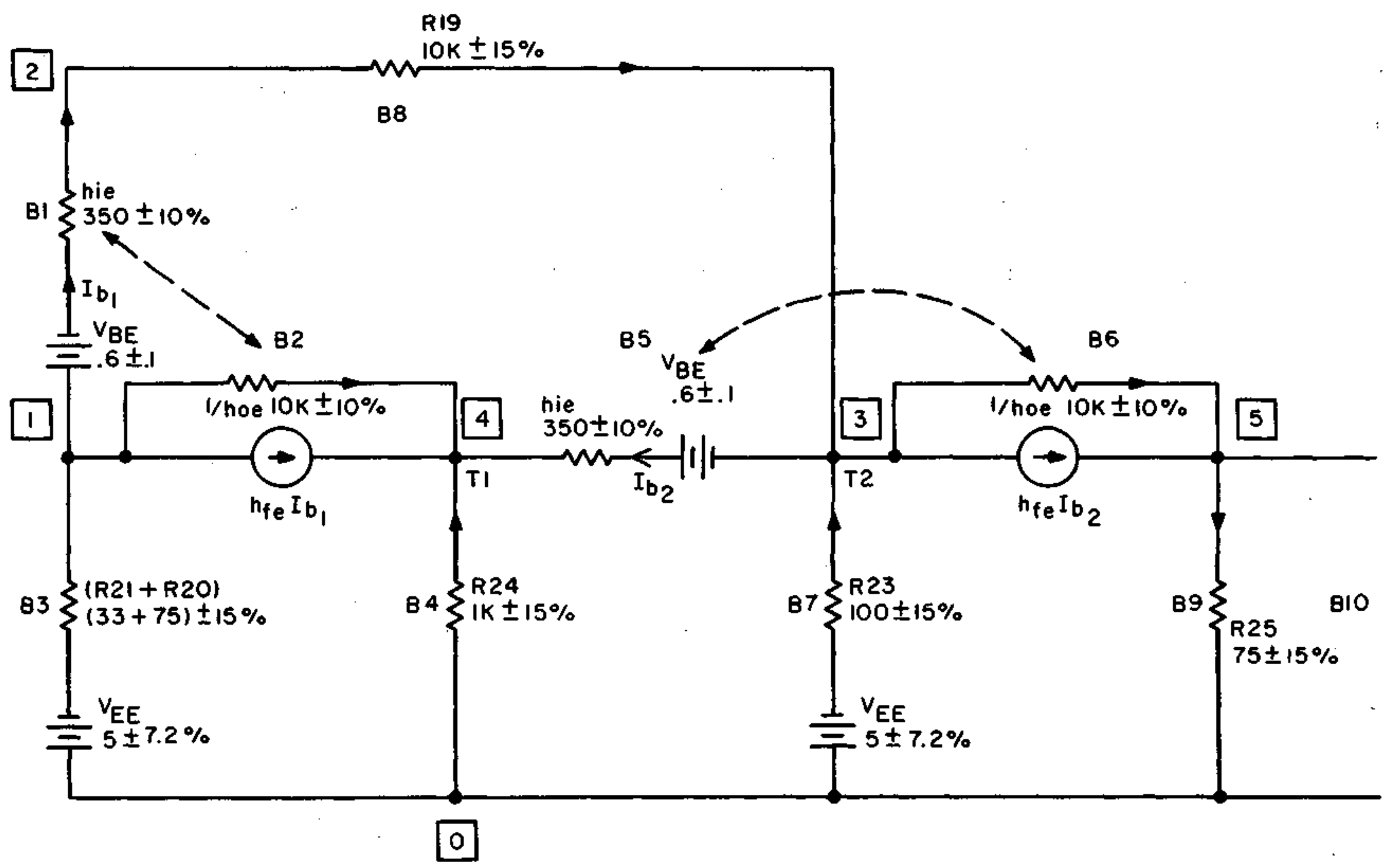

Figure 3I-1 ECAP D.C. ANALYSIS P-B LINE DRIVER

```
       DC ANALYSIS
C      ERTS PB AMPLIFIER LINE DRIVER
C      DATE JUNE 23,1969
B1     N(1,2)   ,R=350 (.10)     ,E=-.6(-.5,-.7)
B2     N(1,4)   ,R=1E4 (.10)
B3     N(0,1)   ,R=405 (.15)     ,E=5.0(.072)
B4     N(0,4)   ,R=1E3 (.15)
B5     N(4,3)   ,R=350 (.10)     ,E=-.6(-.5,-.7)
B6     N(3,5)   ,R=1E4 (.10)
B7     N(0,3)   ,R=100 (.15)     ,E=5.0(.072)
B8     N(2,3)   ,R=1E4 (.15)
B9     N(0,5)   ,R=75  (.15)
B10    N(0,5)   ,R=75  (.05)
T1     B(1,2)   ,BETA=125(50,200)
T2     B(5,6)   ,BETA=125(50,200)
       WORST CASE
       PRINT,WORST CASE
       EXECUTE


WORST CASE SOLUTIONS FOR NODE VOLTAGES

NODE      WCMIN               NOMINAL             WCMAX

 1  PARTIAL W.R.T.   R   2  HAS CHANGED SIGN AT MIN

 1        0.26942415E 01      0.35616121E 01      0.42529214D 01

 2  PARTIAL W.R.T.   R   2  HAS CHANGED SIGN AT MIN

 2        0.20866070E 01      0.29518099E 01      0.36326179D 01

 3  PARTIAL W.R.T.   R   6  HAS CHANGED SIGN AT MIN

 3        0.13918428E 01      0.26717243E 01      0.33832165D 01

 4  PARTIAL W.R.T.   R   6  HAS CHANGED SIGN AT MIN

 4        0.23258448E 01      0.33370152E 01      0.40027866D 01

 5  PARTIAL W.R.T.   R   6  HAS CHANGED SIGN AT MAX

 5        0.37008536E 00      0.88114828E 00      0.19640991D 01
```

```
      DC ANALYSIS
C     ERTS PB AMPLIFIER LINE DRIVER
C     DATE JUNE 23,1969
C     CHANGE R25 AND LOAD TO RN55D75R0F,AND
C     CHANGE R24 TO RC07GF751J TO MEET W/C DYNAMIC RANGE
B1    N(1,2)  ,R=350 (.10)     ,E=-.6(-.5,-.7)
B2    N(1,4)  ,R=1E4 (.10)
B3    N(0,1)  ,R=405 (.15)     ,E=5.0(.072)
B4    N(0,4)  ,     R=750 (.15 )
B5    N(4,3)  ,R=350 (.10)     ,E=-.6(-.5,-.7)
B6    N(3,5)  ,R=1E4 (.10)
B7    N(0,3)  ,R=100 (.15)     ,E=5.0(.072)
B8    N(2,3)  ,R=1E4 (.15)
B9    N(0,5)  ,     R=75  (.042)
B10   N(0,5)  ,     R=75  (.042)
T1    B(1,2)  ,BETA=125(50,200)
T2    B(5,6)  ,BETA=125(50,200)
      WORST CASE
      PRINT,WORST CASE
      EXECUTE
```

WORST CASE SOLUTIONS FOR NODE VOLTAGES

```
NODE      WCMIN                NOMINAL              WCMAX

 1  PARTIAL W.R.T.  R  2  HAS CHANGED SIGN AT MIN

 1  PARTIAL W.R.T.  R  6  HAS CHANGED SIGN AT MIN
 1       0.23704910E 01     0.32769308E 01     0.40333754D 01
 2  PARTIAL W.R.T.  R  2  HAS CHANGED SIGN AT MIN

 2  PARTIAL W.R.T.  R  6  HAS CHANGED SIGN AT MIN
 2       0.17617149E 01     0.26651888E 01     0.34088508D 01
 3  PARTIAL W.R.T.  R  6  HAS CHANGED SIGN AT MIN
 3       0.10345001E 01     0.23296938E 01     0.30667538D 01
 4  PARTIAL W.R.T.  R  6  HAS CHANGED SIGN AT MIN
 4       0.20039473E 01     0.30047874E 01     0.36912239D 01
 5  PARTIAL W.R.T.  R  6  HAS CHANGED SIGN AT MAX
 5       0.49466658E 00     0.10106678E 01     0.20324422D 01
```

```
       DC ANALYSIS
C      ERTS P.B. AMPL.L.D., COMPONENT DISSIPATION
C      N.MALY,JULY 9, 1969, MODIFIED CKT
R1     N(1,2)    ,     R=550      , E=+6
R2     N(1,4)    ,     R=1E4
R3     N(0,1)    ,     R=405      , E=5.0
R4     N(0,4)    ,     R=750
R5     N(4,3)    ,     R=550      , E=+6
R6     N(3,5)    ,     R=1E4
R7     N(0,3)    ,     R=100      , E=5.0
R8     N(2,3)    ,     R=1E4
R9     N(0,5)    ,     R=75
R10    N(0,5)    ,     R=75
T1     B(1,2)    ,     BETA=125
T2     B(5,6)    ,     BETA=125
       PRINT, CV, BV, BA, BP
       EXECUTE
```

BRANCH VOLTAGES

BRANCHES	VOLTAGES			
1- 4	-0.58851718D 00	0.30007808D 00	-0.39136794D 01	-0.30136013D 01
5- 8	-0.56051692D 00	0.30339524D 01	-0.35741182D 01	0.32807833D 00
9- 10	-0.54016581D 00	-0.54016581D 00		

ELEMENT VOLTAGES

BRANCHES	VOLTAGES			
1- 4	0.11482786D-01	0.30007808D 00	0.16863197D 01	-0.30136013D 01
5- 8	0.39483040D-01	0.30339524D 01	0.14258808D 01	0.32807833D 00
9- 10	-0.54016581D 00	-0.54016581D 00		

ELEMENT POWER LOSSES

BRANCHES	POWER LOSSES			
1- 4	0.37672680D-06	0.12396232D-02	0.70214170D-02	0.12109057D-01
5- 8	0.44540297D-05	0.43702503D-01	0.20391357D-01	0.10763538D-04
9- 10	0.38903876D-02	0.38903876D-02		

BRANCH CURRENTS

BRANCHES	CURRENTS			
1- 4	0.32807961D-04	0.41310023D-02	0.41697521D-02	-0.40181350D-02
5- 8	0.11280868D-03	0.14404479D-01	0.14258805D-01	0.32807830D-06
9- 10	-0.72022100D-02	-0.72022100D-02		

APPENDIX 3J

COMPONENT DERATING

FOR

MOTOR/SOLENOID SWITCH

APPENDIX A COMPONENT SPECIFICATIONS

1. Passive Element Derating

a. Resistors

Type	Tolerance		Temp. Charac.			Power Derating	Transient Overload			Failure Rate
	Initial	Initial Plus 10,000 hr Degrad.	R Range	0°C	60°C		Power Rating	Overload X Rated P.	R Change	Per 10^6 hrs.
RCR07-JP	±5%	±15%	R < 1K	±2%	±2.2%	50%		6.2	±2.5%	1
			1.1K < R ≤ 10K	±3%	±2.6%					
RWR- -P	±1%	± 1.8%		±.05%	± .07%	40%				1
RNR- -P	±1%	± 1.9%		±.05%	± .07%	50%	55,57 60	5	± .25%	1
							63 65	4	± .25%	
							70	2.25	± .25%	

b. Capacitors

Type	Tolerance		DC Leakage Current			Voltage Derating	Temp. Charac.		Failure Rate	Radiation
	Initial	Initial Plus 10,000 hr. Degrad.	Cap. in μf	25°C	60°C		0°C	60°	Per 10^6 hrs	Roentgen Per hr.
CSR- -KP	±10%	±30%	8.2	5 μA	31 μA	For 50V Rating use 40 V	-3%	+4.6%	1	10
			18	9	47					
			22	11	58					

2. Transistor Parameter Derating

Parameter	Derating Factor
I_{CBO}	Double every 14°C rise in junction temperature for Germanium. Double every 10°C rise in junction temperature for Silicon. Derate 100% for aging.
V_{BE} (sat)	Decrease 2.5 mV/°C rise in junction temperature. Derate 10% for aging (increase maximum). Derate typical ±20%.
V_{CE} (sat)	Increase 0.2-0.5 mV/°C rise in junction temperature. Derate 10% for aging (increase maximum). Derate typical ±50%.
h_{FE}	Derate 50% of +25°C value for -55°C. Derate 25% for aging (power rating <1 watt). Derate 30% for aging (power rating ≥1 watt).

3. Coil Resistance

The change in coil resistance is given by:

$$R = R_o (1 + \alpha T)$$

where:

R = Resistance at temperature T°C

R_o = Resistance at 0°C

α = Wire temperature coefficient (for copper α = .00393/°C)

COMPONENT SPECIFICATIONS

4. Motor/Solenoid Switch

Design Values							Recommended Values					
Part No.	Type	Nominal Value	Parameter	Limits 0°C	Limits 25°C	Limits 60°C	Type	Nominal Value	Parameter	Limits 0°C	Limits 25°C	Limits 60°C
R1	RCR07	100	max	117.3	115	117.8			max			
			min	82.7	85	82.5			min			
R2	RCR07	3.3K	max	3871	3795	3876	RNR-P	2870	max	2927	2925	2927
			min	2749	2805	2743			min	2913	2815	2913
R3	RCR07	330	max	387	380	388			max			
			min	275	281	274			min			
R4	RCR07	220	max	258	253	274			max			
			min	183	187	183			min			
R5	RCR07	1K	max	1173	1150	1175			max			
			min	827	850	825			min			
R6	RCR20	22	max	25.8	25.3	25.8	RWR-P	10	max	10.2	10.2	10.2
			min	19.1	18.7	19.1			min	9.8	9.8	9.8
R7	RCR07	10K	max	11,730	11,500	11,750			max			
			min	8,270	8,500	8,250			min			
			max						max			
			min						min			
C_1	CSR13 KP	22 µf	max	27.7	28.6	29.9			max			
			min	15	15.4	16.1			min			
C_2	CSR13 KP	18 µf	max	22.7	23.4	24.5	CSR13	8.2 µf	max	10.3	10.6	11
			min	12.2	12.6	13.2			min	5.4	5.7	5.9
			max						max			
			min						min			
R7	M5151/40		max						max			
			min						min			
	RL1	1560	max	1567	1716	1936			max			
			min	1283	1404	1584			min			
	L1		max		1.1H				max			
			min		.975H				min			
	Drop-out Voltage		max	3.37	3.5	4.9			max			
			min	1.07	1.2	2.6			min			
	Operate Time		max		2 ms				max			
			min						min			
	Release Time		max		1.5 ms				max			
			min						min			
	Bounce		max		1.5 ms				max			
			min						min			
	Contact Resistance		max		.2 r				max			
			min						min			
Solenoid	IMC 08-818-20		max						max			
			min						min			
	RL2	4.8	max	4.82	5.28	5.96			max			
			min	3.94	4.32	4.88			min			
	L2		max		3 mH				max			
			min		2.4 mH				min			
	RL3	120	max	121	132	162			max			
			min	99	108	122			min			
	L3		max		35 mH				max			
			min		18 mH				min			
Solenoid	IMC		max						max			
			min						min			
	Holding Force	6 lbs at 24 V	max	7.3	6.6	5.85			max			
			min	6	5.4	4.8			min			
	Holding Force	6.25 lbs at 25 V	max	7.6	6.87	6.1			max			
			min	6.2	5.63	5			min			
			max						max			
			min						min			
K1-K4 K6	8150555-1 (J-J2A)		max						max			
			min						min			
	Pick-up Voltage		max			18			max			
			min						min			
	Drop-out Voltage		max		7				max			
			min						min			
	Operating Voltage		max		29				max			
			min						min			

COMPONENT SPECIFICATIONS (Cont)

Design Values							Recommended Values					
Part No.	Type	Nominal Value	Parameter	Limits 0°C	25°C	60°C	Type	Nominal Value	Parameter	Limits 0°C	25°C	60°C
	RL	320	max	328	352	407			max			
			min	263	288	325			min			
	Operate Time	at 28 V	max		10 ms				max			
			min						min			
	Release Time	at 28 V	max		10 ms				max			
			min						min			
	Bounce	at 28 V	max		1 ms				max			
			min						min			
			max						max			
			min						min			
			max						max			
			min						min			
Power Supply	V_{CC}	24.5	max		25				max			
			min		24				min			
Control Signal	V1	24.5	max		25				max			
			min		24				min			
			max						max			
			min						min			
			max						max			
			min						min			
			max						max			
			min						min			
			max						max			
			min						min			
			max						max			
			min						min			
			max						max			
			min						min			
			max						max			
			min						min			
			max						max			
			min						min			
Q1	2N2907A	P_T	max			210 mw			max			
			min						min			
Ic = 25 mA	V_{CE} (sat)	.15	max	.23	.24	.25			max			
			min		.08				min			
	V_{BE} (sat)	.6	max	.84	.73	.70			max			
			min		.53				min			
	I_{CBO}		max		20 µA	.32 µA			max			
			min						min			
	h_{FE}		max		375				max			
			min	60	71	75			min			
	α_N		max		1				max			
			min	.983	.985	.986			min			
	θ_{J-A}	438°C/W	max						max			
			min						min			
Q2	2N2219A	P_T	max			.55 W	2N2219A		max			
			min						min			
Ic = 96 mA	V_{CE} (sat)	.25	max	.39	.4	.41	I_C = 185mA		max			
			min		.13				min			
	V_{BE} (sat)	.8 V	max	1.06	1.0	.91			max			
			min		.7				min			
	I_{CBO}		max		20 µA	.32 µA			max			
			min						min			
	h_{FE}		max		375				max		375	
			min	56	72	72			min	53	60	60
	α_N		max		1				max			
			min	.983	.985	.986			min			
	θ_{J-A}	188°C/W	max						max			
			min						min			
Q3	2N4399	P_T	max			4 W	Selected 2N4399		max			
			min						min			
Ic = 5A	V_{CE}(sat)	.35	max	.55	.56	.57			max			
			min		.20				min			
	V_{BE}(sat)	.9	max	1.26	1.2	1.1			max			
			min		.3				min			
	I_{CBO}		max	.4mA	2mA	32mA			max			
			min						min			
	h_{FE}	20	max		60				max	53	60	62
			min	11	14	16			min	35	40	41
	θ_{J-A}	34.875°C/W	max					α_N	max		.985	
			min						min		.98	
CR16 CR17	1N645	If surge	max			8A			max			
			min						min			
CR15	1N3191	If surge	max		25A				max			
			min						min			
CR14	1N4970	i Rev. Surge	max		3A				max			
			min						min			
CR14	1N4970	Break-down	max	33.9	34.6	35.8			max			
			min	30.7	31.4	32.5			min			

APPENDIX 3K

WORST CASE CALCULATIONS

WORST CASE CALCULATIONS

1.0 RELAY TIMER

Neglecting the inductive time constant, L/R = .64 ms, which is very small compared to the RC time constant, the relay timer equivalent circuit may be represented by Figure A-1.

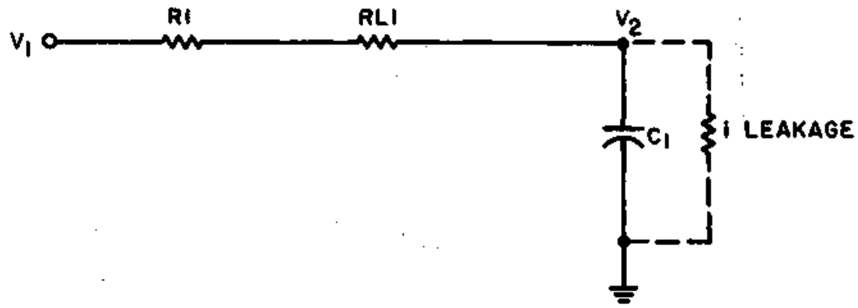

Figure A-1 RELAY TIMER EQUIVALENT CIRCUIT

Also, neglecting the capacitor leakage current, which is very small compared to the charging current during the charging of C1, the voltage across C1 is given by:

$$V_2 = V_1 \left(1 - e^{-t/RC_1}\right) \tag{1}$$

where,

$$R = R_1 + R_{L1} \tag{2}$$

Also, the relay coil voltage is:

$$V_{L1} = \frac{R_{L1}}{R_1 + R_{L1}} (V_1 - V_2) \tag{3}$$

Solving Equation 1:

$$\frac{V_1}{V_1 - V_2} = e^{t/RC_1}$$

and

$$\frac{t}{RC_1} = \ln \frac{V_1}{V_1 - V_2} \tag{4}$$

Solving for V2, from Equation 3,

$$V_2 = V_1 - V_L \left(\frac{R_1 + R_{L1}}{R_{L1}} \right) \tag{5}$$

Substituting Equations 2 and 5 into Equation 4:

$$t = (R_1 + R_{L1})\, C_1\, L_n\, \frac{V_1\, R_{L1}}{V_{L1}\, (R_1 + R_{L1})} \tag{6}$$

Since the drop-out voltage, VL1, exhibits the greatest tolerance, the minimum and maximum timer ON times are dependent on VL1. Minimum TON occurs for V_{L1} maximum and maximum TON occurs for VL1 minimum. Or, for minimum TON, Equation 6 becomes:

$$\underline{T} = (\underline{R}_1 + \underline{R}_{L1})\, \underline{C}_1\ \mathrm{Ln}\, \frac{\underline{V}_1\ \underline{R}_{L1}}{\overline{V}_{L1}\ (\underline{R}_1 + \underline{R}_L)} \tag{7}$$

Substituting worst case values into Equation 7, at 60° C:

$$\underline{T} = (83 + 1584)\ 16.1 \mathrm{x} 10^{-6}\ \mathrm{Ln}\, \frac{24\ (1584)}{4.9\ (83 + 1584)} = 41.5\ \mathrm{ms}$$

For maximum TON, Equation 6 becomes:

$$\overline{T} = (\overline{R}_1 + \overline{R}_{L1})\, \overline{C}_1\ \mathrm{Ln}\, \frac{\overline{V}_1\ \overline{R}_{L1}}{\overline{\overline{V}}_{L1}\ (\overline{R}_1 + \overline{R}_{L1})} \tag{8}$$

or, at 0° C:

$$\overline{T} = (117 + 1567)\ 27.7 \times 10^{-6}\ \mathrm{Ln}\, \frac{25(1567)}{1.07\ (117 + 1567)} = 141\ \mathrm{ms}$$

2.0 SOLENOID DRIVER DRIVE REQUIREMENTS

a. Turn-On Time

In order to determine the transistor regions of operation, the rise time to saturation must be determined. The rise time of Q1 is given by:

$$T = R_2\, C_2\, \mathrm{Ln}\, \frac{V_1}{V_1 - V_{B1}} \tag{9}$$

where,

V_1 = -24.5 ± 2% (shoe control signal)

For the minimum turn-on time, Equation 9 becomes:

$$\underline{T} = \underline{R_2}\, \underline{C_2}\, \mathrm{Ln}\, \frac{\underline{V_1}}{\underline{V_1} - \underline{V_{B1}}} \tag{10}$$

To calculate VB1, from Figure 3-20

$$V_{B1} = V_{E1} + V_{BE1} \tag{11}$$

Since,

$$V_{E1} = I_{E1}\, R_5 + V_{BE1} \tag{12}$$

Then,

$$V_{B1} = I_{E1}\, R_5 + V_{BE1} \tag{13}$$

Also, from Figure 3-20

$$V_{cc} = I_{E1}\, R_5 + V_{CE1} + (I_{c1} - I_{B2})\, R_4 \tag{14}$$

Since,

$$I_c = \alpha_n\, I_E + I_{CB0} \tag{15}$$

Substituting Equation 14 into Equation 13 and solving for IE1:

$$I_{E1} = \frac{V_{cc} - (I_{cB01} - I_{B2})\, R_4 - V_{cE1}}{R_5 + \alpha_N R_4} \tag{16}$$

Maximum VB1 will occur for maximum IE1, therefore:

$$\overline{I}_{E1} = \frac{V_{cc} - (I_{cB01} - I_{B2})\, R_4 - V_{CE1}}{\overline{R}_5 + \alpha_N R_4} \tag{17}$$

Neglecting ICB0, and letting IB2 = 3 mA, then at 60° C:

$$\overline{I}_{E1} = \frac{25 + 3 \times 10^{-3}\ (183) - .1}{1175 + .985\ (183)} = 18.1\ \text{mA}$$

From Equation 13,

$$\underline{V}_{B1} = \underline{I}_{E1}\, \underline{R}_5 + \underline{V}_{BE1} \tag{18}$$

And from Equation 16, minimum IE1 is:

$$\underline{I}_{E1} = \frac{\underline{V}_{cc} - (I_{cB01} - I_{B2})\, \overline{R}_4 - \overline{V}_{CE1}}{\underline{R}_5 + \alpha_N R_4} \tag{19}$$

Neglecting ICB0, and letting IB2 = 2 mA, then solving Equation 19, at 0° C:

$$\underline{I}_{E1} = \frac{24 - 2 \times 10^{-3}\ (258) - .23}{827 + .985\ (258)} = 21.5\ \text{mA}$$

Substituting into Equation 18, at 0° C:

$$\underline{V}_{B1} = 21.5\ \text{mA}\ (827) + .53 = 18.23\ \text{V}$$

Now, let $\overline{V1}$ = 24V, and substituting worst case values into Equation 10, the minimum turn-on time is:

$$\underline{T} = 2913\ (5.9\ \mu t)\ \text{Ln}\ \frac{24}{24 - 18.23} = 24.5\ \text{ms}$$

When $\overline{V}1 = 25V$, $\underline{V}B1 = 22V$, then minimum turn-on time is:

$$\underline{T} = 17.2 \text{ ms Ln } \frac{25}{25-22} = 36.2 \text{ ms}$$

Evidently, turn-on time is minimum for V1 ~ 24V.

Now, for maximum turn-on time, Equation 9 is:

$$\overline{T} = \overline{R}_2 \, \overline{C}_2 \text{ Ln } \frac{\overline{V}_1}{\overline{V}_1 - \overline{V}_{B1}} \tag{20}$$

And, from Equation 13:

$$\overline{V}_{B1} = \overline{I}_{E1} \, \overline{R}_5 + \overline{V}_{BE1} \tag{21}$$

Substituting worst case values into Equation 21, at 60° C:

$$\overline{V}_{B1} = 18.1 \text{ mA } (1175) + .70 = 21.9$$

Using the above results, and substituting into Equation 20, the maximum turn-on is:

$$\overline{T} = 2927 \; (10.3 \; \mu f) \text{ Ln } \frac{25}{25 - 21.9} = 63 \text{ ms}$$

b. Minimum hFE3 required to Drive Q3

Referring to Figure 3-20, Q3 emitter current is given by:

$$V_{cc} = I_{E2} R_6 + V_{BE3} + (I_{E3} + I_{R7}) R_{L2} \tag{22}$$

and,

$$I_{c2} = I_{B3} + \frac{V_{BE3}}{R_7} \tag{23}$$

Also,

$$I_{C2} = \alpha_N I_{E2} + I_{cB02} \tag{24}$$

Or, solving Equation 24 for IE2 and substituting into Equation 23,

$$I_{E2} = \frac{I_{c2} - I_{cB02}}{\alpha_{N2}} = \frac{I_{B3} + \dfrac{V_{BE3}}{R_7} - I_{CB02}}{\alpha_{N2}} \tag{25}$$

since,

$$I_{B3} = \frac{I_{c3}}{h_{FE3}} - \frac{I_{cb03}}{\alpha_{N3}} \tag{26}$$

Then substituting Equations 25 and 26 into Equation 22:

$$V_{cc} = \frac{I_{c3}\, R_6}{h_{FE3}\,\alpha_{N2}} - \left(\frac{I_{c03}}{\alpha_{N3}\,\alpha_{N2}} - \frac{V_{BE3}}{R_7\,\alpha_{N2}} + \frac{I_{cB02}}{\alpha_{N2}}\right) R_6 + V_{cE2} + V_{cE2} + V_{BE3} +$$

$$(I_{E3} - I_{R7})\, R_{L2} \tag{27}$$

Solving Equation 27 for hFE3,

$$hFE3 = \frac{(\alpha_{N3}\, I_{E3} + I_{cB03})\, R_6}{\alpha_{N2}\left[V_{cc} + \left(\dfrac{I_{cb03}}{\alpha_{N3}\ N2} - \dfrac{V_{BE3}}{R_7\,\alpha_{N2}} + \dfrac{I_{cB02}}{\alpha_{N2}}\right) R_6 - V_{CE2} - V_{BE3} - \left(I_{E3} - I_{R7}\right) R_{L2}\right]} \tag{28}$$

Since hFE3 is minimum at low temperature, calculate the maximum hFE3 required at 0° C, which is equivalent to specifying hFE3 for Q3. From the specifications, the solenoid voltage requirement is 20.7V minimum. Therefore, since $\overline{I}E3$ is given by:

$$\overline{I}_{E3} = \frac{\overline{V}_{E3}}{\underline{R_{L2}}} - \frac{\overline{V}_{BE3}}{\underline{R_7}} \tag{29}$$

where,

$$\overline{V}_{E3} = \overline{I}_{RL2}\ \overline{R}_{L2} \tag{30}$$

Then at 0° C, with VE3 = 20.7, from Equation 29:

$$\overline{I}_{E3} = \frac{20.7}{3.94} - \frac{1.26}{8270} = 5.3A$$

Now, neglecting ICB0 at 0° C and IR7, $\overline{hFE3}$ required is:

$$\overline{h}_{FE3} = \frac{N3\ I_{E3}\ R_6}{N2\left[V_{cc} - \frac{\overline{V}_{BE3}\ R_6}{R_7\ \ N2} - \overline{V}_{CE2} - \overline{V}_{BE3} - \overline{I}_{E3}\ R_{\underline{L2}}\right]} \tag{31}$$

Assuming N3 = .97, and substituting worst case values into Equation 31:

$$\overline{h}_{FE3} = \frac{.97\ (5.3)\ (10.2)}{.98\ (24 - \frac{1.26(10.2)}{.98\ (8270)} - .4 - 1.26 - 5.3\ (3.94)} = 33$$

This value is within the limits of Q3 (selected 2N4399), which exhibits an hFE of 35 at 0° C.

Similarly, determine the maximum drive requirements for Q1, Q2. From Figure 1, for Q2, the emitter current is given by:

$$V_{cc} = I_{E2}\ R_6 + V_{cE2} + I_{R7}\ R_7 + I_{RL2}\ R_{L2} \tag{32}$$

Since,

$$V_{BE3} = I_{R7}\ R_7 \tag{33}$$

Then combining Equations 32 and 33, and solving for $\underline{IE2}$. For Vcc and $I_{RL2} \approx I_{E3}$, the minimum possible current from Q2 at 0° C is:

$$\underline{I_{E2}} = \frac{\underline{V_{cc}} - \overline{V}_{cE2} - \overline{V}_{BE3} - \overline{I}_{E3}\ R_{\underline{L2}}}{\overline{R_6}} \tag{34}$$

Substituting worst case parameters into Equation 34:

$$\underline{I}_{E2} = \frac{24 - .39 - 1.26 - 20.7}{10.2} = \frac{1.65}{10.2} = 162 \text{ mA}$$

letting,

$$I_{c2} = \alpha_{N2} I_{E2}$$

Then, IC2 = 160 mA, which is equal to the maximum base current, IB3, required by Q3. Or, using the above results,

$$\bar{I}_{B3} = \frac{\bar{I}_{E3}}{\underline{h}_{FE3}} = \frac{5.3}{33} = 160 \text{ mA}$$

Now, for Q2, minimum hFE2 is given by:

$$\underline{h}_{FE2} = \frac{\bar{I}_{E2}}{I_{B2}} \tag{36}$$

Since $\underline{hFE2}$ is given as 53 at 0° C, then from Equation 36:

$$\bar{I}_{B2} \approx \frac{160}{53} = 3 \text{ mA}$$

To determine Q1 drive capabilities, from Figure 1, the Q1 current is given by:

$$V_{cc} = I_{E1} R_5 + V_{cE1} + (I_{c1} - I_{B2}) R4 \tag{37}$$

since,

$$I_{c1} = \alpha_{N1} I_{E1} + I_{cB01} \tag{38}$$

also,

$$I_{c1} = I_{R4} + I_{B2} \tag{39}$$

Then substituting Equation 38 and 39 into Equation 37, and solving for IE1 available at minimum Vcc,

$$I_{\underline{E1}} = \frac{V_{\underline{cc}} - (I_{cb01} - \overline{I}_{B2})\ \overline{R}_4 - \overline{V}_{cE1}}{\overline{R}_5 + \varphi_{N1}\ \overline{R}_4} \tag{40}$$

Now, neglecting Icbo at 0° C, and letting $\overline{IB2}$ = 3 mA, then substituting worst case values into the above equation.

$$I_{\underline{E1}} = \frac{24 + 3\text{mA}\ (258) - .23}{1173 + .98\ (258)} = 17.2\ \text{mA}$$

Using an alternate approach to determine hFE2, $\overline{IB2}$ available must be calculated for the specified circuit conditions.

Since,

$$I_{B2} = I_{c1} - I_{R4} \tag{41}$$

And, IB2 of interest is $\overline{IB2}$ deliverable under IC1 conditions.

Then from Figure 3-20,

$$V_{c1} = V_{B2} \tag{42}$$

where

$$V_{\underline{c1}} = V_{cc} - \overline{I}_{E2}\ \overline{R}_6 - \overline{V}_{BE2} \tag{43}$$

Evaluating the above equation:

$$V_{\underline{c1}} = 24 - 1.65 - 1.06 = 21.3$$

And since,

$$\overline{I}_{R4} = \frac{V_{cc} - V_{\underline{c}1}}{\underline{R}_4} \tag{44}$$

Using the above values, Equation 44 becomes:

$$\overline{I}_{R4} = \frac{24 - 21.3}{183} = 14.8 \text{ mA}$$

and from Equation 41:

$$\underline{I_{c1}} \approx 14.8 + 3 = 17.8 \text{ mA}$$

The above value is slightly larger than that obtained from Equation 40. Therefore, use the former approach.

To evaluate Q1 drive capabilities, since $\underline{hFE1} = 60$ at 0° C, then, using Equation 36,

$$\overline{I}_{B1} = \frac{17.2}{60} = .29 \text{ mA}$$

From Figure 3-20, the Q1 base current is given by:

$$V_1 = I_{R2} R_2 + V_{BE1} + V_{E1} \tag{45}$$

where,

$$I_{R2} = I_{c2} + I_{B1} \tag{46}$$

and,

$$I_{c2} = -\frac{V_1}{R_2 e} t/_{R_2C_2} \tag{47}$$

Solving Equation 45 for minimum IR2 available:

$$\underline{I_{R2}} = \frac{\underline{V_1} - \overline{V}_{BE1} - \overline{V}_{E1}}{\overline{R}_2} \tag{48}$$

where,

$$V_{E1} = I_{E1} R_5 \tag{49}$$

and for IE1 = 17.2 mA:

$$V_{E1} = 17.2\ (1173) = 20.3V$$

Substituting into Equation 48,

$$I_{R2} = \frac{24 - .84 - 20.3}{2927} = \frac{2.86}{2927} = .97\ \text{mA}$$

Since the above value is greater than the required IB1, it is sufficient to drive Q1 and subsequently Q2.

The effects of maximum Vcc may be evaluated by repeating the above analysis.

From Equation 28, hFE3 required is:

$$\bar{h}_{FE3} = \frac{\alpha_{N3}\ \bar{I}_{E3}\ \bar{R}_6}{\alpha_{N2}\left[\bar{V}_{cc} - \frac{\bar{V}_{BE3}\ \bar{R}_6}{\underline{R}_7\ \alpha_{N2}} - \bar{V}_{CE2} - \bar{V}_{BE3} - \bar{I}_{E3}\ R_{L2}\right]} \tag{50}$$

Substituting worst case values into Equation 50:

$$\bar{h}_{FE3} = \frac{.97\ (5.3)\ (10.2)}{.98\ (25 - .4 - 1.26 - 5.3\ (3.94)} = \frac{52.5}{2.6} = 20$$

Since hFE3 available to 0° C is 35, the above condition is satisfied.

For the required pull-in, the current drive required by Q3 at maximum Vcc is the same as for minimum Vcc. Then, the Q2 voltage drop will be shifted. Or,

$$\bar{V}_{cE2} = \bar{V}_{cE2}\ (\text{sat}) + 1 + 1.39$$

Then, from Equation 34,

$$I_{E2} = 162\ \text{mA}$$

And for Q1, from Equation 40,

$$\underline{I_{E1}} = \frac{\bar{V}_{cc} - (I_{c01} - \bar{I}_{B2})\ \bar{R}_4 - \bar{V}_{CE1}}{\bar{R}_5 + \alpha_{N1}\ \bar{R}_4} \tag{51}$$

And for Vcc = 25,

$$I_{\underline{E1}} = \frac{25.54}{1427} = 17.8 \text{ mA}$$

Maximum IB1 required, however, occurs at maximum IE1 possible, or from Equation 40,

$$\bar{I}_{E1} = \frac{\bar{V}_{cc} - (I_{c01} - \bar{I}_{B2}) R_{\underline{4}} - V_{\underline{CE1}}}{R_{\underline{5}} + \alpha_{N1} R_{\underline{4}}} \qquad (52)$$

Substituting worst case values into Equation 52,

$$\bar{I}_{E1} = \frac{25 - 3 \text{ mA } (191) - .08}{827 + .98\ (191)} = \frac{24.42}{1015} = 23.8 \text{ mA}$$

and from,

$$\bar{I}_{B1} \approx \frac{\bar{I}_{E1}}{h_{\underline{FE}1}} \qquad (53)$$

or,

$$\bar{I}_{B1} = \frac{23.8}{60} = .4 \text{ mA}$$

Now, from Equation 49,

$$\bar{V}_{E1} = \bar{I}_{E1} R_{\underline{5}} = 23.8\ (827) = 19.7 \qquad (54)$$

And from Equation 48,

$$I_{\underline{R2}} = \frac{\bar{V}_1 - \bar{V}_{BE1} - \bar{V}_{E1}}{\bar{R}_2} \qquad (55)$$

Substituting the parameters into Equation 55,

$$I_{\underline{R2}} = \frac{25 - .84 - 19.7}{2927} = \frac{4.46}{2927} = 1.53 \text{ mA}$$

This value is sufficient to drive Q1 at IB1 = .4 mA.

c. Solenoid Pull-In

The solenoid pull-in force is directly proportional to the coil current, IL2. Neglecting transistor reverse saturation current, and R7, then:

$$I_{L2} = I_{E3} \tag{56}$$

or,

$$V_{cc} = I_{E2} R_6 + \overline{V}_{cE2} + \overline{V}_{BE3} + I_{E3} R_{\underline{L2}} \tag{57}$$

since,

$$I_{E2} \approx \frac{I_{E3}}{h_{FE3}} \tag{58}$$

then,

$$I_{E3} = \frac{V_{cc} - V_{BE3} - V_{cE2}}{\frac{R_6}{h_{FE3}} + R_{L2}} \tag{59}$$

Minimum pull-in at 60° C is given by:

$$I_{\underline{E3}} = \frac{V_{\underline{cc}} - \overline{V}_{BE3} - \overline{V}_{cE2}}{\frac{\overline{R}_6}{h_{\underline{FE3}}} + \overline{R}_{L2}} \tag{60}$$

Now, for hFE3 = 41 at 60° C:

$$I_{\underline{E3}} \approx \frac{24 - 1.1 - .57}{\frac{10.2}{42} + 5.96} = \frac{22.33}{6.20} = 3.6A$$

And, since:

$$V_{\underline{E3}} = I_{\underline{E3}} \overline{R}_{L2} \tag{61}$$

E

then for the above values,

$$V_{\underline{E3}} = 3.6\ (5.96) = 21.4V$$

Translated to manufacturer's specifications,

$$V_{Pull-in} = \frac{21.4}{1.16} = 18.5V \text{ at } 25^\circ C$$

which is equivalent to 4.75 lbs. force at 60° C.

Similarly, at 0° C, assuming sufficient hFE3, using Equation 60:

$$I_{\underline{E3}} = \frac{24 - 1.26 - .55}{\frac{10.2}{35} + 4.82} = \frac{2.2}{5.11} = 4.3A$$

from Equation 61:

$$V_{\underline{E3}} = 4.3\ (4.82) = 20.7V$$

and,

$$V_{Pull-in} = \frac{20.7}{.9} = 23V \text{ at } 25^\circ C$$

which is equivalent to 6.5 lbs. force at 0° C.

Maximum pull-in voltage is of little interest, except to determine solenoid stress, which is a maximum of 30V ± 10% at 25° C, or, .9 (30) = 27V ± 10% at 0° C. In addition, VE3 cannot exceed $\overline{V}cc$ = 27V, therefore, maximum allowable solenoid voltage cannot be exceeded in the event Q3 shorts out.

For maximum power supply load, calculate VE3 at 0° C.

Then, from Equation 60,

$$\overline{I}_{E3} = \frac{\overline{V}_{cc} - V_{\underline{BE3}} - V_{\underline{CE2}}}{\frac{R_{\underline{6}}}{h_{\overline{FE3}}} + R_{\underline{L2}}} \qquad (62)$$

And substituting worst case parameters into Equation 62,

$$\overline{I}_{E3} = \frac{25 - .8 - .2}{\frac{9.8}{53} + 3.94} = \frac{24}{4.12} = 5.82A$$

From Equation 61,

$$\overline{V}_{E3} = \overline{I}_{E3} \, R_{\underline{L}2} \tag{63}$$

Or under worst case conditions,

$$V_{E3} = 5.82\ (3.94) = 22.8V$$

d. Transistor Switching Time

1) Turn-On

System specifications require a minimum allowable rise time of 5 ms for a 6 A current step, and approximately 3 ms for a 3.6 A step. Neglecting Q1 base current, the circuit turn-on time is given by:

$$T = R_2 C_2 L_\eta \frac{V_1}{V_1 - V_{B1}} \tag{64}$$

Where, VB1 is dependent on the circuit parameters and worst case variations. For minimum turn-on, Equation 64 becomes:

$$T = \underline{R}_2 \underline{C}_2 L_\eta \frac{\underline{V}_1}{\underline{V}_1 - \underline{V}_{B1}} \tag{65}$$

VB1 will be minimum for IE1 minimum, and IE1 will be minimum when all hFE's are maximum, thus requiring minimum drive. Since hFF's are maximum at 60° C, calculate drive requirements at 60° C.

Thus, letting,

$$I_{C3} = \alpha_{N3} I_{E3} \tag{66}$$

Now, solving Equation 27 for IE3

$$I_{E3}\left(R_{L2}+\frac{\alpha_{N3}R_6}{h_{FE3}\,\alpha_{N2}}\right)=V_{CC}+\left(\frac{I_{cb03}}{\alpha_{N3}\,\alpha_{N2}}-\frac{V_{BE3}}{R_7\,\alpha_{N2}}+\frac{I_{CB02}}{\alpha_{N2}}\right)$$

$$(R_6)-V_{CE2}-V_{BE3}$$

Resulting in:

$$I_{E3}=\frac{V_{cc}+\left(\frac{I_{cb03}}{\alpha_{N3}\,\alpha_{N2}}-\frac{V_{BE3}}{R_7\,\alpha_{N2}}+\frac{I_{cb02}}{\alpha_{N2}}\right)R_6-V_{CE2}-V_{BE3}}{R_{L2}+\frac{\alpha_{N3}R_6}{h_{FE3}\,\alpha_{N2}}} \tag{67}$$

To determine the rise times, ICBO and the IR7 current may be neglected, then

$$I_{E3}=\frac{\underline{V_{cc}}-\overline{V}_{BE3}-\overline{V}_{CE2}}{\frac{\overline{R}_6}{\overline{h}_{FE3}}+\overline{R}_{L2}} \tag{68}$$

And at 60°C

$$\underline{I}_{E3}=\frac{24-1.1-.57}{\frac{10.2}{62}+5.96}=\frac{22.33}{6.12}=3.65\text{A}$$

Since,

$$\underline{I}_{C2}=\frac{\alpha_{N3}\,\underline{I}_{E3}}{\overline{h}_{FE3}} \tag{69}$$

then,

$$\underline{I}_{C2}=\frac{.98\,(3.65)}{62}=58\text{ MA}$$

and,

$$I_{\underline{E}2} = \frac{I_{\underline{C}2}}{\alpha_{N2}} = 59 \text{ MA} \tag{70}$$

Then, since

$$V_{C1} = V_{B2} = V_{CC} - I_{E2} R_6 - V_{BE2} \tag{70}$$

Solve for $\overline{V}C1$, to yield minimum IC1, or

$$\overline{V}_{C1} = V_{\underline{C}C} - I_{\underline{E}2} \overline{R}_6 - V_{\underline{B}E2} \tag{71}$$

And, substituting values into the above equation:

$$\overline{V}_{C1} = 24 - 59 \text{ MA } (10.2) - .7 = 22.7\text{V}$$

To calculate IE1, let

$$I_{C1} = I_{R4} + I_{B2} \tag{72}$$

where,

$$I_{R4} = \frac{V_{CC} - V_{C1}}{R_4} \tag{73}$$

and,

$$I_{B2} = \frac{I_{C2}}{h_{FE2}} \tag{74}$$

For worst case 60°C conditions,

$$I_{\underline{R}4} = \frac{V_{\underline{C}C} - \overline{V}_{C1}}{\overline{R}_4} = \frac{24 - 22.7}{259} = 5 \text{ MA} \tag{75}$$

And,

$$I_{\underline{B2}} = \frac{I_{\underline{C2}}}{\overline{h}_{FE2}} = \frac{58}{66} = .96 \text{ MA} \tag{76}$$

or,

$$I_{\underline{C1}} = 5 + .96 = 5.96 \text{ MA}$$

and,

$$I_{\underline{E1}} = \frac{5.96}{.985} = 6 \text{ MA}$$

Then from,

$$V_{B1} = V_{E1} + V_{BE1} \tag{77}$$

or for minimum VB1,

$$V_{\underline{B1}} = V_{\underline{E1}} + V_{\underline{BE1}} \tag{78}$$

where,

$$V_{\underline{E1}} = I_{\underline{E1}} R_{\underline{5}} \tag{79}$$

Then, at 60°C:

$$V_{\underline{B1}} = 6 \text{ MA } (825) + .53 = 5.47\text{V}$$

Now substituting the above values into Equation 65, at 60°C:

$$\underline{T} = 2913 \ (5.9 \ \mu \text{ f}) \ln \frac{24}{24 - 5.47} = 17.2 \text{ MS } (.2\text{C}) = 4.5 \text{ MS}$$

which exceeds the specified maximum of 3 ms by 150%.

The maximum turn-on time required must be calculated to insure that the solenoid switches before the relay timer drops out. From Equation 64, the maximum turn-on is:

$$\overline{T} = \overline{R}_2 \, \overline{C}_2 \, \ln \frac{\overline{V}_1}{\overline{V}_1 - \overline{V}_{B1}} \tag{80}$$

VB1 will be maximum when IE1 is maximum, which occurs during the maximum drive condition, or at 0°C. Since the drive requirement calculations at 0°C were based on minimum pull-in, $\overline{I}$E3 must be determined at $\overline{V}$cc. Again, from Equation 67:

$$\overline{I}_{E3} = \frac{\overline{V}_{CC} - V_{\underline{B}E3} - \underline{V}_{CE2}}{\frac{\underline{R}6}{h_{\underline{FE}3}} + \underline{R}_{L2}} \tag{81}$$

or at 0°C,

$$\overline{I}_{E3} = \frac{25 - .8 - .2}{\frac{9.8}{35} + 3.94} = 5.7A$$

and,

$$\overline{I}_{C2} = \frac{a_{N3} \overline{I}_{C3}}{h_{\underline{FE}3}} = \frac{.98(5.7)}{35} = 160 \text{ MA}$$

from which,

$$\overline{I}_{E2} = 163 \text{ MA}$$

For maximum IR4, from Equation 70,

$$V_{\underline{C}1} = \overline{V}_{CC} - \overline{I}_{E2} R_6 - \overline{V}_{BE2} \tag{82}$$

And at 0°C,

$$V_{\underline{C}1} = 25 - 163 \text{ MA } (9.8) - 1.06 = 22.34$$

From Equation 73,

$$\overline{I}_{R4} = \frac{\overline{V}_{CC} - \underline{V}_{C1}}{\underline{R}_4}$$

and at 0°C,

$$\overline{I}_{R4} = \frac{25 - 22.34}{191} = 14 \text{ MA}$$

Now, from Equation 74,

$$\overline{I}_{B2} = \frac{\overline{I}_{C2}}{\underline{h}_{FE2}} = \frac{160}{56} = 2.86 \text{ MA}$$

and from Equation 72,

$$\overline{I}_{C1} = 14 + 2.86 = 16.86 \text{ MA} \tag{83}$$

or,

$$\overline{I}_{E1} = \frac{16.86}{.98} 17.2 \text{ MA}$$

And from Equation 77,

$$\overline{V}_{B1} = \overline{V}_{E1} + \overline{V}_{BE1} \tag{84}$$

and,

$$\overline{V}_{B1} = \overline{I}_{E1} \overline{R}_5 + \overline{V}_{BE1} \tag{85}$$

Substituting worst case parameters into Equation 85,

$$\overline{V}_{B1} = 17.2 \text{ MA } (1173) + .84 = 21$$

Substituting worst case parameters into Equation 80,

$$\overline{T} = 2927\ (10.3\ \mu f)\ \ln \frac{25}{25-21} = 30\ (1.82) = 54.5\ MS$$

Since this is greater than the minimum relay timer drop out (41.5 ms), the time required to reach minimum pull-in voltage must be computed. From the manufacturer's specifications, for 4.5 lbs. pull-in at 25°C, VE3 = 18V, and at 0°C, VE3 = .9 (18) = 16.2V.

For this condition,

$$\overline{I}_{E3} = \frac{V_{E3}}{\underline{R_{L2}}} = \frac{16.2}{3.94} = 4.1\ A$$

and,

$$\overline{I}_{C2} = \frac{\alpha_N \overline{I}_{E3}}{\underline{h_{FE3}}} = \frac{.98(4.1)}{35} = 115\ MA$$

Also,

$$\overline{I}_{E2} = 117\ MA$$

From Equation 70,

$$V_{\underline{C1}} = \overline{V}_{CC} - \overline{I}_{E2}\ \underline{R}6 - \overline{V}_{BE2} \tag{86}$$

and at 0°C,

$$V_{\underline{C1}} = 25 - 115\,(9.8) - 1.06 = 22.8V$$

$$\overline{I}_{R4} = \frac{25 - 22.8}{191} = 11.5\ MA$$

From Equation 74,

$$\bar{I}_{B2} = \frac{\bar{I}_{C2}}{\underline{h_{FE2}}} = \frac{115}{56} = 2.05 \text{ MA}$$

And from Equation 72,

$$\bar{I}_{C1} = 11.5 + 2.05 = 13.5 \text{ MA}$$

From Equation 85,

$$\bar{V}_{B1} = 13.5\,(1173) + .84 = 16.64 \text{ V}$$

Substituting the above values into Equation 80,

$$\bar{T} = 2927\ (10.3\ \mu f)\ \ln \frac{25}{25 - 16.64} = 30\ (1.1) = 33 \text{ MS}$$

This result is well within the minimum relay timer dropout.

2) Turn-Off

Since the the transistor switching times are inherently very fast, the driver turn-off is dependent mainly on the decay of C2. This is given by:

$$t = RC\ \text{Ln}\ \frac{E_o}{e_c} \tag{87}$$

or, for one time constant, at 60°C,

$$t_{max} = \bar{R}_3\ \bar{C}_2 = 388\ (11\ \mu f) = 4.27 \text{ MS}$$

and at 0°C,

$$t_{min} = \underline{R_3}\ \underline{C_2} = 275\ (5.4\ \mu f) = 1.49 \text{ MS}$$

Or, turn-off time is primarily due to RC, and is only slightly affected by the inductive time constant L/R = .26 ms.

e. Transistor Power Dissipation

In general, transistor dissipation is given by:

$$P = p\,(t_{off}) + P\,(t_{on}) + P(t_{sw1}) + P(t_{sw2}) \tag{88}$$

where:

t_{OFF} = OFF time

t_{ON} = ON time

t_{SW1} = turn-ON time

t_{SW2} = turn-OFF time

Assuming a linear rise time, the energy dissipated during a switching interval is:

$$W_{tsw} = I_c \frac{V_{CE}\,(off)\,t_{SW}}{6} \tag{89}$$

Neglecting t_{SW} off, storage and delay times, the average power over a cycle is:

$$P_{avg} = \frac{V_{CE\,(ON)}\,I_C\,t_{ON} + V_{CE\,(OFF)}\,I_{CBO}\,t_{off}}{T} + \frac{V_{CE\,(off)}\,I_C\,t_{SW}}{6T} \tag{90}$$

where T = switching period.

Due to system requirements, T min = 2 seconds. From the relay timer, which has a maximum ON of 141 ms,

$$\overline{t}_{ON} + \overline{t}_{SW} = 141 \text{ ms} \tag{91}$$

From Equation 90, it is clear that maximum dissipation occurs for $\overline{t}_{SW}$, $\overline{t}_{ON}$, $\overline{I}_c$, $\overline{V}CE(ON)$, $\overline{I}CBO$, $\overline{V}CE\ (OFF)$. Moreover, the worst condition occurs at 60° C, and maximum P_{avg}. will be computed at 60°C. Since maximum VCE3(ON) results for $\overline{V}CC$, $\overline{V}BE3$, $\overline{V}CE2$, $\underline{hFE3}$ or $(\overline{I}E2)$ and IC3 maximum results for $\underline{RL2}$. Then from Equation 67,

$$\overline{I}_{E3} = \frac{\overline{V}_{CC} + \left(\frac{\overline{I}_{cbo3}}{\alpha_{N3} \alpha_{N2}} - \frac{\overline{V}_{BE3}}{R_7 \alpha_{N2}} + \frac{\overline{I}_{CBO2}}{\alpha_{N2}} \right) \underline{R}_6 - \overline{V}_{CE2} - \overline{V}_{BE3}}{R_{\underline{L2}} + \frac{\alpha_{N3} \underline{R}_6}{h_{\underline{FE3}} \alpha_{N2}}} \tag{92}$$

and substituting into Equation 92,

$$\overline{I}_{E3} = \frac{25 + \left(\frac{32\,\mu A}{.965} - \frac{1.1}{.98(8,250)} + \frac{.32\,\mu A}{.98} \right) 9.8 - .41 - 1.1}{4.88 + \frac{.98\,(9.8)}{.98\,(41)}}$$

and,

$$\overline{I}_{E3} = \frac{25 - .325 - 1.5}{4.88 + .24} = 4.72A$$

$$\overline{I}_{C3} = \alpha_{N3}\, I_{E3} = .98\,(4.72) = 4.62\,A$$

therefore,

$$V_{E3} = \overline{I}_{E3}\, R_{\underline{L2}} = 4.62\ (4.88) = 22.5V$$

$$\overline{V}_{CE3} = \overline{V}_{CC} - V_{E3} = 25 - 22.5 = 2.5V$$

Now, calculate the maximum t_{SW} at 60°C. From Equation 64,

$$\overline{T} = \overline{R}_2\, \overline{C}_2\, \mathrm{Ln} \frac{\overline{V}_1}{\overline{V}_1 - \overline{V}_{B1}} \tag{93}$$

To calculate $\overline{V}B1$, begin with $\overline{I}C3 = 4.62$ A. Then,

$$\overline{I}_{C2} = \frac{\alpha_{N3}\,\overline{I}_{C3}}{h_{FE3}} = \frac{.98\,(4.62)}{41} = 110 \text{ MA}$$

and,

$$\overline{I}_{E2} = \frac{110}{.98} = 112 \text{ MA}$$

From Equation 70, for maximum IR4,

$$V_{C1} = \overline{V}_{CC} - \overline{I}_{E2}\,R_6 - \overline{V}_{BE2}$$

or, substituting values,

$$V_{C1} = 25 - 112\,(9.8) - .91 = 23\text{ V}$$

From Equation 73,

$$\overline{I}_{R4} = \frac{\overline{V}_{CC} - V_{C1}}{R_4} = \frac{25-23}{191} = 10.5 \text{ MA}$$

And from Equation 74,

$$\overline{I}_{B2} = \frac{\overline{I}_{C2}}{h_{FE2}} = \frac{110}{72} = 1.53 \text{ MA}$$

Also, from Equation 72,

$$\overline{I}_{C1} = 10.5 + 1.53 = 12 \text{ MA}$$

or,

$$\overline{I}_{E1} = \frac{12}{.98} = 12.2 \text{ MA}$$

Then, from Equation 85,

$$\overline{V}_{B1} = 12.2 \text{ MA } (1173) + .70 = 15 \text{ V}$$

Substituting the above values into Equation 93, at 60°C,

$$\overline{T}_{60^\circ C} = 3878 \, (11 \, \mu f) \ \ln \frac{25}{25-12} = 42.7 \text{ ms } (.92) = 39 \text{ ms}$$

or, $\overline{t}_{SW}$ = 39 ms,

From Equation 91,

$$\overline{t}_{ON} = 141 - 39 = 102 \text{ ms}$$

and,

$$\overline{t}_{off} = 25 - .141 = 1.86 \text{ sec}$$

Now, substituting the above values into Equation 90, for Q3 with VCE3 (ON) = 2.5, IC3 (ON) = 4.62 A, t_{ON} = 102 ms, t_{OFF} = 1.86 secs., T = 2 secs., VCE OFF = 25.

$$\overline{P}_{Q3} = \frac{2.5\,(4.62)\,102 \text{ ms} + 25\,(32 \text{ mA})\,1.86}{2} + \frac{25\,(4.62)\ 39 \text{ ms}}{6\,(2)} = 1.7 \text{ w}$$

Similarly for Q2, VCE2 (ON) = .41, IC2 (ON) = 110 mA, $\overline{I}$CBO = .32 uA.

Then,

$$\overline{P}_{Q2} = \frac{.41\ (.110)(.102) + 25\ (.32\,\mu A)\,1.86}{2} + \frac{25\ (.110)(39 \text{ ms})}{12} = 11.3 \text{ mw}$$

Also for Q1, IC1 (ON) = 12 mA, VCE (ON) = 8V, $\overline{I}$CBO = .32 uA. Then,

$$\overline{P}_{Q1} = \frac{8\,(12 \text{ mA})(.102) + 25\ (.32\,\mu A)\,1.86}{2} + \frac{25\,(12 \text{ mA})(39 \text{ ms})}{12} = 5.9 \text{ mw}$$

Junction temperature may be represented by,

$$T_J = T_A + \theta_{J\text{-}A}\, P_T \tag{95}$$

where,

$$\theta_{J-A} = \theta_{J-C} + \theta_{C-A} \tag{96}$$

Neglecting thermal capacitance, at $T_A = 60°C$ for Q3.

$$T_J = 60 + 34.875\ (1.7W) = 119.2°C$$

Similarly for Q2,

$$T_J = 60 + 188\ (11.3 \times 10^{-3}) = 62.12°C$$

And for Q1,

$$T_J = 60 + 438\ (5.9 \times 10^{-3}) = 62.58°C$$

To prevent thermal runaway due to thermal regeneration, let

$$\frac{\partial P_T}{\partial T_J} \leq \frac{1}{\theta_{JA}} \tag{97}$$

Assuming,

$$\partial I_{CBO} = {}^{10\%\, I_{CBO} \text{ at } 25°C}/_{°C} \tag{98}$$

then,

$$\partial I_{CBO} = \frac{.1C1}{°C} = {}^{.1\text{ mA}}/_{°C}$$

and,

$$\partial P_J = V_{CC}\, \partial I_{CBO} = 25\ (.1\text{ mA}) = 2.5\text{ mw}/_{°C}$$

or, substituting into Equation 97, for Q3

$$2.5\text{ mw} \leq \frac{1}{34.875} = 28.8\text{ mw}$$

F

For Q2,

$$ICBO = .032\ uA/^\circ C$$

$$J\text{-}A = 188^\circ C/W$$

$$\frac{\partial P_T}{\partial T_J} = 22\ v\ (.032\mu A) = .7\mu W$$

and,

$$.7\ \mu W \leq .0053\ w$$

For Q1,

$$ICBO = 0.32\ uA/^\circ C$$

$$J\text{-}A = 438^\circ C/W$$

$$\frac{\partial P_T}{\partial T_J} = .7\ \mu w$$

and,

$$.7\ \mu w \leq 2.3\ mw$$

Q3 Reliability

Although the junction temperature of Q3 is well within specifications, transistor failure rate is somewhat proportional to junction temperature, and it is desirable to reduce the junction temperature of Q3 with a small heat sink. For example, for a heat sink of 3/32" copper x 5 sq. in., the S-A = 6.8°C/W.

Now since,

$$\theta_{CA} = \theta_{CS} + \theta_{SA}$$

Assuming a very low resistance insulator, $\theta_{C\text{-}S} = .5^\circ C/W$.

Then,

$$\theta_{CA} = 7.3°C/W$$

and,

$$T_J = T_A + (\theta_{JC} + \theta_{CA}) P_T = 60°C + (.875 + 7.3)\ 1.7 = 74°C$$

This results in approximately 40% reduction in junction temperature.

f. Hold Circuit

1) Holding Force

From the manufacturer's specifications, the minimum holding force occurs at VCC minimum, 60°C, or

$$Hold_{min} = 4.8 \text{ lbs}$$

Also, maximum hold occurs at VCC maximum, 0°C, or

$$Hold_{max} = 7.8 \text{ lbs}$$

Since a minimum of 2.5 lbs. is required and 4.5 lbs. is specified, the above force is sufficient.

2) Rise Time

The build-up of current in the hold coil is subject to the time constant:

$$T = L/R$$

or 63.3% of holding force (3 lbs.) will occur at:

$$\overline{T} = \frac{L}{R}$$

Then, at 0°C,

$$\overline{T} = \frac{26.5 \text{ mh}}{99} = .27 \text{ ms}$$

Since the minimum pull-in time is maximum for 41.5-33 = 8.5 ms, the hold force will be sufficient to hold the slug once pull-in force is discontinued.

3) Hold Coil Power Dissipation

Maximum power dissipation occurs at 0°C where the coil resistance is minimum. Thus,

$$\overline{P} = \frac{\overline{V}_2^{\,2}}{\underline{R}} = \frac{625}{99} = 6.3 \text{ W}$$

However, the worst case condition is at 60°C. Or,

$$P_{60°C} = \frac{\overline{V}_2^{\,2}}{\underline{R}} = \frac{625}{122} = 5.1 \text{ W}$$

Since this is continuous power, it is recommended, space permitting, that the coil resistance be increased by using smaller wire, while at the same time, to preserve the holding force, increase the number of turns.

3.0 MOTOR CONTROL

Minimum available relay voltage is:

$$\underline{V_{coil}} = V_{cc} - \overline{I}_{coil}\,\overline{R}_{cont.} \tag{99}$$

where,

$$I \text{ contacts} = I \text{ coil} = \frac{V \text{ coil}}{R \text{ coil}}$$

and,

$$\overline{I}_{coil} = \frac{V_{coil}}{\underline{R}_{coil}} \tag{100}$$

Solving for V coil:

$$V_{\underline{coil}} = \frac{V_{\underline{cc}}}{1 + \frac{\overline{R}_{ct}}{R_{\underline{c2}}}} \tag{101}$$

or

$$V_{\underline{coil}} = \frac{24}{1 + \frac{.2}{263}} = 23.98 \text{ V}$$

<u>Q3 Heat Sink Analysis</u>

Maximum allowable transistor junction temperature for ERTS is 110°C. As shown in Figure A-2, the Q3 heat sink is 6.6 sq. in.

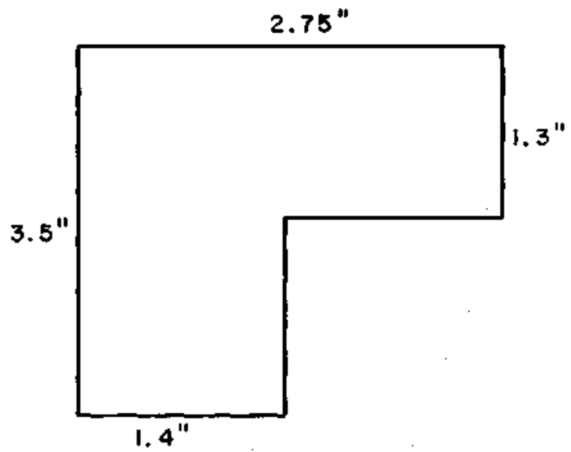

Material: copper clad circuit board (.0028 in. th.)

Figure A-2 Q3 HEAT SINK

Neglecting convection (zero gravity) and conduction, for $A_{heat\ sink} << A_{surface}$, radiant heat transfer is given by:

$$Q = A_1\, e_1\, \sigma\, (T_1^{\,4} - T_2^{\,4}) \quad \text{BTU/hr.} \tag{102}$$

where:

$A1$ = Heat sink area (ft^2)

$e1$ = Emissivity (0.8 for unpolished copper)

σ = Stefan-Boltzman constant (0.173×10^{-8} BTU/hr - ft^3-R^4)

$T1$ = Temperature of heat sink (°Rankine)

$T2$ = Temperature of surrounding surface (°Rankine)

For a uniform heat sink temperature, solving Equation 102 for T_1,

$$T_1 = \left(\frac{Q + A_1 e_1 \sigma T_2^4}{A_1 e_1 \sigma}\right)^{1/4} \tag{103}$$

Since PT = 1.7W, and 1 watt = 3.42 BTU/hr., then,

$$P_T = 1.7\ (3.42) = 5.8 \text{ BTU/hr}$$

and,

$$T_2 = 60°C = 140°F = 140 + 460 = 600°R$$

$$A_1 = 6.6 \text{ in}^2 \cdot \frac{ft^2}{144} = .0458 \text{ ft}^2$$

solving for T1,

$$T_1 = \left(\frac{3.42}{.0458\,(.8)(.173 \times 10^{-8}} + (600)^4\right)^{1/4}$$

or,

$$T_1 = 650°R = 190°F = \frac{5}{9}\ (158) = 87.5°C$$

Now, for a heat sink mounted transistor,

$$T_J = T_C + (\theta_{JC} + \theta_{CS})\, P_T \tag{104}$$

where, for mica,

$$\theta_{C-S} = .5^\circ C/W$$

substituting values into Equation 104,

$$T_J = 87.5 + (.875 + .5)\ 1.7 = 90.7^\circ C$$

which is much less than the allowable junction temperature of 110°C.